

ABSTRACT

WALKER, STEVEN HUNTER. Relative Quantification of *N*-linked Glycans in Complex Mixtures via Stable Isotope Labeling and Enhanced Analysis by Liquid Chromatography Coupled Online to Mass Spectrometry. (Under the direction of Dr. David Charles Muddiman).

Glycomics is a rapidly emerging field due to the ubiquity and functional importance of glycosylation in biological systems. However, the current analytical tools for studying glycomics and glycoproteomics lag decades behind proteomics and, to a larger degree, genomics. Additionally, the increasing advancements in separations and mass spectrometry technology (e.g. the Orbitrap) are not being fully taken advantage of due to the lack of reproducible, robust, and high-throughput front-end glycomics sample preparation strategies. Thus, this dissertation describes an effort to develop a high-throughput chemical derivatization strategy for the relative quantification of *N*-linked glycans, which can be coupled to nearly any glycomics sample preparation procedure with minimal monetary and time cost.

The motivation for this work is the correlation between aberrations in glycosylation and disease. Thus, a strategy capable of systematically comparing and quantifying glycan profiles between samples (e.g. control and cancer samples) would be invaluable in glycan biomarker discovery efforts. Additionally, this work has been primarily developed in the most complex of biological matrices, blood plasma. There are two main reasons for this: 1) because plasma is one of the most complex matrices, it is likely that this technique will be effective when applied to any other biological matrix, and 2) plasma samples can be acquired without invasive

surgery. This means that a screening method derived from biomarkers discovered in plasma will ultimately be inexpensive and non-invasive in practice.

Aside from the possible clinical value of this quantification strategy, this work has made significant contributions to the field of glycomics and fundamental analytical chemistry including both experimental and practical advantages. By developing tunable glycan reagents, it has been shown that these tags are capable of both relatively quantifying *N*-linked glycans and systematically decreasing the detection limits of *N*-linked glycans in plasma samples using mass spectrometry. Because glycomics strategies often involve numerous sample preparation steps, the addition of chemical derivatization typically only further complicates the preparation. However, the strategy presented herein requires only 4 hours of total additional sample preparation time (samples can be processed in parallel), and the reaction products can be immediately analyzed. This is a significant advantage over traditional glycan derivatization strategies such as permethylation and reductive amination.

Finally, this work has also contributed to the fundamentals of analytical chemistry and, more specifically, mass spectrometry. By tuning the glycan reagents with different functional properties, the mechanism for the generation of gas phase ions in electrospray ionization was able to be studied, and using these results, biases in the electrospray process were able to be exploited for the enhanced detection of glycans by mass spectrometry. Furthermore, liquid chromatography of glycans is often coupled online to mass spectrometry for the separation of glycans just before mass analysis, and traditionally, glycans are not able to be retained and

separated using reverse phase chromatography (the most robust separation strategy for biological analytes). However, using the reagents developed and presented herein, the separation of glycans by reverse phase liquid chromatography is not only possible, but it is advantageous, allowing for increased separation efficiency and an increase in the total number of glycans detected. A significant practical advantage of this strategy is the ability to analyze glycan samples on the same instrument platform as a majority of proteomic strategies. This significantly increases the efficiency of joint proteomic and glycomic laboratories and facilitates a more comprehensive systems biology approach to bioanalytical chemistry.

© Copyright 2013 by Steven Hunter Walker

All Rights Reserved

Relative Quantification of *N*-linked Glycans in Complex Mixtures via Stable Isotope
Labeling and Enhanced Analysis by Liquid Chromatography
Coupled Online to Mass Spectrometry

by
Steven Hunter Walker

A dissertation submitted to the Graduate Faculty of
North Carolina State University
in partial fulfillment of the
requirements for the Degree of
Doctor of Philosophy

Chemistry

Raleigh, North Carolina

2013

APPROVED BY:

David C. Muddiman
Professor, Chemistry
Committee Chair

Leslie A. Sombers
Professor, Chemistry

James N. Petite
Professor, Poultry Science

Robert M. Kelly
Professor, Chemical & Biomolecular
Engineering

DEDICATION

This dissertation is dedicated to my family, most importantly my dad - John, my mom - Paige, and my wife - Amber, for their unconditional love and support throughout not only my graduate career but also for the years prior that shaped my life's path. Without the constant encouragement and motivation of my parents, I could not have been at the point in my life I am now. Also, the ability to spend time with my wife and begin our life together has often relieved the stresses of graduate school, and her support has made me a more successful person. Though there are no words to express this to the fullest, I thank you and am forever grateful for the impact each of you has had in my life!

BIOGRAPHY

Steven Hunter Walker was born in Hickory, North Carolina on June 29, 1987 to his parents John and Paige Walker. Hunter attended Fred T. Foard High School just south of Hickory, and upon graduation in 2005, chose to attend the University of North Carolina at Chapel Hill. Here, he earned a Bachelor of Science in Chemistry and graduated with Honors and Distinction. In 2009, Hunter began his Ph.D. studies at North Carolina State University. In 2011, Hunter and his wife, Amber, were married in their hometown of Hickory, North Carolina.

ACKNOWLEDGMENTS

I would first like to gratefully acknowledge my parents and my wife, all to whom this dissertation is dedicated. Their love and support has given me the opportunity to succeed in life and made me the person I am today.

There have been many teachers, professors, and role models who have been instrumental in my life, and I sincerely thank each one of you. However, I would like to individually thank those who have directly impacted my scientific career. During my undergraduate education at the University of North Carolina at Chapel Hill, I was fortunate enough to become involved in undergraduate research. I was mentored by Dr. Tomas Baer in his physical chemistry laboratory, studying chemical thermodynamics using mass spectrometry. It is here that I realized the passion I have for research. Dr. Baer was helpful, motivating, and provided a perspective on science that is not found in the classroom alone. Thus, I am grateful for the impact that both he and his group members had on my decision to attend graduate school.

The person I want to thank the most for my success in scientific research and graduate school is Dr. David Muddiman. I cannot imagine a mentor providing a more successful atmosphere and program to perform cutting-edge research. I have gained so much from him not only in terms of science and research but also what it takes to be successful in all aspects of life. I am grateful for the constant motivation,

inspiration, and effort that he puts in every day so that his graduate students can succeed at the highest level.

Finally, I would like to thank all of the past and current members of the Muddiman group. Each one of you has made me a better scientist and person. The helpful attitude that everyone routinely has is instrumental in the success of the group, and I can only hope that I have adopted this same attitude and carry that with me throughout my life and career. I will be forever grateful for the community that we call the Muddiman group.

TABLE OF CONTENTS

LIST OF TABLES.....	xiii
LIST OF FIGURES	xiv
LIST OF PUBLICATIONS	xvii
LIST OF PRESENTATIONS	xix
CHAPTER 1: An Introduction to the Analysis and Relative Quantification of <i>N</i> -linked Glycans by Liquid Chromatography Coupled Online to Mass Spectrometry.....	1
1.1 Glycomics and Biological Importance.....	1
1.2 <i>N</i> -linked Glycan Analysis Strategies.....	4
1.2.1 Overview	4
1.2.2 Derivatization Strategies.....	7
1.2.3 Relative Quantification Strategies	10
1.3 Glycan Separation by Liquid Chromatography	16
1.3.1 Overview	16
1.3.2 Glycan Separation Strategies.....	16
1.4 Electrospray Ionization	20
1.4.1 Overview	20
1.4.2 The Generation of Gas Phase Ions in Electrospray Ionization	21
1.4.3 Exploiting the Hydrophobic Bias for Increased ESI Efficiency	24
1.5 Fourier Transform Mass Spectrometry	25

1.5.1	Overview	25
1.5.2	Fourier Transform Ion Cyclotron Resonance Mass Spectrometry	27
1.5.3	Orbitrap Mass Spectrometry.....	29
1.5.4	Hybrid Fourier Transform Mass Spectrometry.....	32
1.6	Synopsis of Completed Research	37
1.7	References	43
CHAPTER 2: The Interplay of Permanent Charge and Hydrophobicity in the		
	Electrospray Ionization of Glycans.....	60
2.1	Introduction.....	60
2.2	Experimental	65
2.2.1	Materials.....	65
2.2.2	Synthesis of Reagents.....	66
2.2.3	Fractional Factorial Design.....	67
2.2.4	Charged/Neutral Pair Analysis	70
2.2.5	Nano-Flow Liquid Chromatography	71
2.2.6	LTQ-FTICR Mass Spectrometry	71
2.2.7	Non-Polar Surface Area Calculations	72
2.3	Results and Discussion	72
2.3.1	Hydrazone Formation Optimization	73
2.3.2	Analysis of Charged/Neutral Reagents.....	76
2.3.3	Non-Polar Surface Area Calculations	81
2.4	Conclusions.....	82

2.5	References	84
CHAPTER 3: Hydrophobic Derivatization of <i>N</i> -linked Glycans for Increased Ion		
	Abundance in Electrospray Ionization Mass Spectrometry	90
3.1	Introduction.....	90
3.2	Experimental	94
3.2.1	Materials.....	94
3.2.2	Reagent Synthesis, Purification, and Characterization.....	94
3.2.3	Reagent Analysis for Model Glycan.....	95
3.2.4	Cleavage, Derivatization, and Analysis of Plasma <i>N</i> -linked Glycans .	96
3.2.5	nano-Flow Liquid Chromatography (HILIC).....	97
3.2.6	LTQ-FTICR Mass Spectrometry	97
3.2.7	Non-Polar Surface Area Calculations	98
3.3	Results and Discussion	99
3.3.1	Characterization of Hydrazone Reagents	99
3.3.2	Analysis of the Human Plasma <i>N</i> -linked Glycome using the Phenyl2- GPN Reagent	107
3.4	Conclusion.....	109
3.5	References.....	111
CHAPTER 4: Stable-Isotope Labeled Hydrophobic Hydrazone Reagents for the		
	Relative Quantification of <i>N</i> -linked Glycans by Electrospray Ionization	
	Mass Spectrometry	117
4.1	Introduction.....	117

4.2	Experimental	123
4.2.1	Materials.....	123
4.2.2	Synthesis of Reagents.....	123
4.2.3	<i>N</i> -linked Glycan Derivatization Procedure	124
4.2.4	<i>N</i> -linked Glycan Extraction from Pooled Plasma	124
4.2.5	nano-Flow Hydrophilic Interaction Chromatography.....	125
4.2.6	LTQ-Orbitrap Mass Spectrometry.....	126
4.2.7	Glycan Integration and Relative Quantification.....	127
4.3	Results and Discussion	128
4.4	Conclusions.....	140
4.5	References	141
CHAPTER 5: Systematic Comparison of Reverse Phase and Hydrophilic Interaction Liquid Chromatography Platforms for the Analysis of <i>N</i> - linked Glycans		
		147
5.1	Introduction.....	147
5.2	Experimental	153
5.2.1	Materials.....	153
5.2.2	<i>N</i> -linked Glycan Derivatization Procedure	154
5.2.3	Maltodextrin Sample Preparation	154
5.2.4	<i>N</i> -linked Glycan Extraction from Pooled Plasma	155
5.2.5	nano-Flow Hydrophilic Interaction Chromatography.....	156
5.2.6	nano-Flow Reverse Phase Chromatography.....	157

5.2.7	LTQ-FTICR Mass Spectrometry	157
5.3	Results and Discussion	158
5.4	Conclusions.....	171
5.5	References.....	173
CHAPTER 6: The Use of a Xylosylated Plant Glycoprotein as an Internal Standard Accounting for <i>N</i> -linked Glycan Cleavage and Sample Preparation Variability		
		181
6.1	Introduction.....	181
6.2	Experimental	185
6.2.1	Materials.....	185
6.2.2	Synthesis of Reagents.....	185
6.3	Results and Discussion	187
6.4	Conclusions.....	192
6.5	References.....	194
CHAPTER 7: Individuality Normalization when Labeling with Isotopic Glycan Hydrazide Tags (INLIGHT): A Novel Glycan Relative Quantification Strategy		
		197
7.1	Introduction.....	197
7.2	Experimental	203
7.2.1	Materials.....	203
7.2.2	<i>N</i> -linked Glycan Derivatization Procedure	203
7.2.3	Maltodextrin Sample Preparation	204

7.2.4	<i>N</i> -linked Glycan Extraction from Pooled Plasma	204
7.2.5	cHiPLC nano-Flow Reverse Phase Chromatography.....	205
7.2.6	Q Exactive Mass Spectrometry	205
7.3	Results and Discussion	206
7.4	Conclusions.....	218
7.5	References	220
APPENDICES.....		224
APPENDIX A		225
A.1	Non-Polar Surface Area Calculations.....	225
A.2	Derivatization Reaction.....	226
A.3	Reagent Synthesis	227
A.4	References	235
APPENDIX B		237
B.1	<i>N</i> -linked Glycans Detected from Pooled Human Plasma	237
B.2	Reaction Schemes	240
B.2.1	Experimental Section.....	240
B.2.2	Synthesis of Unlabeled Compounds.....	241
B.2.3	Synthesis and Characterization of Stable-Isotope Labeled Compounds	243
APPENDIX C		246
C.1	Supporting Data and Figures.....	246
APPENDIX D		251

D.1	Glycan Database	251
D.2	Processing Method Details	254
D.2.1	Before you Begin	254
D.2.2	Getting Started.....	254
D.2.3	How to Process.....	262
D.2.4	Extracting the Data to Excel.....	266
APPENDIX E	270
E.1	Reagents and Samples	270
E.2	Sample Preparation.....	271
APPENDIX F	276
F.1	Current Applications and Collaborations	276
F.2	Applications to Ovarian Cancer Biomarker Discovery Efforts.....	278

LIST OF TABLES

Table 2.1	Hydrazide Reagents and NPSA.....	65
Table 2.2	FFD Table for Phenyl-GP Reagent	67
Table 2.3	FFD Table for Phenyl-GPN Reagent	68
Table 2.4	NA2 Equimolar Mixture Abundance Data.....	78
Table 7.1	Abundance Ratios for Example Glycans in AGP-Spiked Plasma Samples	218
Table B.1	Detected Pooled Human Plasma <i>N</i> -linked Glycans	237
Table B.2	Internal Standard Corrected Glycan Ratios.....	238
Table C.1	RP Maltodextrin Peak Widths	248
Table C.2	HILIC Maltodextrin Peak Widths	248
Table C.3	RP and HILIC <i>N</i> -linked Glycans Detected.....	250
Table D.1	Glycan Database	252

LIST OF FIGURES

Figure 1.1	Glycan Biosynthesis.....	2
Figure 1.2	Glycan Analysis Strategies	4
Figure 1.3	Glycan Derivatization Strategies	8
Figure 1.4	General Relative Quantification Strategy using SIL Reagents	11
Figure 1.5	IDAWG Metabolic Labeling and Relative Quantification	15
Figure 1.6	Liquid Chromatography Separation of Glycans.....	19
Figure 1.7	Hydrophobic Bias in Electrospray Ionization	23
Figure 1.8	Glycan Mass Excess Plot.....	26
Figure 1.9	Image Current Detection in FTICR MS	29
Figure 1.10	FTMS Theoretical Duty Cycles	33
Figure 1.11	Resolving Power Comparisons	36
Figure 2.1	Hydrazide Reagent Synthesis.....	66
Figure 2.2	Fractional Factorial Design Results	74
Figure 2.3	Excess Reagent Optimization	75
Figure 2.4	Reaction Efficiency for a Complex Glycan	76
Figure 2.5	Charged and Neutral Reagents	77
Figure 3.1	Exploitation of the Hydrophobic Bias in ESI of Glycans	101
Figure 3.2	Fragmentation Patterns of Derivatized Glycans.....	103
Figure 3.3	Non-Polar Surface Area Calculations for Hydrophobic Tags	105
Figure 3.4	Labile Monosaccharide Glycan Degradation	107

Figure 3.5	Glycan Derivatization in Plasma	109
Figure 4.1	Stable-Isotope Labeled Hydrazide Tag	129
Figure 4.2	Glycan Relative Quantification via SIL Hydrazide Reagents.....	131
Figure 4.3	Quantification in a Simple Glycan Mixture.....	132
Figure 4.4	Internal Standard Correction in Plasma	135
Figure 4.5	Systematic Sample Preparation Variability	138
Figure 5.1	Maltodextrin Separation by RP and HILIC	160
Figure 5.2	Ammonium Adduction in HILIC	164
Figure 5.3	Derivatized and Native Glycan Separation Mechanisms.....	165
Figure 5.4	Modeling of the Reverse Phase Retention Behavior.....	167
Figure 5.5	RP and HILIC Comparison of Plasma Glycans	169
Figure 6.1	Generic Plant Glycoprotein	188
Figure 6.2	HRP Glycan as an Internal Standard	190
Figure 7.1	Isotopic Distribution Overlap	209
Figure 7.2	Maltodextrin Isotopic Overlap Correction and Normalization	210
Figure 7.3	Maltodextrin Relative Quantification Plot.....	213
Figure 7.4	Pooled Human Plasma Sample Preparation Strategy	214
Figure 7.5	Post Data Acquisition Normalization in Plasma	216
Figure A.1	Non-Polar Surface Area Calculations.....	225
Figure A.2	Hydrazone Formation Derivatization Reaction.....	226
Figure B.1	Light and Heavy Glycan Extracted Ion Chromatograms	239
Figure C.1	RP and HILIC Extracted Ion Chromatogram Comparison.....	247

Figure D.1	Xcalibur Home Page	255
Figure D.2	Processing Method Setup Window	256
Figure D.3	Detection Tab and Integration Parameters	258
Figure D.4	Calibration Tab Parameters	259
Figure D.5	Calibration Tab Target Compounds	260
Figure D.6	Levels Tab Parameters	261
Figure D.7	Xcalibur Sequence and Processing	262
Figure D.8	Xcalibur Sequence Setup.....	263
Figure D.9	Xcalibur Sequence Example	264
Figure D.10	View Processed Data in Xcalibur Quan Browser	264
Figure D.11	Area Selection for Glycan Extracted Ion Chromatogram.....	265
Figure D.12	View Spectra of the Extracted Ion Chromatogram	266
Figure D.13	Data List for MATLAB Extraction Program.....	267
Figure D.14	MATLAB Setup	268
Figure D.15	Execute MATLAB Program for Data Extraction	269
Figure F.1	Ovarian Cancer Repository Stages.....	278
Figure F.2	Ovarian Cancer Experimental Design	279
Figure F.3	Ovarian Cancer Glycan Profiling and Correction	280
Figure F.4	Ovarian Cancer Variation.....	281
Figure F.5	Determining Biological Change in Ovarian Cancer	282

LIST OF PUBLICATIONS

1. S. Hunter Walker, Amber D. Taylor, David C. Muddiman. Individuality Normalization when Labeling with Isotopic Glycan Hydrazide Tags (INLIGHT): A Novel Glycan Relative Quantification Strategy. *J. Am. Soc. Mass Spectrom.* Submitted: April 5, 2013.
2. S. Hunter Walker, Amber D. Taylor, David C. Muddiman. The Use of a Xylosylated Plant Glycoprotein as an Internal Standard Accounting for *N*-linked Glycan Cleavage and Sample Preparation Variability. *Rapid Commun. Mass Spectrom.* **2013**, Accepted: March 26, 2013.
3. S. Hunter Walker, Brandon C. Carlisle, David C. Muddiman. Systematic Comparison of Reverse Phase and Hydrophilic Interaction Chromatography Platforms for the Analysis of *N*-linked Glycans. *Anal. Chem.* **2012**, 84, 8198-8206.
4. Shane E. Harton, Sai Venkatesh Pingali, Grady A. Nunnery, Darren A. Baker, S. Hunter Walker, David C. Muddiman, Tadanori Koga, Timothy G. Rials, Volker S. Urban, Paul Langan. Evidence for Complex Molecular Architectures for Solvent-Extracted Lignins. *ACS Macro Lett.* **2012**, 1, 568-573.
5. Tomas Baer, S. Hunter Walker, Nicholas S. Shuman, Andras Bodi. One- and two-dimensional translational energy distributions in the *I*-loss dissociation of $1,2\text{-C}_2\text{H}_4\text{I}_2^+$ and $1,3\text{-C}_3\text{H}_6\text{I}_2^+$: What does this mean? *J. Phys. Chem. A.* **2012**, 116(11), 2833-2844.
6. S. Hunter Walker, David C. Muddiman. Nano-flow Liquid Chromatography Mass Spectrometric Analysis of Glycans in Cancer. *Nanomedicine and Cancer*. Science Publishers, Inc.: Enfield, NH, **2012**.
7. Samantha L. Blake, S. Hunter Walker, David C. Muddiman, Keith R. Beck, David Hinks. Spectral Accuracy and Sulfur Counting Capabilities of the LTQ-FT-ICR and the LTQ-Orbitrap XL for Small Molecule Analysis. *J. Am. Soc. Mass Spectrom.* **2011**, 22(12), 2269-2275.
8. S. Hunter Walker, Januka Budhathoki-Uprety, Bruce M. Novak, David C. Muddiman. Stable-Isotope Labeled Hydrophobic Hydrazide Reagents for the Relative Quantification of *N*-linked Glycans by Electrospray Ionization Mass Spectrometry. *Anal. Chem.* **2011**, 83(17), 6738-6745.

9. S. Hunter Walker, Laura M. Lilley, Monica F. Enamorado, Daniel L Comins, David C. Muddiman. Hydrophobic Derivatization of *N*-linked Glycans for Increased Ion Abundance in Electrospray Ionization Mass Spectrometry. *J. Am. Soc. Mass Spectrom.* **2011**, 22(8), 1309-1317.
10. S. Hunter Walker, Brian N. Papas, Daniel L. Comins, David C. Muddiman. The Interplay of Permanent Charge and Hydrophobicity in the Electrospray Ionization of Glycans. *Anal. Chem.* **2010**, 82(15), 6636-6642.
11. William R. Stevens; S. Hunter Walker; Nicholas S. Shuman; Tomas Baer. Dissociative Photoionization Study of Neopentane: A Path to an accurate Heat of Formation of the *t*-Butyl Ion, *t*-Butyl Iodide, *t*-Butyl Hydroperoxide. *J. Phys. Chem. A.* **2010**, 114(2), 804-810.

LIST OF PRESENTATIONS

1. **Oral** - “High Throughput Stable-Isotope Labeled Derivatization Strategy and Data Analysis for the Relative Quantification of *N*-linked Glycans in Complex Biological Systems” S. Hunter Walker, Amber D. Taylor, David C. Muddiman. *United States Human Proteome Organization Conference*. Baltimore, Maryland, March 2013.
2. **Poster** - “*N*-linked Glycan Relative Quantification Strategy Toward Biomarker Discovery Efforts in Ovarian Cancer *via* Multi-Functional Hydrazide Reagents” S. Hunter Walker, Amber D. Taylor, Brandon C. Carlisle, David C. Muddiman. *National Cancer Institute - Innovative Molecular Analysis Technologies Principal Investigators Meeting*, Houston, Texas, November 2012.
3. **Oral** - “Experimental and Practical Advantages of *N*-linked Glycan Hydrazone Formation Derivatization Toward High-Throughput *N*-linked Glycome Profiling of Plasma” S. Hunter Walker. *Warren Workshop*, Athens, Georgia, August 2012.
4. **Oral** - “Epithelial Ovarian Cancer *N*-linked Glycan Biomarker Discovery Strategy *via* nanoLC Mass Spectrometry” S. Hunter Walker. *FujiFilm Diosynth Biotechnologies*, Cary, North Carolina, March 2012.
5. **Poster** - “Development of Stable-Isotope Labeled Reagents for the Relative Quantification of *N*-linked Glycans *via* Online HILIC Mass Spectrometry” S. Hunter Walker, Januka Budhathoki-Uprety, Laura M. Lilley, Monica F. Enamorado, Daniel L. Comins, Bruce M. Novak, David C. Muddiman. *American Society for Mass Spectrometry Conference*, Denver, Colorado, June 2011.
6. **Oral** - “Development of Stable-Isotope Labeled Reagents for the Relative Quantification of *N*-linked Glycans” S. Hunter Walker. *Triangle Area Mass Spectrometry Meeting*, Research Triangle Park, Durham, North Carolina, April 2011.

7. **Poster** - “Development of Novel Stable-Isotope Labeled Reagents for the Relative Quantification of *N*-linked Glycans and Enhanced Glycan Detection in ESI FTICR Mass Spectrometry” S. Hunter Walker, Januka Budhathoki-Uprety, Laura M. Lilley, Monica F. Enamorado, Daniel L. Comins, Bruce M. Novak, David C. Muddiman. *United States Human Proteome Organization Conference*, Raleigh, North Carolina, June 2011.
8. **Poster** - “Hydrophobic Hydrazide Reagent Library for the Increased Ion Abundance of *N*-linked Glycans in nanoLC (HILIC) LTQ-FTICR MS” S. Hunter Walker, Laura M. Lilley, Daniel L. Comins, David C. Muddiman. *The Federation for Analytical Chemistry and Spectroscopy Societies Conference*, Raleigh, North Carolina, October 2010.
9. **Poster** - “Understanding the Interplay Between a Permanent Charge and Hydrophobicity on the Electrospray Ionization of Glycans and the Application of Hydrazide Hydrophobic Tagging Reagents Toward the Assay of *N*-linked Glycans” S. Hunter Walker; Brian N. Papas, Daniel L. Comins, David C. Muddiman. *American Society for Mass Spectrometry Conference*, Salt Lake City, Utah, May 2010.

CHAPTER 1

An Introduction to the Analysis and Relative Quantification of *N*-linked Glycans by Liquid Chromatography Coupled Online to Mass Spectrometry

1.1 Glycomics and Biological Importance

Glycosylation is a post-translational modification ubiquitous in nature, and it is estimated that more than 50% of all gene products are glycosylated.¹ Furthermore, it is estimated that of the entire translated genome, 0.5-1% of all gene products are involved in the glycosylation process.²⁻³ Glycans take part in regulating numerous biological processes including cell-cell interactions, cellular recognition, adhesion, cell division, immune response, protein folding, and protein stability.⁴ Due to the importance of these roles in biology, aberrations in glycosylation patterns can potentially be detrimental. By monitoring these aberrations, one can potentially correlate up- or down-regulation of these glycans with the onset of disease (e.g. cancer) and develop screening methods based on their quantification.

Glycosylation of proteins can be organized into two main groups: *N*-linked glycans, and *O*-linked glycans.⁵ However, this introduction and following dissertation will focus on *N*-linked glycosylation. *N*-linked glycans are unique from *O*-linked glycans in that there are several available enzymes that can specifically cleave the glycans from proteins, and the most common, peptide: *N*-glycosidase F (PNGase F), is commercially available.⁶ This makes the analysis of *N*-linked glycans much more feasible. Additionally, the presence of a reducing terminus after cleavage is a property necessary for several different types of derivatization,

including hydrazone formation (*vide infra*). *N*-linked glycosylation occurs throughout the secretory pathway in the endoplasmic reticulum and golgi apparatus (**Figure 1.1**).⁴ *N*-linked glycans are synthesized biologically in a semi-template driven process where a core glycan (GlcNAc₂Man₉Glc₃) is synthesized and transferred to the protein via a highly regulated process in the endoplasmic reticulum. However,

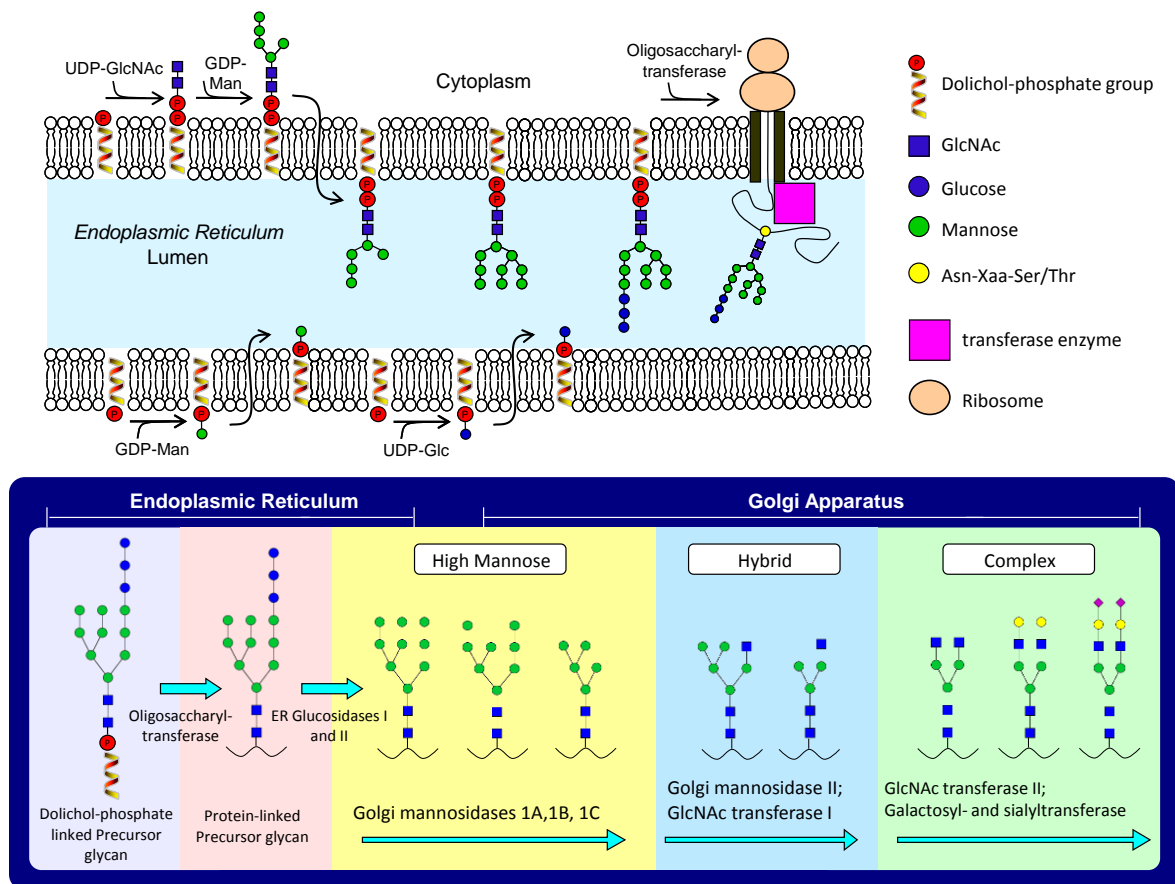


Figure 1.1 – The biosynthetic generation of the *N*-linked glycan precursor attached to every *N*-linked glycoprotein (top). Once attached, the precursor glycan is then trimmed by a series of glycosidases, and monosaccharides are added by a series of glycotransferases in both the endoplasmic reticulum and golgi apparatus (bottom).

once the precursor glycan is attached to the protein, terminal elongation by trimming and addition of monosaccharide units occurs in a non-regulated manner that is determined by substrate levels and the presence of specific glycosidases and glycotransferases.⁵ This terminal elongation mechanism allows for different glycans to be attached to the same glycosylation site on different copies of the same protein. Thus, copies of the same protein located in different parts of the cell or in a different environment may have significantly different glycosylation patterns leading to different protein folding, function, and/or interaction.

The non-regulated terminal elongation facilitates aberrant glycosylation due to changes in environment, such as the onset of disease. Protein glycosylation studies have correlated aberrations in glycosylation patterns with numerous diseases, including cancer. Robbins and coworkers first described the disparity in the size of membrane glycoproteins between healthy and diseased fibroblasts,⁷ and aberrant glycosylation patterns were first linked to cancer in 1978, where it was shown that the glycosylation of α_1 -antitrypsin is altered in lung, prostate, and gastrointestinal cancers.⁸ It is hypothesized that glycans can fulfill the role of being sensitive and specific biomarkers for targeted screening⁹ due to the increased number of studies providing evidence for the correlation of aberrant glycosylation and cancer.¹⁰⁻¹⁴ Additionally, this has been further shown in numerous recent manuscripts demonstrating aberrant glycosylation in several different cancer types¹⁵ including breast,¹⁶⁻¹⁸ prostate,¹⁹⁻²⁰ liver,²¹ ovarian,²²⁻²⁶ pancreatic,²⁷ etc.

1.2 N-linked Glycan Analysis Strategies

1.2.1 Overview

The mass spectrometric (MS) analysis of protein glycosylation has traditionally been difficult in comparison to proteins or nucleotides due to several factors including the structural and isomeric complexity, the hydrophilicity making glycans more difficult to ionize via electrospray ionization (ESI), and the instability of some monosaccharide residues.²⁸ Because of these complexities, there have been

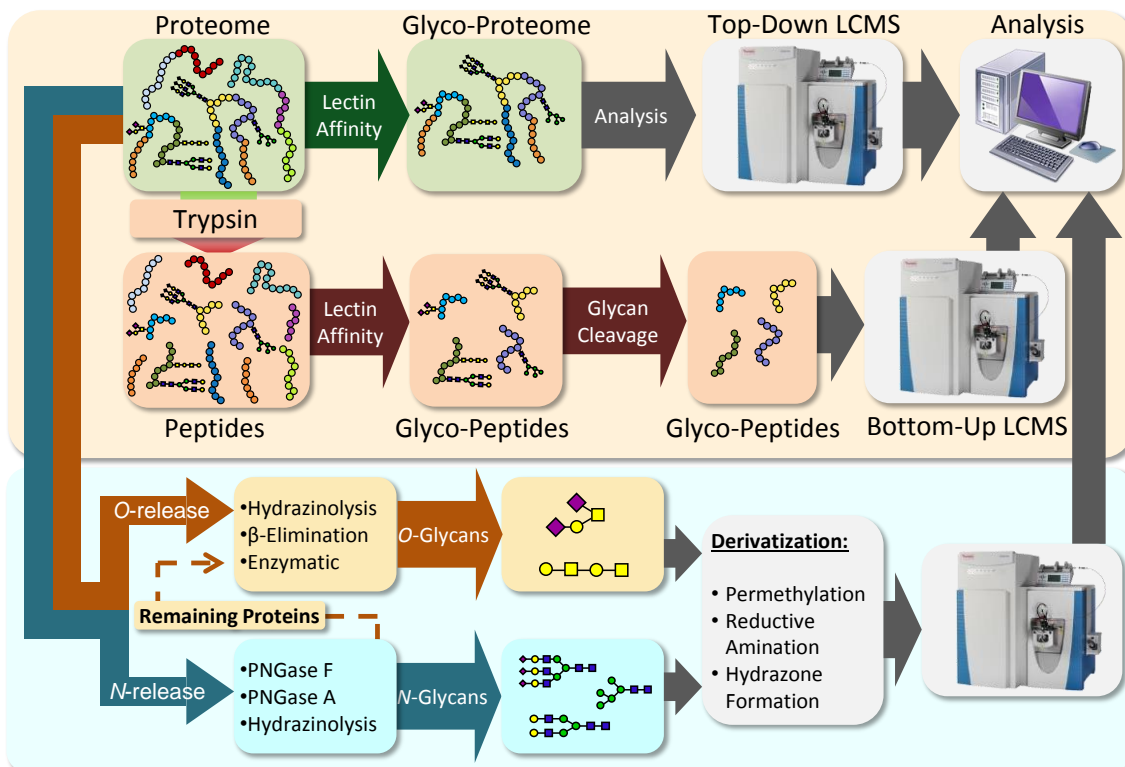


Figure 1.2 – Glycomics encompasses numerous methods for studying protein glycosylation, including studying the glycans attached to proteins (top – beige) and free oligosaccharides (bottom – blue). Each of these strategies is made up of many different technologies to look at different types of glycosylation, different glycosylation sites, and amounts of glycans present.

numerous strategies developed such that protein glycosylation information can be acquired. **Figure 1.2** displays the two major methodologies in which glycans can be analyzed by MS: 1) attached to proteins/peptides (glycoproteomics) or 2) as free oligosaccharides (glycomics). Glycoproteomics (**Figure 1.2 – Top**) is often used to profile not only the glycan, but also the site of glycosylation and protein/peptide sequence.²⁹⁻³¹ This is accomplished in either a ‘top-down’ or ‘bottom-up’ fashion, where the glycoproteins/glycopeptides are enriched using lectin affinity techniques and then analyzed by liquid chromatography coupled online to mass spectrometry (LC-MS).

The second method for studying protein glycosylation is by chemically or enzymatically releasing glycans from the proteins and analyzing the resulting glycan profiles (**Figure 1.2 – Bottom**). Releasing glycans from proteins affords several advantages when analyzing glycans. First, the number of glycans to be detected is significantly less than the number of proteins, and to a larger degree peptides, limiting the complexity of the measurement. Additionally, releasing glycans from proteins also allows access to the reducing terminus of the glycan.⁶ Numerous derivatization techniques take advantage of the free aldehyde group at the reducing terminus of the glycans³²⁻³³ including reductive amination,³⁴⁻³⁸ prazolone formation,^{32, 39-42} aminoxy labeling,⁴³⁻⁴⁴ and hydrazone formation.⁴⁵⁻⁵⁴ This allows for incorporation of hydrophobic tags,^{35-36, 45-46, 50, 55-56} UV and fluorescence labels,^{55, 57-59} and stable isotopes for quantification.^{34, 38, 43-44, 60-61}

There are several methods for the release of *N*-linked glycans, both chemical and enzymatic.⁶²⁻⁶⁴ Enzymatic release of *N*-linked glycans is common due to the widely available Peptide: *N*-glycosidase F (PNGase F) enzyme. PNGase F cleaves the glycans between the asparagine and the reducing end *N*-acetylglucosamine (GlcNAc). The main drawback of PNGase F is that it is unable to cleave core $\alpha(1-3)$ fucosylated glycans often found in plants. However, PNGase A is capable of removing all *N*-linked glycans from proteins⁶⁵⁻⁶⁷ but is currently not well studied and therefore less robust than PNGase F. Additionally, endoglycosidases can be used to release a portion of *N*-linked glycans depending on the specific enzyme.⁶⁸ Enzymatic release is much more limited in *O*-linked glycosylation due to the specificity of the enzymes available (*O*-glycanase).⁶⁹

Cleavage of both *N*-linked and *O*-linked glycans can also be achieved by chemical release methods. The most commonly used chemical release method is hydrazinolysis.⁷⁰⁻⁷⁴ This method is able to semi-selectively cleave *N*-linked and *O*-linked glycans depending on the temperature at which the reaction is carried out. This method has several drawbacks including the use of anhydrous hydrazine, which is extremely toxic and explosive, though a recent report has shown that hydrazine monohydrate can be an acceptable substitute if certain conditions are used.⁷⁴ Additionally, a natural byproduct of hydrazinolysis is the loss of monosaccharide units from the reducing terminus, known as peeling. This is detrimental to glycan analysis because it does not allow derivatization at the

reducing terminus, although studies have recently shown that certain cleavage conditions may yield significantly less peeling.⁷³

An alternative chemical release strategy is reductive β -elimination^{23, 75-77} and has been reported for both *N*-linked and *O*-linked glycans. This technique releases the glycans at the reducing terminus. However, in order to minimize peeling as in hydrozinolysis, it is necessary to reduce the released glycans to alditols.⁶² This is an additional disadvantage, as generally glycan alditols do not have the same capability for derivatization at the reducing terminus. Despite this, β -elimination has been demonstrated in the analysis of *N*-linked glycans cleaved from ovarian cancer samples toward glycan biomarker discovery efforts.²³

1.2.2 Derivatization Strategies

Chemical derivatization, although it can add extensive sample preparation time and/or analytical variability, is often used to enhance the information acquired from MS. Permethylation⁷⁸⁻⁸¹ and peracetylation^{79, 82} are two of the first methods used to derivatize glycans for enhanced MS analysis (**Figure 1.3a**). Though these methods are beneficial and enhance fragmentation spectra as well as increasing glycan ion abundance by incorporating hydrophobic surface area, permethylation and peracetylation convert all hydroxyl, amino, and carboxylic acid groups to their respective ether-functions, and thus, the *m/z* shift is variable for different sized glycans. Additionally, 100% conversion has proven difficult as one must derivatize up to 50 sites per glycan. In contrast, the reducing terminus is a convenient location

for derivatization due to the availability of a free aldehyde group after the enzymatic cleavage of *N*-linked glycans from proteins using PNGase F.⁶ Here, tags with a small, fixed mass shift can be incorporated onto the reagents. Reductive amination (**Figure 1.3b**) is a prominent technique capable of reacting with the reducing terminus of *N*-linked glycans and has been used to enhance several analytical techniques including UV and fluorescence detection^{55, 59, 83-84} and hydrophobic

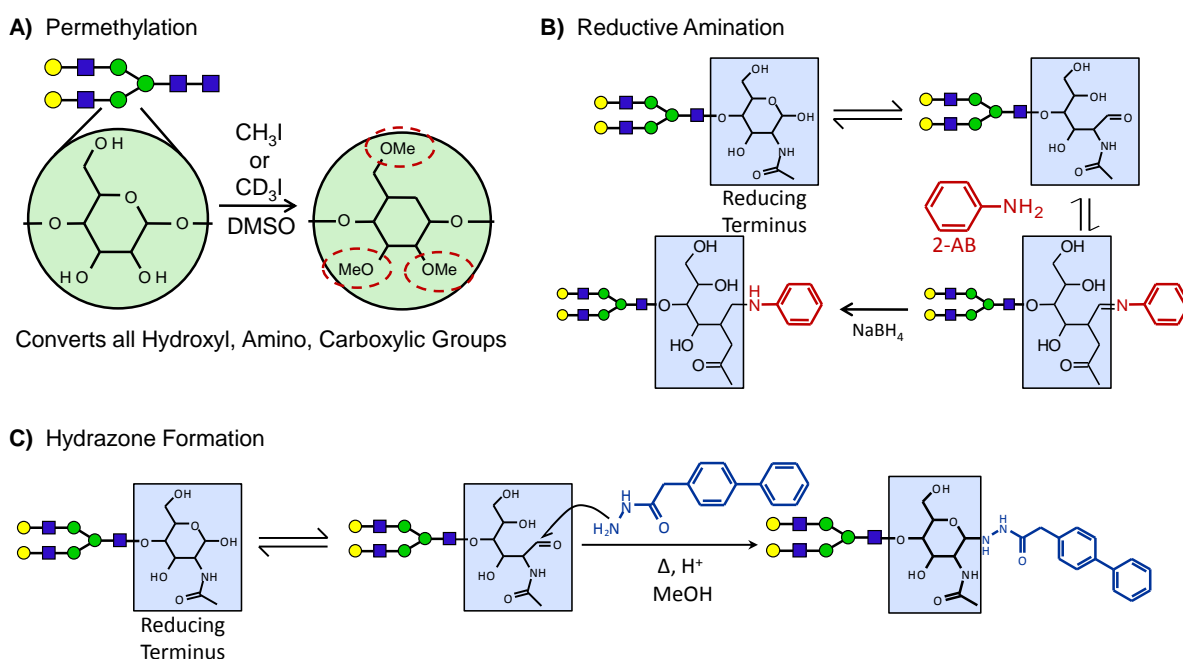


Figure 1.3 – Several common derivatization strategies for *N*-linked glycans. **A)** Permethylation converts all hydroxyl, amino, and carboxylic acid groups to their respective methyl ester. **B)** Reductive amination is the most popular reducing terminus derivatization strategy, and tags such as 2-AB and 2-AA are commercially available. However, reductive amination requires a clean-up step after reaction introducing variability into the method. **C)** Hydrazone formation is also a reducing terminus derivatization strategy. However, the reaction products can be directly injected onto an LC column.

derivatization.³⁴⁻³⁷ Though this method is effective, an additional significant clean-up step is necessary after derivatization, which often increases sample preparation time, the opportunity for sample loss, and the analytical variability in the measurement.

Hydrazone formation (**Figure 1.3c**) is an attractive alternative derivatization strategy in which hydrazide reagents react at the reducing terminus of glycans (much like reductive amination) but does not involve reducing the glycan to a Schiff base using salts such as sodium borohydride.³² Thus, when using hydrazone formation, the product can be directly injected onto the nano-LC column due to the lack of salts necessary in the reaction mixture. Danzylhydrazine⁴⁷ was the first reagent to be coupled to glycans via hydrazone formation for enhanced fluorescence or UV detection.^{52-53, 85} More recently, hydrazone formation has been used for enhanced MS detection,⁴⁵ though an abundance of these reagents is not readily available. Girard's T reagent was first used to increase mass spectral detection in order to incorporate a permanent cationic charge onto the glycan.⁴⁵ However, recent studies have shown decreases in ion abundance when coupling Girard's T reagent to glycans in nanoLC MS,⁴⁶ and it has been shown that hydrophobic derivatives of Girard's T reagent are capable of increasing the ESI efficiency of *N*-linked glycans by more than 4-fold in an LC-MS experiment.⁴⁶

1.2.3 Relative Quantification Strategies

A general scheme for relative quantification of glycans using stable-isotope labeling is presented in **Figure 1.4**. In these types of experiments, two glycan samples are differentially labeled (one light and one heavy), mixed, and analyzed by MS. This allows the two samples to be analyzed in the same LC-MS run, which minimizes the ESI and MS (technical) variability. Additionally, the ideal light and heavy reagents are indistinguishable from each other except for the mass. Thus, the light- and heavy-tagged glycans will behave identically in all facets of analysis but will be separated by mass in the MS. By measuring the ion abundances for the light and heavy peaks for each specific glycan, the relative amounts of each glycan in the two samples can be measured.

Three *N*-linked glycan relative quantification strategies have been developed that involve variations in permethylation: 1) stable-isotope labeling via deuteriomethyl iodide,⁸⁶ 2) stable isotope labeling via $^{13}\text{CH}_3$,⁸⁷ and 3) QUantitation by IsoBaric Labeling (QUIBL) using $^{13}\text{CH}_3\text{I}$ and $^{12}\text{CH}_2\text{DI}$.⁸⁸ Novotny and coworkers utilize permethylation of glycans using either methyl iodide or deuteriomethyl iodide in order to differentially label two glycan samples.⁸⁶ Because the methyl or deuteriomethyl groups are incorporated at each hydroxyl, amino and carboxylic acid group, each glycan will have a 3 Da mass shift per functional group methylated. In a similar study, Orlando and coworkers, permethylate with $^{13}\text{CH}_3$.⁸⁷ Again, the labels are incorporated at each of the hydroxyl, amino, and carboxylic acid groups, and the mass shift is variable per glycan.

Orlando and coworkers also exploit permethylation for the quantification of glycans, however, $^{13}\text{CH}_3\text{I}$ or $^{12}\text{CH}_2\text{DI}$ are used to differentially permethylate samples.⁸⁸ In this case, the two derivatization groups have the same nominal mass, but an exact mass difference of 0.002922 Da is observed per methylation site. Since all *N*-linked glycans have at least 20 methylation sites, the mass shift is >

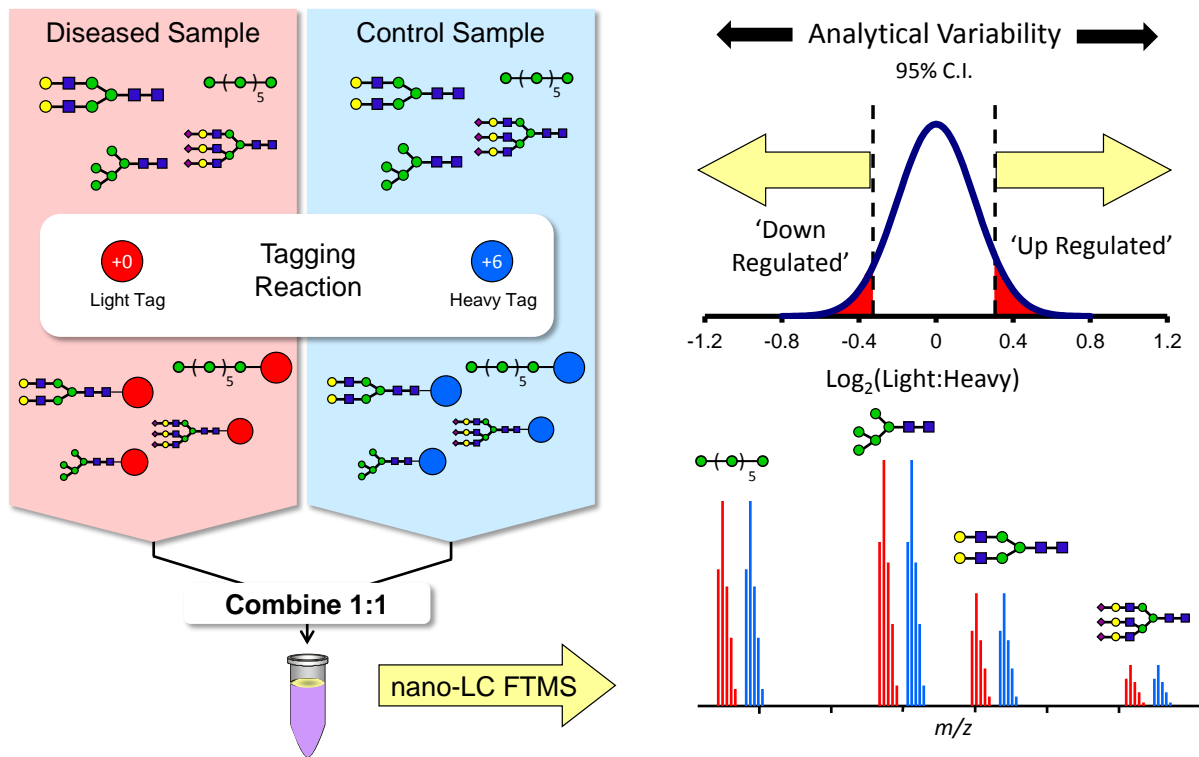


Figure 1.4 – A generic schematic for the relative quantification of *N*-linked glycans using stable-isotope labeling and analysis by LC-MS. Two samples are differentially labeled, mixed, and analyzed in the same LC-MS run. However, in the mass spectrum, each glycan from the two samples is separated by mass and relatively quantified based on ion abundance.

0.058 Da, and a mass spectrometer with 30,000 resolving power is able to resolve these two m/z . All of these methods are used to relatively quantify glycans from two separate samples in the same mass spectrometric run. Additionally, both samples are prepared individually and then mixed together before mass spectrometric analysis. This technique affords the advantage that ionization and measurement variability from run to run by ESI/MALDI MS analysis is exactly the same for both samples.

One major disadvantage to these studies where permethylation is used to incorporate stable isotopes is that due to the numerous hydroxyl, amino, and carboxylic groups present in oligosaccharides (~5 per monosaccharide and 7-18 monosaccharides per *N*-linked glycan), a 0.1% change in the permethylation efficiency between two samples can result in a 3-10% difference in ion abundance depending on the type and size of the glycan. Thus, the two samples must be permethylated with identical efficiency in order to confidently quantify glycans. Additionally, all of these methods use deuterium labeling, which is known to have a different chromatographic shift than hydrogen in LC. Thus, a multiple deuterio-labeled glycan can elute from a liquid chromatography column at a different time and in different mobile phases causing a possible change in ionization efficiency between the two samples and skew quantification.

Two other relative quantification strategies involve derivatization by stable-isotope labeled reductive amination reagents, GRIL³⁸ and tetraplex stable-isotope coded tags.³⁴⁻³⁵ Cummings and coworkers have developed Glycan Reductive

Isotope Labeling (GRIL) utilizing [$^{12}\text{C}_6$]aniline and [$^{13}\text{C}_6$]aniline in order to differentially label glycan samples, combine 1:1, and analyze in the same MS.³⁸ A comparable method has been developed by Zaia and coworkers,³⁴⁻³⁵ where a reductive amination reagent has been developed such that 4 tags can be used all with a different number of deuterium atoms incorporated (+0, +4, +8, +12). This is the first reagent that has the ability of tetraplex quantification of glycans. The authors were able to quantify the relative amounts of *N*-linked glycans from the plasma of four different species in the same mass spectrum. However, the mass shift of only 4 Da per tag is an inherent disadvantage to this method and creates overlapping isotopic distributions which involve theoretical simulations to deconvolute the data and determine relative abundances. Additionally, deuterium is used which can cause a chromatographic shift, introducing ionization and mass spectrometric variability (*vide supra*).

Tandem mass tags (TMTs) are a specific type of SIL tags for derivatization in a unique method of SIL-MS relative quantification, originally developed for proteomics measurements.⁸⁹⁻⁹⁰ This technique uses isobaric tagging reagents made up of a mass reporter group, a mass normalization group, and a cleavable linker between the two groups. The TMTs are synthesized such that stable isotopes are incorporated in the mass reporter group for the first tag, and stable isotopes are incorporated in the mass normalization group for the second tag. Thus, in full scan MS, the two tags cannot be differentiated from each other. However, when dissociating in MS/MS, the cleavable linker is fragmented. Thus, the reporter group

pair (one with SIL and one without) is separated by mass, detected, and the ion abundance ratios are used for relative quantification. This technique is often preferred over standard light/heavy SIL-MS strategies because the latter inherently is two-times as complex, due to two m/z peaks for each analyte. In contrast, in TMT experiments, the tags are isobaric and are detected as one m/z per analyte until it is chosen for fragmentation.

Recently, TMTs have been developed for glycans using hydrazide and aminoxy reagents.⁴³ However, in this study, a non-labeled tag was also synthesized so that light/heavy relative quantification in the full scan MS can be compared to the TMT approach. It was shown that using these TMTs, this technology is not capable of quantifying as well as the previously reported light/heavy SIL strategy. This is thought to be due to the cleavable linker having a higher energy of fragmentation than the glycosidic bonds in glycans. This results in over-fragmentation and a low signal-to-noise ratio for the reporter ions. These experiments do suggest that well-designed TMTs could be beneficial to the field.

Orlando and coworkers have developed a novel method to metabolically label glycans in cell culture (**Figure 1.5**), Isotopic Detection of Aminosugars With Glutamine (IDAWG).⁹¹ In glycan biosynthesis, the only method for the incorporating nitrogen into glycan molecules is through the hexosamine biosynthetic pathway. Here, the side chain of glutamine is the sole donor source of nitrogen for the production of aminosugars and sugar nucleotides, molecules which transfer individual monosaccharides to glycans during glycan biosynthesis. By doping in

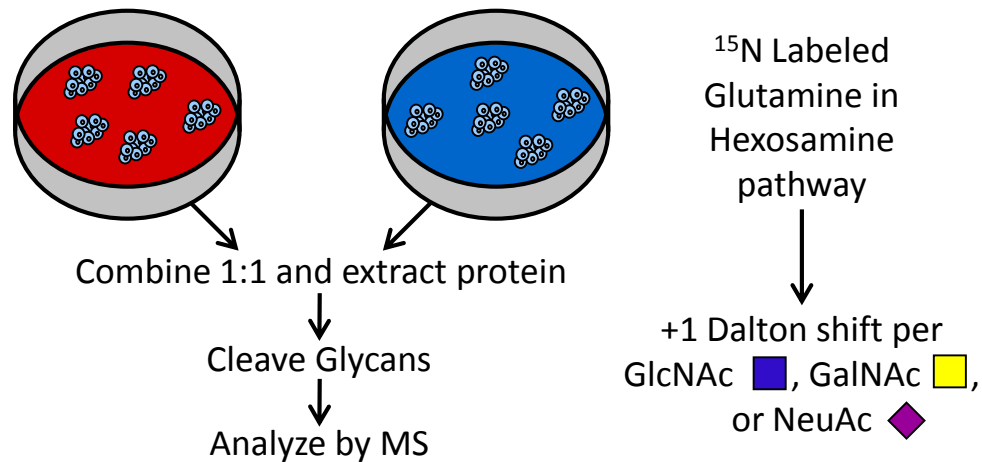


Figure 1.5 – IDAWG relative quantification strategy for glycans using metabolic labeling in cell culture. This method is advantageous over chemical derivatization because it reduces the amount of parallel sample preparation, thus reducing the variability of the method.

only ¹⁵N labeled glutamine into a glutamine deprived media, one can grow cells with glycans that are differentially label at the all monosaccharides containing nitrogen and incorporate a 1 Da mass shift per HexNAc, GalNAc, and NeuAc in the glycans. This method has a significant advantage over all previous derivatization techniques in that after the cells are grown they can be mixed together and all subsequent sample preparation steps are performed in the same vial, significantly reducing the sample preparation variability. However, the main drawback is that this study can only be performed in which an organism can be metabolically labeled with ¹⁵N, which is limited to cell culture at present.

1.3 Glycan Separation by Liquid Chromatography

1.3.1 Overview

The analysis of *N*-linked glycans from complex biological samples such as cell lysates, tissue lysates, or plasma involves measuring on the order of 100 analytes with significantly different molecular properties, molecular weights, and endogenous abundances. Because of this, it is often necessary to perform liquid chromatography (LC) separation prior to MS analysis. This allows hydrophobic molecules to elute at different times than more hydrophilic molecules, which reduces competition in the ESI process (*vide infra*). Additionally, the large dynamic range of *N*-linked glycans hinders analysis due to the fixed number of charges allowed to be detected at one time in FTMS instruments. Thus, separation of high abundance glycans from lower abundant glycans allows for lower abundant glycans to comprise a larger fraction of the total ions in the mass spectrometer, increasing the ion abundance, decreasing detection limits, and increasing the dynamic range of the instrument.

1.3.2 Glycan Separation Strategies

Many different types of liquid chromatography platforms have been used in the separation of glycans⁹²⁻⁹³ including both normal⁹⁴ and reverse phase (RP)⁹⁵, ion exchange¹⁶, on- and off-line, and capillary and chip-based systems^{93, 96-97}. Native glycans are not retained in RPLC due to the polar nature of the glycans and nonpolar nature of the stationary phase. However, RPLC can be used to

separate derivatized glycans when the derivatization imparts enough nonpolar molecules that the glycans are retained (permethylation or hydrophobic derivatization).⁹⁸ The two stationary phases that are most commonly used to separate native glycans are bonded HILIC stationary phases⁹⁹⁻¹⁰⁰ and graphitized carbon stationary phases.¹⁰¹⁻¹⁰²

HILIC and graphitized carbon separation techniques efficiently separate native and reduced oligosaccharides; however, both techniques involve “mixed-mode” separation methods that are a combination of hydrophobic/partitioning and ionic/adsorption interaction that must be further studied in order to elucidate the exact mechanism of separation.⁹⁹⁻¹⁰³ A recent study compared the two nano-flow LC techniques using Amide-80 stationary phase (HILIC) and graphitized carbon stationary phase.²³ The authors reported excellent performance for both separation techniques; however, heavily sialylated glycans were permanently retained on the graphitized carbon stationary phase (a problem also reported in an alternate study¹⁰²), and the life of the graphitized carbon column was much shorter than that of the HILIC column. Additionally, the development and miniaturization of HILIC stationary phases have exceeded that of graphitized carbon stationary phases.¹⁰¹

HILIC has been used frequently for the separation of both native^{23, 94, 104-106} and derivatized^{34, 38, 46} glycans in online LC-MS experiments⁹² and is often used for glycomic analyses due to the strong retention of polar compounds in comparison to RP stationary phases. HILIC is analogous to a normal phase chromatographic method where a polar stationary phase is used, and water is the strong eluent.

Analytes are separated by a mixture of partitioning between a water-enriched layer on the surface of the stationary phase and adsorption to the stationary phase.^{99-100, 107-108} An amide stationary phase allows for a water-enriched layer to form on the surface of the stationary phase, and, depending on the hydrophilicity of the analyte, molecules spend different amounts of time in this stagnant water layer. Thus, partitioning results in separation by hydrophobicity with the most hydrophilic molecules being retained on the column and the hydrophobic molecules eluting first (opposite to RPLC). Additionally, molecules can be retained on the column by adsorbing to the stationary phase. Molecules that participate in adsorption typically have physical properties that facilitate interaction with the functional groups on the stationary phase, such as molecules that have large dipole interactions, hydrogen bonding, etc.

Glycan analysis strategies often evolve and benefit from previous or current proteomic strategies. One of the most effective proteomic strategies is online separation by RPLC coupled online to ESI MS. However, the translation of this technology to the field of glycomics has been difficult for numerous reasons including the lack of retention on RP columns and the suppressed ESI response of the much more hydrophilic glycans. Derivatization of *N*-linked glycans can be used to increase the hydrophobicity enough for glycan separation by RP chromatography (**Figure 1.6**). There are several disadvantages in HILIC that have been reported in comparison to RP chromatography including peak fronting and tailing, column bleed, irreversible sorption, and slow equilibration times.¹⁰⁹ These problems can be

overcome by switching the HILIC stationary phase¹⁰⁹ or increasing the buffer concentration.¹¹⁰ Additionally, HILIC separation efficiency is generally accepted to

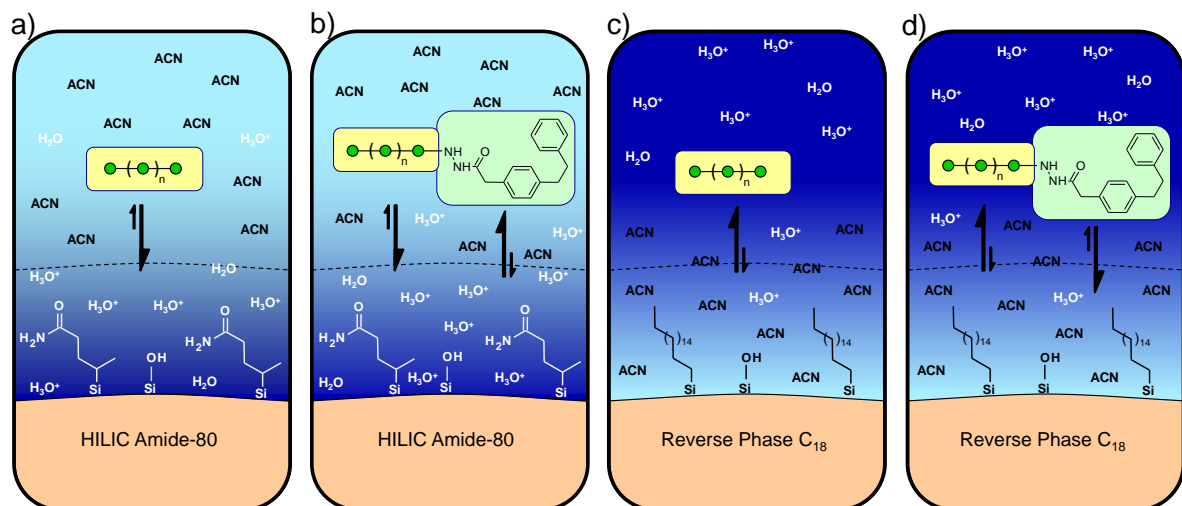


Figure 1.6 – The observed retention behavior of native and derivatized *N*-linked glycans in HILIC (a and b) and RP (c and d) chromatography. The magnitude of the arrows indicates the observed relative amount of interaction of the glycan with the stationary phase. The *N*-linked glycan shown is a general hexose structure to demonstrate the collective behavior of the maltodextrin glycans.

be inferior to RP chromatography,¹¹¹⁻¹¹² and though this depends on the analyte and the type and amount of buffer reagent, peak widths tend to be broader in HILIC than RP chromatography. This decreases the peak capacity of the separation and increases the possibility for competition of analytes in the electrospray droplet, which can significantly hinder glycan analysis. This inferiority is thought to be due to the relatively limited studies of the fundamental chemistry of HILIC in comparison to RP and the relative newness of the separation technique (Alpert coined the term HILIC

in 1990⁹⁹).¹¹² Furthermore, researchers must choose from a large collection of different HILIC stationary phases, each of which is often optimized for a specific type of analyte and/or has limited studies of separation efficiency.¹¹² Our group has generated data previously that show a range of separation efficiencies depending on the *N*-linked glycan composition in HILIC with the peak widths (FWHM) ranging from just under 1 minute to several minutes.²³ This is in contrast to the same chromatography instrument platform using RP C₁₈ stationary phase for peptide analysis, which consistently produces peak widths \leq 30 seconds.¹¹³ This disparity leads one to the hypothesis that it is possible to significantly enhance the analysis of *N*-linked glycans by separating glycans with RP chromatography rather than HILIC.

1.4 Electropray Ionization

1.4.1 Overview

In mass spectrometry, the first process that must occur before detecting the analyte of interest is to generate gas phase ions. For non-volatile analytes, such as large biomolecules, this had proven to be a challenging task. However, upon the invention of electropray ionization (ESI),¹¹⁴ it became possible to generate multiply-charged gas phase ions from analytes in solution. Today, in biological studies where the analytes are typically large (> 1 kDa), ESI is one of the two ionization sources most often employed along with Matrix Assisted Laser Desorption/Ionization (MALDI). MALDI is an enticing choice for the ionization of glycans due to the short analysis times, the high throughput of samples, and the tolerance for contamination

such as salts. However, ESI is often chosen in glycan analysis for 2 reasons: 1) MALDI imparts more internal energy into the molecules during ionization than ESI (known to cause in-source fragmentation of the glycosidic bonds primarily with sialic acid residues²³), and 2) ESI can be directly coupled to liquid chromatography for the online fractionation of glycan samples just prior to injection into the MS. The primary reason that ESI is not ubiquitous for glycan analysis is the fact that ESI creates an inherent bias for the ionization of hydrophobic molecules (*vide infra*).¹¹⁵ This is an extreme hurdle for glycan analysis due to the hydrophilic and polar nature of the sugar residues.

The invention of nano-flow ESI¹¹⁶ has significantly enhanced the analysis of glycans in MS and allows underivatized, native glycans to be analyzed with ion abundance and signal-to-noise ratios comparable to peptide analysis.¹¹⁷ In nanospray, lower flow rates generate smaller droplets with a larger surface to volume ratio,¹¹⁶ and this increases the surface activity of the more solvated, hydrophilic glycans, increasing the ionization efficiency entering the MS. Several studies have shown the increased sensitivity, ion abundance, and decreased detection limits of glycans when moving from micro- to nano-flow ESI,^{95, 117} and can be rationalized by understanding the mechanism of electrospray.

1.4.2 The Generation of Gas Phase Ions in Electrospray Ionization

ESI is a soft ionization source (limited source fragmentation) that affords the advantage of multiple charging of large biomolecules. The ESI mechanism is still in

debate, but in general, it has been accepted that the analytes are dissolved in small droplets that have a surplus of charge (H^+ in positive mode) on the surface due to the electrochemical reaction in the capillary floating at ~ 2 kV and are ejected from the electrospray emitter tip in the form of a “Taylor cone”.¹¹⁸ These droplets undergo a series of desolvation and fission processes and eventually produce individual gas-phase ions. The ion formation mechanism from electrospray droplets typically adopts one of two theories, either the charged residue model¹¹⁹⁻¹²⁰ or the ion evaporation model.¹²¹⁻¹²³ Dole et. al.¹¹⁹⁻¹²⁰ proposed the charged residue model, where the droplets undergo several “Coulombic explosions” that eventually give rise to progeny droplets containing only one analyte molecule. This droplet is further desolvated until all the solvent is evaporated leaving only a gas-phase analyte ion. The ion evaporation model, proposed by Iribarne and Thomson,¹²¹⁻¹²³ and later supported by Fenn,¹¹⁵ also describes a series of desolvation and Coulombic fission events. However, in this scenario, the fission events and desolvation result in progeny droplets with a charge density so great that the electrostatic field at the droplet surface is sufficient to eject the surface analytes from the droplet as gas-phase ions. Recently, it has been hypothesized that both mechanisms are present in ESI depending on the physical and chemical properties of the solvents and analytes.¹²⁴

In either model, the hydrophobic bias detrimental to glycan analysis is introduced at two different stages during the ESI process (**Figure 1.7**). First, as the droplets are being desolvated, they reach the Rayleigh limit, and when this occurs,

several droplets (estimated at $20^{125-126}$) are ejected from the surface of the droplet.¹²⁷ When these smaller progeny droplets are ejected, they are composed of

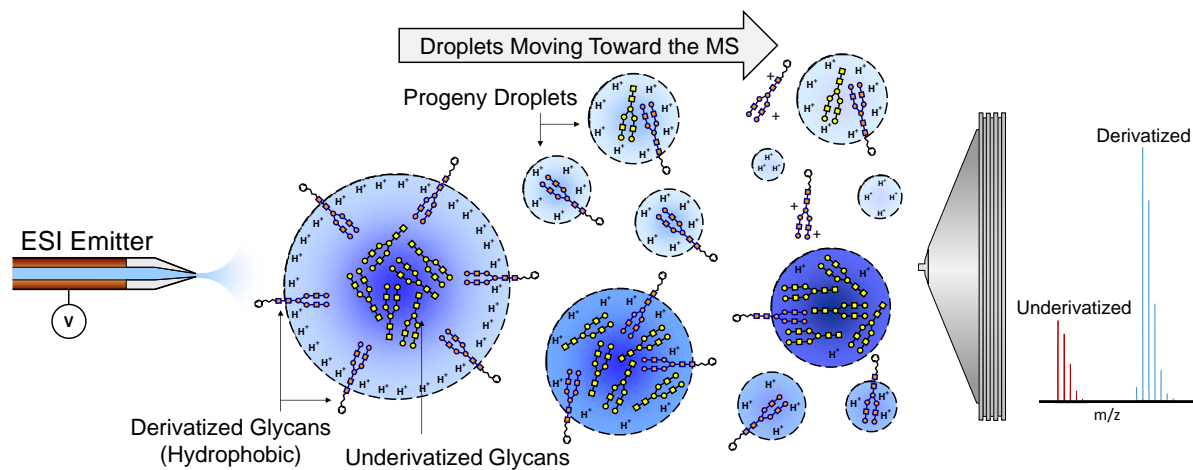


Figure 1.7 – A depiction of the hydrophobic bias in ESI. As the droplets are moving toward the MS, they are being desolvated, and the charge to surface area ratio is increasing, creating coulombic repulsion. Progeny droplets are ejected from the surface, and the hydrophobic molecules are enriched in these droplets. It is from these droplets that gas phase ions are formed, creating the hydrophobic bias.

solvent, analyte, and an abundance of charge from the surface of the parent droplet. Because the more hydrophobic molecules will have a higher surface activity in the parent droplet than the hydrophilic analytes,¹²⁸ the hydrophobic molecules are significantly enriched in the progeny droplets, and it is these droplets which go on to form gas-phase ions. Moreover, the hydrophilic molecules remain in the larger parent droplet that has a decreased charge to volume ratio, further decreasing the chance for the hydrophilic molecules to be ionized.¹¹⁷

The second stage of hydrophobic bias occurs in the progeny droplets. In order to form gas-phase ions, the analytes must overcome the surface tension of the droplet. Hydrophilic molecules interact more favorably with the solvent in these progeny droplets, resulting in a higher free energy of solvation in comparison to more hydrophobic molecules.^{115, 129} Due to this interaction with the solvent, hydrophobic analytes require less energy to be ejected as gas phase ions. This two-stage hydrophobic bias in ESI has made the MS and MS/MS analysis of glycans much more difficult than that of proteins and peptides but can be exploited to enhance ESI efficiency.

1.4.3 Exploiting the Hydrophobic Bias for Increased ESI Efficiency

The hydrophobic bias in ESI has been exploited for large biomolecules in order to increase ionization efficiency, thereby decreasing detection limits. The hydrophobic bias was first utilized when researchers observed that one strand of PCR product had a biased ion abundance over the complimentary strand in ESI MS.¹²⁹ The researchers were then able to take advantage of this bias when the ionization efficiency of a nucleic acid 20-mer was selectively enhanced by adding an alkyl chain to the 5' terminus. The hydrophobic bias was then used to enhance the signals of peptides and proteins.¹³⁰⁻¹³⁸ In these studies, hydrophobic small molecules were used to derivatize peptide and protein functional groups such as primary amines,¹³⁷ the guanidine group on arginine,¹³⁸ and the thiol group on cysteine.¹³⁰⁻¹³⁶ The most beneficial of these studies reports a >2000-fold

enhancement in the ion abundance of a peptide when derivatized with a hydrophobic molecule.¹³⁵

Due to the hydrophilic nature of glycans in comparison to peptides and proteins, it is hypothesized that derivatization of glycans with hydrophobic moieties has the potential to significantly enhance glycan analysis by ESI MS. There have been several reports of increasing glycan ion abundance in ESI MS via derivatization,^{35-36, 45-46, 50, 55-56} but few of these studies have actively sought to develop reagents with extensive hydrophobic properties in order to significantly increase ESI efficiency. A recent study has modified Girard's T reagent (which has been shown to increase glycan ion abundance⁴⁵) to accomplish this task, and it was shown that glycan ion abundance can be increased more than 4-fold in comparison to the native glycan.⁴⁶

1.5 Fourier Transform Mass Spectrometry

1.5.1 Overview

N-linked glycan analysis by mass spectrometry is often significantly less complex than typical proteomic experiments, which can contain tens of thousands of analytes. Though glycans are significantly more complex structurally and biosynthetically than proteins due to their non-linear nature, branching, and isomeric possibilities,¹³⁹ nature significantly limits the number of compositions of *N*-linked glycans actually observed.^{96, 140} Though each composition can be made up of numerous isobaric isoforms, these are indistinguishable in a mass spectrometer,

and a high resolving power mass spectrometer is capable of uniquely measuring nearly all possible *N*-linked glycan compositions.^{43, 96, 140}

In order to profile all *N*-linked glycans by LC-MS, without pre-fractionation, it is necessary to use a MS that is capable of sensitive and high mass measurement accuracy (MMA) analysis. An example of this is presented in **Figure 1.8**, where it is shown that by measuring only the exact mass of analytes, the mass excess (exact mass minus the nominal mass) is capable distinguishing between classes of

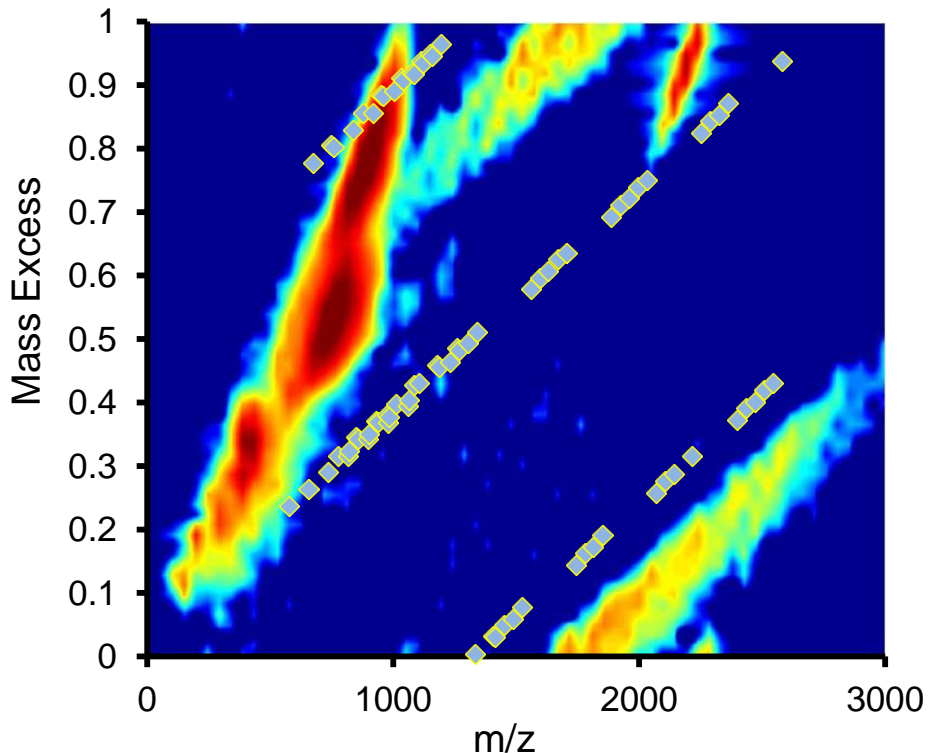


Figure 1.8 – A density plot of the mass excess vs. the *m/z* for a lipid database. The *N*-linked plasma glycan mass excess values are overlaid and are shown to fall in ‘forbidden’ zones in the lipid density plot.

biomolecules. The density plot in **Figure 1.8** consists of the mass excess vs. the m/z of a lipid database. The mass excess of *N*-linked glycans found in human plasma is overlaid. It is seen that the glycans generally fall into 'forbidden' zones (dark blue regions) in the lipid density plot. This information adds confidence to the measurement and identification of *N*-linked glycans.

An additional strategy that researchers often use to add confidence to the measurement of a glycan, is the use of tandem MS that allows for both precursor mass analysis and also selection and fragmentation of a specific m/z value. These experiments are often performed using hybrid mass spectrometers, where ion trapping and detection can occur simultaneously (*vide infra*). Fourier Transform mass spectrometers (FTMS) satisfy each of these requirements, and recent developments in ion optics and mass analyzer technology have significantly improved the speed and quality at which these measurements can be made.

1.5.2 Fourier Transform Ion Cyclotron Resonance Mass Spectrometry

Fourier Transform ion cyclotron resonance (FTICR) mass spectrometers are the first generation of FTMS instruments and provide high mass MMA (<5 ppm) and high resolving power ($RP_{m/z=400} = 100,000$) measurements.¹⁴¹ Resolving power is the ability of the mass spectrometer to separate ions with similar m/z , and in FTMS instruments is proportional to the amount of time that the analytes are measured. MMA is the measure of how accurately a mass spectrometer can measure mass.

This is described in **Equation 1.1**, where M_{exp} is the experimental mass and M_{theo} is the theoretical mass.

$$\text{MMA (ppm)} = \frac{M_{\text{exp}} - M_{\text{theo}}}{M_{\text{theo}}} \times 10^6 \quad \text{Equation 1.1}$$

FTICR instruments are able to acquire very accurate mass analysis data by taking advantage of the m/z dependence of gas phase ions in a magnetic field. The FTICR mass analyzer (ICR cell) is located within the bore of a superconducting magnet with a homogeneous magnetic field, and once ions are introduced into the FTICR cell, they assume a natural cyclotron motion due to the Lorentz force.¹⁴²⁻¹⁴⁵ An RF voltage is applied to the two excitation plates and the ions are excited in order to increase the radius of cyclotron motion (**Figure 1.9**).¹⁴⁴⁻¹⁴⁵ This will cause phase coherence of ions with the same m/z , and as the ion packet passes by the detection plates, a current is induced, which is then measured over a given time period, producing a sinusoidal time domain. The time domain is a combination of signals of different ion packets that must be de-convoluted using a fast Fourier Transform.¹⁴⁶ A fast Fourier Transform converts the time domain of each packet of ions into a frequency spectrum which can subsequently be converted into a mass spectrum using **Equation 1.2**. The frequency (ω_0) is directly proportional to the inverse of the m/z and the magnetic field (B_0). In an FTICR, the resolving power is proportional to the magnetic field strength (B_0) and the time of acquisition (**Equation 1.3**).

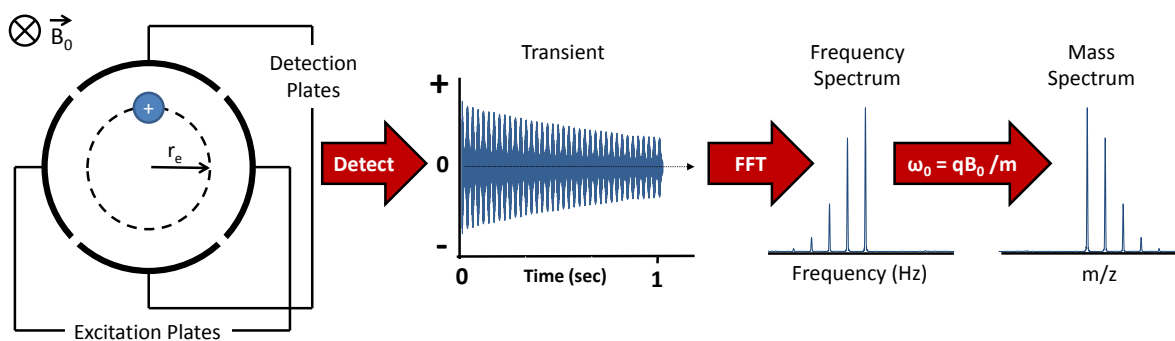


Figure 1.9 – A schematic of the detection of ions in *FTICR MS*. Upon excitation of the ions in the ICR cell, the ion cyclotron motion is detected in the form of a sinusoidal time domain. This time domain is Fast Fourier transformed into a frequency spectrum, which is then converted to a mass spectrum.

$$\omega_0 = \frac{qB_0}{m} \quad \text{Equation 1.2}$$

$$\text{Resolving Power} = \frac{m}{\Delta m} = \frac{1.274 \times 10^7 B_0 T_{\text{acq}} / n}{m/z} \quad \text{Equation 1.3}$$

1.5.3 Orbitrap Mass Spectrometry

The next generation of FTMS instruments is based on electrostatic fields rather than magnetic; the Orbitrap mass spectrometer is similar to FTICR instruments in that ions are trapped in the analysis cell, and sinusoidal frequencies are measured in order to achieve high resolving power and high MMA. However, the main difference is that an electric field is used to stabilize the ions in the Orbitrap rather than a magnetic field as in FTICR. The ability to trap ions using only an electric field was first demonstrated in 1923 when Kingdon¹⁴⁷ showed that ions can be trapped using a metal can with a charged wire spanning the axis of the can. In

this experiment, ions were generated by electric discharge and attracted toward the charged wire and neutralized. However, those ions that have enough tangential velocity were able to avoid impact, and these ions orbit the wire for an extended period of time. Electrostatic trapping has become increasingly more effective,¹⁴⁸ but it was not until advances in charged particle optics that the electrostatic fields were improved enough to use this trapping strategy for mass analysis.¹⁴⁹⁻¹⁵⁰

Though mass analysis was reported using electrostatic trapping, it was necessary to further improve the electric field homogeneity, ion injection strategy, and ion detection in order to generate a robust mass analyzer. In 2000, Makarov developed the Orbitrap mass analyzer which made use of highly precise engineering and machining, and this technology is the basis of what is currently the most advanced mass analysis instrumentation. The Orbitrap is made of two outer electrode 'cups' facing each other and separated by a dielectric ring. A central electrode runs along the axis of the electrodes, which is analogous to the charged wire in the Kingdon experiments. When ions are introduced into the Orbitrap, they move in a trajectory which combines three different cyclic motions in all three dimensions: 1) rotational motion around the central electrode, 2) radial motion, and 3) axial oscillation along the axis of the central electrode due to opposing electric fields on each of the electrodes. Of these three motions, only axial motion is independent of initial velocities and proportional to the m/z of the ion. Thus, this is the sinusoidal motion that is measured, fast Fourier Transformed into a frequency

signal, and converted to an m/z value based on **Equation 1.4**, where ω is the axial frequency, e is the elementary charge, and k is the field curvature (constant).

$$\omega = \sqrt{\frac{e \cdot k}{(m/z)}}$$

Equation 1.4

Ions must be introduced into the Orbitrap in a coherent packet in order to achieve high resolving power due to the lack of phase coherence in an electric field. This is accomplished by using an external ion storage device called a C-trap.¹⁵¹ This is a significant advancement in the development of the Orbitrap because it allowed for coupling with a continuous ionization strategy, such as ESI. Additionally, the C-trap allows for coupling Orbitrap mass analyzers with other mass analyzers in order to generate hybrid instruments, which significantly increase the analysis capabilities of Orbitrap mass spectrometers. The first commercial Orbitrap was introduced in 2005 and coupled with a linear ion trap mass analyzer to generate the LTQ-Orbitrap.¹⁵²⁻¹⁵⁴ Since 2005, several improvements on Orbitrap technology have been introduced such as a high-field compact Orbitrap¹⁵⁵ and a benchtop Exactive mass spectrometer.¹⁵⁶⁻¹⁵⁸ Additionally, several iterations of hybrid Orbitrap mass spectrometers were commercialized, such as the LTQ-Orbitrap Velos,¹⁵⁹⁻¹⁶⁰ which incorporates a higher energy collision cell, and the LTQ-Orbitrap Elite,¹⁵⁵ which incorporates the high-field Orbitrap.

1.5.4 Hybrid Fourier Transform Mass Spectrometry

Hybrid mass spectrometers are a combination of two or more mass analyzers, and each mass analyzer can be used as a mass filter, a detector, or both.¹⁶¹ The first Fourier Transform hybrid mass spectrometer was a linear ion trap coupled to a FTICR mass spectrometer (LTQ-FTICR).¹⁶² The main advantage of hybrid instruments is that the LTQ-FTICR is capable of simultaneous trapping and detection and/or simultaneous detection in both the LTQ and FTICR, allowing for the acquisition of both a high mass accuracy scan and a MS/MS scan to occur in parallel. With these capabilities, it is possible to collect high mass accuracy and MS/MS data for 10 analytes on a ~3 sec timescale (**Figure 1.10a**). Thus, for a complex mixture, this is less than the timescale of peak widths in LC, allowing for mass analysis of numerous analytes. Because of this, data dependent acquisition (DDA) has been developed.¹⁶³ In complex mixtures, DDA allows for intensity-based selection of eluting analytes to be subsequently fragmented. In the LTQ-FTICR, a full scan mass spectrum in the FTICR is used to determine the most abundant masses (usually a fixed number such as 10 – top 10 experiment). These masses are then individually isolated in the LTQ, fragmented, and the product ion spectra are collected. This top 10 cycle happens in ~3 sec. When this is completed, the former 10 most abundant m/z ions are put on an exclude list, and the next 10 most abundant ions are chosen for isolation and fragmentation. This process continually repeats throughout a LC gradient, allowing for mass analysis data on thousands of analytes per injection.

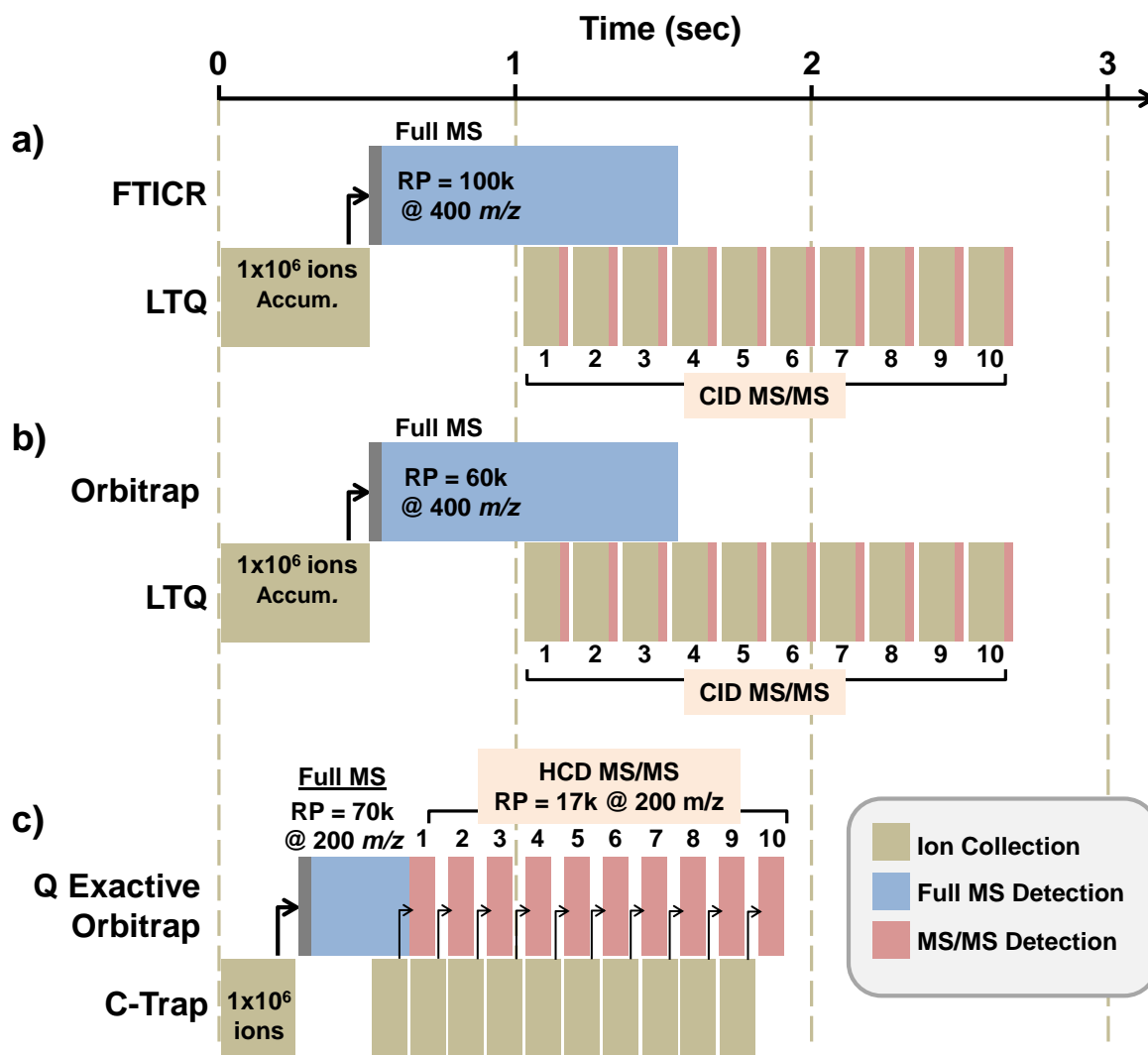


Figure 1.10 – A comparison of the theoretical duty cycles for hybrid FTMS instruments. The LTQ-FTICR (a) and LTQ-Orbitrap (b) instruments function similarly. However, the recently developed Q Exactive (c) is capable of detecting both full MS and product ion MS/MS in the Orbitrap with high resolving power and MMA. Additionally, the entire process occurs more rapidly due to simultaneous ion collection in the C-trap.

When the Orbitrap was invented, it was immediately coupled with a LTQ in a near identical setup to the LTQ-FTICR.¹⁵³⁻¹⁵⁴ The Orbitrap is thought to be a more sensitive instrument due to the more efficient ion transfer into the Orbitrap in comparison to FTICR. Additionally, FTICR instruments are extremely costly to maintain in comparison to an Orbitrap. Because a superconducting magnet is used in FTICR, it must be continuously cooled by liquid Helium and liquid nitrogen. With the rising cost of cryogenics, it can cost a baseline of tens of thousands of dollars per year to maintain a single FTICR instrument. Thus, the hybrid LTQ-Orbitrap allows for a significant and practical advantage over LTQ-FTICR instruments with comparable (or better) data acquisition (**Figure 1.10b**).

A recent iteration in Fourier Transform hybrid instruments is the benchtop Q Exactive MS.¹⁵⁶ This instrument consists of a quadrupole mass analyzer coupled to an Orbitrap. This instrument is unique in several ways in comparison to the LTQ-Orbitrap instruments. First, the Q Exactive has been engineered such that it has a much smaller footprint than the LTQ-Orbitrap and is now a benchtop mass spectrometer. Additionally, the Orbitrap has been manufactured so that the data can be processed using an enhanced Fourier Transform (eFT). The eFT function allows for mass analysis in nearly half the time for the same resolving power, increasing the speed at which DDA can occur. Additionally, the Q Exactive is equipped with a higher energy collision (HCD) cell, allowing for parallel fragmentation outside of the Orbitrap and further increasing the efficiency of the Q Exactive.

There is a significant difference between having a quadrupole mass filter and a linear ion trap coupled to an Orbitrap. The major disadvantage of having a quadrupole mass filter is that it is not capable of trapping or detecting analytes. Though this is the case, a significant advantage of the Q Exactive is that all ions are detected in the Orbitrap, which affords high resolving power and mass accuracy to both precursor and product ion spectra. Though it takes more time to acquire spectra in an Orbitrap in comparison to a linear ion trap, the eFT algorithm and ability to trap ions in the C-trap in parallel with detection allows for a precursor scan and up to 12 product ion scans to be collected in under 3 sec, which is faster than previous LTQ-Orbitrap generations, while collecting higher mass accuracy data for all scans.

The development of the Orbitrap has generated a debate about which type of instrument, magnetic (FTICR) or electric (Orbitrap), is the future of FTMS technology. The major benefit of FTICR mass spectrometry is that higher resolving power can be achieved by increasing the magnetic field strength, and the Orbitrap (until the invention of the high-field orbitrap) does not have this capability. **Figure 1.11a** shows a theoretical plot of FTICR resolving power vs. m/z for a 1 s acquisition time using several different magnetic fields. Thus, if the mass analysis of a biological system (such as intact proteins) requires higher resolving power, a FTICR MS is capable (in theory) of being produced that can measure this. However, the currently manufactured Orbitrap instrument resolving powers vs. m/z are plotted in **Figure 1.11b** over top of the dashed FTICR plot in **Figure 1.11a**, where it is seen

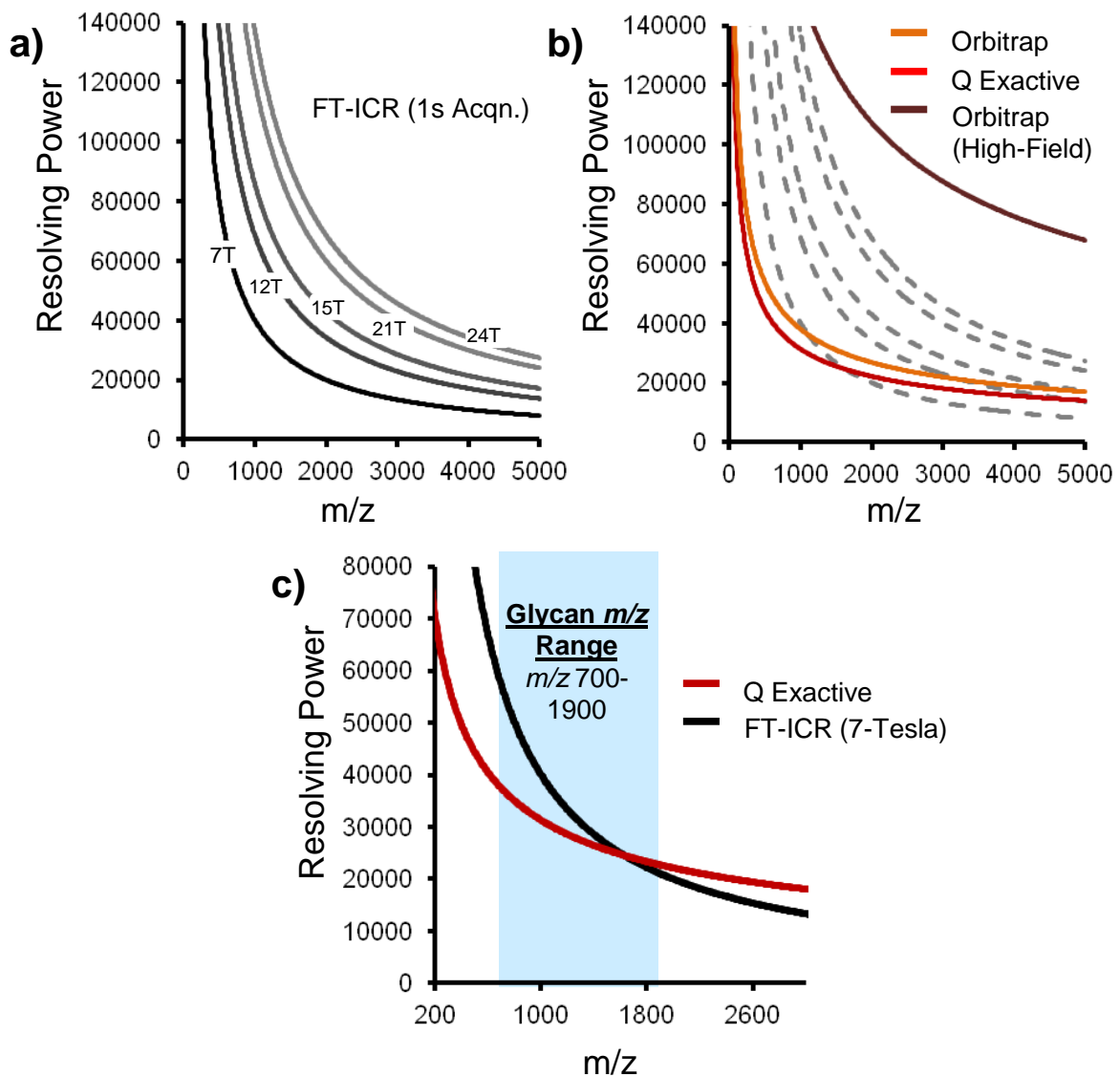


Figure 1.11 – a) The correlation between resolving power and m/z for FTICR instruments with varying magnetic fields at a 1 s acquisition time. **b)** The resolving power vs. m/z for Orbitrap FTMS instruments overlaying the previous FTICR data. The Orbitrap and high-field Orbitrap acquire data for ~ 0.75 s, and the Q Exactive acquires data for ~ 0.33 s. **c)** The comparison of a commercially available 7 T FTICR and the Q Exactive. The m/z range which glycans are routinely measured is shaded in blue. Thus at these m/z values, the shortened acquisition time for the Q Exactive is more beneficial than the marginally better resolving powers in the FTICR instrument.

that the high-field Orbitrap is capable of measuring all m/z values at a higher resolving power than even the FTICR instruments with the largest magnetic fields.

Figure 1.11a-b display the leading edge of FTMS advancements in technology. However, a comparison of the resolving power vs. m/z plot for a practical and commercially available 7 Tesla FTICR and the Q Exactive is shown in **Figure 1.11c**. It can be seen that the Q Exactive is comparable to the resolving power achieved in FTICR. Additionally, for the measurement of *N*-linked glycans (m/z range shaded in blue), the FTICR and Q Exactive are able to generate data with comparable resolving powers, all of which are sufficient to separate all *N*-linked glycan compositions. Thus, when performing mass analysis of *N*-linked glycans, it is more practical to use a Q Exactive MS due to the shortened acquisition time in the precursor scan and more efficient duty cycle (**Figure 1.10c**).

1.6 Synopsis of Completed Research

The analysis of *N*-linked glycans is often hindered by the lack of high-throughput analysis strategies translational across laboratories, the hydrophilicity of the glycans, and the lack of quantification strategies available. This dissertation describes a novel technology that addresses each of these shortcomings via glycan derivatization with hydrophobic, SIL reagents. **Chapter 2** describes in detail the hydrazone formation derivatization technique, which is able to efficiently couple hydrazide reagents (derivatives of Girard's P reagent) to the reducing terminus of *N*-linked glycans, or any glycan with a free aldehyde group at the reducing terminus.

Numerous conditions for hydrazone formation have been reported in the literature,^{45, 47, 51-53, 164-165} and these conditions were used as the starting factors in a design of experiments (DOE) fractional factorial design (FFD)¹⁶⁶ for the optimization of the hydrazone formation reaction. Upon optimization, it was shown that >95% reaction efficiency can be achieved for both simple sugars and complex *N*-linked glycan standards. Additionally, in order to direct the synthesis of hydrophobic reagents, the effect of derivatization with a permanently charged tag was studied. By synthesizing a reagent pair that is structurally and molecularly identical to one another except for the substitution of a pyridinium ion for a phenyl group, it was shown that the neutral tagging reagents significantly out-perform their charged counterparts. This study was used as the foundation for future *N*-linked glycan derivatization and quantification strategies due to the high efficiency of reaction, and it allowed one to make hypothesis-driven predictions for the synthesis of reagents for the increased ESI efficiency.

Because it was shown in **Chapter 2** that the neutral reagents significantly out-perform their charged counterparts, a library of solely neutral reagents has been synthesized in order to systematically exploit the hydrophobic bias for *N*-linked glycans in ESI and is described in **Chapter 3**. By synthesizing hydrazide reagents with increasing hydrophobicity, it is shown that the ESI efficiency of derivatized glycans is proportional to the hydrophobicity of the tagging reagent. Non-polar surface area (NPSA) calculations were used to estimate the hydrophobicity of the tag, and this correlation will be used in future studies to generate even more

effective glycan hydrazide reagents. Additionally, the optimal hydrazide reagent from the library was used to derivatize *N*-linked glycan cleaved from pooled human plasma. Derivatization efficiency of the plasma *N*-linked glycome was >95%, and the total glycan signal from all derivatized glycans was significantly greater than for native glycans, demonstrating the successful exploitation of the hydrophobic bias in ESI even in the most complex of mixtures.

Though the data in **Chapter 3** leads one to infer that more hydrophobic reagents could be even more effective, reagent development was put on hold so that SIL reagents could be synthesized. In **Chapter 4**, the most effective reagent from **Chapter 3**, P2GPN, was synthesized in both the native form and with $^{13}\text{C}_6$ stable isotopes in the terminal phenyl ring. This allowed one to differentially label two glycan samples, mix the samples together, and analyze in the same LC-MS run. Because the only differences between the tagged glycans are the stable-isotope labels, both the light- and heavy-tagged glycans behave identically in the chromatographic separation and ESI process. However, the light- and heavy-tagged glycans are separated using mass spectrometry, and each glycan can then be relatively quantified based on the relative ion abundances. The effectiveness of this strategy in both simple glycan mixtures and pooled human plasma are presented, and an internal standard is incorporated to correct for systematic variability due to parallel sample preparation.

Because this relative quantification experiment incorporates not only stable isotopes, but also hydrophobicity, **Chapter 5** presents the separation of

hydrophobic-tagged glycans by RPLC. This is both a practical and experimental advantage over traditional glycomics separation strategies such as HILIC and graphitized carbon. Experimentally, it is shown that glycans are separated with a much higher efficiency in RPLC in comparison to HILIC. This leads to an increase of ~40% in the number of unique glycan compositions which are able to be detected. Additionally, the RPLC platform for the separation of glycans is identical to that of typical bottom-up proteomic experiments. This is a significant advantage in research groups who study both proteomics and glycomics due to the minimal time to switch between sample sets (it can often take 1-2 days to re-equilibrate a RP nano-LC system to or from HILIC).

The fundamental strategy for the derivatization, separation, and quantitative MS analysis of *N*-linked glycans has been optimized such that glycans from even the most complex of samples, plasma, can be relatively quantified. However, before this strategy can be applied to large biological samples, the analytical variability of the strategy had to be minimized, and a reproducible data analysis strategy had to be developed. **Chapter 6** describes the incorporation of a glycoprotein internal standard, horseradish peroxidase (HRP), in order to account for systematic global sample preparation variability. A glycoprotein internal standard is advantageous in comparison to a free glycan because any variability in the PNGase F cleavage reaction cannot be taken into account using a free oligosaccharide. However, using an oligosaccharide that must be cleaved from a glycoprotein as an internal standard allows for variability in every step of sample preparation to be accounted for. HRP

was used due to the commercial availability and the presence of xylosylated glycans, which are not found in mammalian biosynthetic pathways, preventing glycans from HRP skewing plasma glycan quantification. Additionally, it was shown that when using the HRP glycan as an internal standard, all systematic bias due to parallel sample preparation variability is eliminated.

Glycomics data analysis strategies are severely lagging behind proteomics, and often, bioinformatic strategies are incompatible across different laboratories. Thus, **Chapter 7** details the reproducible analysis strategy for relative quantification of *N*-linked glycans using the SIL reagents, recently-coined as the INLIGHT (Individuality Normalization when Labeling with Isotopic Glycan Hydrazide Tags) strategy. Because the SIL reagents only have a mass shift of 6 Da, large molecular weight glycans often have isotopic distribution overlap. This overlap is corrected for by calculating a molecular weight factor based on theoretical isotopic distribution. Also, a total glycan normalization procedure is presented such that systematic variability in the biological system (such as different total glycosylation levels between samples) can be accounted for. Finally, to show the power of the quantification strategy, certain pooled plasma samples were spiked with a specific glycoprotein. These samples were compared to each other and to neat pooled plasma. The glycans that have been reported to be attached to the spiked glycoprotein were determined to be significantly different than the neat pooled plasma samples, demonstrating the ability for this strategy to relatively quantify the amounts of glycans across samples.

The **Appendices** contain supplemental material, where numerous details, syntheses, calculations, analysis processes, and data tables are presented. **Appendices A-D** contain supporting information for **Chapters 3, 4, 5, and 7**, respectively. **Appendix E** contains a detailed data sheet and procedure for the sample preparation (cleavage, purification, derivatization, and relative quantification) of *N*-linked glycans from plasma samples. Finally, **Appendix F** presents the current and future applications of the INLIGHT relative quantification strategy for *N*-linked glycans. Preliminary data is presented on the largest-scale glycan relative quantification studies to date, where the INLIGHT strategy is applied biomarker discovery efforts in ovarian cancer in collaboration with the Mayo Clinic (Rochester, MN).

1.6 References

- (1) Apweiler, R.; Hermjakob, H.; Sharon, N. On the frequency of protein glycosylation, as deduced from analysis of the SWISS-PROT database. *BBA-Gen. Subjects*, **1999**, *1473*, 4-8.
- (2) Begley, T. P., *Wiley Encyclopedia of Chemical Biology* **2009**, *2*, 785.
- (3) Varki, A.; Marth, J. Oligosaccharides in vertebrate development. *Seminars Dev. Biol.*, **1995**, *6*, 127-138.
- (4) Varki, A.; Cummings, R. D.; Esko, J. D.; Freeze, H. H.; Stanley, P.; Bertozzi, C. R.; Hart, G. W.; Etzler, M. E., *Essentials of Glycobiology, 2nd edition* **2009**.
- (5) Taylor, M. E.; Drickamer, K., *Introduction to Glycobiology*, 2nd ed.; Oxford University Press Inc.: New York, 2006.
- (6) Tarentino, A. L.; Trimble, R. B.; Plummer, T. H. Enzymatic Approaches for Studying the Structure, Synthesis, and Processing of Glycoproteins. *Meth. Cell Biology*, **1989**, *32*, 111-139.
- (7) Wu, H. C.; Meezan, E.; Black, P. H.; Robbins, P. W. Comparative Studies on Carbohydrate-Containing Membrane Components of Normal and Virus-Transformed Mouse Fibroblasts .I. Glucosamine-Labeling Patterns in 3t3 Spontaneously Transformed 3t3 and Sv-40-Transformed 3t3 Cells. *Biochem.*, **1969**, *8*, 2509-&.
- (8) Rostenberg, I.; Guizarvazquez, J.; Penaloza, R. Altered Carbohydrate Content of Alpha-1-Antitrypsin in Patients with Cancer. *J. Natl. Cancer Inst.*, **1978**, *61*, 961-965.
- (9) Packer, N. H.; von der Lieth, C. W.; Aoki-Kinoshita, K. F.; Lebrilla, C. B.; Paulson, J. C.; Raman, R.; Rudd, P.; Sasisekharan, R.; Taniguchi, N.; York, W. S. Frontiers in glycomics: Bioinformatics and biomarkers in disease - An NIH White Paper prepared from discussions by the focus groups at a workshop on the NIH campus, Bethesda MD (September 11-13, 2006). *Proteomics*, **2008**, *8*, 8-20.
- (10) Casey, R. C.; Oegema, T. R.; Skubitz, K. M.; Pambuccian, S. E.; Grindle, S. M.; Skubitz, A. P. N. Cell membrane glycosylation mediates the adhesion, migration, and invasion of ovarian carcinoma cells. *Clin. Exp. Metastasis*, **2003**, *20*, 143-152.

- (11) Zhao, Y. Y.;Takahashi, M.;Gu, J. G.;Miyoshi, E.;Matsumoto, A.;Kitazume, S.;Taniguchi, N. Functional roles of N-glycans in cell signaling and cell adhesion in cancer. *Cancer Science*, **2008**, *99*, 1304-1310.
- (12) Gorelik, E.;Galili, U.;Raz, A. On the role of cell surface carbohydrates and their binding proteins (lectins) in tumor metastasis. *Cancer and Metastasis Reviews*, **2001**, *20*, 245-277.
- (13) Hakomori, S. Aberrant Glycosylation in Cancer Cell-Membranes as Focused on Glycolipids - Overview and Perspectives. *Cancer Res.*, **1985**, *45*, 2405-2414.
- (14) Hammoud, Z. T.;Mechref, Y.;Hussein, A.;Bekesova, S.;Zhang, M.;Kesler, K. A.;Novotny, M. V. Comparative glycomic profiling in esophageal adenocarcinoma. *J. Theorac. Cardiovasc. Surg.*, **2010**, *139*, 1216-1223.
- (15) Fuster, M. M.;Esko, J. D. The sweet and sour of cancer: Glycans as novel therapeutic targets. *Nat. Rev. Cancer*, **2005**, *5*, 526-542.
- (16) Abd Hamid, U. M.;Royle, L.;Saldoval, R.;Radcliffe, C. M.;Harvey, D. J.;Storr, S. J.;Pardo, M.;Antrobus, R.;Chapman, C. J.;Zitzmann, N.;Robertson, J. F.;Dwek, R. A.;Rudd, P. M. A strategy to reveal potential glycan markers from serum glycoproteins associated with breast cancer progression. *Glycobiology*, **2008**, *18*, 1105-1118.
- (17) Kirmiz, C.;Li, B. S.;An, H. J.;Clowers, B. H.;Chew, H. K.;Lam, K. S.;Ferrige, A.;Alecio, R.;Borowsky, A. D.;Sulaimon, S.;Lebrilla, C. B.;Miyamoto, S. A serum glycomics approach to breast cancer biomarkers. *Mol. Cell Proteomics*, **2007**, *6*, 43-55.
- (18) Kyselova, Z.;Mechref, Y.;Kang, P.;Goetz, J. A.;Dobrolecki, L. E.;Sledge, G. W.;Schnaper, L.;Hickey, R. J.;Malkas, L. H.;Novotny, M. V. Breast cancer diagnosis and prognosis through quantitative measurements of serum glycan profiles. *Clin. Chem.*, **2008**, *54*, 1166-1175.
- (19) de Leoz, M. L. A.;Young, L. J. T.;An, H. J.;Kronewitter, S. R.;Kim, J. H.;Miyamoto, S.;Borowsky, A. D.;Chew, H. K.;Lebrilla, C. B. High-Mannose Glycans are Elevated during Breast Cancer Progression. *Mol. Cell Proteomics*, **2011**, *10*, 1-9.
- (20) Kyselova, Z.;Mechref, Y.;Al Bataineh, M. M.;Dobrolecki, L. E.;Hickey, R. J.;Vinson, J.;Sweeney, C. J.;Novotny, M. V. Alterations in the serum glycome due to metastatic prostate cancer. *J. Proteome Res.*, **2007**, *6*, 1822-1832.

- (21) Isailovic, D.;Kurulugama, R. T.;Plasencia, M. D.;Stokes, S. T.;Kyselova, Z.;Goldman, R.;Mechref, Y.;Novotny, M. V.;Clemmer, D. E. Profiling of human serum glycans associated with liver cancer and cirrhosis by IMS-MS. *J. Proteome Res.*, **2008**, *7*, 1109-1117.
- (22) An, H. J.;Miyamoto, S.;Lancaster, K. S.;Kirmiz, C.;Li, B. S.;Lam, K. S.;Leiserowitz, G. S.;Lebrilla, C. B. Profiling of glycans in serum for the discovery of potential biomarkers for ovarian cancer. *J. Proteome Res.*, **2006**, *5*, 1626-1635.
- (23) Bereman, M. S.;Williams, T. I.;Muddiman, D. C. Development of a nanoLC LTQ Orbitrap Mass Spectrometric Method for Profiling Glycans Derived from Plasma from Healthy, Benign Tumor Control, and Epithelial Ovarian Cancer Patients. *Anal. Chem.*, **2009**, *81*, 1130-1136.
- (24) Gehrke, C. W.;Waalkes, T. P.;Borek, E.;Swartz, W. F.;Cole, T. F.;Kuo, K. C.;Abeloff, M.;Ettinger, D. S.;Rosenshein, N.;Young, R. C. Quantitative Gas-Liquid-Chromatography of Neutral Sugars in Human-Serum Glycoproteins - Fucose, Mannose, and Galactose as Predictors in Ovarian and Small Cell Lung-Carcinoma. *J. Chromatogr.*, **1979**, *162*, 507-528.
- (25) Saldova, R.;Royle, L.;Radcliffe, C. M.;Hamid, U. M. A.;Evans, R.;Arnold, J. N.;Banks, R. E.;Hutson, R.;Harvey, D. J.;Antrobus, R.;Petrescu, S. M.;Dwek, R. A.;Rudd, P. M. Ovarian cancer is associated with changes in glycosylation in both acute-phase proteins and IgG. *Glycobiology*, **2007**, *17*, 1344-1356.
- (26) Williams, T. I.;Toups, K. L.;Saggese, D. A.;Kalli, K. R.;Cliby, W. A.;Muddiman, D. C. Epithelial ovarian cancer: Disease etiology, treatment, detection, and investigational gene, metabolite, and protein biomarkers. *J. Proteome Res.*, **2007**, *6*, 2936-2962.
- (27) Zhao, Y. Y.;Takahashi, M.;Gu, J. G.;Miyoshi, E.;Matsumoto, A.;Kitazume, S.;Taniguchi, N. Functional roles of N-glycans in cell signaling and cell adhesion in cancer. *Cancer Sci.*, **2008**, *99*, 1304-1310.
- (28) Zaia, J. Mass Spectrometry and Glycomics. *OMICS*, **2010**, *14*, 401-418.
- (29) Novotny, M. V.;Alley, W. R.;Mann, B. F. Analytical glycobiology at high sensitivity: current approaches and directions. *Glycoconjugate J.*, **2013**, *30*, 89-117.
- (30) Zhang, Y.;Yin, H. R.;Lu, H. J. Recent progress in quantitative glycoproteomics. *Glycoconjugate J.*, **2012**, *29*, 249-258.

- (31) Lazar, I. M.;Lee, W.;Lazar, A. C. Glycoproteomics on the rise: Established methods, advanced techniques, sophisticated biological applications. *Electrophoresis*, **2013**, *34*, 113-125.
- (32) Lamari, F. N.;Kuhn, R.;Karamanos, N. K. Derivatization of carbohydrates for chromatographic, electrophoretic and mass spectrometric structure analysis. *J. Chromatogr., B*, **2003**, *793*, 15-36.
- (33) Ruhaak, L. R.;Zauner, G.;Huhn, C.;Bruggink, C.;Deelder, A. M.;Wuhrer, M. Glycan labeling strategies and their use in identification and quantification. *Anal. Bioanal. Chem.*, **2010**, *397*, 3457-3481.
- (34) Bowman, M. J.;Zaia, J. Comparative Glycomics Using a Tetraplex Stable-Isotope Coded Tag. *Anal. Chem.*, **2010**, *82*, 3023-3031.
- (35) Bowman, M. J.;Zaia, J. Tags for the stable isotopic labeling of carbohydrates and quantitative analysis by mass spectrometry. *Anal. Chem.*, **2007**, *79*, 5777-5784.
- (36) Poulter, L.;Burlingame, A. L. Desorption Mass-Spectrometry of Oligosaccharides Coupled with Hydrophobic Chromophores. *Methods Enzymol.*, **1990**, *193*, 661-688.
- (37) Harvey, D. J. Electrospray mass spectrometry and fragmentation of *N*-linked carbohydrates derivatized at the reducing terminus. *J. Am. Soc. Mass Spectrom.*, **2000**, *11*, 900-915.
- (38) Xia, B. Y.;Feasley, C. L.;Sachdev, G. P.;Smith, D. F.;Cummings, R. D. Glycan reductive isotope labeling for quantitative glycomics. *Anal. Biochem.*, **2009**, *387*, 162-170.
- (39) Saba, J. A.;Shen, X. D.;Jamieson, J. C.;Perreault, H. Investigation of different combinations of derivatization, separation methods and electrospray ionization mass spectrometry for standard oligosaccharides and glycans from ovalbumin. *J. Mass Spectrom.*, **2001**, *36*, 563-574.
- (40) Nielsen, T. C.;Rozek, T.;Hopwood, J. J.;Fuller, M. Determination of urinary oligosaccharides by high-performance liquid chromatography/electrospray ionization-tandem mass spectrometry: Application to Hunter syndrome. *Anal. Biochem.*, **2010**, *402*, 113-120.

- (41) Suzuki, S.;Kakehi, K.;Honda, S. Comparison of the sensitivities of various derivatives of oligosaccharides in LC/MS with fast atom bombardment and electrospray ionization interfaces. *Anal. Chem.*, **1996**, *68*, 2073-2083.
- (42) Honda, S.;Akao, E.;Suzuki, S.;Okuda, M.;Kakehi, K.;Nakamura, J. High-Performance Liquid-Chromatography of Reducing Carbohydrates as Strongly Ultraviolet-Absorbing and Electrochemically Sensitive 1-Phenyl-3-Methyl-5-Pyrazolone Derivatives. *Anal. Biochem.*, **1989**, *180*, 351-357.
- (43) Hahne, H.;Neubert, P.;Kuhn, K.;Etienne, C.;Bomgarden, R.;Rogers, J. C.;Kuster, B. Carbonyl-Reactive Tandem Mass Tags for the Proteome-Wide Quantification of N-Linked Glycans. *Anal. Chem.*, **2012**, *84*, 3716-3724.
- (44) Uematsu, R.;Furukawa, J.;Nakagawa, H.;Shinohara, Y.;Deguchi, K.;Monde, K.;Nishimura, S. I. High throughput quantitative glycomics and glycoform-focused proteomics of murine dermis and epidermis. *Mol. Cell. Proteomics*, **2005**, *4*, 1977-1989.
- (45) Naven, T. J. P.;Harvey, D. J. Cationic derivatization of oligosaccharides with Girard's T reagent for improved performance in matrix-assisted laser desorption/ionization and electrospray mass spectrometry. *Rapid Commun. Mass Spectrom.*, **1996**, *10*, 829-834.
- (46) Bereman, M. S.;Comins, D. L.;Muddiman, D. C. Increasing the hydrophobicity and electrospray response of glycans through derivatization with novel cationic hydrazides. *Chem. Comm.*, **2010**, *46*, 237-239.
- (47) Avigad, G. Dansyl Hydrazine as a Fluorimetric Reagent for Thin-Layer Chromatographic Analysis of Reducing Sugars. *J. Chromatogr.*, **1977**, *139*, 343-347.
- (48) Lattova, E.;Perreault, H. Profiling of N-linked oligosaccharides using phenylhydrazine derivatization and mass spectrometry. *J. Chromatogr. A*, **2003**, *1016*, 71-87.
- (49) Lattova, E.;Perreault, H. Labelling saccharides with phenylhydrazine for electrospray and matrix-assisted laser desorption-ionization mass spectrometry. *J. Chromatogr. B*, **2003**, *793*, 167-179.
- (50) Johnson, D. W. A modified Girard derivatizing reagent for universal profiling and trace analysis of aldehydes and ketones by electrospray ionization tandem mass spectrometry. *Rapid Commun. Mass Spectrom.*, **2007**, *21*, 2926-2932.

- (51) Shinohara, Y.;Sota, H.;Kim, F.;Shimizu, M.;Gotoh, M.;Tosu, M.;Hasegawa, Y. Use of a Biosensor Based on Surface-Plasmon Resonance and Biotinyl Glycans for Analysis of Sugar Binding Specificities of Lectins. *J. Biochem*, **1995**, *117*, 1076-1082.
- (52) Karamanos, N. K.;Tsegenidis, T.;Antonopoulos, C. A. Analysis of Neutral Sugars as Dinitrophenyl-Hydrazones by High-Performance Liquid-Chromatography. *J. Chromatogr.*, **1987**, *405*, 221-228.
- (53) Miksik, I.;Gabriel, J.;Deyl, Z. Microemulsion electrokinetic chromatography of diphenylhydrazones of dicarbonyl sugars. *J. Chromatogr. A*, **1997**, *772*, 297-303.
- (54) Lattova, E.;Perreault, H. Method for investigation of oligosaccharides using phenylhydrazine derivatization. *Methods Mol. Biol.*, **2009**, *534*, 65-77.
- (55) Yoshino, K.;Takao, T.;Murata, H.;Shimonishi, Y. Use of the Derivatizing Agent 4-Aminobenzoic Acid 2-(Diethylamino)Ethyl Ester for High-Sensitivity Detection of Oligosaccharides by Electrospray-Ionization Mass-Spectrometry. *Anal. Chem.*, **1995**, *67*, 4028-4031.
- (56) Chang, Y. L.;Liao, S. K. S.;Chen, Y. C.;Hung, W. T.;Yu, H. M.;Yang, W. B.;Fang, J. M.;Chen, C. H.;Lee, Y. C. Tagging saccharides for signal enhancement in mass spectrometric analysis. *J. Mass Spectrom.*, **2011**, *46*, 247-255.
- (57) Anumula, K. R. Advances in fluorescence derivatization methods for high-performance liquid chromatographic analysis of glycoprotein carbohydrates. *Anal. Biochem.*, **2006**, *350*, 1-23.
- (58) Chen, X. Y.;Flynn, G. C. Analysis of N-glycans from recombinant immunoglobulin G by on-line reversed-phase high-performance liquid chromatography/mass spectrometry. *Anal. Biochem.*, **2007**, *370*, 147-161.
- (59) Hase, S.;Ikenaka, T.;Matsushima, Y. A Highly Sensitive Method for Analyses of Sugar Moieties of Glycoproteins by Fluorescence Labeling. *J. Biochem.*, **1981**, *90*, 407-414.
- (60) Zhang, P.;Zhang, Y.;Xue, X. D.;Wang, C. J.;Wang, Z. F.;Huang, L. J. Relative quantitation of glycans using stable isotopic labels 1-(d0/d5) phenyl-3-methyl-5-pyrazolone by mass spectrometry. *Anal. Biochem.*, **2011**, *418*, 1-9.
- (61) Orlando, R. Quantitative Glycomics. *Methods Mol. Biol.*, **2010**, *600*, 31-49.

- (62) Geyer, H.;Geyer, R. Strategies for analysis of glycoprotein glycosylation. *Biochim. Biophys. Acta*, **2006**, *1764*, 1853-1869.
- (63) Zaia, J. Mass spectrometry of oligosaccharides. *Mass Spectrom. Rev.*, **2004**, *23*, 161-227.
- (64) Mechref, Y.;Novotny, M. V. Structural investigations of glycoconjugates at high sensitivity. *Chem. Rev.*, **2002**, *102*, 321-369.
- (65) Takahashi, N.;Nishibe, H. Almond Glycopeptidase Acting on Aspartylglycosylamine Linkages - Multiplicity and Substrate-Specificity. *Biochim. Biophys. Acta*, **1981**, *657*, 457-467.
- (66) Nishibe, H.;Takahashi, N. The Release of Carbohydrate Moieties from Human-Fibrinogen by Almond Glycopeptidase without Alteration in Fibrinogen Clottability. *Biochim. Biophys. Acta*, **1981**, *661*, 274-279.
- (67) Takahashi, N.;Nishibe, H. Some Characteristics of a New Glycopeptidase Acting on Aspartylglycosylamine Linkages. *J. Biochem.*, **1978**, *84*, 1467-1473.
- (68) Yamamoto, K. Microbial Endoglycosidases for Analyses of Oligosaccharide Chains in Glycoproteins. *J. Biochem.*, **1994**, *116*, 229-235.
- (69) O'Neill, R. A. Enzymatic release of oligosaccharides from glycoproteins for chromatographic and electrophoretic analysis. *J. Chromatogr. A*, **1996**, *720*, 201-215.
- (70) Patel, T.;Bruce, J.;Merry, A.;Bigge, C.;Wormald, M.;Jaques, A.;Parekh, R. Use of Hydrazine to Release in Intact and Unreduced Form Both N-Linked and O-Linked Oligosaccharides from Glycoproteins. *Biochem.*, **1993**, *32*, 679-693.
- (71) Anumula, K. R. Unique anthranilic acid chemistry facilitates profiling and characterization of Ser/Thr-linked sugar chains following hydrazinolysis. *Anal. Biochem.*, **2008**, *373*, 104-111.
- (72) Merry, A. H.;Neville, D. C. A.;Royle, L.;Matthews, B.;Harvey, D. J.;Dwek, R. A.;Rudd, P. M. Recovery of intact 2-aminobenzamide-labeled O-glycans released from glycoproteins by hydrazinolysis. *Anal. Biochem.*, **2002**, *304*, 91-99.

- (73) Kozak, R. P.;Royle, L.;Gardner, R. A.;Fernandes, D. L.;Wuhrer, M. Suppression of peeling during the release of O-glycans by hydrazinolysis. *Anal. Biochem.*, **2012**, *423*, 119-128.
- (74) Nakakita, S. I.;Sumiyoshi, W.;Miyanishi, N.;Hirabayashi, J. A practical approach to N-glycan production by hydrazinolysis using hydrazine monohydrate. *Biochem. Biophys. Res. Comm.*, **2007**, *362*, 639-645.
- (75) Schiffman, G.;Kabat, E. A.;Thompson, W. Immunochemical Studies on Blood Groups 30 - Cleavage of a B + H Blood-Group Substances by Alkali. *Biochem.*, **1964**, *3*, 113-&.
- (76) Huang, Y. P.;Konse, T.;Mechref, Y.;Novotny, M. V. Matrix-assisted laser desorption/ionization mass spectrometry compatible beta-elimination of O-linked oligosaccharides. *Rapid Commun. Mass Spectrom.*, **2002**, *16*, 1199-1204.
- (77) Huang, Y. P.;Mechref, Y.;Novotny, M. V. Microscale nonreductive release of O-linked glycans for subsequent analysis through MALDI mass spectrometry and capillary electrophoresis. *Anal. Chem.*, **2001**, *73*, 6063-6069.
- (78) Ciucanu, I.;Kerek, F. A Simple and Rapid Method for the Permethylation of Carbohydrates. *Carbohydr. Res.*, **1984**, *131*, 209-217.
- (79) Dell, A. Preparation and Desorption Mass-Spectrometry of Permethyl and Peracetyl Derivatives of Oligosaccharides. *Methods in Enzymology*, **1990**, *193*, 647-660.
- (80) Guillard, M.;Gloerich, J.;Wessels, H. J. C. T.;Morava, E.;Wevers, R. A.;Lefeber, D. J. Automated measurement of permethylated serum N-glycans by MALDI-linear ion trap mass spectrometry. *Carbohydrate Research*, **2009**, *344*, 1550-1557.
- (81) Kang, P.;Mechref, Y.;Novotny, M. V. High-throughput solid-phase permethylation of glycans prior to mass spectrometry. *Rapid Commun. Mass Spectrom.*, **2008**, *22*, 721-734.
- (82) Bourne, E. J.;Stacey, M.;Tatlow, J. C.;Tedder, J. M. Studies on Trifluoroacetic Acid .1. Trifluoroacetic Anhydride as a Promoter of Ester Formation between Hydroxy-Compounds and Carboxylic Acids. *J. Chem. Soc.*, **1949**, 2976-2979.

- (83) Pabst, M.;Kolarich, D.;Poltl, G.;Dalik, T.;Lubec, G.;Hofinger, A.;Altmann, F. Comparison of fluorescent labels for oligosaccharides and introduction of a new postlabeling purification method. *Anal. Biochem.*, **2009**, *384*, 263-273.
- (84) Schwaiger, H.;Oefner, P. J.;Huber, C.;Grill, E.;Bonn, G. K. Capillary Zone Electrophoresis and Micellar Electrokinetic Chromatography of 4-Aminobenzonitrile Carbohydrate-Derivatives. *Electrophoresis*, **1994**, *15*, 941-952.
- (85) Mopper, K.;Johnson, L. Reversed-Phase Liquid-Chromatographic Analysis of Dns-Sugars - Optimization of Derivatization and Chromatographic Procedures and Applications to Natural Samples. *J. Chromatogr.*, **1983**, *256*, 27-38.
- (86) Kang, P.;Mechref, Y.;Kyselova, Z.;Goetz, J. A.;Novotny, M. V. Comparative glycomic mapping through quantitative permethylation and stable-isotope labeling. *Anal. Chem.*, **2007**, 6064-6073.
- (87) Alvarez-Manilla, G.;Warren, N. L.;Abney, T.;Atwood, J.;Azadi, P.;York, W. S.;Pierce, M.;Orlando, R. Tools for glycomics: relative quantitation of glycans by isotopic permethylation using (CH₃I)-C-13. *Glycobiology*, **2007**, 677-687.
- (88) Atwood, J.;Cheng, L.;Alvarez-Manilla, G.;Warren, N.;York, W.;Orlando, R. Quantitation by isobaric labeling: Applications to glycomics. *Journal of Proteome Research*, **2008**, 367-374.
- (89) Thompson, A.;Schafer, J.;Kuhn, K.;Kienle, S.;Schwarz, J.;Schmidt, G.;Neumann, T.;Hamon, C. Tandem mass tags: A novel quantification strategy for comparative analysis of complex protein mixtures by MS/MS (vol 15, pg 1895, 2003). *Anal. Chem.*, **2003**, *75*, 4942-4942.
- (90) Dayon, L.;Hainard, A.;Licker, V.;Turck, N.;Kuhn, K.;Hochstrasser, D. F.;Burkhard, P. R.;Sanchez, J. C. Relative quantification of proteins in human cerebrospinal fluids by MS/MS using 6-plex isobaric tags. *Anal. Chem.*, **2008**, *80*, 2921-2931.
- (91) Orlando, R.;Lim, J.;Atwood, J.;Angel, P.;Fang, M.;Aoki, K.;Alvarez-Manilla, G.;Moremen, K.;York, W.;Tiemeyer, M.;Pierce, M.;Dalton, S.;Wells, L. IDAWG: Metabolic Incorporation of Stable Isotope Labels for Quantitative Glycomics of Cultured Cells. *Journal of Proteome Research*, **2009**, 3816-3823.

- (92) Wuhrer, M.;Deelder, A. M.;Hokke, C. H. Protein glycosylation analysis by liquid chromatography-mass spectrometry. *J. Chromatogr. B: Anal. Technol. Biomed. Life Sci.*, **2005**, *825*, 124-133.
- (93) Kirsch, S.;Bindila, L. Nano-LC and HPLC-chip-ESI-MS: an emerging technique for glycobioanalysis. *Bioanalysis*, **2009**, *1*, 1307-1327.
- (94) Wuhrer, M.;Koeleman, C. A. M.;Deelder, A. M.;Hokke, C. N. Normal-phase nanoscale liquid chromatography - Mass spectrometry of underivatized oligosaccharides at low-femtomole sensitivity. *Anal. Chem.*, **2004**, *76*, 833-838.
- (95) Karlsson, N. G.;Wilson, N. L.;Wirth, H. J.;Dawes, P.;Joshi, H.;Packer, N. H. Negative ion graphitised carbon nano-liquid chromatography/mass spectrometry increases sensitivity for glycoprotein oligosaccharide analysis. *Rapid Commun. Mass Spectrom.*, **2004**, *18*, 2282-2292.
- (96) Chu, C. S.;Ninonuevo, M. R.;Clowers, B. H.;Perkins, P. D.;An, H. J.;Yin, H. F.;Killeen, K.;Miyamoto, S.;Grimm, R.;Lebrilla, C. B. Profile of native N-linked glycan structures from human serum using high performance liquid chromatography on a microfluidic chip and time-of-flight mass spectrometry. *Proteomics*, **2009**, *9*, 1939-1951.
- (97) Bindila, L.;Peter-Katalinic, J. Chip-Mass Spectrometry for Glycomic Studies. *Mass Spectrom. Rev.*, **2009**, *28*, 223-253.
- (98) Alley, W. R.;Madera, M.;Mechref, Y.;Novotny, M. V. Chip-based Reversed-phase Liquid Chromatography-Mass Spectrometry of Permethylated N-Linked Glycans: A Potential Methodology for Cancer-biomarker Discovery. *Anal. Chem.*, **2010**, *82*, 5095-5106.
- (99) Alpert, A. J. Hydrophilic-Interaction Chromatography for the Separation of Peptides, Nucleic-Acids and Other Polar Compounds. *J. Chromatogr.*, **1990**, *499*, 177-196.
- (100) Hemstrom, P.;Irgum, K. Hydrophilic interaction chromatography. *J. Sep. Sci.*, **2006**, *29*, 1784-1821.
- (101) Ruhaak, L. R.;Deelder, A. M.;Wuhrer, M. Oligosaccharide analysis by graphitized carbon liquid chromatography-mass spectrometry. *Anal. Bioanal. Chem.*, **2009**, *394*, 163-174.

- (102) Pabst, M.;Altmann, F. Influence of electrosorption, solvent, temperature, and ion polarity on the performance of LC-ESI-MS using graphitic carbon for acidic oligosaccharides. *Anal. Chem.*, **2008**, *80*, 7534-7542.
- (103) Fan, J. Q.;Kondo, A.;Kato, I.;Lee, Y. C. High-Performance Liquid-Chromatography of Glycopeptides and Oligosaccharides on Graphitized Carbon Columns. *Anal. Biochem.*, **1994**, *219*, 224-229.
- (104) Dixon, R. B.;Bereman, M. S.;Petitte, J. N.;Hawkrigde, A. M.;Muddiman, D. C. One-year plasma N-linked glycome intra-individual and inter-individual variability in the chicken model of spontaneous ovarian adenocarcinoma. *Int. J. Mass Spectrom.*, **2011**, *305*, 79-86.
- (105) Bereman, M. S.;Young, D. D.;Deiters, A.;Muddiman, D. C. Development of a Robust and High Throughput Method for Profiling N-Linked Glycans Derived from Plasma Glycoproteins by NanoLC-FTICR Mass Spectrometry. *J. Proteome Res.*, **2009**, *8*, 3764-3770.
- (106) Butler, M.;Quelhas, D.;Critchley, A. J.;Carchon, H.;Hebestreit, H. F.;Hibbert, R. G.;Vilarinho, L.;Teles, E.;Matthijs, G.;Schollen, E.;Argibay, P.;Harvey, D. J.;Dwek, R. A.;Jaeken, J.;Rudd, P. M. Detailed glycan analysis of serum glycoproteins of patients with congenital disorders of glycosylation indicates the specific defective glycan processing step and provides an insight into pathogenesis. *Glycobiology*, **2003**, *13*, 601-622.
- (107) Nguyen, H. P.;Schug, K. A. The advantages of ESI-MS detection in conjunction with HILIC mode separations: Fundamentals and applications. *J. Sep. Sci.*, **2008**, *31*, 1465-1480.
- (108) Gregor, H. P.;Bregman, J. I. Studies on Ion-Exchange Resins .4. Selectivity Coefficients of Various Cation Exchangers Towards Univalent Cations. *J. Colloid Sci.*, **1951**, *6*, 323-347.
- (109) Snyder, L. R.;Kirkland, J. J.;Dolan, J. W., *Introduction to Modern Liquid Chromatography*, 3 ed.; Wiley: Hoboken, NJ, USA, 2009.
- (110) Kadar, E. P.;Wujcik, C. E. Remediation of undesirable secondary interactions encountered in hydrophilic interaction chromatography during development of a quantitative LC-MS/MS assay for a dipeptidyl peptidase IV (DPP-IV) inhibitor in monkey serum. *J. Chromatogr. B*, **2009**, *877*, 471-476.

- (111) Thaysen-Andersen, M.;Engholm-Keller, K.;Roepstorff, P., in *Hydrophilic Interaction Liquid Chromatography (HILIC) and Advanced Applications*, ed. P. G. Wang, W. He. CRC Press: Boca Raton, FL, 2011, pp 551-575.^
- (112) Ikegami, T.;Tomomatsu, K.;Takubo, H.;Horie, K.;Tanaka, N. Separation efficiencies in hydrophilic interaction chromatography. *J. Chromatogr. A*, **2008**, *1184*, 474-503.
- (113) Andrews, G. L.;Shuford, C. M.;Burnett, J. C.;Hawkridge, A. M.;Muddiman, D. C. Coupling of a vented column with splitless nanoRPLC-ESI-MS for the improved separation and detection of brain natriuretic peptide-32 and its proteolytic peptides. *J. Chromatogr. B*, **2009**, *877*, 948-954.
- (114) Fenn, J. B.;Mann, M.;Meng, C. K.;Wong, S. F.;Whitehouse, C. M. Electrospray Ionization for Mass-Spectrometry of Large Biomolecules. *Science*, **1989**, *246*, 64-71.
- (115) Fenn, J. B. Ion Formation from Charged Droplets - Roles of Geometry, Energy, and Time. *J. Am. Soc. Mass Spectrom.*, **1993**, *4*, 524-535.
- (116) Wilm, M. S.;Mann, M. Electrospray and Taylor-Cone Theory, Does Beam of Macromolecules at Last. *Int. J. Mass Spectrom. Ion Processes*, **1994**, *136*, 167-180.
- (117) Bahr, U.;Pfenninger, A.;Karas, M.;Stahl, B. High sensitivity analysis of neutral underivatized oligosaccharides by nanoelectrospray mass spectrometry. *Anal. Chem.*, **1997**, *69*, 4530-4535.
- (118) Taylor, G. Disintegration of Water Drops in Electric Field. *Proc. Royal Soc. London. Series a. Math and Phys. Sci.*, **1964**, *280*, 383-397.
- (119) Dole, M.;Mack, L. L.;Hines, R. L. Molecular Beams of Macroions. *J. Chem. Phys.*, **1968**, *49*, 2240-&.
- (120) Mack, L. L.;Kralik, P.;Rheude, A.;Dole, M. Molecular Beams of Macroions .2. *J. Chem. Phys.*, **1970**, *52*, 4977-&.
- (121) Iribarne, J. V.;Dziedzic, P. J.;Thomson, B. A. Atmospheric-Pressure Ion Evaporation Mass-Spectrometry. *Int. J. Mass Spectrom Ion Processes*, **1983**, *50*, 331-347.

- (122) Iribarne, J. V.;Thomson, B. A. Evaporation of Small Ions from Charged Droplets. *J. Chem. Phys.*, **1976**, *64*, 2287-2294.
- (123) Thomson, B. A.;Iribarne, J. V. Field-Induced Ion Evaporation from Liquid Surfaces at Atmospheric-Pressure. *J. Chem. Phys.*, **1979**, *71*, 4451-4463.
- (124) Kebarle, P.;Verkerk, U. H. Electrospray: From Ions in Solution to Ions in the Gas Phase, What We Know Now. *Mass Spectrom. Rev.*, **2009**, *28*, 898-917.
- (125) Gomez, A.;Tang, K. Q. Charge and Fission of Droplets in Electrostatic Sprays. *Phys. Fluids*, **1994**, *6*, 404-414.
- (126) Kebarle, P.;Tang, L. From Ions in Solution to Ions in the Gas-Phase - the Mechanism of Electrospray Mass-Spectrometry. *Anal. Chem.*, **1993**, *65*, A972-A986.
- (127) Duft, D.;Achtzehn, T.;Muller, R.;Huber, B. A.;Leisner, T. Coulomb fission - Rayleigh jets from levitated microdroplets. *Nature*, **2003**, *421*, 128-128.
- (128) Cech, N. B.;Enke, C. G. Effect of affinity for droplet surfaces on the fraction of analyte molecules charged during electrospray droplet fission. *Anal. Chem.*, **2001**, *73*, 4632-4639.
- (129) Null, A. P.;Nepomuceno, A. I.;Muddiman, D. C. Implications of hydrophobicity and free energy of solvation for characterization of nucleic acids by electrospray ionization mass spectrometry. *Anal. Chem.*, **2003**, *75*, 1331-1339.
- (130) Frahm, J. L.;Bori, I. D.;Comins, D. L.;Hawkrige, A. M.;Muddiman, D. C. Achieving augmented limits of detection for peptides with hydrophobic alkyl tags. *Anal. Chem.*, **2007**, *79*, 3989-3995.
- (131) Mirzaei, H.;Regnier, F. Enhancing electrospray ionization efficiency of peptides by derivatization. *Anal. Chem.*, **2006**, *78*, 4175-4183.
- (132) Yang, W. C.;Mirzaei, H.;Liu, X. P.;Regnier, F. E. Enhancement of amino acid detection and quantification by electrospray ionization mass spectrometry. *Anal. Chem.*, **2006**, *78*, 4702-4708.
- (133) Shuford, C. M.;Comins, D. L.;Whitten, J. L.;Burnett, J. C.;Muddiman, D. C. Improving limits of detection for B-type natriuretic peptide using PC-IDMS: An application of the ALiPHAT strategy. *Analyst*, **2010**, *135*, 36-41.

- (134) Williams, D. K.;Comins, D. L.;Whitten, J. L.;Muddiman, D. C. Evaluation of the ALiPHAT Method for PC-IDMS and Correlation of Limits-of-Detection with Nonpolar Surface Area. *J. Am. Soc. Mass. Spectrom.*, **2009**, *20*, 2006-2012.
- (135) Williams, D. K.;Meadows, C. W.;Bori, I. D.;Hawkrige, A. M.;Comins, D. L.;Muddiman, D. C. Synthesis, characterization, and application of iodoacetamide derivatives utilized for the ALiPHAT strategy. *J. Am. Chem. Soc.*, **2008**, *130*, 2122-2123.
- (136) Shuford, C. M.;Muddiman, D. C. Capitalizing on the hydrophobic bias of electrospray ionization through chemical modification in mass spectrometry-based proteomics. *Expert Rev. Proteomics*, **2011**, *8*, 317-323.
- (137) Kulevich, S. E.;Frey, B. L.;Kreitingner, G.;Smith, L. M. Alkylating Tryptic Peptides to Enhance Electrospray Ionization Mass Spectrometry Analysis. *Anal. Chem.*, **2010**, *82*, 10135-10142.
- (138) Foettinger, A.;Leitner, A.;Lindner, W. Derivatisation of arginine residues with malondialdehyde for the analysis of peptides and protein digests by LC-ESI-MSMS. *J. Mass Spectrom.*, **2006**, *41*, 623-632.
- (139) Werz, D. B.;Ranzinger, R.;Herget, S.;Adibekian, A.;von der Lieth, C. W.;Seeberger, P. H. Exploring the structural diversity of mammalian carbohydrates ("Glycospace") by statistical databank analysis. *ACS Chem. Biol.*, **2007**, *2*, 685-691.
- (140) Kronewitter, S. R.;An, H. J.;de Leoz, M. L.;Lebrilla, C. B.;Miyamoto, S.;Leiserowitz, G. S. The development of retrosynthetic glycan libraries to profile and classify the human serum N-linked glycome. *Proteomics*, **2009**, *9*, 2986-2994.
- (141) Xian, F.;Hendrickson, C. L.;Marshall, A. G. High Resolution Mass Spectrometry. *Analytical Chemistry*, **2012**, *84*, 708-719.
- (142) Marshall, A.;Hendrickson, C.;Jackson, G. Fourier transform ion cyclotron resonance mass spectrometry: A primer. *Mass Spectrometry Reviews*, **1998**, 1-35.
- (143) Baldeschwieler, J. D. Ion Cyclotron Resonance Spectroscopy. *Science*, **1968**, *159*, 263-&.
- (144) Comisarow, M. B.;Marshall, A. G. Fourier-Transform Ion-Cyclotron Resonance Spectroscopy. *Chem. Phys. Lett*, **1974**, *25*, 282-283.

- (145) Comisarow, M. B. Theory of Fourier-Transform Ion-Cyclotron Resonance Mass-Spectroscopy. Signal Modeling for Ion-Cyclotron Resonance. *Journal of Chemical Physics*, **1978**, 4097-4104.
- (146) Cooley, J. W.; Tukey, J. W. An Algorithm for Machine Calculation of Complex Fourier Series. *Math. Comput.*, **1965**, 19, 297-&.
- (147) Kingdon, K. H. A method for the neutralization of electron space charge by positive ionization at very low gas pressures. *Phys. Rev.*, **1923**, 21, 408-418.
- (148) Perry, R. H.; Cooks, R. G.; Noll, R. J. Orbitrap Mass Spectrometry: Instrumentation, Ion Motion and Applications. *Mass Spectrom. Rev.*, **2008**, 27, 661-699.
- (149) Korsunskii, M. I.; Bazakutsa, V. A. A Study of the Ion-Optical Properties of a Sector-Shaped Electrostatic Field of the Difference Type. *Soviet Physics-Tech. Phys.*, **1958**, 3, 1396-1409.
- (150) Knight, R. D. Storage of Ions from Laser-Produced Plasmas. *Appl. Phys. Lett.*, **1981**, 38, 221-223.
- (151) Hardman, M.; Makarov, A. A. Interfacing the orbitrap mass analyzer to an electrospray ion source. *Anal. Chem.*, **2003**, 75, 1699-1705.
- (152) Scigelova, M.; Makarov, A. Orbitrap mass analyzer - Overview and applications in proteomics. *Proteomics*, **2006**, 16-21.
- (153) Makarov, A.; Denisov, E.; Lange, O.; Horning, S. Dynamic range of mass accuracy in LTQ orbitrap hybrid mass spectrometer (vol 17, pg 977, 2006). *J. Am. Soc. Mass Spectrom.*, **2006**, 17, 1758-1758.
- (154) Hu, Q. Z.; Noll, R. J.; Li, H. Y.; Makarov, A.; Hardman, M.; Cooks, R. G. The Orbitrap: a new mass spectrometer. *J. Mass Spectrom.*, **2005**, 40, 430-443.
- (155) Michalski, A.; Damoc, E.; Lange, O.; Denisov, E.; Nolting, D.; Muller, M.; Viner, R.; Schwartz, J.; Remes, P.; Belford, M.; Dunyach, J. J.; Cox, J.; Horning, S.; Mann, M.; Makarov, A. Ultra High Resolution Linear Ion Trap Orbitrap Mass Spectrometer (Orbitrap Elite) Facilitates Top Down LC MS/MS and Versatile Peptide Fragmentation Modes. *Mol. Cell. Proteomics*, **2012**, 11.
- (156) Michalski, A.; Damoc, E.; Hauschild, J. P.; Lange, O.; Wieghaus, A.; Makarov, A.; Nagaraj, N.; Cox, J.; Mann, M.; Horning, S. Mass Spectrometry-based

- Proteomics Using Q Exactive, a High-performance Benchtop Quadrupole Orbitrap Mass Spectrometer. *Mol. Cell. Proteomics*, **2011**, *10*.
- (157) Bateman, K. P.;Kellmann, M.;Muenster, H.;Papp, R.;Taylor, L. Quantitative-Qualitative Data Acquisition Using a Benchtop Orbitrap Mass Spectrometer. *J. Am. Soc. Mass Spectrom.*, **2009**, *20*, 1441-1450.
- (158) Geiger, T.;Cox, J.;Mann, M. Proteomics on an Orbitrap Benchtop Mass Spectrometer Using All-ion Fragmentation. *Mol. Cell. Proteomics*, **2010**, *9*, 2252-2261.
- (159) Olsen, J. V.;Nielsen, M. L.;Damoc, N. E.;Griep-Raming, J.;Moehring, T.;Makarov, A.;Schwartz, J.;Horning, S.;Mann, M. Characterization of the Velos, an Enhanced LTQ Orbitrap, for Proteomics. *Mol. Cell. Proteomics*, **2009**, S40-S40.
- (160) Olsen, J. V.;Schwartz, J. C.;Griep-Raming, J.;Nielsen, M. L.;Damoc, E.;Denisov, E.;Lange, O.;Remes, P.;Taylor, D.;Splendore, M.;Wouters, E. R.;Senko, M.;Makarov, A.;Mann, M.;Horning, S. A Dual Pressure Linear Ion Trap Orbitrap Instrument with Very High Sequencing Speed. *Mol. Cell. Proteomics*, **2009**, *8*, 2759-2769.
- (161) Glish, G. L.;Burinsky, D. J. Hybrid mass spectrometers for tandem mass Spectrometry. *J. Am. Soc. Mass Spectrom.*, **2008**, *19*, 161-172.
- (162) Syka, J. E. P.;Marto, J. A.;Bai, D. L.;Horning, S.;Senko, M. W.;Schwartz, J. C.;Ueberheide, B.;Garcia, B.;Busby, S.;Muratore, T.;Shabanowitz, J.;Hunt, D. F. Novel linear quadrupole ion trap/FT mass spectrometer: Performance characterization and use in the comparative analysis of histone H3 post-translational modifications. *J. Proteome Res.*, **2004**, *3*, 621-626.
- (163) Stahl, D. C.;Swiderek, K. M.;Davis, M. T.;Lee, T. D. Data-controlled automation of liquid chromatography tandem mass spectrometry analysis of peptide mixtures. *J. Am. Soc. Mass Spectrom.*, **1996**, *7*, 532-540.
- (164) Hull, S. R.;Turco, S. J. Separation of Dansyl Hydrazine-Derivatized Oligosaccharides by Liquid-Chromatography. *Anal. Biochem.*, **1985**, *146*, 143-149.
- (165) Gil, G. C.;Kim, Y. G.;Kim, B. G. A relative and absolute quantification of neutral N-linked oligosaccharides using modification with carboxymethyl trimethylammonium hydrazide and matrix-assisted laser desorption/ionization time-of-flight mass spectrometry. *Anal. Biochem.*, **2008**, *379*, 45-59.

(166) Louvar, J. F. Simplify Experimental Design. *Chemical Eng. Prog.*, **2010**, 106, 35-40.

CHAPTER 2

The Interplay of Permanent Charge and Hydrophobicity in the Electrospray Ionization of Glycans

The following work was reprinted with permission from: Walker, S. H.; Papas, B. N.; Comins, D. L.; Muddiman, D. C. *Analytical Chemistry* **2010**, 82(15), 6636-6642. Copyright 2010 American Chemical Society. The original publication may be accessed directly via the World Wide Web.

2.1 Introduction

The derivatization of molecules for enhanced detection in mass spectrometry (MS) has a long history dating back to the use of trimethylsilylating agents to increase the volatility of alcohols¹ and GC-MS analysis², which is still widely practiced today. Upon the invention of electrospray ionization (ESI)³, a need to enhance ionization of large biomolecules arose, and hydrophobicity has commonly been exploited to accomplish this goal. Hydrophobic tags have been coupled to nucleic acids⁴ and peptides⁵⁻⁹; the latter has demonstrated as much as a 2000-fold improvement¹⁰. The ability to adapt these methods and apply them to glycomics analysis affords a significant opportunity due to the fact that the assay of glycans is difficult in comparison to peptides.

Glycans have traditionally been difficult to ionize given their hydrophilicity and lack of basic sites able to be protonated, and several methods have been implemented to modify glycans for enhanced mass spectrometric ionization and detection including permethylation¹¹⁻¹², peracetylation^{11, 13}, and derivatization at the reducing terminus of the sugar¹⁴. Permethylation¹¹⁻¹² and peracetylation^{11, 13} have

been shown to increase the glycan abundance and give valuable MS/MS data but often have time consuming wet chemistry steps and are not useful with larger glycans due to incomplete reaction dispersing the glycan signal across several different m/z channels. Thus, the exploration of alternate glycan analysis strategies is necessary in order to further develop the field of glycomics.

Enzymatic cleavage of *N*-linked glycans from proteins allows access to the glycan's reducing terminus where the terminal sugar resides in equilibrium between the closed hemi-acetal and reactive aldehyde forms¹⁵. Reductive amination involves converting the open-ring aldehyde reducing sugar to an amine and has been used for the hydrophobic tagging of glycans¹⁶⁻¹⁹ and for the incorporation fluorescent or UV absorbing tags²⁰⁻²³. However, a major limitation of coupling this methodology to ESI is the fact that salts contaminate the sample, and a cumbersome clean up step is required after derivatization and prior to online separations. Not only will this take more time, but clean up methods such as solid phase extraction can incur significant losses and increases analytical variability. These side effects are not favorable for the assay of glycans using electrospray ionization, yet there is another derivatization procedure that is capable of high reaction efficiency at the reducing terminus: hydrazone formation. A recent study compares the fragmentation patterns of these two derivatization strategies when analyzing a variety of oligosaccharides²⁴.

Dansylhydrazine (DHZ) was the first hydrazide coupled to glycans for enhanced fluorescence detection²⁵, and since, many more hydrazide reagents have been utilized in mass spectrometry for fluorescence and UV detection²⁶⁻²⁷. However,

Harvey and coworkers first used cationic hydrazone formation for the increased detection of glycans in MALDI- and ESI-MS²⁸. They reported a 10-fold decrease in detection limits could be achieved when incorporating a permanent charge on the tagging reagent (Girard's T reagent), and no clean up was required between reaction and introduction on the chromatography column. In contrast, it has recently been reported that the Girard's T reagent decreases the abundance of detected glycans in ESI-MS²⁹. These two contradicting studies have prompted this work to determine how modifying glycans with the permanent charge affects the ESI response in conjunction with the use of hydrophobic tags to enhance glycan ion abundance. Though previous studies have shown different fragmentation patterns using charged reagents in fast atom bombardment MS³⁰, studies from this group show little difference in the fragmentation when coupling fixed-charge reagents to *N*-linked glycans²⁹.

Fenn has shown that in an electrospray droplet, hydrophobic analytes are concentrated near the surface of the droplet, more hydrophilic molecules are more solvated near the center, and the surplus protons generated from the oxidation of water in the ESI capillary build up on the surface of the droplet³¹. This creates a bias which allows the hydrophobic analytes (being less solvated and near the surface) to be inherently more likely to acquire charge and be ejected as gas-phase ions as the droplet is desolvated. Though this is accepted and has been demonstrated for the hydrophobic properties of different molecules^{4-10, 32}, the effect of a permanent charge fixed on a molecule has not been explicitly studied. Researchers have been hesitant

to incorporate a permanent charge hypothesizing that it would have a negative effect in the fragmentation patterns of the glycans and could cause partial or total loss of the tag¹⁸. Recently, though, it has been shown that CID fragmentation patterns of a charged complex glycan are not negatively affected by a permanently charged tag nor is the tag lost during fragmentation²⁹. Given these results, charged hydrazide reagents are now considered a viable avenue toward the hydrophobic tagging of glycans. However, charged hydrazide tags have not been utilized in hydrophobic tagging of glycans, aside from Girard's reagents T and P, because they are not commercially available. This can be surmounted by the synthesis of specific hydrazide reagents with characteristics hypothesized to most efficiently enhance ESI response.

In order that the hydrazone tagging method can be further applied to the profiling of entire glycomes, the derivatization reaction must occur stoichiometrically. If this is not the case, then this method will be detrimental to glycan analysis by increasing the number of m/z channels and retention times a given glycan analyte is partitioned into, decreasing the signal-to-noise and increasing the limit of detection. Fractional factorial design (FFD) is a design of experiments (DOE) optimization process in which a large number of variables (>3) can be simultaneously analyzed, significantly reducing the amount of time and cost required to examine a large experimental space³³. Using FFD, the relevancy of several independent variables operating on one dependant variable can be measured using a combination of experiments in which each independent variable is varied at two levels (e.g., one low

and one high). Subsequently, the variables that significantly affect the dependant variable being measured are able to be isolated and further optimized under controlled conditions. This DOE procedure is an efficient method to analyze the numerous variables affecting glycan tagging reactions, minimizing both the time and cost required.

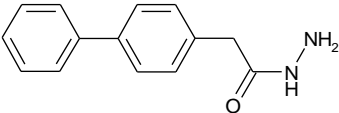
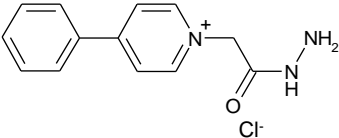
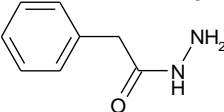
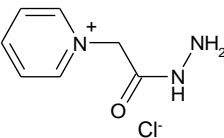
Herein, two pairs (one synthesized and one commercially available) of related molecules, in which one reagent in each pair contains a permanent charge, are used to determine whether or not a fixed cationic charge is beneficial to glycan analysis. These charged/neutral molecules only differ in that the charged molecule has a quaternary ammonium substituted for a carbon atom, which allows for the direct comparison of ESI response with the hydrophobic properties of the molecules held constant. Moreover, a DOE optimization is presented where a FFD is used in order to determine which independent variables affect the tagging reaction efficiency. These significant variables were further optimized to provide a final optimized tagging procedure for glycan hydrazone formation. Finally, discussions relating hydrophobicity, hydrophilic interaction (liquid) chromatography (HILIC) retention time, and non polar surface area calculations (NPSA) are included in order to determine the optimal properties of glycan tagging reagents and to direct future synthesis for the enhanced detection of glycans by ESI-MS.

2.2 Experimental

2.2.1 Materials

Maltoheptaose, Gal₂Man₃GlcNAc₄ (NA2) glycan, Phenylacetic hydrazide (GPN), acetic acid, ammonium acetate, ethyl chloroacetate, hydrazine hydrate, 4-phenylpyridine, and ethyl phenylacetate were all purchased from Sigma Aldrich (St Louis, MO). Girard's reagent P (GP) was purchased from TCI America (Portland, OR). HPLC grade ACN, water, and MeOH were all purchased from Burdick & Jackson (Muskegon, MI).

Table 2.1 – Reagents, abbreviations, and NPSA

Abbreviation	Structure	NPSA ^a
Phenyl-GPN		181
Phenyl-GP		180
GPN		109
GP		108

^aNon-Polar Surface Area

2.2.2 Synthesis of Reagents

The reagents and abbreviations used throughout this study are presented in **Table 2.1**. The hydrazide tagging reagents, phenyl-GP and phenyl-GPN, were synthesized according to **Figure 2.1**. For the charged reagents, R groups are attached to the pyridine ring of esters (II), which are reacted with hydrazine hydrate to effect amide bond formation between the hydrazine and the ester group. This allows numerous derivatives to be prepared and tested in order to discover the optimum tag, while ensuring the ability to incorporate ≥ 6 ^{13}C stable isotopes for future relative quantification studies. The same amide bond is formed in the neutral reagents between the hydrazine and ester group, and many neutral esters are commercially available that can be used as the starting material.

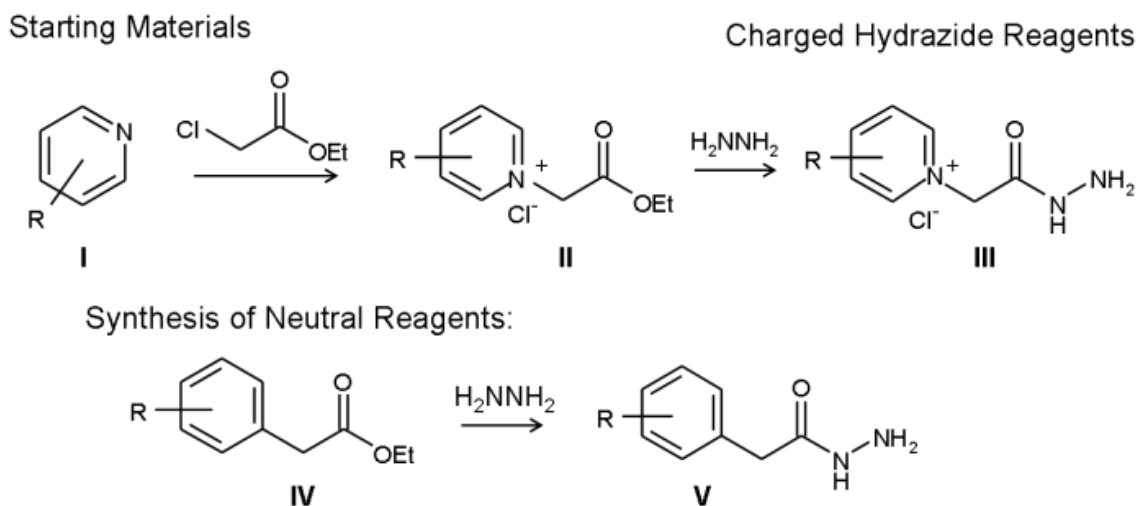


Figure 2.1 – Short synthetic routes to charged (III) and neutral (V) hydrazide reagents starting with pyridinium salts (II) or esters (IV). Amide bond formation between the ester function and hydrazine gives the desired hydrazides.

2.2.3 Fractional Factorial Design of Experiments

Two separate FFD experiments were conducted in which aliquots of maltoheptaose (~0.17 nmol) were dried, and to separate dried samples, the appropriate reagent solution was added and reacted according to **Table 2.2** and **Table 2.3** for the phenyl-GP and phenyl-GPN reagents, respectively. After reaction,

Table 2.2 – FFD reaction table for the phenyl-GP reagent.

Sample Number	Temperature (°C)	Solvent Composition	Reaction Time (min)	Excess Reagent (mol)	Reaction Volume (µL)
1	50	MeOH/Acetic Acid	15	25x	250
2	50	MeOH/Acetic Acid	15	300x	50
3	50	MeOH/Acetic Acid	180	25x	50
4	50	MeOH/Acetic Acid	180	300x	250
5	50	Water/Acetic Acid	15	25x	50
6	50	Water/Acetic Acid	15	300x	250
7	50	Water/Acetic Acid	180	25x	250
8	50	Water/Acetic Acid	180	300x	50
9	90	MeOH/Acetic Acid	15	25x	50
10	90	MeOH/Acetic Acid	15	300x	250
11	90	MeOH/Acetic Acid	180	25x	250
12	90	MeOH/Acetic Acid	180	300x	50
13	90	Water/Acetic Acid	15	25x	250
14	90	Water/Acetic Acid	15	300x	50
15	90	Water/Acetic Acid	180	25x	50
16	90	Water/Acetic Acid	180	300x	250

samples were dried *in vacuo* at 35°C and reconstituted in 200 µL of HILIC initial conditions (20:80 mobile phase A:B) for nanoLC MS analysis. An FFD analysis of the phenyl-GP reagent was carried out at a resolution of 4 ($\frac{1}{2} 2^5$) in order to determine the significance of the reaction time, temperature, volume, mol excess (XS) of tagging reagent, and solvent composition. The second set of FFD experiments were carried out using the phenyl-GPN reagent and a FFD with a resolution of 4 ($\frac{1}{2} 2^4$). A resolution of 4 implies that all the main effects of the individual variables can be clearly distinguished, and some two-factor interactions can be distinguished. Also, a *full factorial design* would comprise 64 (2^5) and 32 (2^4)

Table 2.3 – FFD reaction table for the phenyl-GPN reagent.

Sample Number	Temperature (°C)	Time (min)	Excess Reagent (mol)	Volume (µL)
1	50	15	25x	50
2	50	15	300x	250
3	50	180	25x	250
4	50	180	300x	50
5	90	15	25x	250
6	90	15	300x	50
7	90	180	25x	50
8	90	180	300x	250

experiments for the phenyl-GP and phenyl-GPN reagents, respectively. However, in this study a *fractional factorial design* is used where only 1/2 the experiments are enough to achieve a resolution of 4.

The independent variables studied were reaction time, temperature, volume, and mol XS. In both cases, the samples were analyzed randomly in triplicate, and the peak areas in the extracted ion chromatograms (EIC) were used to determine tagging efficiency. The data were then modeled using JMP v8.0 software (SAS, Cary, NC). It was necessary to perform two FFD studies to ensure that the permanent charge does not affect the tagging reaction efficiencies. Also, the inclusion of solvent composition in the phenyl-GPN FFD experiment was not possible due to the tag's insolubility in water. This is acceptable due to the fact that in the phenyl-GP FFD, the solvent composition was not determined to have any effect on the glycan tagging efficiency. Each of the variables included in the FFD studies was chosen by studying literature hydrazone formation reaction conditions. Currently, there is a wide variety of reaction conditions for the formation of hydrazones and no standardized or ubiquitous procedures³⁴⁻³⁶. Thus, it was necessary to use a time- and cost-efficient method to study all the possible reaction conditions.

Since the amount of mol XS was determined to be a significant factor in both experiments (*vide infra*), an optimization of this parameter was performed by adding 10-, 20-, 40-, 80-, 160-, 320-, 640-, 1280-, 2560-, and 5120-fold excess tag in 100 μ L of 85:15 (v/v) MeOH:Acetic Acid to separate dried maltoheptaose aliquots and

reacted in parallel for 3 hr at 75 °C. Samples were dried *in vacuo* at 35 °C and reconstituted in 200 µL of HILIC initial conditions for nanoLC MS analysis. All reaction efficiencies were calculated using EIC integrated peak areas according to

Equation 2.1:

$$\frac{[\text{Peak Area}(\text{Tagged Glycan})]}{[\text{Peak Area}(\text{Tagged Glycan})] + [\text{Peak Area}(\text{Free Glycan})]} \times 100 \quad (\text{Eqn. 2.1})$$

2.2.4 Charged/Neutral Pair Analysis

Five aliquots of glycan (~0.17 nmol) were dried, and reagent solutions of the 4 different tags (~3500 mol XS) in 100 µL of 85:15 (v/v) MeOH:acetic acid were added to separate reaction vials containing the dried glycan sample. For the 5th sample, 100 µL of 85:15 (v/v) MeOH:acetic acid was added to the dried glycan sample with no reagent present. Each vial was heated at 75 °C for 3 hr., and then the solvent was evaporated off *in vacuo* at 35 °C. Each sample was then reconstituted in 200 µL of HILIC initial conditions, and 30 µL of each of the 5 samples were combined in a sample vial to form an equimolar mixture so that ~1 pmol of each was introduced on column. Each sample was also analyzed individually in order to determine reaction efficiency. All samples were run randomly, in triplicate.

2.2.5 *Nano-flow Liquid Chromatography*

Hydrophilic interaction liquid chromatography (HILIC) was performed on an Eksigent nanoLC-2D system (Dublin, CA) running under a vented-column configuration³⁷ as described previously³⁸. Briefly, mobile phase A and B consisted of 50 mM ammonium acetate (pH 4.5) and 100% ACN, respectively. Ten microliters of sample were injected onto a 100 μ m ID IntegraFrit trap column packed in-house to ~3.2 cm with Amide-80 stationary phase (TOSOH Bioscience, San Jose, CA). The analytical column consisted of a 75 μ m ID capillary coupled to a 15 μ m PicoFrit tip packed in-house to ~10 cm with Amide-80 stationary phase. Glycans were eluted at 500 nL/min, and the gradient was ramped from 20 to 60 % solvent A over 37 min, with a total run time of 1 hr as previously reported³⁸. IntegraFrit and PicoFrit columns were from New Objective (Woburn, MA).

2.2.6 *LTQ-FTICR Mass Spectrometry*

The mass spectrometer used was a hybrid linear ion trap, Fourier transform ion cyclotron resonance mass spectrometer (Thermo Fisher Scientific, San Jose, CA) outfitted with a 7 Tesla superconducting magnet. Mass calibration was performed as specified by the manufacturer. Spectra were acquired in data dependent mode, where each precursor ion scan in the ICR cell determined up to 5 m/z values that would be fragmented during subsequent MS/MS scans in the ion trap. If the same m/z value is chosen twice within 30 s, the m/z was placed on an exclude list, and the dynamic exclusion was set to 2 min in order to reduce

oversampling. A 2 kV potential was applied to a zero dead volume union to induce electrospray ionization, and the capillary and tube lens voltages were set to 42 V and 120 V, respectively, with a heated capillary temperature of 225 °C. An AGC of 1×10^6 (maximum injection time of 1 s) was set in the ICR cell with a $100,000_{FWHM}$ at 400 m/z resolving power. For MS/MS in the ion trap, the normalized collision energy was set to 22 with an AGC of 1×10^4 and a maximum injection time of 400 ms. Xcalibur software (version 2.0.5) was used for peak integration and data analysis.

2.2.7 Non-Polar Surface Area Calculations

NPSA's were calculated for each of the four reagents in order to estimate the hydrophobicity of the reagents. Each molecule is considered to be at a standard geometry. Spheres with van der Waals radii appropriate for each atom are placed at each atomic origin. The exposed surface area (area not contained within another sphere) is then calculated using standard numerical integration schemes as implemented in Mathematica (Version 7, 2008; Wolfram Research, Inc., Champaign, IL). The total NPSA for a molecule then is the sum of the visible surface areas for each non-polar atom, which excludes oxygens, carbons bonded to oxygen, nitrogens, and hydrogens bonded to either oxygen or nitrogen.

2.3 Results and Discussion

Glycans were analyzed by positive ion mass spectrometry in order to determine the effects of a positive permanent charge on glycan analysis. Though

recent studies have shown the benefits of negative ion MS in the tandem MS of glycans³⁹⁻⁴⁶, the positively charged derivatives are not amenable to negative ion mode. Also, much of the literature for the negative ion MS of glycans does not involve derivatization. This will be necessary in future studies from this group involving stable isotope labeling for the relative quantification of glycans. Each glycan was detected by both protonation and ammonium adduction allowing two different fragmentation patterns; the ammonium adduction should not allow for internal rearrangement according to recent studies on using large groups for cationization⁴⁷⁻⁵¹.

2.3.1 *Hydrazone Formation Optimization*

In both FFD experiments, it was shown that the amount of excess reagent is a significant variable in the efficiency of the reaction (**Figure 2.2**). In the phenyl-GPN experiment, the reaction volume was also determined to affect the reaction efficiency. This is not unexpected as either reducing the volume or increasing the mol excess will effectively increase the concentration of reagent; thus, these two variables are strongly related, and only optimizing the excess reagent was sufficient to achieve 95-98% reaction efficiency. The amount of excess reagent (phenyl-GPN) needed in a 100- μ L solution was optimized as shown in **Figure 2.3**. Amounts of excess reagent greater than ~5,000-fold were deemed insignificant using a t-test to compare measurements (analyzed in triplicate). Using ~3500 mol XS in all

subsequent studies resulted in $\geq 97\%$ reaction efficiency coupling the reagents to the NA2 complex glycan (**Figure 2.4**).

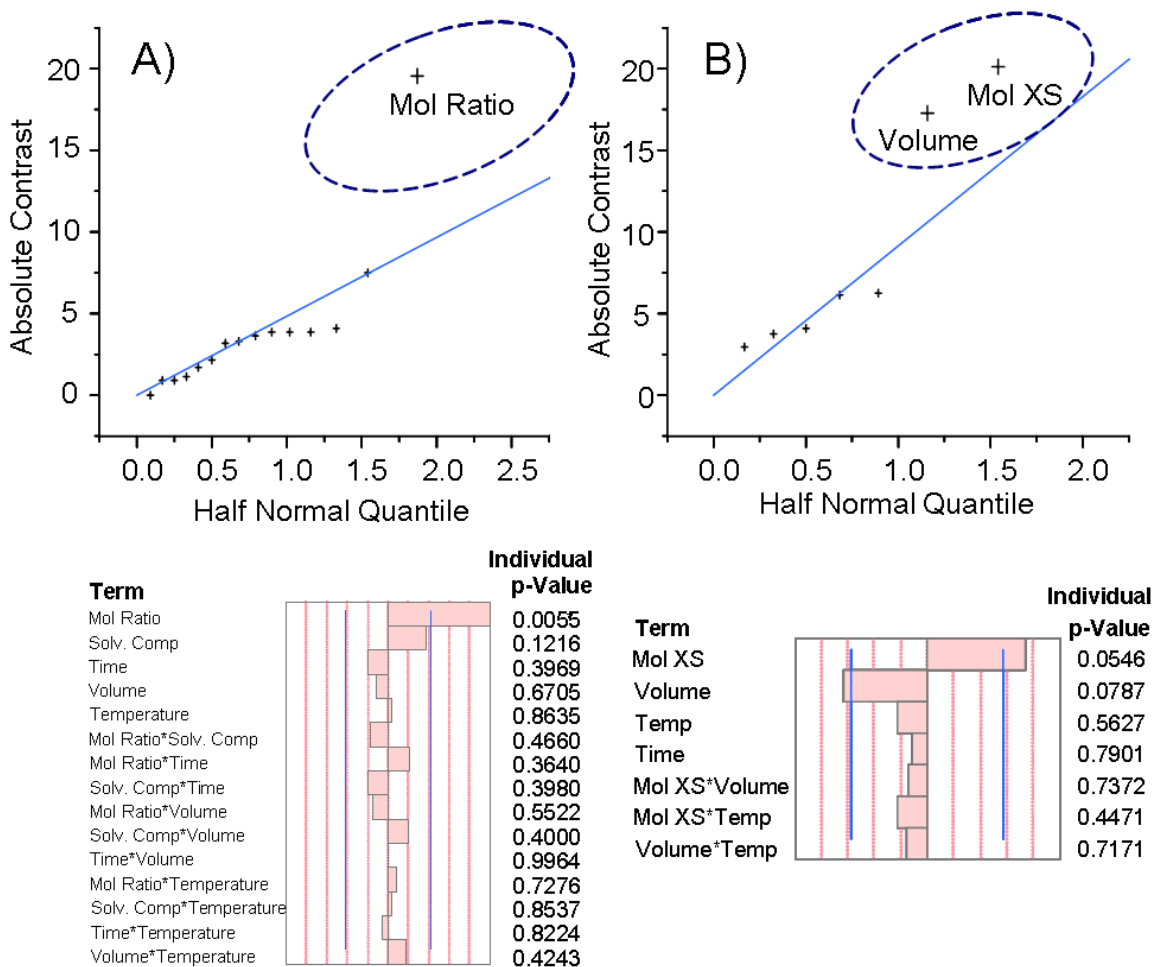


Figure 2.2 – JMP v8.0 FFD results for the reaction of maltoheptaose and Girard's P derivatives. A) derivatization using phenyl-GP, and B) derivatization using phenyl-GPN. Hashed circles (- -) indicate significant variables. Absolute contrast denotes the probability that a variable is significant, and the half normal quantile is the probability assuming no significance. Variables which fall above the curve are deemed significant. The tabular representation is below showing the p-values for each variable in comparison to the cut-off value of 0.1.

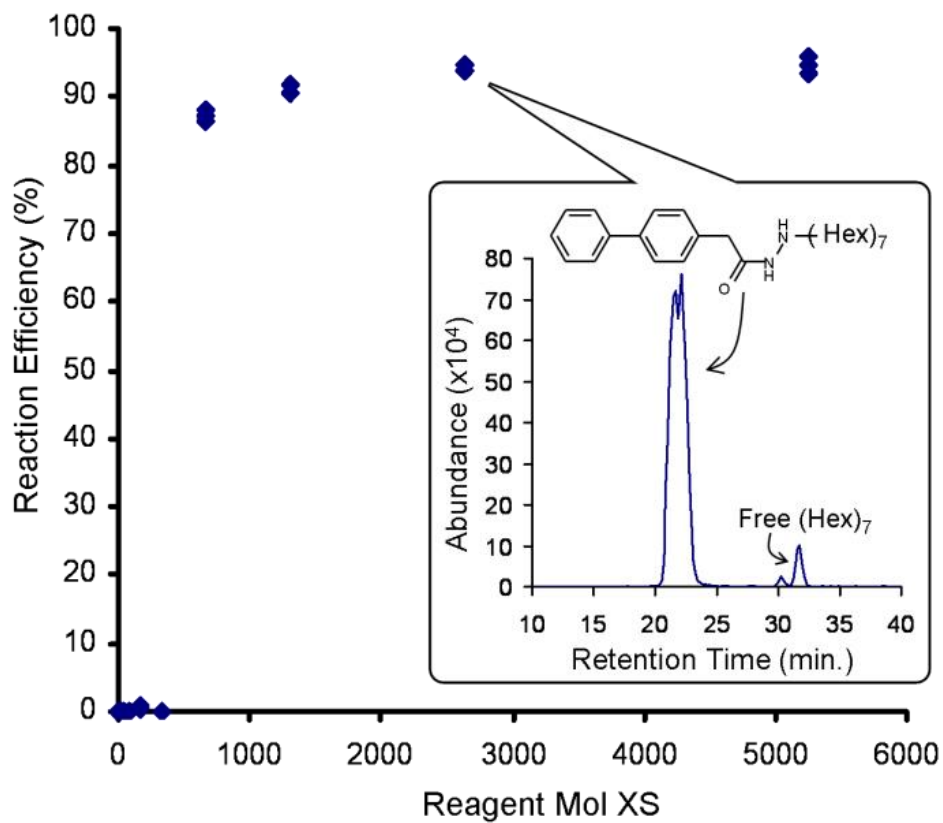


Figure 2.3 – The optimization of the mol XS (with respect to the amount of glycan) of the reagent needed to be added to the reaction mixture in order to ensure that stoichiometric reaction conditions occurred.

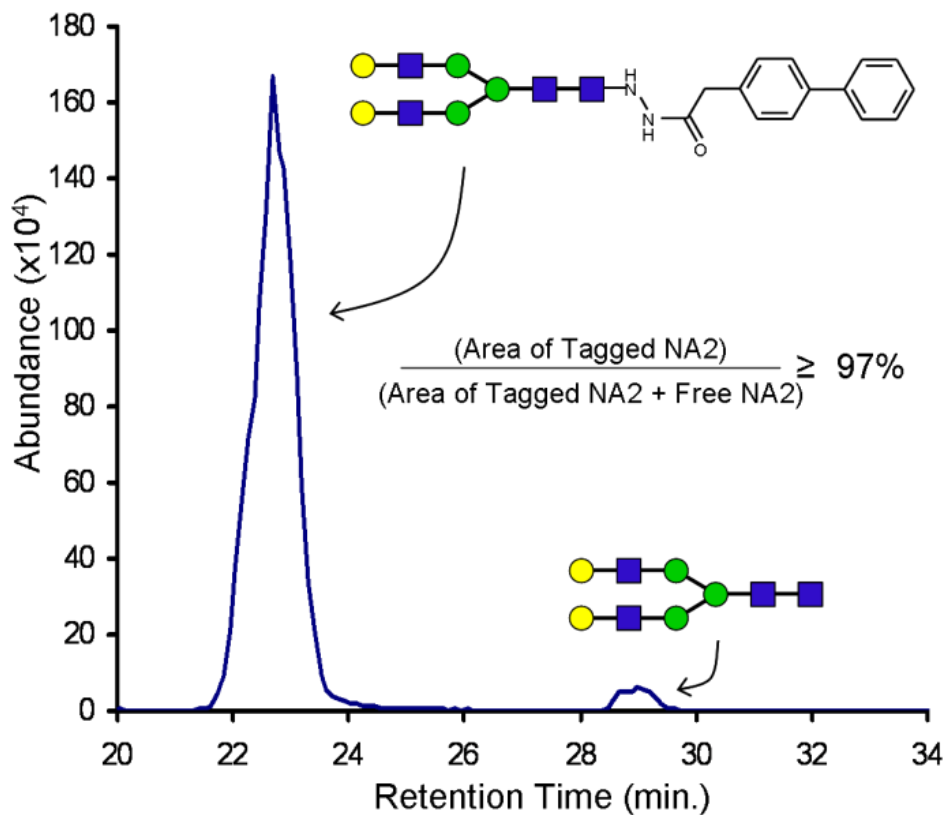


Figure 2.4 – The extracted ion chromatogram of the phenyl-GPN tagged NA2 glycan and the unreacted free NA2 glycan at the optimized reaction conditions determined by the FFD studies. This shows a 97% reaction efficiency for the NA2 glycan.

2.3.2 Analysis of Charged/Neutral Reagents

Two sets of reagents (**Table 2.1**), in which the molecules in each pair differ only by the incorporation of a permanent cationic charge (via quaternary ammonium) in one of the molecules, were analyzed to determine the role of a permanent charge with respect to electrospray ionization. Maltoheptaose (data not shown) and a

complex glycan, NA2, were used to determine the affect of a permanent charge by analyzing an equimolar mixture of each tagging reagent coupled to the oligosaccharide. The EICs for the NA2 glycan are shown in **Figure 2.5**. In both

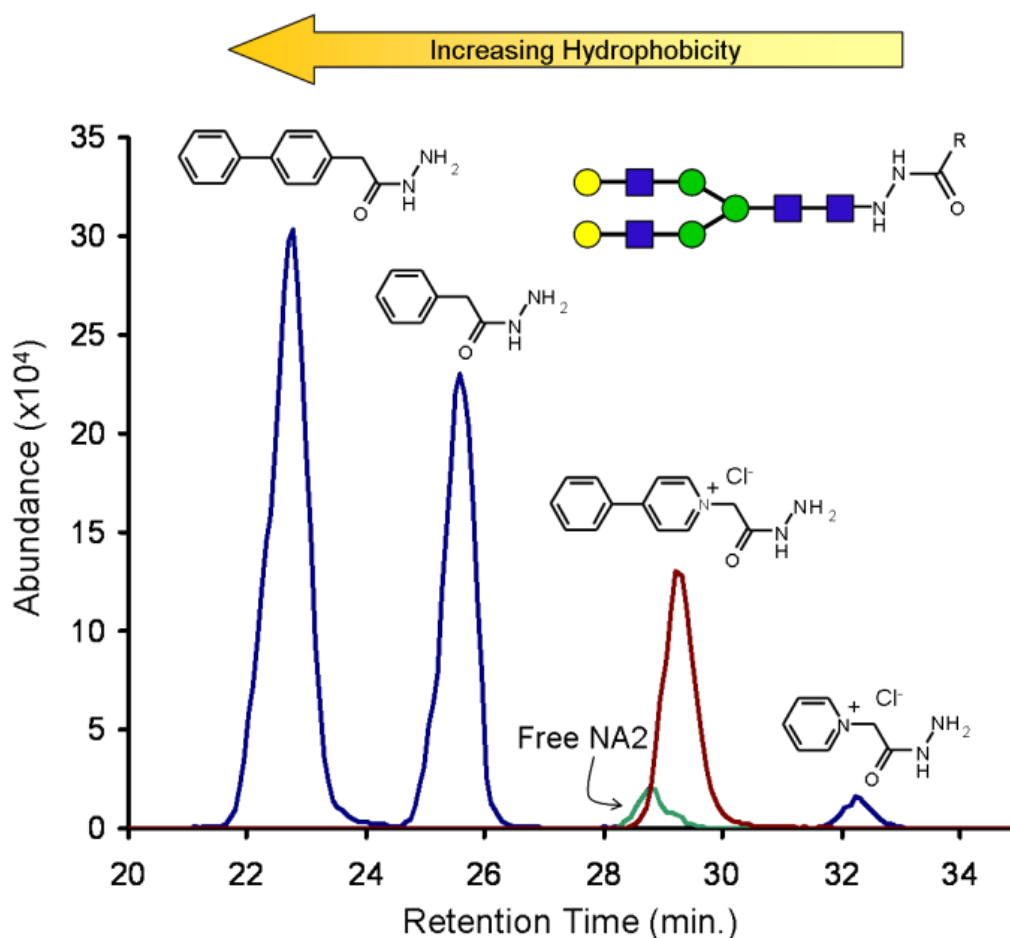


Figure 2.5 – The extracted ion chromatogram of the equimolar mixture made from the NA2 glycan with each tag. The phenyl-GP glycan and the free glycan EIC's are overlaid to show overlapping retention, and the phenyl-GP glycan out-competes the free glycan for excess charge in the electrospray droplet. determined by the FFD studies. This shows a 97% reaction efficiency for the NA2 glycan.

cases (synthesized and commercially available) the neutral tagging reagent outperformed its charged equivalent, and the results are displayed in **Table 2.4**. In the equimolar mixture displayed in **Figure 2.5**, only ~1 pmol of each glycan was introduced onto the chromatography column. This shows that at small amounts of

Table 2.4 – Retention times and relative abundance data for the NA2 glycan equimolar mixture.

Molecule	Retention Time (min)	Fold Increase^a
Phenyl-GPN ^b + NA2	22.8	18
GPN ^b + NA2	25.5	11
Phenyl-GP ^c + NA2	29.2	7
Free NA2	29.1	1
GP ^c + NA2	32.23	<1

^aRelative to free glycan
^bNeutral Reagent
^cCharged Reagent

glycan, a clean-up step after derivatization is not necessary. The starting amount of glycan was much more (~170 pm) in order to minimize the variability in the sample preparation of the equimolar mixture. When pipetting small volumes and small concentrations, a minute amount of variability in the precision of equipment can cause a substantial difference in the concentrations of each species.

These results show that the phenyl-GPN reagent provides an 18-fold increase in electrospray response in comparison to the free NA2 glycan, but these results must be interpreted with caution. Since the phenyl-GP glycan elutes during the same time window as the free glycan, the ionization of the free glycan is suppressed causing the 'fold increase' to be overestimated. Nonetheless, the relative peak areas of the co-eluting phenyl-GP and free NA2 glycans suggest that the phenyl-GP glycan is still more competitive than the free glycan for the surface charge in the electrospray droplet. If this is the case and it is assumed that the hydrophobicity is the only variable determining HILIC retention time (the less retention, the more hydrophobic), then one can argue that a charged moiety on a molecule enhances the ionization. However, recent studies have described HILIC as separating compounds based on a mixed-mode mechanism, where a combination of partitioning and adsorption (due to coulombic interactions or hydrogen bonding) take place⁵²⁻⁵⁴. This study supports these conclusions, and it is hypothesized here that the permanent charge causes the phenyl-GP glycan to be retained longer (due to adsorption) than if the retention mechanism was only based on the hydrophobicity of the molecule (partitioning). Thus, one would conclude that the reason the two molecules elute together is due to a combination of partitioning and adsorption of the phenyl-GP tagged glycan, and the phenyl-GP glycan is actually more hydrophobic, allowing for an increased ESI response relative to the free glycan even though an equimolar mixture of the two analytes elute at the same retention time in HILIC.

Though the phenyl-GP glycan and the free NA2 elute at the same time and the free NA2 signal is suppressed, this does not affect the analysis of the charged and neutral reagents. In this study, the information of concern is how the neutral reagents perform compared to their charged equivalent. From the EIC in **Figure 2.5**, it is clear that the two neutral reagents have enhanced abundances in comparison to the charged reagents, and though previously proposed that a permanent cationic charge would enhance ionization²⁸, this study supports the conclusion that the positive charge actually causes the molecule to be more solvated in the electrospray droplet, less competitive for the excess surface charge, and have a decreased ESI response in comparison with its neutral analogue.

Using these two pairs of reagents, the ESI response in relation to hydrophobicity of the tags was also able to be studied. The two neutral molecules (phenyl-GPN and GPN) only differ by the addition of a phenyl group. The phenyl-GPN glycan eluted almost 4 minutes earlier than the GPN glycan and the detected abundance was increased by ~2-fold. This was also the case with the charged molecules, where the phenyl-GP glycan elutes 4 minutes earlier and has an increased relative abundance to the GP glycan. This suggests that the hydrophobic tagging of glycans will follow similar trends as the hydrophobic tagging of peptides; thus, these synthesized reagents can be further developed to incorporate branched, alkyl, or ring hydrophobic regions in order to further enhance ESI response.

2.3.3 *Non-Polar Surface Area Calculations*

The NPSA of the 4 reagent molecules in this experiment have been calculated and are listed in **Table 2.1**. For both pairs, the equivalent charged and neutral reagents' NPSA calculations are essentially the same, meaning that one should assume that the molecules' hydrophobicities are equivalent, and the ESI responses should be equal as well. However, this is not the case, and the decreased ESI response for an addition of a permanent charge cannot be accounted for by the molecular composition of each reagent. The only other variable that can be accountable for the difference in retention time and abundance is the permanent charge. It is proposed that the cationic charge solvates favorably into the center of the electrospray droplet, causing it to be less competitive for the excess surface charge. Thus, the droplet must undergo much more desolvation in order for the charged reagent glycans to be able to acquire enough charge to be ejected into the gas phase, and by this time, much of the surface charge has already been depleted by the less solvated, more hydrophobic, neutrally tagged glycans.

The HILIC retention times (**Table 2.4**) corroborate these results as well. Because HILIC is a variant of normal phase chromatography, the glycans with the most hydrophobic tags should elute earlier than the free glycan or glycans with more hydrophilic tags, which is clearly shown in **Figure 2.5**. Also, it should be noted that even though the phenyl-GP and GP reagents have a greater NPSA than the free glycan (NPSA ~ 0), the permanent charge causes these tagged glycans to elute after the free glycan, which from the HILIC retention times, one would conclude that

they are more hydrophilic. Though the hydrophobicity of these tags has been increased, the permanent charge negates any positive effect that these tags afford glycans in the electrospray droplet.

2.4 Conclusions

An equimolar mixture of tagged glycans revealed two important trends in the analysis of glycans: 1) as in peptides, the incorporation of increasingly hydrophobic tags increases the ESI response of glycans, and 2) a permanent charge does not enhance ionization, but causes the tagged glycans to be more solvated in the electrospray droplet decreasing the abundance in MS. It was also shown that the optimized procedure affords complex *N*-linked glycans $\geq 97\%$ reaction efficiency, which is necessary in order to avoid the glycan signal being dispersed over several different *m/z* channels. NPSA calculations were also performed in order to confirm that the physical properties of the molecules in each reagent pair are equally hydrophobic without accounting for the effects of a permanent charge. This allowed the permanent charge to be treated as the only independent variable, and conclusions were able to be drawn based solely on the comparative abundance of the charged and neutrally tagged glycans. The results presented here will allow one to make hypothesis-driven predictions for the synthesis of reagents that will further enhance the electrospray ionization of glycans, allowing for decreased limits of detection in glycomics applications such as identifying glycans cleaved from

proteins, quantifying glycans, and detecting relative changes in glycan population towards biomarker discovery.

Future studies will move toward developing neutral hydrazide reagents for the maximum enhancement of glycan signal in ESI-MS. In both cases studied herein, and in previous studies^{16, 18, 29}, the electrospray ionization efficiency of *N*-linked glycans is increased as the hydrophobicity of the tags is increased. Though the trends presented here will be valuable to glycan analysis, further work must be done to determine the types of hydrophobic groups most conducive to glycan analysis. A wide range of hydrazide tagging reagents must be studied in order to determine specific hydrophobic properties (linear, branched, aliphatic or aromatic rings) that will most effectively enhance glycan analysis. In addition, the neutral reagents used in this study will be amenable to glycan analysis in the negative ion mode. This is a highly advantageous scenario as the complimentary information able to be derived from analyzing glycans in the positive and negative ion mode in parallel will require no extra sample preparation yet yield significantly more data. It is through approaches like these that all possible characteristics and properties of glycans can be exploited, and sample preparation can be optimized in order to detect the least abundant glycans in biological samples, acquire the most informative fragmentation spectra, and ensure a thorough assay of the *N*-linked glycome.

2.5 References

- (1) Sharkey, A. G.;Friedel, R. A.;Langer, S. H. Mass Spectra of Trimethylsilyl Derivatives. *Anal. Chem.*, **1957**, 29, 770-776.
- (2) Sweeley, C. C.;Bentley, R.;Makita, M.;Wells, W. W. Gas-Liquid Chromatography of Trimethylsilyl Derivatives of Sugars and Related Substances. *J. Am. Chem. Soc.*, **1963**, 85, 2497-&.
- (3) Yamashita, M.;Fenn, J. B. Electrospray Ion-Source - Another Variation on the Free-Jet Theme. *J. Phys. Chem.*, **1984**, 88, 4451-4459.
- (4) Null, A. P.;Nepomuceno, A. I.;Muddiman, D. C. Implications of hydrophobicity and free energy of solvation for characterization of nucleic acids by electrospray ionization mass spectrometry. *Anal. Chem.*, **2003**, 75, 1331-1339.
- (5) Mirzaei, H.;Regnier, F. Enhancing electrospray ionization efficiency of peptides by derivatization. *Anal. Chem.*, **2006**, 78, 4175-4183.
- (6) Yang, W. C.;Mirzaei, H.;Liu, X. P.;Regnier, F. E. Enhancement of amino acid detection and quantification by electrospray ionization mass spectrometry. *Anal. Chem.*, **2006**, 78, 4702-4708.
- (7) Frahm, J. L.;Bori, I. D.;Comins, D. L.;Hawkrige, A. M.;Muddiman, D. C. Achieving augmented limits of detection for peptides with hydrophobic alkyl tags. *Anal. Chem.*, **2007**, 79, 3989-3995.
- (8) Williams, D. K.;Comins, D. L.;Whitten, J. L.;Muddiman, D. C. Evaluation of the ALiPHAT Method for PC-IDMS and Correlation of Limits-of-Detection with Nonpolar Surface Area. *J. Am. Soc. Mass. Spectrom.*, **2009**, 20, 2006-2012.
- (9) Shuford, C. M.;Comins, D. L.;Whitten, J. L.;Burnett, J. C.;Muddiman, D. C. Improving limits of detection for B-type natriuretic peptide using PC-IDMS: An application of the ALiPHAT strategy. *Analyst*, **2010**, 135, 36-41.
- (10) Williams, D. K.;Meadows, C. W.;Bori, I. D.;Hawkrige, A. M.;Comins, D. L.;Muddiman, D. C. Synthesis, characterization, and application of iodoacetamide derivatives utilized for the ALiPHAT strategy. *J. Am. Chem. Soc.*, **2008**, 130, 2122-2123.

- (11) Dell, A. Preparation and Desorption Mass-Spectrometry of Permethy and Peracetyl Derivatives of Oligosaccharides. *Methods in Enzymology*, **1990**, 193, 647-660.
- (12) Ciucanu, I.;Kerek, F. A Simple and Rapid Method for the Permethylation of Carbohydrates. *Carbohydr. Res.*, **1984**, 131, 209-217.
- (13) Bourne, E. J.;Stacey, M.;Tatlow, J. C.;Tedder, J. M. Studies on Trifluoroacetic Acid .1. Trifluoroacetic Anhydride as a Promoter of Ester Formation between Hydroxy-Compounds and Carboxylic Acids. *J. Chem. Soc.*, **1949**, 2976-2979.
- (14) Lamari, F. N.;Kuhn, R.;Karamanos, N. K. Derivatization of carbohydrates for chromatographic, electrophoretic and mass spectrometric structure analysis. *J. Chromatogr., B*, **2003**, 793, 15-36.
- (15) Tarentino, A. L.;Trimble, R. B.;Plummer, T. H. Enzymatic Approaches for Studying the Structure, Synthesis, and Processing of Glycoproteins. *Meth. Cell Biology*, **1989**, 32, 111-139.
- (16) Poulter, L.;Burlingame, A. L. Desorption Mass-Spectrometry of Oligosaccharides Coupled with Hydrophobic Chromophores. *Methods Enzymol.*, **1990**, 193, 661-688.
- (17) Harvey, D. J. Electrospray mass spectrometry and fragmentation of N-linked carbohydrates derivatized at the reducing terminus. *J. Am. Soc. Mass Spectrom.*, **2000**, 11, 900-915.
- (18) Bowman, M. J.;Zaia, J. Tags for the stable isotopic labeling of carbohydrates and quantitative analysis by mass spectrometry. *Anal. Chem.*, **2007**, 79, 5777-5784.
- (19) Bowman, M. J.;Zaia, J. Comparative Glycomics Using a Tetraplex Stable-Isotope Coded Tag. *Anal. Chem.*, **2010**, 82, 3023-3031.
- (20) Hase, S.;Ikenaka, T.;Matsushima, Y. A Highly Sensitive Method for Analyses of Sugar Moieties of Glycoproteins by Fluorescence Labeling. *J. Biochem.*, **1981**, 90, 407-414.
- (21) Schwaiger, H.;Oefner, P. J.;Huber, C.;Grill, E.;Bonn, G. K. Capillary Zone Electrophoresis and Micellar Electrokinetic Chromatography of 4-Aminobenzonitrile Carbohydrate-Derivatives. *Electrophoresis*, **1994**, 15, 941-952.

- (22) Yoshino, K.;Takao, T.;Murata, H.;Shimonishi, Y. Use of the Derivatizing Agent 4-Aminobenzoic Acid 2-(Diethylamino)Ethyl Ester for High-Sensitivity Detection of Oligosaccharides by Electrospray-Ionization Mass-Spectrometry. *Anal. Chem.*, **1995**, *67*, 4028-4031.
- (23) Pabst, M.;Kolarich, D.;Poltl, G.;Dalik, T.;Lubec, G.;Hofinger, A.;Altmann, F. Comparison of fluorescent labels for oligosaccharides and introduction of a new postlabeling purification method. *Anal. Biochem.*, **2009**, *384*, 263-273.
- (24) Lattova, E.;Snovida, S.;Perreault, H.;Krokhin, O. Influence of the labeling group on ionization and fragmentation of carbohydrates in mass spectrometry. *J. Am. Soc. Mass Spectrom.*, **2005**, *16*, 683-696.
- (25) Avigad, G. Dansyl Hydrazine as a Fluorimetric Reagent for Thin-Layer Chromatographic Analysis of Reducing Sugars. *J. Chromatogr.*, **1977**, *139*, 343-347.
- (26) Karamanos, N. K.;Tsegenidis, T.;Antonopoulos, C. A. Analysis of Neutral Sugars as Dinitrophenyl-Hydrazones by High-Performance Liquid-Chromatography. *J. Chromatogr.*, **1987**, *405*, 221-228.
- (27) Miksik, I.;Gabriel, J.;Deyl, Z. Microemulsion electrokinetic chromatography of diphenylhydrazones of dicarbonyl sugars. *J. Chromatogr. A*, **1997**, *772*, 297-303.
- (28) Naven, T. J. P.;Harvey, D. J. Cationic derivatization of oligosaccharides with Girard's T reagent for improved performance in matrix-assisted laser desorption/ionization and electrospray mass spectrometry. *Rapid Commun. Mass Spectrom.*, **1996**, *10*, 829-834.
- (29) Bereman, M. S.;Comins, D. L.;Muddiman, D. C. Increasing the hydrophobicity and electrospray response of glycans through derivatization with novel cationic hydrazides. *Chem. Comm.*, **2010**, *46*, 237-239.
- (30) Domon, B.;Mueller, D. R.;Richter, W. J. Tandem Mass-Spectrometric Analysis of Fixed-Charge Derivatized Oligosaccharides. *Organic Mass Spectrometry*, **1994**, *29*, 713-719.
- (31) Fenn, J. B. Ion Formation from Charged Droplets - Roles of Geometry, Energy, and Time. *J. Am. Soc. Mass Spectrom.*, **1993**, *4*, 524-535.
- (32) Cech, N. B.;Enke, C. G. Relating electrospray ionization response to nonpolar character of small peptides. *Anal. Chem.*, **2000**, *72*, 2717-2723.

- (33) Louvar, J. F. Simplify Experimental Design. *Chemical Engineering Progress*, **2010**, *106*, 35-40.
- (34) Hull, S. R.;Turco, S. J. Separation of Dansyl Hydrazine-Derivatized Oligosaccharides by Liquid-Chromatography. *Anal. Biochem.*, **1985**, *146*, 143-149.
- (35) Shinohara, Y.;Sota, H.;Kim, F.;Shimizu, M.;Gotoh, M.;Tosu, M.;Hasegawa, Y. Use of a Biosensor Based on Surface-Plasmon Resonance and Biotinyl Glycans for Analysis of Sugar Binding Specificities of Lectins. *J. Biochem*, **1995**, *117*, 1076-1082.
- (36) Gil, G. C.;Kim, Y. G.;Kim, B. G. A relative and absolute quantification of neutral N-linked oligosaccharides using modification with carboxymethyl trimethylammonium hydrazide and matrix-assisted laser desorption/ionization time-of-flight mass spectrometry. *Anal. Biochem.*, **2008**, *379*, 45-59.
- (37) Andrews, G. L.;Shuford, C. M.;Burnett, J. C.;Hawkridge, A. M.;Muddiman, D. C. Coupling of a vented column with splitless nanoRPLC-ESI-MS for the improved separation and detection of brain natriuretic peptide-32 and its proteolytic peptides. *J. Chromatogr. B*, **2009**, *877*, 948-954.
- (38) Bereman, M. S.;Young, D. D.;Deiters, A.;Muddiman, D. C. Development of a Robust and High Throughput Method for Profiling N-Linked Glycans Derived from Plasma Glycoproteins by NanoLC-FTICR Mass Spectrometry. *J. Proteome Res.*, **2009**, *8*, 3764-3770.
- (39) Wheeler, S. F.;Harvey, D. J. Negative ion mass spectrometry of sialylated carbohydrates: Discrimination of N-acetylneuraminic acid linkages by MALDI-TOF and ESI-TOF mass spectrometry. *Anal. Chem.*, **2000**, *72*, 5027-5039.
- (40) Chai, W. G.;Piskarev, V.;Lawson, A. M. Negative ion electrospray mass spectrometry of neutral underivatized oligosaccharides. *Anal. Chem.*, **2001**, *73*, 651-657.
- (41) Chai, W. G.;Piskarev, V.;Lawson, A. M. Branching pattern and sequence analysis of underivatized oligosaccharides by combined MS/MS of singly and doubly charged molecular ions in negative-ion electrospray mass spectrometry. *J. Am. Soc. Mass Spectrom.*, **2002**, *13*, 670-679.
- (42) Pfenninger, A.;Karas, M.;Finke, B.;Stahl, B. Structural analysis of underivatized neutral human milk oligosaccharides in the negative ion mode

- by nano-electrospray MSn (Part 2: Application to isomeric mixtures). *J. Am. Soc. Mass Spectrom.*, **2002**, *13*, 1341-1348.
- (43) Pfenninger, A.;Karas, M.;Finke, B.;Stahl, B. Structural analysis of underivatized neutral human milk oligosaccharides in the negative ion mode by nano-electrospray MSn (Part 1: Methodology). *J. Am. Soc. Mass Spectrom.*, **2002**, *13*, 1331-1340.
- (44) Harvey, D. J. Fragmentation of negative ions from carbohydrates: Part 1. Use of nitrate and other anionic adducts for the production of negative ion electrospray spectra from N-linked carbohydrates. *J. Am. Soc. Mass Spectrom.*, **2005**, *16*, 622-630.
- (45) Harvey, D. J. Fragmentation of negative ions from carbohydrates: Part 2. Fragmentation of high-mannose N-linked glycans. *J. Am. Soc. Mass Spectrom.*, **2005**, *16*, 631-646.
- (46) Harvey, D. J. Fragmentation of negative ions from carbohydrates: Part 3. Fragmentation of hybrid and complex N-linked glycans. *J. Am. Soc. Mass Spectrom.*, **2005**, *16*, 647-659.
- (47) Kovacik, V.;Hirsch, J.;Kovac, P.;Heerma, W.;Thomasoates, J.;Haverkamp, J. Oligosaccharide Characterization Using Collision-Induced Dissociation Fast-Atom-Bombardment Mass-Spectrometry - Evidence for Internal Monosaccharide Residue Loss. *J. Mass Spectrom.*, **1995**, *30*, 949-958.
- (48) Brull, L. P.;Heerma, W.;ThomasOates, J.;Haverkamp, J.;Kovacik, V.;Kovac, P. Loss of internal 1->6 substituted monosaccharide residues from underivatized and per-O-methylated trisaccharides. *J. Am. Soc. Mass Spectrom.*, **1997**, *8*, 43-49.
- (49) Ernst, B.;Muller, D. R.;Richter, W. J. False sugar sequence ions in electrospray tandem mass spectrometry of underivatized sialyl-Lewis-type oligosaccharides. *Int. J. Mass Spectrom Ion Proc.*, **1997**, *160*, 283-290.
- (50) Brull, L. P.;Kovacik, V.;Thomas-Oates, J. E.;Heerma, W.;Haverkamp, J. Sodium-cationized oligosaccharides do not appear to undergo 'internal residue loss' rearrangement processes on tandem mass spectrometry. *Rapid Commun. Mass Spectrom.*, **1998**, *12*, 1520-1532.
- (51) Harvey, D. J.;Mattu, T. S.;Wormald, M. R.;Royle, L.;Dwek, R. A.;Rudd, P. M. "Internal residue loss": Rearrangements occurring during the fragmentation of

- carbohydrates derivatized at the reducing terminus. *Anal. Chem.*, **2002**, *74*, 734-740.
- (52) Hemstrom, P.;Irgum, K. Hydrophilic interaction chromatography. *J. Sep. Sci.*, **2006**, *29*, 1784-1821.
- (53) Nguyen, H. P.;Schug, K. A. The advantages of ESI-MS detection in conjunction with HILIC mode separations: Fundamentals and applications. *J. Sep. Sci.*, **2008**, *31*, 1465-1480.
- (54) Dejaegher, B.;Heyden, Y. V. HILIC methods in pharmaceutical analysis. *J. Sep. Sci.*, **2010**, *33*, 698-715.

CHAPTER 3

Hydrophobic Derivatization of *N*-linked Glycans for Increased Ion Abundance in Electrospray Ionization Mass Spectrometry

The following work was reprinted with permission from: Walker, S. H.; Lilley, L. M.; Enamorado, M. F.; Comins, D. L.; Muddiman, D. C. *Journal of the American Society for Mass Spectrometry* **2011**, 22(8), 1309-1317. Copyright 2011 Springer. The original publication may be accessed directly via the World Wide Web.

3.1 Introduction

The inherent hydrophobic bias in electrospray ionization (ESI) has been exploited in numerous studies first for nucleic acids¹, then peptides and proteins²⁻⁷, and most recently glycans⁸⁻¹⁴ in order to increase the ion abundance of analytes in mass spectrometry (MS). While these techniques frequently introduce an additional wet chemistry step in sample preparation, the benefits have been shown to outweigh the time and cost; a >2000-fold improvement in peptide signal has been reported⁷. The addition of hydrophobic functions to molecules *via* chemical derivatization will not only increase the ion abundance in ESI but can also have other beneficial aspects, such as the ability to incorporate stable isotopes for quantification^{10, 15} and the enhanced information acquired from fragmentation spectra in the permethylation of glycans¹⁶. Analysis of glycans by ESI has been hampered by the hydrophilicity of the sugar functional groups causing them to have a higher free energy of solvation and be more difficult to desorb from the electrospray droplet in the generation of gas-phase ions. Thus, derivatization using hydrophobic reagents can be used to aid in overcoming this obstacle. Imparting additional hydrophobic functions onto glycan

molecules allows the glycans to be less solvated and have a higher surface activity in the precursor electrospray droplet. As this droplet is desolvated on the way to the MS, a series of Coulombic fission events occur where a number of smaller progeny droplets (estimated to be $\sim 20^{17}$) are ejected from the surface of the original droplet¹⁷⁻¹⁹. In comparison with the native glycans, the more hydrophobic, derivatized glycans are more likely to have a higher surface activity and are significantly enriched in the progeny droplets²⁰. It is these progeny droplets that are further desolvated and eventually produce gas-phase ions²¹, creating the hydrophobic bias in ESI.

Permethylation²²⁻²⁴ and peracetylation^{23, 25} are two of the first methods used to derivatize glycans for enhanced MS analysis. These methods have been shown to enhance fragmentation spectra²⁶⁻²⁷ and increase the glycan ion abundance. However, permethylation and peracetylation convert all hydroxyl, amino, and carboxylic acid groups to their methyl- and acetyl-ether functions, respectively, and thus, the m/z shift due to the derivatization is variable for different sized glycans. Additionally, 100% conversion has proven difficult and is variable for different *N*-linked glycans. For example, due to the numerous hydroxyl, amino, and carboxylic groups present in oligosaccharides (~ 5 per monosaccharide and 7-18 monosaccharides per *N*-linked glycan), a 0.1% change in the permethylation efficiency can result in a 3-10% efficiency difference depending on the type and size of the glycan. In contrast, the reducing terminus is a convenient location for derivatization due to the availability of a free aldehyde group after the enzymatic cleavage of *N*-linked glycans from proteins using peptide: *N*-glycosidase F (PNGase

F). Moreover, stable isotope labels with a small, fixed mass shift can be incorporated onto the reagents while simultaneously increasing the hydrophobicity. Reductive amination is a prominent technique capable of reacting with the reducing terminus of *N*-linked glycans and has been used to enhance several analytical techniques including UV and fluorescence detection²⁸⁻³¹ and hydrophobic derivatization^{9-10, 32-33}. Two studies have shown the ability to incorporate hydrophobic tagging and isotopic labeling using reductive amination derivatization^{10, 15}. Though this method is effective, an additional significant clean-up step is necessary after derivatization due to salt contamination, which often increases sample preparation time, the opportunity for sample loss, and the analytical variability in the measurement.

Hydrazone formation is an attractive alternative derivatization strategy in which hydrazide reagents react at the reducing terminus of glycans much like reductive amination but does not involve reducing the glycan to a Schiff base using salts such as sodium borohydride³⁴. Thus, when using hydrazone formation, the product can be directly injected onto the nano-LC column due to the lack of salts necessary in the reaction mixture. In addition, >95% reaction efficiency can be routinely achieved using hydrazone formation as a means of hydrophobic tagging of glycans¹³. Danzylhydrazine³⁵ was the first of many reagents to be coupled to glycans via hydrazone formation for enhanced fluorescence or UV detection³⁶⁻³⁸. More recently, hydrazone formation has been used for enhanced MS detection^{8, 12-13}, though an abundance of these reagents is not readily available. Several different

hydrazide reagents have been developed and used to increase glycan abundance^{8, 12-13}. Girard's T reagent was first used to increase mass spectral detection in order to incorporate a permanent cationic charge onto the glycan¹². However, recent studies have shown decreases in ion abundance when coupling Girard's T reagent to glycans in nanoLC MS⁸, and it has been shown that neutral reagents are significantly better than preformed cations when coupled to *N*-linked glycans^{8, 13}.

Herein, a small library of hydrazide reagents has been synthesized and is used to derivatize glycans in order to determine the type of hydrophobic structure that most effectively increases the ion abundance of glycans in ESI-MS. The reagents studied are exclusively neutral compounds due to the compatibility in positive and negative mode MS and due to recent studies showing decreased electrospray response when incorporating a permanent charge on the reagent (*vide supra*)¹³. Additionally, the non-polar surface areas (NPSA) for all the reagents have been calculated in order to give a theoretical estimate of the hydrophobicity of the reagents as it has been shown that the NPSA correlates directly with the hydrophobicity of the analytes in peptide analysis⁵⁻⁶. Furthermore, the compatibility of the hydrazone reagents with complex mixtures and the advantages present are demonstrated by the derivatization of *N*-linked glycans found in human plasma.

3.2 Experimental

3.2.1 Materials

The (Gal-GlcNAc)₂Man₃GlcNAc₂ (NA2) glycan, (NeuAc-Gal-GlcNAc)₂Man₃(Fuc)(GlcNAc)₂ (A2F) glycan, trifluoroacetic acid (TFA), acetic acid, ammonium acetate, ethyl chloroacetate, and β-mercaptoethanol were all purchased from Sigma Aldrich (St Louis, MO). Phenylacetic acid, 3-phenylpropionic acid, 4-phenylbutanoic acid, 5-phenylpentanoic acid, ethynyl benzene, ethyl 2-(4-bromophenyl)acetate, hydrazine hydrate, 4-phenylpyridine, and ethyl phenylacetate were purchased from VWR (West Chester, PA). Peptide: *N*-Glycosidase F (2.5 mU/μL), denaturing solution (1 M β-mercaptoethanol and 2% (w/w) SDS), and the detergent solution (15% nonidet P40) were purchased from Prozyme (San Leandro, CA). Pooled human plasma was purchased from Innovative Research (Novi, MI). High performance liquid chromatography grade acetonitrile (ACN), water, and methanol (MeOH) were all purchased from Burdick & Jackson (Muskegon, MI). IntegraFrit and PicoFrit columns were purchased from New Objective (Woburn, MA) and the TSK-Gel Amide-80 stationary phase was from TOSOH Bioscience (San Jose, CA). The graphitized solid phase extraction cartridges were purchased from Alltech (Deerfield, IL).

3.2.2 Reagent Synthesis, Purification, and Characterization

Five hydrazide reagents were synthesized: 2-phenylacetohydrazide (GPN), 3-phenylpropanehydrazide (GPN2), 4-phenylbutanehydrazide (GPN3), 5-

phenylpentanehydrazide (GPN4), and 4-phenethylbenzohydrazide (phenyl2-GPN). The mono-phenyl reagents were synthesized by Fischer esterification, converting a carboxylic acid to a methyl ester followed by reaction with hydrazine hydrate in absolute ethanol at 90°C to form the hydrazide. The bi-phenyl reagent (phenyl2-GPN) was synthesized by reacting ethynyl benzene with ethyl 2-(4-bromophenyl)acetate in the presence of a catalyst and the triple bond was hydrogenated in absolute ethanol over Pd/C. As with the mono-phenyl reagents the ester was converted to a hydrazide function *via* reaction with hydrazine hydrate in absolute ethanol incubated at 90°C. Synthesis schemes, purification methods, and characterization data have been extensively detailed in the supplemental material (**Appendix A**).

3.2.3 Reagent Analysis for Model Glycan

A 2 mg/mL solution of each individual reagent was made in 85:15 MeOH:acetic acid (v/v). The NA2 glycan was aliquotted into 6 microcentrifuge tubes (170 pmol in each tube), dried, and 100 µL (~3500 mol XS) of the synthesized reagents (GPN, GPN2, GPN3, GPN4, and phenyl2-GPN) were added to separate dried glycan samples so that 5 of the tubes have a different tag in each tube and the final glycan sample has no tag (only 100 µL of reaction solvent was added). The six samples were allowed to incubate at 75°C for three hours, and the samples were dried *in vacuo*. A reaction diagram with starting materials and the final derivatized glycan structure is presented in the supplemental material (**Figure A.1**). The

samples were then reconstituted in HILIC initial conditions (80% ACN and 20% 50 mM ammonium acetate in water), and the six glycan samples were combined in an equimolar mixture so that ~1 pmol of each was injected on column in a 10 μ L injection and analyzed using nanoLC LTQ-FTICR MS.

3.2.4 Cleavage, Derivatization, and Analysis of Plasma N-linked Glycans

Fifty microliters of lyophilized pooled human plasma was reconstituted in 250 μ L of 50 mM tris-HCl buffer (pH 7.5) and denatured by adding 28 μ L of 2% SDS/1 M β -mercaptoethanol and incubating at 95°C for 5 min. The solution was allowed to cool to room temperature, and 5 μ L of PNGase F (12.5 mU) was added. The reaction was allowed to proceed for 18 hr. at 37°C. The reaction was then quenched with 500 μ L of 0.1% TFA. The glycans were extracted using graphitized carbon solid phase extraction (SPE), which has been described in detail previously³⁹, and the glycan samples were dried *in vacuo*.

The derivatization procedure for plasma glycans was optimized to decrease the amount of peeling for labile capping sugar units such as sialic acid and fucose. A 1 mg/ml solution of phenyl2-GPN reagent in 75:25 MeOH:Acetic acid solution was prepared. To the dried glycan sample, 100 μ L of the reagent solution was added and allowed to react for 3 hrs at 56°C in an incubator. The glycans were then dried *in vacuo* and reconstituted in HILIC initial conditions.

3.2.5 *nano-Flow Liquid Chromatography (HILIC)*

Separation of derivatized glycans was performed using online hydrophilic interaction (liquid) chromatography (HILIC)³⁹. An Eksigent nanoLC-2D system equipped with an AS1 autosampler (Dublin, CA) was used with a vented-column setup as described previously⁴⁰. TSK-Gel Amide-80 stationary phase with a 5 μm particle size (TOSOH Bioscience) was used to pack the trap and analytical columns, and both were packed in house. The trap column (360 μm O.D., 100 μm I.D. IntegraFrit) was packed to ~ 3.2 cm, and the analytical column (360 μm O.D., 75 μm I.D. with a 15 μm PicoFrit tip) was packed to ~ 10 cm. Mobile phase A and B were 50 mM ammonium acetate (pH 4.5) and 100% ACN, respectively. Onto the trap, 10 μL of sample were injected at the initial gradient conditions (20% solvent A), washed at high organic solvent (93% B), and eluted at 500 nL/min. The gradient was ramped from 20 to 60 % Solvent A over 37 min with a total run time of 60 min. A shallower gradient was used with the plasma glycans that included an additional washing step in high organic solvent (93% B). The gradient for plasma glycans was ramped from 20 to 55% solvent A over 37 min, and the total run time was 70 min.

3.2.6 *LTQ-FTICR Mass Spectrometry*

A hybrid linear ion trap Fourier Transform ion cyclotron resonance mass spectrometer (Thermo Fisher Scientific, San Jose, CA) equipped with a 7 Tesla superconducting magnet was used to acquire precursor and product ion mass spectra. Electrospray ionization was performed by applying a 2 kV potential to a

zero dead volume union preceding the trap column. The ions were introduced into a stainless steel capillary heated to 225 °C, and the capillary and tube lens voltages were set to 42 V and 120 V, respectively. The AGC in the ICR cell was set to 1×10^6 ions with a maximum injection time of 1 s. In the LTQ, the AGC was set to 8×10^3 ions with a maximum injection time of 80 ms and a normalized collision energy of 22. The instrument was operated in data dependent mode where up to 3 MS/MS spectra were collected per precursor scan. An include list was generated consisting of the 3 most intense m/z values in the precursor scan (FTICR), and these ions were subsequently fragmented (LTQ). If the same m/z value is chosen twice in 30 s, the m/z was placed on an exclude list for 30 s. Additionally, a 5000 count threshold was used to ensure quality MS/MS spectra. The mass spectrometer was calibrated according to manufacturer protocol and Xcalibur software (v. 2.0.5) was used for peak integration and data analysis.

3.2.7 Non-Polar Surface Area Calculations

The NPSA were calculated as reported previously⁵. Due to the numerous hydrophilic functions, such as hydroxyl groups, that comprise glycans, the NPSA of the sugar units are deemed negligible. Thus, only the NPSA of the hydrophobic tagging reagents are taken into account. The NPSA of the reagents were calculated by using standard Van der Waal's radii and bond lengths⁴¹. Other previous studies have used computer modeling to integrate the NPSA of reagents¹³ and alternate assumptions^{6, 8} in the determination of NPSA; thus, a detailed description of the

assumptions, formulas, and calculations is included in the supplemental material (**Figure A.2**) in order to present a single method for NPSA calculations of hydrophobic tagging reagents.

3.3 Results and Discussion

3.3.1 Characterization of Hydrazone Reagents

Five neutral reagents were synthesized in order to increase the relative abundance of *N*-linked glycans in ESI MS, analyze the types of hydrophobic groups that most effectively increase the electrospray response of glycans in MS, and direct the future synthesis of hydrazone reagents *en route* to determining an optimal tag for enhanced glycan analysis and quantification. Neutral reagents were chosen due to former studies showing the decreased ion abundance of glycans derivatized with permanently charged (+) reagents¹³. Furthermore, neutral reagents are compatible in both the positive and negative ion modes in ESI MS. Since the negative ion mode has shown to be advantageous to glycan analysis (more informative fragmentation patterns and the enhanced analysis of glycans with acidic sugar residues such as sialic acid)⁴²⁻⁴⁸, the neutral reagents allow one to explore more experimental space without any additional sample preparation when switching between positive and negative modes. Two types of reagents have been synthesized: mono-phenyl and bi-phenyl. A set of mono-phenyl reagents was synthesized in order to vary the alkyl chain length from 1-4 methylene units between the reactive site and the phenyl group. This will allow one to evaluate the affect of lengthening the hydrocarbon

chain length with respect to the relative glycan response in ESI-MS. In addition, another set of molecules has been synthesized that contains bi-phenyl reagents. These two types of hydrophobic groups differ in their types of bonds (sigma vs. pi), geometry (tetrahedral vs. planar), chemical structure, and localization of the electrons. The different characteristics of the reagents will allow for different solvent-analyte interactions in the electrospray droplet, and the characteristics most beneficial will be incorporated into future reagents in order to further enhance the ionization efficiency of glycans.

The synthesis and purification of the reagents were efficient and were confirmed by the accurate mass spectra of the derivatized NA2 glycan in the FT ICR MS. Each reagent was coupled to the glycan and run individually in order to determine reaction efficiency and purity (data not shown). All reagents reacted nearly stoichiometrically with >95% efficiency, and there were no spectra in which there were more than two *N*-linked glycan peaks (tagged and free glycan), implying that there were no impurities or partial synthetic products present capable of reaction with the glycans. In addition, this is also evidence that the tags do not degrade in the reaction conditions or in the ionization source before analysis in the MS. Several characterization methods have been employed in order to confirm the synthesis of the reagents including ^1H NMR, ^{13}C NMR, IR and high resolution MS, and are included in the supplemental material.

The effects of the hydrophobic hydrazide reagents were analyzed by creating an equimolar mixture of the NA2 glycan derivatized with each synthesized reagent,

and the derivatized glycans show significant increases in ion abundance in comparison to the native glycan (**Figure 3.1b**). The extracted ion chromatograms (EIC) of each reagent are displayed to show the retention time and relative abundance of each tagged glycan. The reagents synthesized in this experiment (**Figure 3.1a**) were chosen to observe the effectiveness of incorporating linear

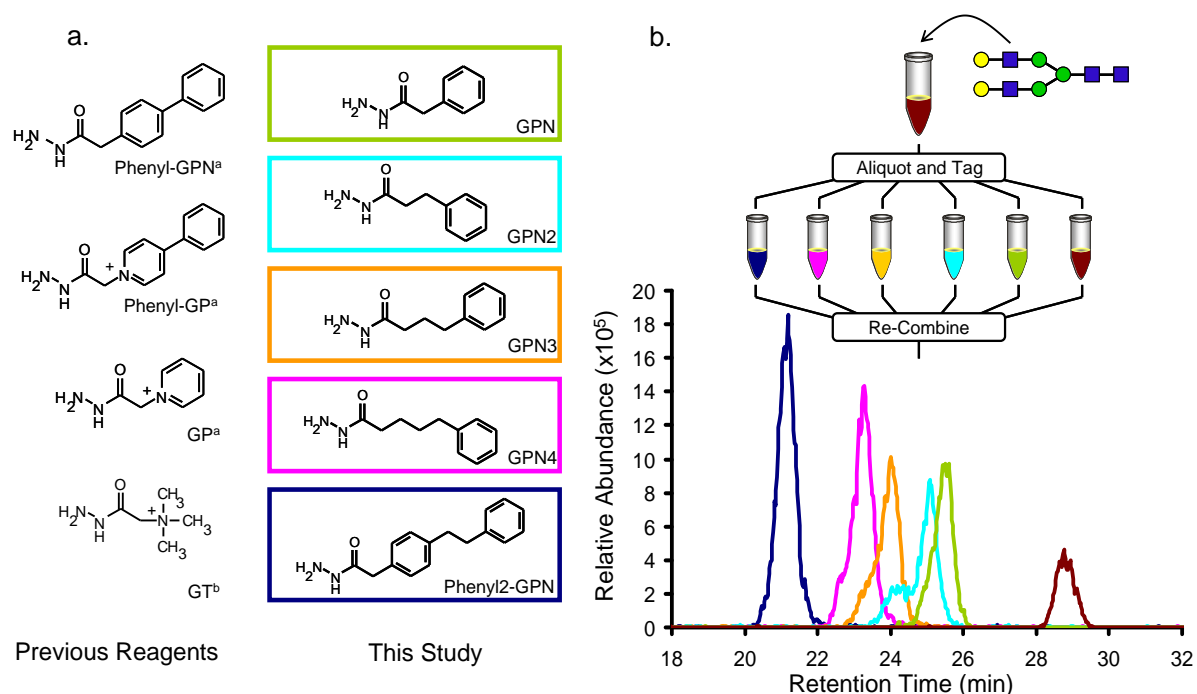


Figure 3.1 – a) The reagents analyzed in this and in previous experiments (^aRef. 1; ^bRef. 2). **b)** The EIC's of each of the current (boxed) reagents coupled to the NA2 glycan. The HILIC elution order is from the most hydrophobic reagents to the least (phenyl2-GPN, GPN4, GPN3, GPN2, GPN, native glycan). The relative abundances follow the same trend, as expected.

alkane hydrophobic groups and additional phenyl groups onto the reagents. One phenyl group on the tagging reagent is necessary for the incorporation of stable isotopes ($^{13}\text{C}_6$) for future quantification studies, but as previously shown, a second phenyl group significantly increases the ion abundance of tagged glycans¹³. It was hypothesized that alkyl groups are more hydrophobic than phenyl groups due to the delocalization of the *pi* bonds in the phenyl ring, and a larger increase in electrospray response would be expected for the reagents with linear alkanes. As the number of methylene groups is increased, the ion abundance increased, although it was not until the addition of 3 additional methylene groups (GPN4) that the electrospray response of the derivatized NA2 glycan increased equivalently to that of the reagent with two phenyl groups and no methylene groups (phenyl-GPN). In addition, the combination of two additional alkyl groups and two phenyl groups produced a reagent that outperformed any reagent synthesized to date. This evidence leads one to infer that the best method to increase the electrospray response of glycans is to add several phenyl rings to the reagents with the possibility of incorporating short alkyl chains between the rings.

In order to further characterize the derivatized glycans and to confirm the stability of the reagents throughout the sample preparation and MS analysis, the MS/MS spectra of the two most successful reagents, phenyl₂-GPN and GPN4, are shown in **Figure 3.2a** and **3.2b**, respectively. These spectra show similar fragmentation in both types of reagents, mono- and bi-phenyl. In no spectrum has fragmentation of the reagent been observed, and the tag is never cleaved from the

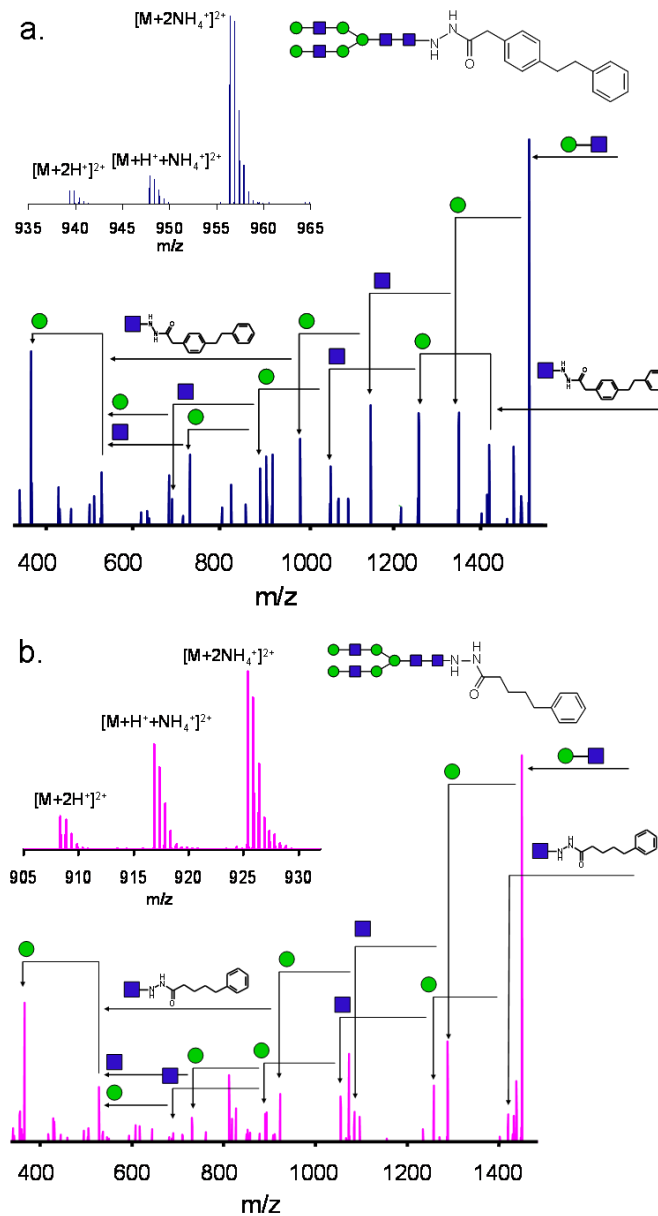


Figure 3.2 – The MS/MS data of the **a)** phenyl2-GPN and **b)** GPN4 reagents. The two fragmentation spectra show similar patterns, and in no case was a loss or fragmentation of the tagging reagent observed. In addition, the composition of the glycan was able to be determined using the MS/MS spectra. The insets are the high mass measurement accuracy FT-ICR precursor ions, showing the monoisotopic peak ($[M+2H^+]^{2+}$) and the ammonium adduction peaks ($[M+H^++NH_4^+]^{2+}$ and $[M+2NH_4^+]^{2+}$). In both **a** and **b**, squares and circles denote N-acetylglucosamine (HexNAc) and hexose (Hex) monosaccharide residues, respectively.

terminal GlcNAc residue, which allows for the determination of y and b glycosidic bond cleavages per Domon and Costello²⁶. These fragmentation spectra show that the composition of unknown glycans can be determined using either the high mass measurement accuracy of the precursor scan, by the MS/MS spectra, or a combination of both. The signal-to-noise (S/N) ratios of the fragmentation spectra show good quality with only ~1 pmol introduced onto column, and nearly all the fragmentation products are present. This was not the case for the native glycans, where several fragmentation peaks were not able to be distinguished from the noise.

Non-polar surface area (NPSA) calculations are used to estimate the hydrophobicity of the hydrazide reagents. By estimating the hydrophobicity of the reagents, the most successful reagent will be able to be predicted. **Figure 3.3a** demonstrates the correlation between the NPSA calculations and the experimental ion abundances for the NA2 glycan derivatized with several different reagents. In general, as the NPSA, or hydrophobicity, of the reagent is increased, the signal of the derivatized glycan is increased as well. Based on this experimental data, future synthetic routes can be developed based on the NPSA and predict the types of hydrophobic reagents that will most effectively enhance the glycan ion abundance. This directed synthetic approach will allow only the reagents with the best chance of further increasing glycan ion abundance to be tested, and as the library continues to grow, the correlation between NPSA and relative glycan abundance will become more evident and lead toward the best possible hydrophobic reagent. However, increasing the hydrophobicity too much will be possible, leading to analytes that are

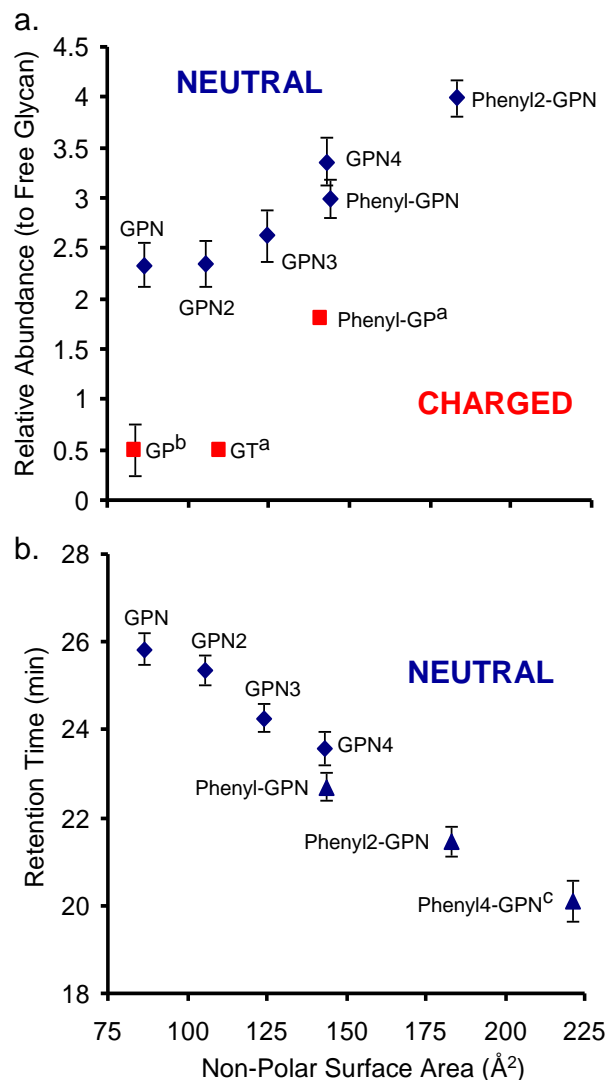


Figure 3.3 – a) The abundance of the derivatized glycan (relative to the free glycan) has been plotted vs. the NPSA of the reagents. Diamonds denote neutral reagents, and squares represent charged reagents (^aRef. 1; ^bRef. 2). **b)** The retention time of the derivatized glycan is plotted vs. the NPSA of the reagents. Diamonds represent mono-phenyl reagents, and triangles represent bi-phenyl reagents. The error bars in both **a** and **b** indicate 95% confidence intervals ($3 \leq n \leq 5$). ^cThe phenyl4-GPN reagent was synthesized (identical to phenyl2-GPN, except that it contains a 4-C chain between the phenyl rings), but the recrystallization purification was only minimally successful, and thus, it was analyzed for retention time purposes only and not for quantitative analysis.

not retained on a HILIC column or reagents that are not soluble in the reaction conditions.

Separation by HILIC allows for another metric for the estimation of the hydrophobicity of the species present. In HILIC, the more hydrophobic species elute earlier, allowing for an estimation of the hydrophobicity of the analytes based on the retention time. Though HILIC is considered to be a “mixed-mode” separation method where both partitioning and adsorption mechanisms are involved in separation⁴⁹⁻⁵², the reagents used in this experiment are chemically similar, and thus, the retention mechanisms are assumed to be similar. **Figure 3.3b** is a plot of retention time (RT) vs. NPSA and shows an additional correlation between the experimental (RT) and calculated (NPSA) hydrophobicity. The two types of reagents, mono- and bi-phenyl, both show linear trends in which the retention time increases as the reagents become less hydrophobic. However, the slopes and intercepts of these lines differ, which implies slightly different separation mechanisms between the two types of reagents coupled to glycans. Though the reagents GPN4 and phenyl-GPN have nearly identical NPSA, the retention time between the two derivatized glycans is significantly different. Thus, the different types of bonds, the localization of electrons, and the geometry of the reagents are the differences between the two analytes and interact in different ways with the stationary phase. Though HILIC separation mechanism, retention times, and stationary phase interactions are not fully understood, this study shows that with all other properties held constant, the glycans derivatized with reagents primarily

composed of alkyl chains interact more with the stationary phase than glycans derivatized with the bi-phenyl reagents.

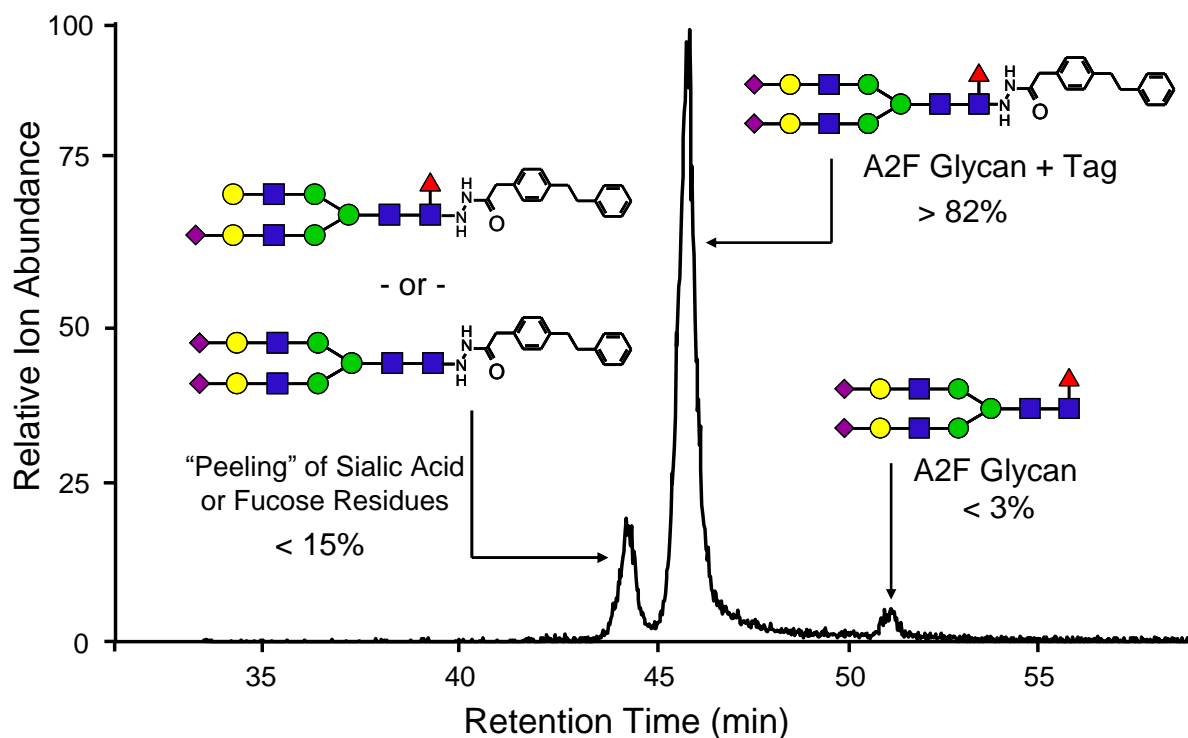


Figure 3.4 – The EIC of the native and tagged A2F glycan after derivatization with phenyl2-GPN at 56°C for 3 hr in 25:75 acetic acid:MeOH. This shows > 95% conversion to the derivatized glycan, however there is still a small amount of peeling, or loss of sialic acid or fucose.

3.3.2 Analysis of the Human Plasma N-Linked Glycome using the Phenyl2-GPN Reagent

In order to demonstrate the compatibility and effectiveness of the novel glycan hydrophobic reagents in complex mixtures, the N-linked glycans from pooled human plasma were cleaved, derivatized with phenyl2-GPN, and analyzed. Initially,

intact sialylated glycans were not able to be detected. Upon further investigation, it was determined that the high reaction temperature combined with acidic conditions (75°C in 15% acetic acid for 3 hr) was causing peeling, or loss of labile sugar residues (most notably NeuAc). Thus, numerous reaction conditions were tested using a model glycan, A2F, which contains 2 terminal sialic acid residues and one core fucose. It was found that a lower temperature and higher acidity (56°C in 25:75 acetic acid:MeOH for 3 hr) provided near complete conversion to the derivatized glycan (> 95%) and minimized the peeling (**Figure 3.4**). These conditions were used in all the subsequent studies containing complex glycans with sialic acid or fucose residues.

Figure 3.5 shows the analysis of *N*-linked glycans cleaved from plasma, both native and derivatized. The base peak chromatograms have been overlaid in **Figure 3.5a** and the derivatized glycans show on average a 4-fold increase in total ion abundance with certain negatively charged glycans showing up to a 10-fold increase. **Figure 3.5b** shows the derivatization efficiency of the glycans in a complex mixture. The > 97% reaction efficiency in plasma displays the robustness of the derivatization even in the most complex of samples, plasma. Additionally, **Figure 3.5c** demonstrates the advantage of derivatizing negatively charged sialylated glycans, which are often difficult to ionize in the positive ion mode. When analyzing native glycans, the tri-sialylated A3 glycan is only minutely detected. It is shown that the signal of the native A3 glycan is only slightly above the noise, whereas >10-fold S/N is detected for the derivatized A3 glycan. This provides more

statistically accurate isotopic ratios which yield higher quality data and will lead to the accurate quantification of *N*-linked glycans over a wider dynamic range.

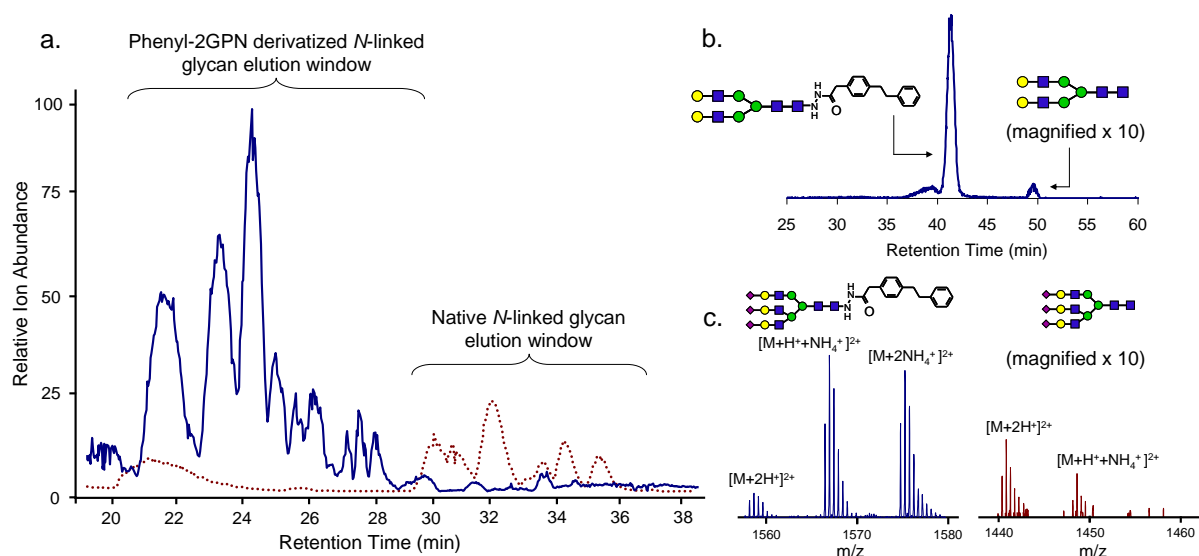


Figure 3.5 – The compatibility of the phenyl₂-GPN hydrophobic hydrazide reagent with glycans cleaved from complex mixtures: **a)** the base peak chromatogram of the derivatized *N*-linked glycans (solid line) overlaid with the base peak chromatogram of the native *N*-linked glycans (dotted line); an average of 4-fold increase in glycan ion abundance is observed for all glycan species. **b)** the EIC and reaction efficiency of the NA₂ glycan cleaved from plasma proteins; **c)** the mass spectra of the tri-sialylated A₃ glycan both native and derivatized.

3.4 Conclusion

The hydrazide reagents are effective in increasing the glycan ion abundance in ESI FTICR MS, and as the reagents become more hydrophobic, the ion abundance is increased further. The addition of a second phenyl ring has been

found to have the greatest effect on the glycan response, and future studies will continue to incorporate this multi-phenyl structure into the tagging reagents. To date, no reagents have suffered from degradation or decreased ion abundance due to solubility issues. This is evidence that there are still possibilities to make reagents that are even more hydrophobic, will still be compatible with the reaction solvents and nanoLC conditions, and can further increase the ion abundance of glycans.

The increased total ion abundance of the derivatized glycans cleaved from plasma proteins imparts several advantages for glycan analysis, including the facilitated detection of lower abundant glycan species. By increasing the ion abundance of these glycans by an average of 4-fold and some negatively charged glycans up to 10-fold, the number of *N*-linked glycans detected in plasma was increased by ~10%. This glycan derivatization procedure, which adds <4 hours total of sample preparation time, is an effective tool in enhancing the profiling of *N*-linked glycans in complex samples.

3.5 References

- (1) Null, A. P.;Nepomuceno, A. I.;Muddiman, D. C. Implications of hydrophobicity and free energy of solvation for characterization of nucleic acids by electrospray ionization mass spectrometry. *Anal. Chem.*, **2003**, *75*, 1331-1339.
- (2) Frahm, J. L.;Bori, I. D.;Comins, D. L.;Hawkridge, A. M.;Muddiman, D. C. Achieving augmented limits of detection for peptides with hydrophobic alkyl tags. *Anal. Chem.*, **2007**, *79*, 3989-3995.
- (3) Mirzaei, H.;Regnier, F. Enhancing electrospray ionization efficiency of peptides by derivatization. *Anal. Chem.*, **2006**, *78*, 4175-4183.
- (4) Yang, W. C.;Mirzaei, H.;Liu, X. P.;Regnier, F. E. Enhancement of amino acid detection and quantification by electrospray ionization mass spectrometry. *Anal. Chem.*, **2006**, *78*, 4702-4708.
- (5) Shuford, C. M.;Comins, D. L.;Whitten, J. L.;Burnett, J. C.;Muddiman, D. C. Improving limits of detection for B-type natriuretic peptide using PC-IDMS: An application of the ALiPHAT strategy. *Analyst*, **2010**, *135*, 36-41.
- (6) Williams, D. K.;Comins, D. L.;Whitten, J. L.;Muddiman, D. C. Evaluation of the ALiPHAT Method for PC-IDMS and Correlation of Limits-of-Detection with Nonpolar Surface Area. *J. Am. Soc. Mass. Spectrom.*, **2009**, *20*, 2006-2012.
- (7) Williams, D. K.;Meadows, C. W.;Bori, I. D.;Hawkridge, A. M.;Comins, D. L.;Muddiman, D. C. Synthesis, characterization, and application of iodoacetamide derivatives utilized for the ALiPHAT strategy. *J. Am. Chem. Soc.*, **2008**, *130*, 2122-2123.
- (8) Bereman, M. S.;Comins, D. L.;Muddiman, D. C. Increasing the hydrophobicity and electrospray response of glycans through derivatization with novel cationic hydrazides. *Chem. Comm.*, **2010**, *46*, 237-239.
- (9) Bowman, M. J.;Zaia, J. Tags for the stable isotopic labeling of carbohydrates and quantitative analysis by mass spectrometry. *Anal. Chem.*, **2007**, *79*, 5777-5784.
- (10) Bowman, M. J.;Zaia, J. Comparative Glycomics Using a Tetraplex Stable-Isotope Coded Tag. *Anal. Chem.*, **2010**, *82*, 3023-3031.

- (11) Gouw, J. W.;Burgers, P. C.;Trikoupis, M. A.;Terlouw, J. K. Derivatization of small oligosaccharides prior to analysis by matrix-assisted laser desorption/ionization using glycidyltrimethylammonium chloride and Girard's reagent T. *RCMS*, **2002**, *16*, 905-912.
- (12) Naven, T. J. P.;Harvey, D. J. Cationic derivatization of oligosaccharides with Girard's T reagent for improved performance in matrix-assisted laser desorption/ionization and electrospray mass spectrometry. *Rapid Commun. Mass Spectrom.*, **1996**, *10*, 829-834.
- (13) Walker, S. H.;Papas, B. N.;Comins, D. L.;Muddiman, D. C. The Interplay of Permanent Charge and Hydrophobicity in the Electrospray Ionization of Glycans. *Anal. Chem.*, **2010**, *82*, 6636-6642.
- (14) Ruhaak, L. R.;Zauner, G.;Huhn, C.;Bruggink, C.;Deelder, A. M.;Wuhrer, M. Glycan labeling strategies and their use in identification and quantification. *Anal. Bioanal. Chem.*, **2010**, *Published online 12 March 2010*.
- (15) Xia, B. Y.;Feasley, C. L.;Sachdev, G. P.;Smith, D. F.;Cummings, R. D. Glycan reductive isotope labeling for quantitative glycomics. *Anal. Biochem.*, **2009**, *387*, 162-170.
- (16) Reinhold, V. N.;Reinhold, B. B.;Costello, C. E. Carbohydrate Molecular-Weight Profiling, Sequence, Linkage, and Branching Data - Es-MS and CID. *Anal. Chem.*, **1995**, *67*, 1772-1784.
- (17) Kebarle, P.;Tang, L. From Ions in Solution to Ions in the Gas-Phase - the Mechanism of Electrospray Mass-Spectrometry. *Anal. Chem.*, **1993**, *65*, A972-A986.
- (18) Kebarle, P.;Verkerk, U. H. Electrospray: From Ions in Solution to Ions in the Gas Phase, What We Know Now. *Mass Spectrom. Rev.*, **2009**, *28*, 898-917.
- (19) Gomez, A.;Tang, K. Q. Charge and Fission of Droplets in Electrostatic Sprays. *Phys. Fluids*, **1994**, *6*, 404-414.
- (20) Cech, N. B.;Enke, C. G. Effect of affinity for droplet surfaces on the fraction of analyte molecules charged during electrospray droplet fission. *Anal. Chem.*, **2001**, *73*, 4632-4639.
- (21) Fenn, J. B. Ion Formation from Charged Droplets - Roles of Geometry, Energy, and Time. *J. Am. Soc. Mass Spectrom.*, **1993**, *4*, 524-535.

- (22) Ciucanu, I.;Kerek, F. A Simple and Rapid Method for the Permethylation of Carbohydrates. *Carbohydr. Res.*, **1984**, *131*, 209-217.
- (23) Dell, A. Preparation and Desorption Mass-Spectrometry of Permethyl and Peracetyl Derivatives of Oligosaccharides. *Methods in Enzymology*, **1990**, *193*, 647-660.
- (24) Guillard, M.;Gloerich, J.;Wessels, H. J. C. T.;Morava, E.;Wevers, R. A.;Lefeber, D. J. Automated measurement of permethylated serum N-glycans by MALDI-linear ion trap mass spectrometry. *Carbohydrate Research*, **2009**, *344*, 1550-1557.
- (25) Bourne, E. J.;Stacey, M.;Tatlow, J. C.;Tedder, J. M. Studies on Trifluoroacetic Acid .1. Trifluoroacetic Anhydride as a Promoter of Ester Formation between Hydroxy-Compounds and Carboxylic Acids. *J. Chem. Soc.*, **1949**, 2976-2979.
- (26) Domon, B.;Costello, C. E. A Systematic Nomenclature for Carbohydrate Fragmentations in Fab-MS MS Spectra of Glycoconjugates. *Glycoconjugate Journal*, **1988**, *5*, 397-409.
- (27) Zhao, C.;Xie, B.;Chan, S. Y.;Costello, C. E.;O'Connor, P. B. Collisionally activated dissociation and electron capture dissociation provide complementary structural information for branched permethylated oligosaccharides. *Journal of the American Society for Mass Spectrometry*, **2008**, *19*, 138-150.
- (28) Hase, S.;Ikenaka, T.;Matsushima, Y. A Highly Sensitive Method for Analyses of Sugar Moieties of Glycoproteins by Fluorescence Labeling. *J. Biochem.*, **1981**, *90*, 407-414.
- (29) Pabst, M.;Kolarich, D.;Poltl, G.;Dalik, T.;Lubec, G.;Hofinger, A.;Altmann, F. Comparison of fluorescent labels for oligosaccharides and introduction of a new postlabeling purification method. *Anal. Biochem.*, **2009**, *384*, 263-273.
- (30) Schwaiger, H.;Oefner, P. J.;Huber, C.;Grill, E.;Bonn, G. K. Capillary Zone Electrophoresis and Micellar Electrokinetic Chromatography of 4-Aminobenzonitrile Carbohydrate-Derivatives. *Electrophoresis*, **1994**, *15*, 941-952.
- (31) Yoshino, K.;Takao, T.;Murata, H.;Shimonishi, Y. Use of the Derivatizing Agent 4-Aminobenzoic Acid 2-(Diethylamino)Ethyl Ester for High-Sensitivity Detection of Oligosaccharides by Electrospray-Ionization Mass-Spectrometry. *Anal. Chem.*, **1995**, *67*, 4028-4031.

- (32) Harvey, D. J. Electrospray mass spectrometry and fragmentation of N-linked carbohydrates derivatized at the reducing terminus. *J. Am. Soc. Mass Spectrom.*, **2000**, *11*, 900-915.
- (33) Poulter, L.; Burlingame, A. L. Desorption Mass-Spectrometry of Oligosaccharides Coupled with Hydrophobic Chromophores. *Methods Enzymol.*, **1990**, *193*, 661-688.
- (34) Lamari, F. N.; Kuhn, R.; Karamanos, N. K. Derivatization of carbohydrates for chromatographic, electrophoretic and mass spectrometric structure analysis. *J. Chromatogr., B*, **2003**, *793*, 15-36.
- (35) Avigad, G. Dansyl Hydrazine as a Fluorimetric Reagent for Thin-Layer Chromatographic Analysis of Reducing Sugars. *J. Chromatogr.*, **1977**, *139*, 343-347.
- (36) Karamanos, N. K.; Tsegenidis, T.; Antonopoulos, C. A. Analysis of Neutral Sugars as Dinitrophenyl-Hydrazones by High-Performance Liquid-Chromatography. *J. Chromatogr.*, **1987**, *405*, 221-228.
- (37) Miksik, I.; Gabriel, J.; Deyl, Z. Microemulsion electrokinetic chromatography of diphenylhydrazones of dicarbonyl sugars. *J. Chromatogr. A*, **1997**, *772*, 297-303.
- (38) Mopper, K.; Johnson, L. Reversed-Phase Liquid-Chromatographic Analysis of Dns-Sugars - Optimization of Derivatization and Chromatographic Procedures and Applications to Natural Samples. *J. Chromatogr.*, **1983**, *256*, 27-38.
- (39) Bereman, M. S.; Young, D. D.; Deiters, A.; Muddiman, D. C. Development of a Robust and High Throughput Method for Profiling N-Linked Glycans Derived from Plasma Glycoproteins by NanoLC-FTICR Mass Spectrometry. *J. Proteome Res.*, **2009**, *8*, 3764-3770.
- (40) Andrews, G. L.; Shuford, C. M.; Burnett, J. C.; Hawkridge, A. M.; Muddiman, D. C. Coupling of a vented column with splitless nanoRPLC-ESI-MS for the improved separation and detection of brain natriuretic peptide-32 and its proteolytic peptides. *J. Chromatogr. B*, **2009**, *877*, 948-954.
- (41) Oxtoby, D. W.; Gillis, H. P.; Nachtrieb, N. H., *Principles of Modern Chemistry*, 4th ed.; Saunders College Pub.: Fort Worth, 1999.

- (42) Wheeler, S. F.;Harvey, D. J. Negative ion mass spectrometry of sialylated carbohydrates: Discrimination of N-acetylneuraminic acid linkages by MALDI-TOF and ESI-TOF mass spectrometry. *Anal. Chem.*, **2000**, *72*, 5027-5039.
- (43) Chai, W. G.;Piskarev, V.;Lawson, A. M. Branching pattern and sequence analysis of underivatized oligosaccharides by combined MS/MS of singly and doubly charged molecular ions in negative-ion electrospray mass spectrometry. *J. Am. Soc. Mass Spectrom.*, **2002**, *13*, 670-679.
- (44) Chai, W. G.;Piskarev, V.;Lawson, A. M. Negative ion electrospray mass spectrometry of neutral underivatized oligosaccharides. *Anal. Chem.*, **2001**, *73*, 651-657.
- (45) Pfenninger, A.;Karas, M.;Finke, B.;Stahl, B. Structural analysis of underivatized neutral human milk oligosaccharides in the negative ion mode by nano-electrospray MS_n (Part 2: Application to isomeric mixtures). *J. Am. Soc. Mass Spectrom.*, **2002**, *13*, 1341-1348.
- (46) Harvey, D. J. Fragmentation of negative ions from carbohydrates: Part 3. Fragmentation of hybrid and complex N-linked glycans. *J. Am. Soc. Mass Spectrom.*, **2005**, *16*, 647-659.
- (47) Harvey, D. J. Fragmentation of negative ions from carbohydrates: Part 2. Fragmentation of high-mannose N-linked glycans. *J. Am. Soc. Mass Spectrom.*, **2005**, *16*, 631-646.
- (48) Harvey, D. J. Fragmentation of negative ions from carbohydrates: Part 1. Use of nitrate and other anionic adducts for the production of negative ion electrospray spectra from N-linked carbohydrates. *J. Am. Soc. Mass Spectrom.*, **2005**, *16*, 622-630.
- (49) Alpert, A. J. Hydrophilic-Interaction Chromatography for the Separation of Peptides, Nucleic-Acids and Other Polar Compounds. *J. Chromatogr.*, **1990**, *499*, 177-196.
- (50) Hemstrom, P.;Irgum, K. Hydrophilic interaction chromatography. *J. Sep. Sci.*, **2006**, *29*, 1784-1821.
- (51) Nguyen, H. P.;Schug, K. A. The advantages of ESI-MS detection in conjunction with HILIC mode separations: Fundamentals and applications. *J. Sep. Sci.*, **2008**, *31*, 1465-1480.

- (52) Dejaegher, B.;Heyden, Y. V. HILIC methods in pharmaceutical analysis. *J. Sep. Sci.*, **2010**, 33, 698-715.

CHAPTER 4

Stable-Isotope Labeled Hydrophobic Hydrazide Reagents for the Relative Quantification of *N*-linked Glycans by Electrospray Ionization Mass Spectrometry

The following work was reprinted with permission from: Walker, S. H.; Budhathoki-Uprety, J.; Novak, B. M.; Muddiman, D. C. *Analytical Chemistry* **2011**, 83(17), 6738-6745. Copyright 2011 American Chemical Society. The original publication may be accessed directly via the World Wide Web.

4.1 Introduction

Glycosylation is one of the most common post-translational modifications in biological systems, estimated to occur in more than 50% of translated gene products.¹ Furthermore, of the entire translated genome, 0.5-1% of all gene products are involved in glycosylation.² Glycans are ubiquitous in biological processes regulating cell-cell interactions, cellular recognition, cell division and adhesion, immune response, and protein stability.³ Due to the importance of glycosylation, aberrations in the glycosylation patterns are often found to be detrimental to the biological system. In 1969, Robbins and coworkers first reported aberrations in glycosylation by describing the disparity in the size of membrane glycoproteins between healthy and diseased fibroblasts.⁴ Furthermore, aberrant glycosylation was first linked to cancer in 1978 where aberrant glycosylation patterns of α_1 -antitrypsin were discovered in lung, prostate, and gastrointestinal cancers.⁵ Since then, numerous studies have provided evidence for the correlation between aberrant glycosylation and cancer,⁶⁻¹¹ and now, researchers believe that glycans may be possible candidates for sensitive and specific disease biomarkers.¹² Recent

studies have supported these earlier findings demonstrating aberrant glycosylation in many different types of cancers,¹³ including breast,¹⁴⁻¹⁶ prostate,¹⁷⁻¹⁸ liver,¹⁹ ovarian,²⁰⁻²⁴ pancreatic,²⁵ etc. However, there are no ubiquitous methodologies used to detect, profile, and quantify these changes in glycosylation.

Relatively few glycan quantification strategies have been developed; however, since 2007, the relative quantification of *N*-linked glycans via the incorporation of stable-isotope labeling has produced several novel methodologies.^{3, 26} These involve using common glycan derivatization strategies such as permethylation,²⁷⁻²⁹ reductive amination,³⁰⁻³² and hydrazone formation (this study) to incorporate chemically similar but isotopically differentiated labels that can be used to separate the glycans by mass, allowing relative quantification in MS. Additionally, metabolic incorporation of stable isotopes has been shown by Orlando and coworkers³³ where cells can be grown in “heavy media” differentially labeling the glycans and allowing for separation by mass (*vide infra*).

Two *N*-linked glycan quantification strategies involve variations in permethylation: 1) stable-isotope labeling via deuteriomethyl iodide³⁴ and 2) QUantitation by IsoBaric Labeling (QUIBL) using ¹³CH₃I and ¹²CH₂DI.²⁸ Novotny and coworkers utilize permethylation of glycans using either methyl iodide or deuteriomethyl iodide in order to differentially label two glycan samples.²⁹ Because the methyl or deuteriomethyl groups are incorporated at each hydroxyl, amino and carboxylic acid group, each glycan will have a 3 Da mass shift per functional group methylated. Orlando and coworkers also exploit permethylation for the quantification

of glycans; however, $^{13}\text{CH}_3\text{I}$ or $^{12}\text{CH}_2\text{DI}$ are used to differentially permethylate samples.²⁸ In this case the two derivatization groups have the same nominal mass, but an exact mass difference of 0.002922 Da is observed per methylation site. Since all *N*-linked glycans have at ≥ 20 methylation sites, the mass shift is ≥ 0.058 Da, which high resolving power instruments ($\geq 30,000$) can distinguish. Both of these methods are used to relatively quantify glycans from two separate samples in the same LC-MS analysis. Additionally, both samples are prepared individually and then mixed together prior to LC-MS. This technique affords the advantage that ionization and measurement variability from run to run by ESI or MALDI MS analysis is identical for both samples. A disadvantage present in these studies is that the permethylation efficiency of each sample must be identical. Due to the numerous hydroxyl, amino, and carboxylic groups present in oligosaccharides, a 0.1% change in the permethylation efficiency between two samples can result in a 3-10% efficiency difference (depending on glycan size). Thus, the two samples must be permethylated with equal efficiency in order to confidently quantify glycans. Additionally, both of these methods use deuterium labeling, which is known to have a different chromatographic shift than hydrogen in LC.³⁵⁻³⁷ Thus, a multiple deuterio-labeled glycan can elute from a liquid chromatography column at a different time and in different mobile phases introducing analytical variability into the analysis, which negates the usefulness of mixing the two samples together before LC MS.

Two other relative quantification strategies involve derivatization by stable-isotope labeled reductive amination reagents, GRIL³² and tetraplex stable-isotope

coded tags.³⁰⁻³¹ Cummings and coworkers have developed Glycan Reductive Isotope Labeling (GRIL) utilizing [¹²C₆]aniline and [¹³C₆]aniline in order to differentially label glycan samples, combine 1:1, and analyze in the same MS.³² A comparable method has been developed by Zaia and coworkers,³⁰⁻³¹ where a reductive amination reagent has been developed such that 4 tags can be used all with a different number of deuterium atoms incorporated (+0, +4, +8, +12). This is the first reagent that has the ability of tetraplex quantification of glycans. The authors were able to quantify the relative amounts of *N*-linked glycans from the plasma of four different species in the same mass spectrum. However, the mass shift of only 4 Da per tag is an inherent disadvantage to this method and creates overlapping isotopic distributions, which involve theoretical simulations to extract the correct ion abundances of the tetraplex quadruplets. Additionally, deuterium is used which can cause a chromatographic shift, introducing ionization and mass spectrometric variability (*vide supra*).

Orlando and coworkers have developed a novel method to metabolically label glycans in cell culture, Isotopic Detection of Aminosugars With Glutamine (IDAWG).³³ In glycan biosynthesis, the only method for the incorporation of nitrogen into glycan molecules is through the hexosamine biosynthetic pathway. Here, the side chain of glutamine is the sole donor source of nitrogen for the production of aminosugars and sugar nucleotides, molecules which transfer individual monosaccharides to glycans during glycan biosynthesis. By doping only ¹⁵N-labeled glutamine into a glutamine deprived media, one can grow cells with glycans that are

differentially labeled at all monosaccharides containing nitrogen and incorporate a 1 Da mass shift per HexNAc, GalNAc, and NeuAc into the glycans. This method has a significant advantage over all previous stable-isotope labeled techniques in that after the cells are grown, they are mixed together, and all subsequent sample preparation steps are performed in the same vial, significantly reducing the sample preparation variability between the two samples. However, the primary drawback is that this study can only be performed in a living organism that is capable of being metabolically labeled with ^{15}N , which is presently limited to cell culture.

Hydrazone formation is an attractive alternative derivatization strategy which, until now, has not been exploited for the incorporation of stable-isotope labels and relative quantification of glycans. Comparable to reductive amination (GRIL,³² *vide supra*), hydrazone formation reacts at the reducing terminus of the glycans and is capable of incorporating a fixed mass shift for the differential mass labeling of two samples. However, hydrazone formation is a more facile method for derivatization that does not involve reduction with sodium borohydride,³⁸⁻⁴² a method which requires a significant cleanup step, increasing time and analytical variability. A detailed method for hydrazone formation derivatization of *N*-linked glycans has been recently published.⁴³⁻⁴⁴ These manuscripts detail the methods, advantages, shortcomings, and results of nanoLC MS analysis of hydrazone derivatization of *N*-linked glycans vs. native *N*-linked glycans. Briefly, it has been shown that the addition of a hydrophobic, hydrazone reagent can significantly increase the ion abundance of glycans in ESI.⁴³⁻⁴⁵ Additionally, a plasma glycan sample can be

derivatized and directly loaded onto the nanoLC column in <4 hr without a cleanup step. It is shown that the P2GPN reagent increases the ion abundance of all types of glycans in ESI, allowing for a ~10% increase in glycan identifications in human plasma vs. native glycans.⁴³ The reaction efficiency has been meticulously optimized⁴⁴ and is shown to be >95% for model glycans and for glycans cleaved from plasma.⁴³ Further details on the derivatization reaction, effects on the glycans, fragmentation, etc. have been previously reported.³⁹⁻⁴⁵

Herein, a relative quantification strategy for *N*-linked glycans via stable-isotope labeled hydrophobic hydrazide reagents is presented which builds upon the methodologies^{23, 46-47} and rapid (<4 hr) derivatization strategy⁴³⁻⁴⁵ developed by this group for glycan analysis in epithelial ovarian cancer. The P2GPN hydrazide reagent has been synthesized in its natural isotopic form and with the incorporation of ¹³C₆ stable isotopes. The 'light' and 'heavy' reagents have been characterized and applied to a simple mixture of glycans. Additionally, the relative quantification strategy was applied to pooled human plasma, and the analytical variability of the sample preparation, method, and instrument was measured. Furthermore, maltoheptaose was spiked in at the onset of all sample preparation in order to correct for sample preparation variations between the two samples. It is shown that the internal standard significantly reduces the difference in the systematic bias between the two samples due to parallel processing.

4.2 Experimental

4.2.1 Materials

Maltoheptaose, (Gal-GlcNAc)₂Man₃GlcNAc₂ (NA2) glycan, (NeuAc-Gal-GlcNAc)₂Man₃(Fuc)(GlcNAc)₂ (A2F) glycan, hydrazine monohydrate, bromobenzene, tetrakis(triphenyl phosphine) palladium(0), triphenyl phosphine, copper(I)iodide, triethyl amine, and palladium on charcoal were all purchased from Sigma Aldrich (St. Louis, MO). Man₉GlcNAc₂ (MAN9) was purchased from Fisher Scientific (Houston, TX). Ethyl 4-ethynylphenylacetate was purchased from Spectra Group Limited, Inc. (Millbury, OH). ¹³C₆-bromobenzene was purchased from Cambridge Isotope Laboratories, Inc. (Andover, MA). Pooled human plasma was purchased from Innovative Research (Novi, MI). IntegraFrit and PicoFrit capillaries were purchased from New Objective (Woburn, MA). These columns were packed in-house with TSK-Gel Amide-80 stationary phase from TOSOH Bioscience (San Jose, CA). Graphitized solid phase extraction columns were purchased from Alltech (Deerfield, IL). Peptide: *N*-glycosidase F (2.5 mU/μL) and the denaturing solution (1 M β-mercaptoethanol and 2% (w/w) SDS) were purchased from Prozyme (San Leandro, CA).

4.2.2 Synthesis of Reagents

The bi-phenyl reagent, 4-phenethylbenzohydrazide (P2GPN), was synthesized in its native and ¹³C₆-isotopically labeled forms. The stable-isotope labeled and native reagents were synthesized by identical methods; however, the

incorporation of $^{13}\text{C}_6$ was achieved by starting with ^{13}C -labeled bromobenzene. The synthesis mechanism was comparable to the previous report.⁴³ Briefly, the bromobenzene was coupled to ethyl 4-ethynylphenylacetate via a Sonogashira coupling⁴⁸ and the triple bond was hydrogenated. The ethyl ester was then converted to the hydrazide group completing the 4-phenethylbenzohydrazide reagent. Extensive synthesis and characterization data are provided in the supplemental material (**Appendix B**).

4.2.3 *N-linked Glycan Derivatization Procedure*

The derivatization reaction was performed as described previously.⁴³ The lyophilized glycans were reconstituted in a 1 mg/ml solution of the phenyl2-GPN reagent in 75:25 (v/v) MeOH:acetic acid solution. This mixture was then incubated for 3.5 hr at 56°C. The reaction solution was immediately placed in a -80°C freezer for 30 min to quench the reaction. The mixture was then lyophilized to dryness and stored at -20°C. The glycans were reconstituted in 50 μL of HILIC mobile phase (initial conditions) for LC-MS analysis. Where relative quantification was performed, the two samples being compared were mixed, vortexed, and analyzed in the same nanoLC MS run.

4.2.4 *N-linked Glycan Extraction from Pooled Plasma*

In the experiments herein, 100 μL (10 $\mu\text{g}/\text{mL}$) of internal standard (maltoheptaose) was added to 50 μL of pooled human plasma and the solution was

lyophilized to dryness. The glycan cleavage procedure has been described in detail previously.^{43, 46} Briefly, the lyophilized plasma containing the internal standard was reconstituted in 250 μ L of 50 mM tris-HCl buffer (pH 7.5) and the proteins were denatured at 95°C for 5 min by adding 28 μ L of 2% SDS/1M β -mercaptoethanol. The solution was allowed to sit for 20 min until room temperature was achieved, and then 5 μ L of PNGase F (2.5 mU/ μ L) were added to the plasma sample. The solution was then incubated for 18 hr at 37°C and subsequently quenched with 500 μ L of 0.1% TFA. The glycans were then separated from the proteins using solid phase extraction (SPE) equipped with a graphitized carbon cartridge as described in detail previously.⁴⁶ The eluted fractions were then dried down, combined, and derivatized (*vide supra*).

4.2.5 nano-Flow Hydrophilic Interaction Chromatography

Derivatized glycans were separated prior to MS analysis via hydrophilic interaction chromatography (HILIC) as described previously.^{43-44, 46} A vented column setup⁴⁹ was used with an Eksigent nanoLC-1D PLUS system equipped with an AS1 autosampler (Dublin, CA). Both the trap and analytical columns were packed in-house with TSK-Gel Amide-80 stationary phase (5 μ m particle size). The analytical column consists of a 75 μ m I.D. capillary packed to 10 cm, and the trap column consists of a 100 μ m I.D. capillary packed to 10 cm. Mobile phase A consists of 50 mM ammonium acetate (pH 4.5) and mobile phase B consists of 100% ACN. Gradient elution was used in which the solvent composition was varied from 20 to

55% solvent A over 37 minutes. The glycans were loaded onto the trap column in 80:20 solvent B:A and an initial wash step was used at 93% B before beginning the gradient, and after the end of the gradient, the column was washed with 85% A giving a total run time, including re-equilibration, of 70 min.

4.2.6 *LTQ-Orbitrap Mass Spectrometry*

A hybrid linear ion trap Orbitrap mass spectrometer (Thermo Fisher Scientific, San Jose, CA) was used for all LC-MS glycan analysis data presented herein. Ionization of glycans was achieved by applying a 2 kV potential to a zero dead volume union creating an electric field over the capillary and inducing gas-phase ionization of the glycan analytes. Upon ionization, the analytes enter a heated (225°C) capillary and travel through a series of ion guides before being detected. The capillary and tube lens voltages were 42 V and 120 V, respectively, and the AGC in the Orbitrap was set to 1×10^6 ions with a maximum injection time of 500 ms. A resolving power of 60,000 was used in the Orbitrap, allowing for ~1 scan/sec. The AGC in the LTQ was set to 8×10^3 with a maximum injection time of 80 ms and normalized collision energy (NCE) of 22. Data dependent mode was used to acquire precursor and fragmentation spectra. Up to 5 MS/MS spectra were acquired per precursor Orbitrap scan based on the most abundant m/z values. A 10,000 count threshold was used and m/z values chosen twice in 30 s were placed on an exclude list for an additional 30 s. Calibration was performed according to the

manufacturer protocol and Xcalibur software (v. 2.0.7) was used for data analysis and peak integration.

4.2.7 Glycan Integration and Relative Quantification

The glycan ratios were calculated by integrating the areas under each extracted ion chromatogram (EIC) of the 'light' and 'heavy' labeled glycan. The chromatograms of a specifically labeled glycan were extracted using the monoisotopic peak(s). Because significant ammonium adduction was observed, these m/z values ($[M+nH^++mNH_4^+]^{(n+m)+}$) were also summed in the EIC. Additionally, if more than one charge-state was present, then both charge-states' $[M+nH^+]^{n+}$ and ammonium adducted peaks were summed in the EIC. For relative quantification, the ratio of the area under EIC of the 'heavy':'light' for each glycan was calculated. This raw glycan ratio was then 'corrected' by using the 'heavy':'light' ratio of the spiked-in internal standard, maltoheptaose. The maltoheptaose glycan ratio was calculated using the same EIC and integration as described above. Maltoheptaose serves as an important internal standard to correct for the differences in sample preparation systematic error including derivatization reaction variability, SPE recovery variability, glycan interaction with vials, stationary phases, etc. Additionally, correcting with maltoheptaose takes into account the slightly different isotopic distributions due to the number of possible natural ^{13}C 's in each molecule and the incomplete incorporation of $^{13}C_6$ (vide infra).

4.3 Results and Discussion

The 'light' and 'heavy' forms of the P2GPN reagent were synthesized by identical mechanisms only differing in the source of bromobenzene. The heavy labeled compound was characterized by high resolution FT-ICR MS, and the mass spectrum is shown in **Figure 4.1a**. It is seen that ~95% of the compound consists of successful incorporation of the $^{13}\text{C}_6$ isotope labels. Additionally, the data show peaks at $^{13}\text{C}_5$ and $^{13}\text{C}_0$ isotope incorporation corresponding to <5% and <1% relative abundance, respectively. It is paramount in the relative quantification strategy by differential labeling that no cross-reaction occurs after the two samples are mixed together. Because hydrazone formation derivatization does not require the removal of excess hydrazide reagent, there is the possibility of the unreacted 'light' tag reacting with the 'heavy' sample and vice versa. A control study was performed in which an extracted glycan sample from pooled plasma was tagged with the 'heavy' reagent. Additionally, a blank vial was prepared in parallel and tagged with the 'light' reagent. These two samples were then mixed together and analyzed. The result is shown in **Figure 4.1b**, where it is observed that less than 1% of the example glycan is derivatized with the $^{13}\text{C}_0$ reagent, indicating that there is $\leq 1\%$ cross-reactivity after mixing. However, the actual cross-reactivity is significantly less because the $^{13}\text{C}_0$ peak is also attributed to the isotopic purity of the $^{13}\text{C}_6$ reagent (**Figure 4.1a**).

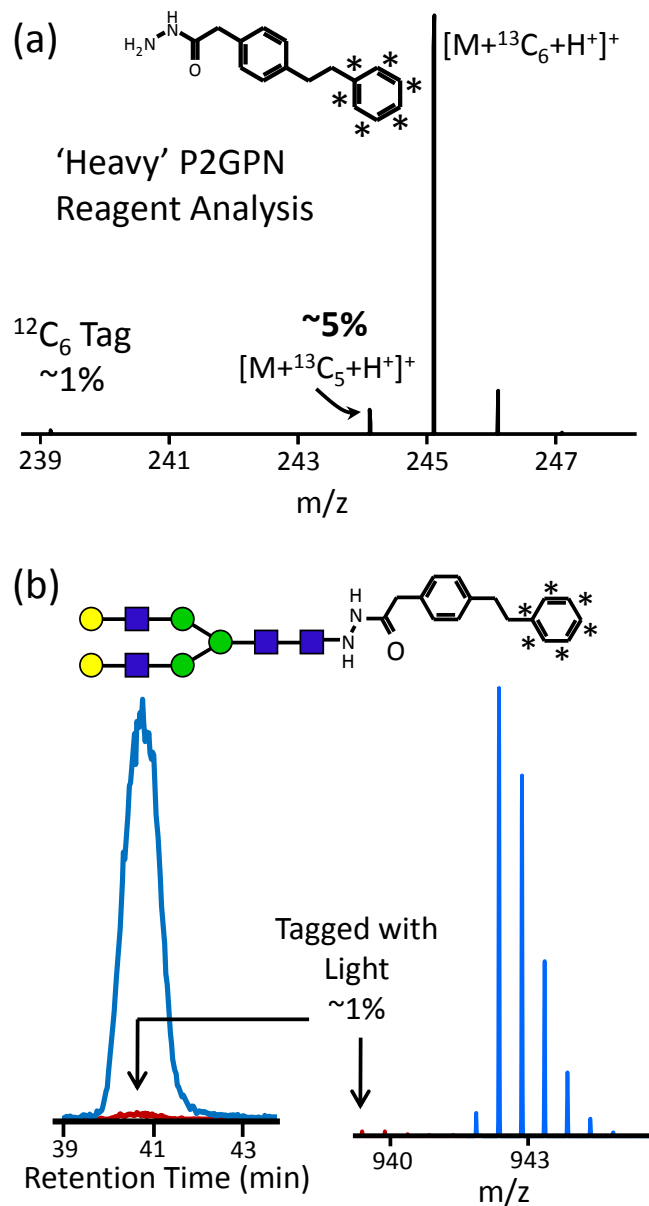


Figure 4.1 – Characterization of the heavy P2GPN reagent: a) the high resolving power mass spectrum of the ¹³C₆-labeled P2GPN. The ¹³C₆ was incorporated at 95%, while the ¹³C₀ and ¹³C₅ side products account for 1 and 5%, respectively. b) a control study in which one plasma sample was tagged with the 'heavy' reagent and a blank vial was tagged with the 'light'. The samples were mixed together and negligible cross-reaction was observed, as the 1% of 'light' sample was observed from the incomplete incorporation of the ¹³C₆.

In order to further characterize the behavior of the 'light' and 'heavy' reagents, glycans were cleaved from two aliquots of a pooled human plasma sample in parallel and were derivatized with the 'light' and 'heavy' reagent, respectively. These two samples were then mixed in a 1:1 ratio and analyzed. **Figure 4.2** displays the near identical behavior of the 'light' and 'heavy' tagged glycans with respect to chromatographic, MS, and collision induced dissociation (CID) performance. It is imperative that the chromatographic performance of the same 'light' and 'heavy' tagged are identical in order to ensure conserved retention times, mobile phases in which the glycans elute, and conditions in the ESI droplet. If these are not identical for the differentially tagged pair, then the ionization efficiency in ESI may be significantly different causing the MS to systematically bias the glycan ratios. For example, **Figure 4.2** shows the EIC of an example Hex₅HexNAc₄Fuc glycan where the 'light' and 'heavy' tagged glycan co-elute from the HILIC column. Thus, there is no isotopic retention effect. A table included in the supplemental material lists the retention times for each pair of detected glycans (**Table B.1**).

There also cannot be an isotopic bias in the MS detection of the differentially labeled glycans. The precursor ions detected in the orbitrap are shown for the 'light' and 'heavy' forms of an example glycan (**Figure 4.2**). A 1:1 ratio is detected; however, it is observed that the isotopic distributions of the 'light' and 'heavy' form have slightly different isotopic abundances for the A+1 through A+5 peaks. This is expected due to the different number of possible natural ¹³C sites in the tags. Additionally, the product-ion spectra are overlaid for the 'light' and 'heavy' forms of

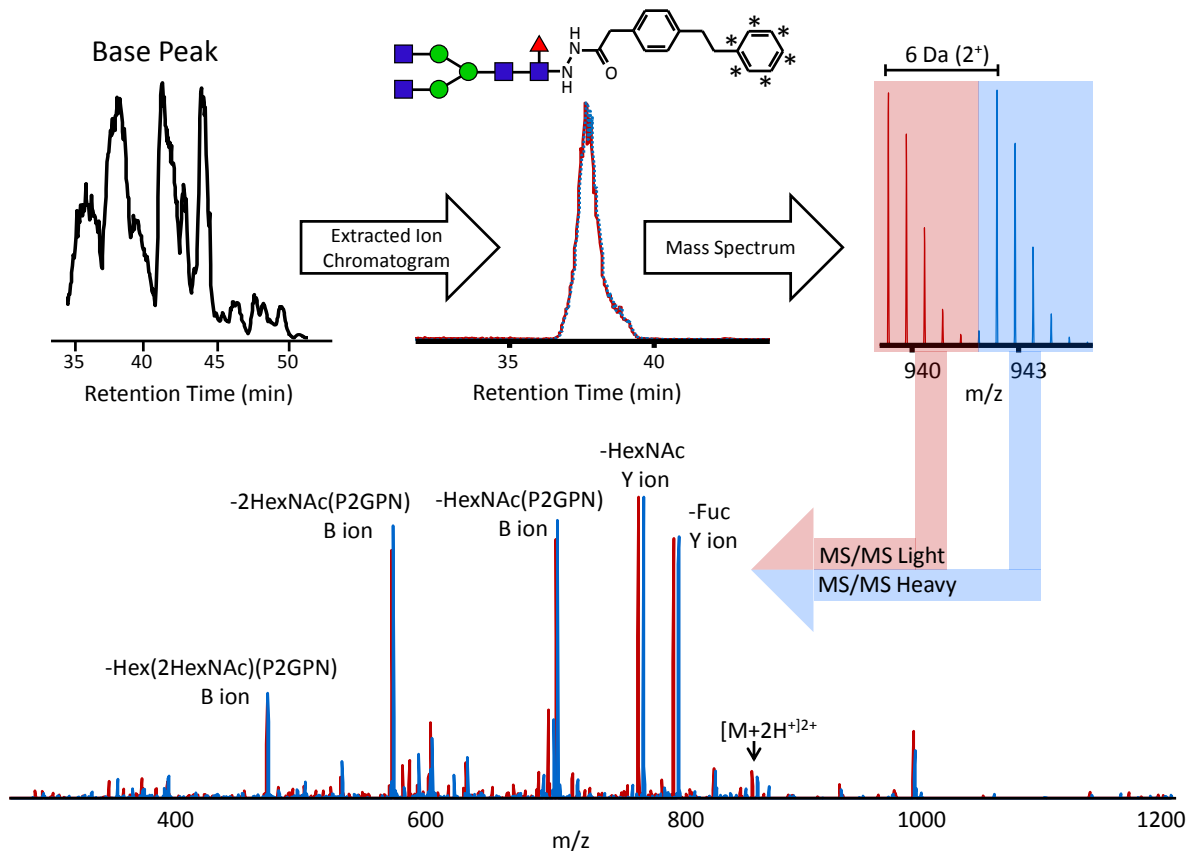


Figure 4.2 – Chromatographic, MS, and MS/MS characterization of a 1:1 derivatized human plasma mixture. There is no retention time shift, and the precursor ions are detected in a 1:1 ratio. Additionally, it is shown that there is no isotope effect on the fragmentation of the derivatized glycans.

the example glycan. It is shown that the stable-isotope labeled tag does not affect the fragmentation patterns of the glycans any differently than the 'light' reagent. Furthermore, whether or not a fragment is a 'Y' or 'B' ion⁵⁰ can be easily distinguished by determining if the peaks overlap or have a 6 Da shift. If there is a 6 Da shift between the 'light' and 'heavy' tagged fragments, then this means that the tag is still present, thus the reducing terminus is intact and is a 'Y' ion.

In order to test the quantification capabilities of these reagents, a simple mixture of three glycans (NA2, MAN9, and A2F) plus an internal standard, maltoheptaose, were divided into aliquots, and various amounts of NA2 glycan were spiked into each vial so that there were 5 different NA2 'light' to 'heavy' sets (ratios: 5:1, 2:1, 1:1, 1:2, and 1:5). These samples were tagged with either the 'light' or

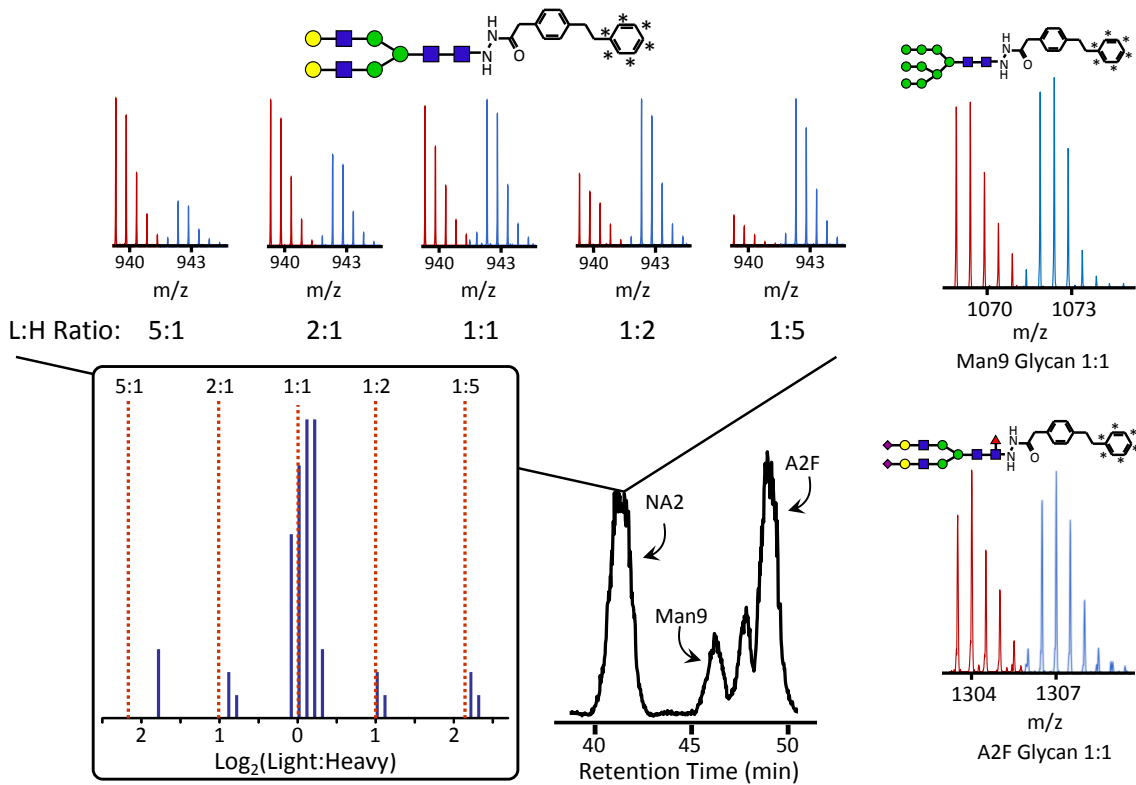


Figure 4.3 – A simple mixture of 3 model *N*-linked glycans (NA2, A2F, and MAN9) plus the internal standard, maltoheptaose, in a 1:1 mixture. Also, the NA2 glycan mixture was spiked in at varying concentration ratios of 5:1, 2:1, 1:1, 1:2, and 1:5 (upper inset). The histogram shows the experimental relative quantification data, where glycans with a 1:1 ratio are centered around 0 in the $\text{log}_2(\text{H:L})$ plot, and the NA2 ratios are near the expected values and clearly distinct from each other and the 1:1 glycan samples.

'heavy' reagent and the two mixtures were combined 1:1. The results are shown in **Figure 4.3** where the maltoheptaose corrected histogram shows the analytical variability of the method and how well a change in concentration can be detected by mass spectrometry. The analytical variability is shown by the histogram of the 1:1 glycans, which are centered around 0 in the $\log_2(\text{H:L})$ plot. Additionally, it is seen that the expected ratios of the NA2 glycan were able to be recovered. The inset, shown above the base peak chromatogram, displays example spectra of the 'light' and 'heavy' pairs at each of the NA2 ratios. The relative abundance of the $[\text{M}+\text{nH}^+]^{n+}$ peaks are indicative of the spiked-in ratios, and the $\log_2(\text{H:L})$ histogram shows clear distinction between each of the varied concentrations.

In all *N*-linked glycan quantification experiments, maltoheptaose has been spiked in at the onset of sample preparation in order to account for the difference in systematic error between samples prepared in parallel. The analysis of *N*-linked glycans cleaved from plasma proteins involves numerous sample preparation steps that can lead to different measured abundance ratios in MS. This is unfortunate for the present relative quantification strategy, as samples undergo preparation in parallel but in a different vial with at least slightly different conditions. Though the samples are processed in parallel and efforts are taken to minimize differences in time, temperature, solvent composition, etc., other factors that cannot be controlled also contribute to this difference in systematic error, such as glycan recovery from a specific vial or SPE column, binding to pipette tips, variable reaction efficiency, etc. In order to take into account these variations between samples, an internal standard

was introduced into the plasma at the onset of the sample preparation. The internal standard must possess several properties: 1) it must have the same physical properties as the *N*-linked glycans being analyzed, 2) it must not be present on any proteins found in the biological sample of interest, and 3) it must have similar HILIC chromatographic properties as *N*-linked glycans. In these studies, maltoheptaose was used as the internal standard. Maltoheptaose is a straight-chain polysaccharide containing 7 hexose sugar units, and this standard fulfills criteria 2 and 3; however, criteria 1 is only partially fulfilled in that *N*-linked glycans are made up with monosaccharides other than just hexose, such as *N*-acetylglucose amine and *N*-acetylneuraminic acid, residues not present in maltoheptaose.

Figure 4.4 demonstrates the utility of spiking maltoheptaose into 2 aliquots of plasma samples before sample preparation. The four example glycans shown all have an increase in ion abundance in the 'heavy' sample. However, this is also the case for the internal standard, and if the internal standard ratio is used to correct for the 'light' vs. 'heavy' abundance of the *N*-linked glycans, then the *N*-linked glycan ratios are significantly closer to 1:1. Maltoheptaose is capable of accounting for two types of systematic error in these measurements: 1) the variable sample preparation conditions, efficiencies, and recoveries for each sample and 2) the bias due to the incorporation of $^{13}\text{C}_6$ stable isotopes. Having discussed the possible types of variations derived from parallel processing, the differences in the 'light' and 'heavy' abundance due to the isotopic distributions arise from the incomplete incorporation of the $^{13}\text{C}_6$ isotopes and the statistical probabilities in which natural ^{13}C

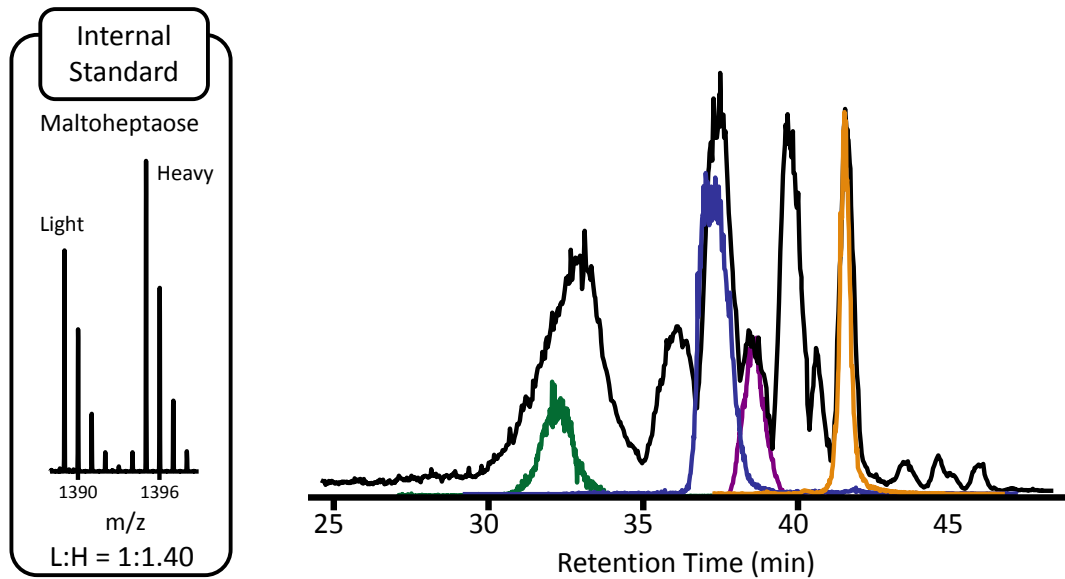
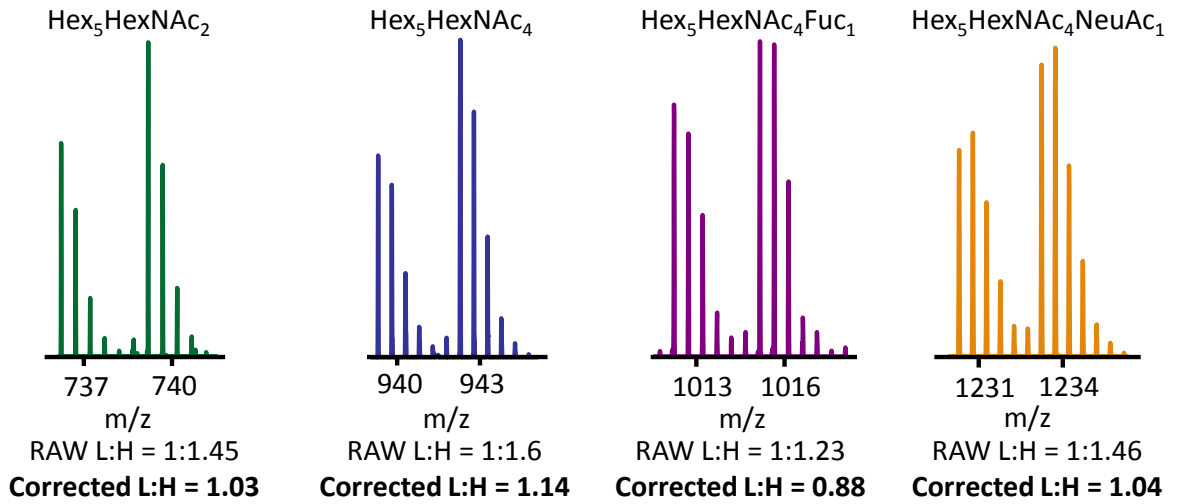


Figure 4.4 – Maltoheptaose is spiked into all of the samples at the onset of sample preparation. This allows one to track the variations in the sample preparation, since each is prepared in parallel then mixed together after derivatization. In plasma, 4 example glycans have been chosen to show the effect of the internal standard on correcting the glycan ratios. Here, almost a 50% difference in the sample preparation systematic error can be corrected using the ratios of the ‘light’ to ‘heavy’ internal standard.

is incorporated into a molecule. In the former, the ~95% incorporation of the $^{13}\text{C}_6$ isotopes will cause the $[\text{M}+\text{nH}^+]^{\text{n}+}$ peak to be only 95% the abundance of the 'light' reagent. Additionally, since $^{13}\text{C}_6$ has been artificially synthesized into the molecules, there are fewer opportunities for natural incorporation of ^{13}C in the 'heavy' reagent than in the 'light' reagent. These isotope effects cause the $[\text{M}+\text{nH}^+]^{\text{n}+}$ peak of the 'heavy' tagged glycans to have a greater abundance (by ~4.5%) than the $[\text{M}+\text{nH}^+]^{\text{n}+}$ peak of the 'light' tagged glycans. Though these instances arise, these changes in the isotopic distribution are conserved for all *N*-linked glycans and maltoheptaose. Thus, using the maltoheptaose 'light' to 'heavy' ratio will correct for these isotopic differences in addition to a majority of the sample preparation variations. A table has been included in the supplemental material listing the glycan compositions detected and the raw and corrected and ratios (**Table B.2**).

The example glycans in **Figure 4.4** were chosen to represent a majority of the *N*-linked glycan types including high mannose, complex, sialylated, and fucosylated. From these data, the internal standard is able to quantitatively correct for a majority of the difference in systematic error between samples incurred during sample preparation; however, a t-test shows that the 95% confidence interval of the corrected distribution still does not include 0. Thus, it is possible that an internal standard with properties more closely related to *N*-linked glycans can more effectively correct for sample preparation systematic error differences. While maltoheptaose is comprised of the most common hexose monosaccharide units, there are no HexNAc, NeuAc, or Fuc residues present. This might hinder the

effectiveness of the internal standard. Also, NeuAc (sialic acid) is a labile residue, and if the conditions in the sample preparation are slightly different, there could be variable peeling that would not be able to be taken into account. Thus, a more comprehensive internal standard, or set of internal standards, may be a more effective strategy in the future to more accurately correct for any sample preparation bias. Furthermore, maltoheptaose elutes much earlier and has a significantly broader (10x) peak shape than a majority of the *N*-linked glycans. This also is not optimal when using maltoheptaose as an internal standard. However, the cost-effective maltoheptaose has shown to correct for a majority of the differences in systematic error due to parallel sample preparation, and further investigation is needed to determine whether a more expensive internal standard or panel of internal standards will more effectively account for the sample preparation variability.

In order to determine the analytical variability of the relative quantification strategy, two aliquots of a pooled plasma sample were processed in parallel and tagged with the 'light' and 'heavy' reagents, respectively. Biologically identical aliquots were used in order to minimize the biological and sample variability. This will allow one to analyze only the variability in the analytical method, sample preparation, and instrument performance (the variability should be negligible here due to the samples being mixed together before ionization and mass analysis). **Figure 4.5** displays the results of this analysis. The histogram shows two distributions: 1) the raw, uncorrected $\log_2(H:L)$ data (red) and 2) the internal standard corrected $\log_2(H:L)$ data (black). As mentioned previously and further

shown here, the internal standard is effective in correcting for a majority of the systematic error, including all classes of *N*-linked glycans (high mannose, hybrid, and complex).

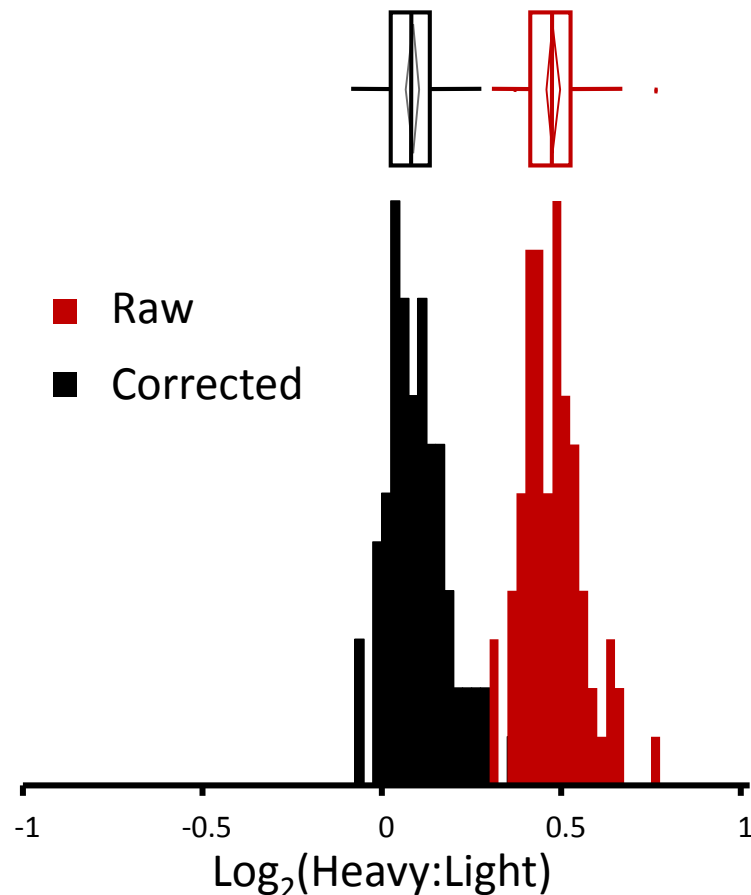


Figure 4.5 – The histogram of 27 *N*-linked glycans cleaved and quantified using the P2GPN reagent pair from 2 aliquots of pooled human plasma. The red distribution is the raw glycan log₂(H:L) ratios, whereas the black distribution is the internal standard corrected ratios. The narrow distribution indicates the minimal analytical variability between two 1:1 glycan samples cleaved from a complex mixture. Confidence intervals (95%) are shown above the distributions (Diamonds) along with the quantiles of the distribution (boxes).

The histogram comprises the relative quantification of 27 glycan species analyzed in triplicate. The width of the distribution is less than 0.5 on a \log_2 scale. This leads one to infer that changes in *N*-linked glycosylation in different biological samples as little as 30% may be able to be detected using the methods presented herein. The mean of the corrected *N*-linked glycan distribution is slightly larger than 0, and a t-test has shown that the 95% confidence interval does not include 0. This is thought to be due to the isotopic distribution overlap in the high molecular weight *N*-linked glycans. In the small glycans, the 6 Da shift is sufficient so that any overlapping isotopic distribution is negligible. However, as the sizes of the glycans get larger, there is more probability that natural ^{13}C is incorporated in the glycans. Thus, the A+6 isotopic distribution peak for the 'light'-tagged glycan begins to become more significant in the spectra and skew the relative quantification data. The internal standard corrects for most isotopic effects, such as the incomplete incorporation of $^{13}\text{C}_6$ into the 'heavy' tag. However, maltoheptaose is a relatively small oligosaccharide, and in the case of overlapping distributions, there is no overlap in the 'light' and 'heavy' forms of maltoheptaose. Therefore, maltoheptaose effectively corrects for variability in the sample preparation, but a panel of standards with varying molecular weights is a possible solution for more accurately correcting for the molecular weight bias.

4.4 Conclusion

The stable-isotope labeled reagents have been shown to be a viable strategy for the relative quantification of *N*-linked glycans in simple and complex mixtures. The P2GPN 'light' and 'heavy' reagents have near identical properties with respect to chromatographic, MS, and MS/MS performance. These reagents have shown the possibility for relative quantification of *N*-linked glycans from the most complex of mixtures, pooled plasma, and it is hypothesized that the small analytical variability will afford the advantage of detecting subtle changes in glycosylation patterns. These reagents have the potential to quantify the aberrations in glycosylation in numerous studies related to disease and cancer. However, further variability analyses are necessary to determine biologically relevant cutoff values in order to determine significant change. These studies will determine the effectiveness of the stable-isotope labeled hydrazide reagents and how well this quantification method can be applied to biological systems.

4.5 References

- (1) Apweiler, R.; Hermjakob, H.; Sharon, N. On the frequency of protein glycosylation, as deduced from analysis of the SWISS-PROT database. *BBA-Gen. Subjects*, **1999**, *1473*, 4-8.
- (2) Begley, T. P., *Wiley Encyclopedia of Chemical Biology* **2009**, *2*, 785.
- (3) Varki, A.; Cummings, R. D.; Esko, J. D.; Freeze, H. H.; Stanley, P.; Bertozzi, C. R.; Hart, G. W.; Etzler, M. E., *Essentials of Glycobiology* **2009**.
- (4) Wu, H. C.; Meezan, E.; Black, P. H.; Robbins, P. W. Comparative Studies on Carbohydrate-Containing Membrane Components of Normal and Virus-Transformed Mouse Fibroblasts .I. Glucosamine-Labeling Patterns in 3t3 Spontaneously Transformed 3t3 and Sv-40-Transformed 3t3 Cells. *Biochemistry*, **1969**, *8*, 2509-2517.
- (5) Rostenberg, I.; Guizarvazquez, J.; Penaloza, R. Altered Carbohydrate Content of Alpha-1-Antitrypsin in Patients with Cancer. *J. Natl. Cancer Inst.*, **1978**, *61*, 961-965.
- (6) Hakomori, S. Aberrant Glycosylation in Cancer Cell-Membranes as Focused on Glycolipids - Overview and Perspectives. *Cancer Res.*, **1985**, *45*, 2405-2414.
- (7) Casey, R. C.; Oegema, T. R.; Skubitz, K. M.; Pambuccian, S. E.; Grindle, S. M.; Skubitz, A. P. N. Cell membrane glycosylation mediates the adhesion, migration, and invasion of ovarian carcinoma cells. *Clin. Exp. Metastasis*, **2003**, *20*, 143-152.
- (8) Zhao, Y. Y.; Takahashi, M.; Gu, J. G.; Miyoshi, E.; Matsumoto, A.; Kitazume, S.; Taniguchi, N. Functional roles of N-glycans in cell signaling and cell adhesion in cancer. *Cancer Sci.*, **2008**, *99*, 1304-1310.
- (9) Gorelik, E.; Galili, U.; Raz, A. On the role of cell surface carbohydrates and their binding proteins (lectins) in tumor metastasis. *Cancer Metast. Rev.*, **2001**, *20*, 245-277.
- (10) Hammoud, Z. T.; Mechref, Y.; Hussein, A.; Bekesova, S.; Zhang, M.; Kesler, K. A.; Novotny, M. V. Comparative glycomic profiling in esophageal adenocarcinoma. *J. Theorac. Cardiovasc. Surg.*, **2010**, *139*, 1216-1223.

- (11) Kim, Y. S.;Yoo, H. S.;Ko, J. H. Implication of Aberrant Glycosylation in Cancer and Use of Lectin for Cancer Biomarker Discovery. *Protein Pept. Lett.*, **2009**, *16*, 499-507.
- (12) Packer, N. H.;von der Lieth, C. W.;Aoki-Kinoshita, K. F.;Lebrilla, C. B.;Paulson, J. C.;Raman, R.;Rudd, P.;Sasisekharan, R.;Taniguchi, N.;York, W. S. Frontiers in glycomics: Bioinformatics and biomarkers in disease - An NIH White Paper prepared from discussions by the focus groups at a workshop on the NIH campus, Bethesda MD (September 11-13,2006). *Proteomics*, **2008**, *8*, 8-20.
- (13) Fuster, M. M.;Esko, J. D. The sweet and sour of cancer: Glycans as novel therapeutic targets. *Nat. Rev. Cancer*, **2005**, *5*, 526-542.
- (14) Kirmiz, C.;Li, B. S.;An, H. J.;Clowers, B. H.;Chew, H. K.;Lam, K. S.;Ferrige, A.;Alecio, R.;Borowsky, A. D.;Sulaimon, S.;Lebrilla, C. B.;Miyamoto, S. A serum glycomics approach to breast cancer biomarkers. *Mol. Cell. Proteomics*, **2007**, *6*, 43-55.
- (15) Abd Hamid, U. M.;Royle, L.;Saldova, R.;Radcliffe, C. M.;Harvey, D. J.;Storr, S. J.;Pardo, M.;Antrobus, R.;Chapman, C. J.;Zitzmann, N.;Robertson, J. F.;Dwek, R. A.;Rudd, P. M. A strategy to reveal potential glycan markers from serum glycoproteins associated with breast cancer progression. *Glycobiology*, **2008**, *18*, 1105-1118.
- (16) Kyselova, Z.;Mechref, Y.;Kang, P.;Goetz, J. A.;Dobrolecki, L. E.;Sledge, G. W.;Schnaper, L.;Hickey, R. J.;Malkas, L. H.;Novotny, M. V. Breast cancer diagnosis and prognosis through quantitative measurements of serum glycan profiles. *Clin. Chem.*, **2008**, *54*, 1166-1175.
- (17) Kyselova, Z.;Mechref, Y.;Al Bataineh, M. M.;Dobrolecki, L. E.;Hickey, R. J.;Vinson, J.;Sweeney, C. J.;Novotny, M. V. Alterations in the serum glycome due to metastatic prostate cancer. *J. Proteome Res.*, **2007**, *6*, 1822-1832.
- (18) de Leoz, M. L. A.;An, H. J.;Kronewitter, S.;Kim, J.;Beecroft, S.;Vinall, R.;Miyamoto, S.;White, R. D.;Lam, K. S.;Lebrilla, C. Glycomic approach for potential biomarkers on prostate cancer: Profiling of N-linked glycans in human sera and pRNS cell lines. *Disease Markers*, **2008**, *25*, 243-258.
- (19) Isailovic, D.;Kurulugama, R. T.;Plasencia, M. D.;Stokes, S. T.;Kyselova, Z.;Goldman, R.;Mechref, Y.;Novotny, M. V.;Clemmer, D. E. Profiling of human serum glycans associated with liver cancer and cirrhosis by IMS-MS. *J. Proteome Res.*, **2008**, *7*, 1109-1117.

- (20) Gehrke, C. W.;Waalkes, T. P.;Borek, E.;Swartz, W. F.;Cole, T. F.;Kuo, K. C.;Abeloff, M.;Ettinger, D. S.;Rosenshein, N.;Young, R. C. Quantitative Gas-Liquid-Chromatography of Neutral Sugars in Human-Serum Glycoproteins - Fucose, Mannose, and Galactose as Predictors in Ovarian and Small Cell Lung-Carcinoma. *J. Chromatogr.*, **1979**, *162*, 507-528.
- (21) An, H. J.;Miyamoto, S.;Lancaster, K. S.;Kirmiz, C.;Li, B. S.;Lam, K. S.;Leiserowitz, G. S.;Lebrilla, C. B. Profiling of glycans in serum for the discovery of potential biomarkers for ovarian cancer. *J. Proteome Res.*, **2006**, *5*, 1626-1635.
- (22) Saldoval, R.;Royle, L.;Radcliffe, C. M.;Hamid, U. M. A.;Evans, R.;Arnold, J. N.;Banks, R. E.;Hutson, R.;Harvey, D. J.;Antrobus, R.;Petrescu, S. M.;Dwek, R. A.;Rudd, P. M. Ovarian cancer is associated with changes in glycosylation in both acute-phase proteins and IgG. *Glycobiology*, **2007**, *17*, 1344-1356.
- (23) Bereman, M. S.;Williams, T. I.;Muddiman, D. C. Development of a nanoLC LTQ Orbitrap Mass Spectrometric Method for Profiling Glycans Derived from Plasma from Healthy, Benign Tumor Control, and Epithelial Ovarian Cancer Patients. *Anal. Chem.*, **2009**, *81*, 1130-1136.
- (24) Williams, T. I.;Toups, K. L.;Saggese, D. A.;Kalli, K. R.;Cliby, W. A.;Muddiman, D. C. Epithelial ovarian cancer: Disease etiology, treatment, detection, and investigational gene, metabolite, and protein biomarkers. *J. Proteome Res.*, **2007**, *6*, 2936-2962.
- (25) Zhao, J.;Qiu, W. L.;Simeone, D. M.;Lubman, D. M. N-linked glycosylation profiling of pancreatic cancer serum using capillary liquid phase separation coupled with mass spectrometric analysis. *J. Proteome Res.*, **2007**, *6*, 1126-1138.
- (26) Orlando, R. Quantitative Glycomics. *Methods Mol. Biol.*, **2010**, *600*, 31-49.
- (27) Alvarez-Manilla, G.;Warren, N. L.;Abney, T.;Atwood, J.;Azadi, P.;York, W. S.;Pierce, M.;Orlando, R. Tools for glycomics: relative quantitation of glycans by isotopic permethylation using (CH₃)₂C-¹³. *Glycobiology*, **2007**, 677-687.
- (28) Atwood, J. A.;Cheng, L.;Alvarez-Manilla, G.;Warren, N. L.;York, W. S.;Orlando, R. Quantitation by isobaric labeling: Applications to glycomics. *J. Proteome Res.*, **2008**, 367-374.

- (29) Kang, P.;Mechref, Y.;Kyselova, Z.;Goetz, J. A.;Novotny, M. V. Comparative glycomic mapping through quantitative permethylation and stable-isotope labeling. *Anal. Chem.*, **2007**, 6064-6073.
- (30) Bowman, M. J.;Zaia, J. Tags for the stable isotopic labeling of carbohydrates and quantitative analysis by mass spectrometry. *Anal. Chem.*, **2007**, *79*, 5777-5784.
- (31) Bowman, M. J.;Zaia, J. Comparative Glycomics Using a Tetraplex Stable-Isotope Coded Tag. *Anal. Chem.*, **2010**, *82*, 3023-3031.
- (32) Xia, B. Y.;Feasley, C. L.;Sachdev, G. P.;Smith, D. F.;Cummings, R. D. Glycan reductive isotope labeling for quantitative glycomics. *Anal. Biochem.*, **2009**, *387*, 162-170.
- (33) Orlando, R.;Lim, J. M.;Atwood, J. A.;Angel, P. M.;Fang, M.;Aoki, K.;Alvarez-Manilla, G.;Moremen, K. W.;York, W. S.;Tiemeyer, M.;Pierce, M.;Dalton, S.;Wells, L. IDAWG: Metabolic Incorporation of Stable Isotope Labels for Quantitative Glycomics of Cultured Cells. *J. Proteome Res.*, **2009**, 3816-3823.
- (34) Kang, P.;Mechref, Y.;Klouckova, I.;Novotny, M. V. Solid-phase permethylation of glycans for mass spectrometric analysis. *Rapid Commun. Mass Spectrom.*, **2005**, *19*, 3421-3428.
- (35) Filer, C. N. Isotopic fractionation of organic compounds in chromatography. *J. Labelled Compd. Radiopharm.*, **1999**, 169-197.
- (36) Gygi, S. P.;Rist, B.;Gerber, S. A.;Turecek, F.;Gelb, M. H.;Aebbersold, R. Quantitative analysis of complex protein mixtures using isotope-coded affinity tags. *Nat. Biotechnol.*, **1999**, 994-999.
- (37) Filer, C. N.;Fazio, R.;Ahern, D. G. (+/-)-[methyl-H-3 and methyl-H-2]mianserin - participants in a dramatic instance of HPLC isotopic fractionation. *J. Org. Chem.*, **1981**, 3344-3346.
- (38) Gouw, J. W.;Burgers, P. C.;Trikoupi, M. A.;Terlouw, J. K. Derivatization of small oligosaccharides prior to analysis by matrix-assisted laser desorption/ionization using glycidyltrimethylammonium chloride and Girard's reagent T. *RCMS*, **2002**, *16*, 905-912.
- (39) Naven, T. J. P.;Harvey, D. J. Cationic derivatization of oligosaccharides with Girard's T reagent for improved performance in matrix-assisted laser

- desorption/ionization and electrospray mass spectrometry. *Rapid Commun. Mass Spectrom.*, **1996**, *10*, 829-834.
- (40) Lattova, E.;Perreault, H. Labelling saccharides with phenylhydrazine for electrospray and matrix-assisted laser desorption-ionization mass spectrometry. *J. Chromatogr. B*, **2003**, *793*, 167-179.
- (41) Lattova, E.;Perreault, H. Profiling of N-linked oligosaccharides using phenylhydrazine derivatization and mass spectrometry. *J. Chromatogr. A*, **2003**, *1016*, 71-87.
- (42) Ruhaak, L. R.;Zauner, G.;Huhn, C.;Bruggink, C.;Deelder, A. M.;Wuhrer, M. Glycan labeling strategies and their use in identification and quantification. *Anal. Bioanal. Chem.*, **2010**, *Published online 12 March 2010*.
- (43) Walker, S. H.;Lilley, L. M.;Enamorado, M. F.;Comins, D. L.;Muddiman, D. C. Hydrophobic Derivatization of N-linked Glycans for Increased Ion Abundance in Electrospray Ionization Mass Spectrometry. *J. Am. Soc. Mass Spectrom.*, **2011**, DOI: 10.1007/s13361-011-0140-x.
- (44) Walker, S. H.;Papas, B. N.;Comins, D. L.;Muddiman, D. C. Interplay of Permanent Charge and Hydrophobicity in the Electrospray Ionization of Glycans. *Anal. Chem.*, **2010**, *82*, 6636-6642.
- (45) Bereman, M. S.;Comins, D. L.;Muddiman, D. C. Increasing the hydrophobicity and electrospray response of glycans through derivatization with novel cationic hydrazides. *Chem. Comm.*, **2010**, *46*, 237-239.
- (46) Bereman, M. S.;Young, D. D.;Deiters, A.;Muddiman, D. C. Development of a Robust and High Throughput Method for Profiling N-Linked Glycans Derived from Plasma Glycoproteins by NanoLC-FTICR Mass Spectrometry. *J. Proteome Res.*, **2009**, *8*, 3764-3770.
- (47) Dixon, R. B.;Bereman, M. S.;Petitte, J. N.;Hawkridge, A. M.;Muddiman, D. C. One-Year Plasma N-linked Glycome Intra-Individual and Inter-Individual Variability in the Chicken Model of Spontaneous Ovarian Adenocarcinoma. *Int. J. Mass Spectrom.*, **2010**, doi: 10.1016/j.ijms.2010.05.023.
- (48) Sonogashira, K.;Tohda, Y.;Hagihara, N. Convenient synthesis of acetylenes - catalytic substitutions of acetylenic hydrogen with bromoalkenes, iodoarenes, and bromopyridines. *Tetrahedron Lett.*, **1975**, 4467-4470.

- (49) Andrews, G. L.;Shuford, C. M.;Burnett, J. C.;Hawkridge, A. M.;Muddiman, D. C. Coupling of a vented column with splitless nanoRPLC-ESI-MS for the improved separation and detection of brain natriuretic peptide-32 and its proteolytic peptides. *J. Chromatogr. B*, **2009**, *877*, 948-954.
- (50) Domon, B.;Costello, C. E. A Systematic Nomenclature for Carbohydrate Fragmentations in Fab-MS MS Spectra of Glycoconjugates. *Glycoconjugate J.*, **1988**, *5*, 397-409.

CHAPTER 5

Systematic Comparison of Reverse Phase and Hydrophilic Interaction Liquid Chromatography Platforms for the Analysis of N-linked Glycans

The following work was reprinted with permission from: Walker, S. H.; Carlisle, B. C.; Muddiman, D. C. *Analytical Chemistry* **2012**, 84, 8198-8206. Copyright 2012 American Chemical Society. The original publication may be accessed directly via the World Wide Web.

5.1 Introduction

Glycosylation is a post-translational protein modification that is ubiquitous in biological systems¹⁻² and plays a significant role in numerous biological processes including cell-cell interactions, cellular recognition, protein stability, and immune response.³ Therefore, it is important to develop efficient, high-throughput strategies in order to analyze and understand these modifications. Many current glycomic strategies have evolved and benefitted from existing proteomic strategies, which are comprised mainly of some fractionation method followed by mass spectrometric analysis. One of the most effective proteomic strategies is online separation by reverse phase (RP) liquid chromatography (LC) coupled online to electrospray ionization (ESI) mass spectrometry (MS). However, the translation of this technology to the field of glycomics has been difficult for numerous reasons including the lack of retention on RP columns and the suppressed ESI response of the much more hydrophilic glycans. Thus, researchers have adapted this strategy to use more compatible separation techniques⁴ (hydrophilic interaction chromatography and graphitized carbon chromatography) and derivatization

techniques⁵⁻⁶ (permethylation, reductive amination, and hydrazone formation) in order to overcome the inherent disadvantages in the analysis of glycans.

When analyzing *N*-linked glycans cleaved from complex mixtures (such as plasma) in ESI MS, the separation of glycans prior to MS analysis is necessary due to the wide dynamic range and variable ionization efficiencies that can cause analyte suppression. Thus, numerous chromatographic techniques have been adapted for glycan separation including hydrophilic interaction (liquid) chromatography (HILIC), graphitized carbon chromatography, and less frequently RP chromatography.⁴ Chromatography is effective in increasing the peak capacity of the measurement and facilitating the detection of lower abundant glycans.⁷

HILIC has been used frequently for the separation of both native⁸⁻¹² and derivatized¹³⁻¹⁷ glycans in online LC-MS experiments⁴ and is often used for glycomic analyses due to the strong retention of polar compounds in comparison to RP stationary phases. However, there are several disadvantages that have been reported in comparison to RP chromatography including peak fronting and tailing, column bleed, irreversible sorption, and slow equilibration times.¹⁸ These problems can be overcome by switching the HILIC stationary phase¹⁸ or increasing the buffer concentration.¹⁹ Additionally, HILIC separation efficiency is generally accepted to be inferior to RP chromatography,²⁰⁻²¹ and though this depends on the analyte and the type and amount of buffer reagent, peak widths tend to be broader in HILIC than RP chromatography. This decreases the peak capacity of the separation and increases the possibility for competition of analytes in the electrospray droplet, which can

significantly hinder glycan analysis. This inferiority is thought to be due to the relatively limited studies of the fundamental chemistry of HILIC in comparison to RP and the relative newness of the separation technique (Alpert coined the term HILIC in 1990²²).²¹ Furthermore, researchers must choose from a large collection of different HILIC stationary phases, each of which is often optimized for a specific type of analyte and/or has limited studies of separation efficiency.²¹ Our group has generated data previously that show a range of separation efficiencies depending on the *N*-linked glycan composition in HILIC with the peak widths (FWHM) ranging from just under 1 minute to several minutes.^{13, 23} This is in contrast to the same chromatography instrument platform using RP C₁₈ stationary phase for peptide analysis, which consistently produces peak widths \leq 30 seconds.²⁴ This disparity leads one to the hypothesis that it is possible to significantly enhance the analysis of *N*-linked glycans by separating glycans with RP chromatography rather than HILIC.

RP chromatography is not compatible with native glycan analysis due to the lack of interaction of the glycans with the non-polar stationary phase. However, glycans that are derivatized either at the reducing terminus^{6, 25-38} or permethylated^{4, 39-40} are able to be retained on a C₁₈ column. This is due to the increase in hydrophobicity of the derivatized glycan molecule so that the derivatized glycans will interact (either by partitioning or adsorption⁴¹) more effectively with the stationary phase and be retained on a RP column.^{4, 7} However, there have been minimal studies demonstrating the inherent advantages of using each separation technique for glycan analysis.

Glycan derivatization at the reducing terminus is common in *N*-linked glycan analysis due to the enzymatic cleavage of *N*-linked glycans from proteins using PNGase F.⁴² Upon cleavage, *N*-linked glycans are left intact with an accessible reducing terminus at the core HexNAc residue. Reductive amination is a prominent derivatization strategy at the reducing terminus that has been used for the incorporation of hydrophobic tags,^{33, 43-45} UV and fluorescent tags,^{28, 30, 38, 46} as well as the incorporation of stable isotope labeled tags for relative quantification.¹⁶⁻¹⁷ Depending on the derivatization reagent, studies have demonstrated that reductively aminated glycans are capable of being retained on a reverse phase column.^{33, 38} Recent reports have shown the separation of reductively aminated glycans by both HILIC^{16, 44} and RP^{33, 38} chromatography, and the development of commercialized kits (e.g. GlycoProfile for 2-AB labeling) for glycan derivatization have made glycan analysis using this derivatization strategy popular and versatile.

Pyrazolone derivatization of carbohydrates has also been used to facilitate MS and UV detection.⁶ The tag 1-phenyl-3-methyl-5-pyrazolone (PMP) is a common pyrazolone reagent that has been used frequently to derivatize glycans, and several reports have described separation of PMP-derivatized glycans using RP chromatography.^{6, 27, 31, 47-48} Perreault and coworkers²⁷ compared separation and detection efficiencies of both RP chromatography and HILIC (NH₂ column) of PMP-glycans cleaved from ovalbumin and found that HILIC provided better glycan chromatographic resolution, but RP chromatography provided more sensitive ESI. Additionally, the glycan profiles were found to be different depending on the

separation method used. PMP-derivatization of glycans was also used in the profiling of urinary oligosaccharides in mucopolysaccharidosis (MPS) type II (Hunter syndrome).³¹ The authors were able to separate the derivatized glycans and use the glycan profiles to distinguish between unaffected control samples and MPS II patients, leading to possible diagnosis strategies for Hunter syndrome.

Hydrazone formation is a similar derivatization strategy to reductive amination and pyrazolone derivatization in which hydrazine or hydrazide reagents can react with the reducing terminus of oligosaccharides. Dansylhydrazine was the first reagent used in the hydrazone derivatization of glycans,⁴⁹ and since, numerous reagents have been employed.^{6, 13-15, 25, 50-54} Hydrazone chemistry is often chosen for glycan derivatization due to the relatively simple and stable reaction that does not require a clean-up step after derivatization.^{14, 25, 50, 55} Numerous reaction conditions are presented in the literature,^{32, 52-53, 56-57} and recent studies from this group have shown consistent reaction efficiencies of hydrazide reagents with all classes of *N*-linked glycans to be $\geq 95\%$.¹³⁻¹⁴ Mopper and coworkers have demonstrated the RP separation of dansylhydrazine derivatized glycans,³² and Perreault and coworkers have demonstrated the RP separation of glycans derivatized with the phenylhydrazine reagent.^{25-26, 55} The latter authors were able to separate *N*-linked glycan standards and *N*-linked glycans cleaved from ovalbumin, both derivatized with phenylhydrazine, on C₈ and C₁₈ columns.

Permethylation is an alternative derivatization strategy in which all hydroxyl, amino, and carboxylic acid groups are converted to their respective methyl-ether

functions. This modification substantially increases the hydrophobicity of the glycans and allows for retention on a RP (C₁₈) column. This was first demonstrated by Vouros and coworkers, where a standard maltooligosaccharide ladder and standard branched complex *N*-linked glycans were permethylated and separated by RP chromatography.³⁹ A more recent study has demonstrated a chip-based RP separation of permethylated glycans.⁴⁰ The authors profiled the *N*-linked glycans in blood serum in search of diagnostic markers to distinguish breast cancer patients from controls. Permethylated glycans can yield more informative MS/MS spectra, and often, branching patterns can be determined.⁵⁸⁻⁶⁰

The derivatization steps necessary for glycan separation by RP chromatography often require a significant amount of additional sample preparation time, sample clean up procedures, and an increase in the analytical variability of the sample preparation strategy. However, often the benefits of glycan derivatization can outweigh these downfalls by providing more glycan structural information,⁵⁸⁻⁶⁰ more glycome coverage,¹³ the ability to relatively quantify glycans,^{16-17, 23, 61-65} and facilitated detection either by increased ion abundance in MS^{13, 15, 44-45, 50} or by adding a fluorescent or UV tag.^{28-29, 46, 49, 66-67}

Herein, we demonstrate that the separation of hydrazone derivatized *N*-linked glycans by RP chromatography has several significant advantages in comparison to HILIC including an increased number of detectable glycans, increased peak capacity due to better chromatographic resolution, reduced complexity of the spectra due to

the lack of ammonium adduction, reduced equilibration times, an increase in laboratory efficiency, and increased repeatability across laboratories currently equipped with instrumentation for proteomic analyses. Each of these advantages will be discussed with specific examples and data, which were collected on the same LC platform for both chromatographic techniques (the platforms only differed in the packing material of the trap and analytical chromatography columns). RP and HILIC separation will be discussed with respect to two samples: 1) maltodextrin oligosaccharide ladder and 2) *N*-linked glycans cleaved from pooled human plasma. In both samples, the number of glycans detected was greater when separated by RP chromatography rather than HILIC. Thus, hydrophobic derivatization of *N*-linked glycans and separation by RP chromatography is a significant advantage over separation by HILIC and a significant advancement in the development of a high-throughput strategy for the analysis of *N*-linked glycans.

5.2 Experimental

5.2.1 Materials

The hydrazide reagent, 4-phenethylbenzohydrazide, used for *N*-linked glycan derivatization was synthesized previously²³ in the Department of Chemistry at North Carolina State University. Peptide: *N*-glycosidase F (PNGase F) was purchased from New England BioLabs (Ipswich, MA). The maltodextrin oligosaccharide ladder was purchased from V-Labs, Inc. (Covington, LA). TSK-Gel Amide-80 and Magic C₁₈AQ stationary phases were purchased from TOSOH Bioscience (San Jose, CA)

and Michrom BioResources (Auburn, CA), respectively. Pooled human plasma, acetic acid, ammonium acetate, ammonium bicarbonate, dithiothreitol, and formic acid were all purchased from Sigma Aldrich (St. Louis, MO). HPLC grade acetonitrile, water, and methanol were purchased from Burdick & Jackson (Muskegon, MI).

5.2.2 N-linked Glycan Derivatization Procedure

N-linked glycans were derivatized with 4-phenethylbenzohydrazide (P2PGN) via hydrazone formation, as described previously.¹³ Briefly, immediately prior to reaction, a 1 mg/mL solution of P2GPN reagent was made in 75:25 (v/v) MeOH:acetic acid solution. One hundred microliters of the reagent solution were then added to the lyophilized glycan sample, and the sample was vortexed, centrifuged, and allowed to incubate at 56° C for 3 hr. The samples were then immediately lyophilized to dryness and stored at -20° C.

5.2.3 Maltodextrin Sample Preparation

Aliquots were made such that upon lyophilization, each contained 50 µg of maltodextrin ladder. No further sample preparation was performed until derivatization with either the light or heavy P2GPN reagent. After derivatization, the glycans were reconstituted in 200 µL of the LC initial conditions.

5.2.4 *N-linked Glycan Extraction from Pooled Plasma*

Pooled plasma aliquots were prepared by pipetting 50 μL into individual vials, and 1 μg of internal standard (maltoheptaose) was added to each sample. The samples were then lyophilized to dryness. The glycan cleavage and extraction methodology has been developed and described in detail previously,^{10, 68} and the following briefly outlines the procedure used in this experiment with the deviations elaborated on from previous publications. The lyophilized pooled human plasma and internal standard were reconstituted in 191 μL of 100 mM ammonium bicarbonate buffer, vortexed, and centrifuged. In order to denature the proteins, 2 μL of 1 M dithiothreitol (DTT) were added to make a final concentration of 10 mM DTT. The plasma sample was then incubated in 95° C for 15 s followed by incubation at 25° C for 15 s. The denaturation heat cycle was repeated 3 additional times. Following denaturation, 2 μL (1000 units) of PNGase F (glycerol free) were added to the sample for *N*-linked glycan cleavage. The mixture was vortexed, centrifuged, and allowed to incubate at 37° C for 18 hr. Following incubation, ethanol precipitation was performed to crudely separate the glycans from the remaining proteins and plasma matrix.⁶⁸ This was accomplished by adding 800 μL of chilled ethanol to the sample and letting it incubate for 1 hr at -80° C. The sample was then centrifuged at 13,200 rpm, and the supernatant was extracted and lyophilized. Solid phase extraction (SPE) was then performed on the sample to remove any other contamination, remaining plasma matrix, or protein and has been described previously.¹⁰ The SPE fractions were then combined, lyophilized, and stored at -20°

C. After derivatization, the glycans were reconstituted in 200 μ L of the LC initial conditions.

5.2.5 *nano-Flow Hydrophilic Interaction Chromatography*

Both derivatized and native *N*-linked glycans were separated by online HILIC prior to mass analysis, as described previously.^{9-10, 13} An Eksigent nanoLC-1D PLUS system (Eksigent, Dublin, CA) equipped with an HTS PAL autosampler (LEAP Technologies, Carrboro, NC) was set up to run in the vented column configuration.²⁴ The trap and analytical columns were packed in-house with TSK-Gel Amide-80 stationary phase (TOSOH Bioscience, San Jose, CA). A 100 μ m inner diameter IntegraFrit capillary (New Objective, Woburn, MA) was packed to 5 cm and used as the trap column, and a 75 μ m inner diameter PicoFrit (New Objective, Woburn, MA) was packed to 15 cm and used as the analytical column. Mobile phase A consisted of 50 mM ammonium acetate in water (pH 4.5), and mobile phase B was 100% acetonitrile. *N*-linked glycan samples were reconstituted in a 20/80% (v/v) ratio of mobile phase A/B and loaded onto the trap column at 2 μ L/min in the same solvent conditions. The sample was washed on the trap column for approximately 10 column washes, and then, a gradient elution was performed where mobile phase B was varied from 80% to 45% over 35 min at a flow rate of 500 nL/min. Column equilibration in 20% mobile phase A and column washing in 15% mobile phase B were performed at the beginning of the gradient, and a final column re-equilibration

was performed in the final 10 min of the run in 20% mobile phase A for a total run time of 70 min.

5.2.6 nano-Flow Reverse Phase Chromatography

The same equipment and vented-column set-up was used for reverse phase chromatography as stated above for HILIC. The columns were the same dimensions but were packed with Magic C₁₈AQ stationary phase (Michrom Bioresources, Auburn, CA). The stationary phase consisted of 5 µm particles with 200 Å pore size. Mobile phase A consisted of 98/2/0.2% water/acetonitrile/formic acid, and mobile phase B was 2/98/0.2% water/acetonitrile/formic acid. Sample was reconstituted in a solution of 95/5/0.2% water/acetonitrile/formic acid solution and loaded onto the trap column at 2 µL/min in mobile phase A. Approximately 10 column washes were performed with mobile phase A, and then the sample was eluted from the trap column at 500 nL/min using a gradient elution. The column was allowed to equilibrate for 5 min at 98% mobile phase A, and the gradient was ramped from 20% to 35% B over 33 min. The column was washed in 98% B for 5 min and allowed to re-equilibrate at the initial gradient conditions for 10 min for a total run time of 55 min.

5.2.7 LTQ-FT-ICR Mass Spectrometry

Mass analysis was performed on a hybrid linear ion trap Fourier transform ion cyclotron resonance (LTQ-FT-ICR) mass spectrometer (Thermo Fisher Scientific,

San Jose, CA) equipped with a 7 Tesla superconducting magnet. The instrument was calibrated per the manufacturer specifications. ESI was achieved by attaching 2.25 kV to the trap column union. The capillary was heated to 225° C with the capillary and tube lens voltages set at 42 and 120 V, respectively. Data dependent acquisition was performed such that for every precursor scan in the ICR cell, a maximum of 5 ms/ms fragmentation scans were collected in the ion trap determined by the most intense precursor ions. However, the second time a specific *m/z* was chosen for ms/ms, it was placed on an exclude list for 3 min, allowing for lower abundant analytes to be chosen for ms/ms as well. The ions were dissociated in the ion trap using collision induced dissociation with a normalized collision energy (NCE) of 28. An AGC of 8×10^3 with a maximum injection time of 100 ms was used in the ion trap scans, and an AGC of 1×10^6 with a maximum injection time of 500 ms was used in the FT scans. The glycans were identified manually by accurate mass (composition identification) and analyzed using Xcalibur software (v.2.0.7).

5.3 Results and Discussion

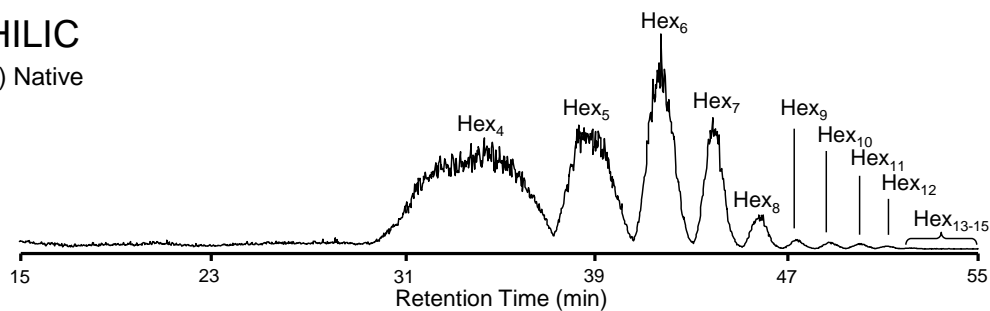
The separation of *N*-linked glycans by RP chromatography affords several advantages including an increase in separation efficiency, an increase in the number of glycans detected, and practical advantages such as the ability to use a more widely employed LC-MS technique (e.g. proteomic analyses). In order to demonstrate these advantages, two samples, maltodextrin and *N*-linked glycans cleaved from pooled human plasma, were used to compare the effectiveness of

HILIC and RP chromatography on the separation of both native and hydrazide derivatized glycans. As HILIC has been shown to effectively retain and separate native and derivatized glycans,^{10, 13} this was used as the control separation method. The *N*-linked glycans cleaved from plasma and the maltodextrin samples were first analyzed by HILIC coupled online with LTQ FT-ICR MS in order to insure sample integrity. Aliquots of the same samples (stored frozen at -20°C) were then analyzed by online RP chromatography coupled to FT-ICR MS using the same LC instrument platform.

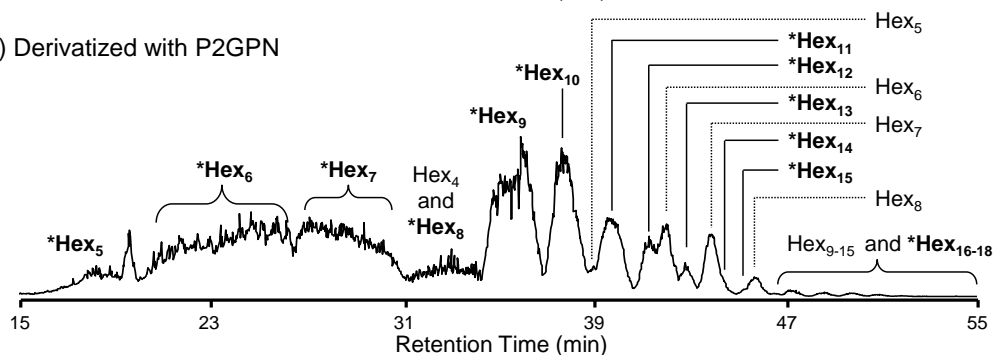
Figure 5.1 contains the base peak chromatograms for both native and derivatized maltodextrin samples on HILIC (**5.1a** and **5.1b**, respectively) and RP chromatography (**5.1c** and **5.1d**, respectively). As shown previously, both native and derivatized glycans are retained and separated by HILIC.^{10, 13-15, 23} In contrast, **Figure 5.1c** shows that there is no retention of native maltodextrin on the RP column, as is expected due to the polar nature of the glycans and the non-polar nature of the C₁₈ stationary phase. Upon derivatization of maltodextrin, **Figure 5.1d** shows that maltodextrin is capable of being separated and retained on a RP C₁₈ column. It must be mentioned that these are the optimized HILIC and RP gradients for derivatized glycans. Though the gradient for RP analysis of native glycans begins at >20% B, studies were also performed in RP starting at 2% B in order to optimize the native glycan retention. However, there were no conditions in which native glycans were retained on RP chromatography.

HILIC

a) Native



b) Derivatized with P2GPN



Reverse Phase

c) Native



d) Derivatized with P2GPN

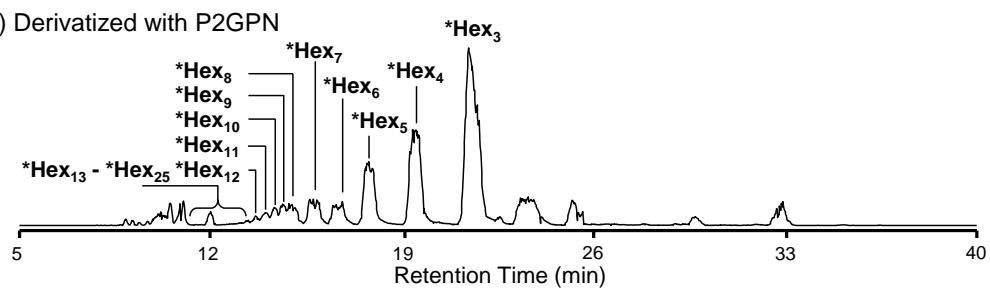


Figure 5.1 – The base peak chromatograms of both native and derivatized (**bold with ***) maltodextrin (Hex_n) oligosaccharides analyzed by HILIC (**a** and **b**, respectively) and RP chromatography (**c** and **d**, respectively).

Several additional important observations are made from the base peak chromatograms in **Figure 5.1**. The HILIC base peak chromatograms show that the separation efficiency for both native and derivatized glycans varies as a function of the glycan retention time. This is in contrast to the separation by RP chromatography, where the peak widths are uniform throughout the chromatogram. It is important in the analysis of *N*-linked glycans to have as narrow peak widths as possible in order to reduce the amount of possible co-elution and peak suppression due to the more easily ionized or more abundant glycans. In the HILIC chromatograms, the glycans that elute over a large time window are the more hydrophobic and more abundant glycans, meaning that these glycans will likely elute at the same time as, and out-compete, the more hydrophilic, less abundant glycans. **Figure C.1** in the supplemental material contains example extracted ion chromatograms (EIC) for both HILIC and RP chromatography to further show the superior resolution for RP chromatography.

Though the fact that HILIC is capable of retaining both native and derivatized *N*-linked glycans is often viewed as an advantage, **Figure 5.1b** shows that these two species often have overlapping analytes, and this is a disadvantage when one is only interested in analyzing the derivatized *N*-linked glycans. During derivatization, $\leq 5\%$ of each glycan remains untagged. Though this seems like a small number, when the dynamic range of the sample comprises orders of magnitude, 5% of an abundant analyte is capable of out-competing lower abundant analytes in the electrospray droplet (e.g. Hex₇ and *Hex₁₄ in **Figure 5.1b**). In contrast, the RP

chromatography of derivatized glycans has no contamination by the un-reacted glycan. This is a significant advantage in comparison to HILIC and decreases the competition in the electrospray droplet and AGC ion trap capacity for the low abundant glycans.

The final important piece of data from **Figure 5.1** is the total number of unique glycan compositions detected in each chromatographic system. There are 12 glycan compositions detected in **Figure 5.1a**, 14 in **Figure 5.1b**, 0 in **Figure 5.1c**, and 23 in **Figure 5.1d**. This shows that independent of the chromatographic technique, it is always better to derivatize the *N*-linked glycans with hydrophobic hydrazide reagents than to analyze their native counterparts. However, **Figure 5.1** also shows that it is significantly more productive (~65% more compositions detected) to separate derivatized glycans by RP chromatography than HILIC. There are several differences in the two chromatography techniques that are possible reasons for this outcome. First, as mentioned above (**Figure C.1**), the efficiency of RP chromatography is more uniform throughout the glycan retention window, and in general, the peak widths are narrower. The oligosaccharide peak widths are compared in the supplemental material for the same 15 glycans (only oligosaccharides that were detected in both HILIC and RP techniques). The HILIC peak widths have a range of 0.34-10.37 min with a mean of 2.23 min and standard deviation of 2.87 (**Table C.1**). In contrast, the RP peak widths have a range of 0.34-1.1 min with a mean of 0.49 min and a standard deviation of 0.18 (**Table C.2**). Because peak broadening spreads the analytes out over a longer retention time, the

detection limit will be lower for chromatographic techniques with narrower peak widths (*i.e.*, higher concentration). Additionally, the elution overlap of un-reacted glycans with lower abundant, derivatized glycans in HILIC causes competition in the electrospray droplet. This hinders the ionization of the lower abundant glycans, causing fewer glycans to be detected in HILIC.

Furthermore, the efficiency of HILIC is often increased and the peak tailing minimized by addition of an acidic buffer such as ammonium acetate or ammonium formate.^{19, 69} However, the addition of ammonium salts into the buffer often has an adverse affect on detection due to the ammonium adduction in ESI. **Figure 5.2** shows the difference in mass spectra between HILIC (top/blue) and RP chromatography (bottom/red) for three different glycan compositions (**Figure 5.2a** from maltodextrin and **Figure 5.2b** and **Figure 5.2c** cleaved from human plasma – *vide infra*). It must be noted that all the glycans are detected in light and heavy pairs due to the derivatization with both the native and stable-isotope labeled glycan reagents (as published previously for the relative quantification of *N*-linked glycans²³). This was necessary to confirm that the light and heavy tagged glycans are affected identically in RP chromatography with no chromatographic shift due to the incorporation of ¹³C₆.

The absence of ammonium acetate in the RP solvent system allows for only the detection of the $[M+nH^+]^{n+}$ peak, whereas ammonium adduction is detected in the HILIC spectra due to the buffer system containing ammonium acetate. This

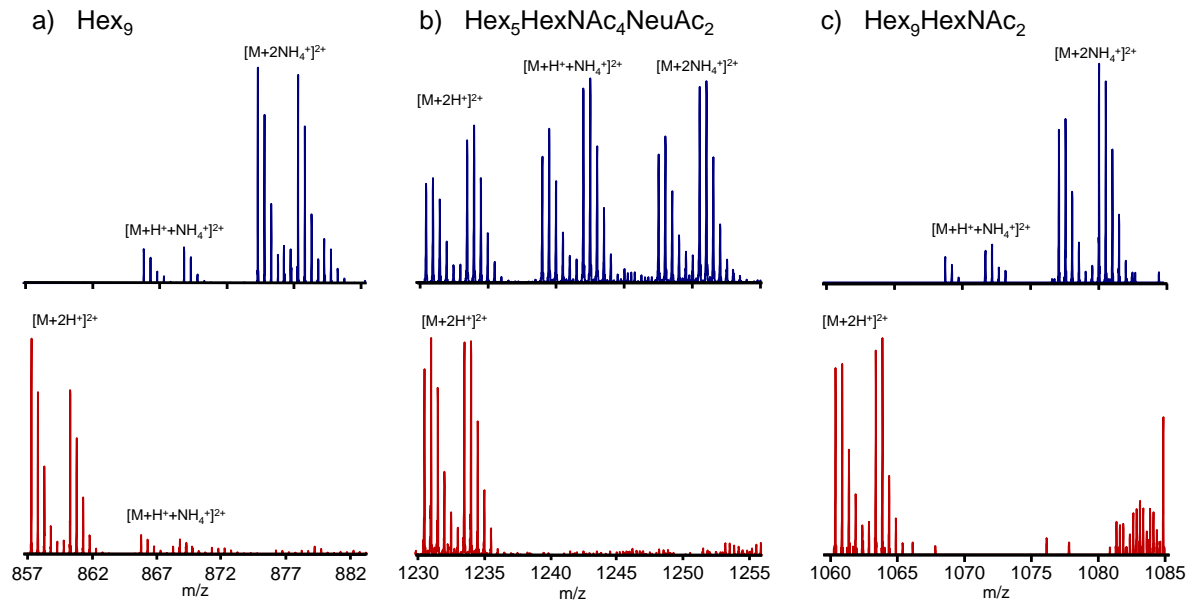


Figure 5.2 – Example mass spectra for (a) a hexose oligosaccharide in the maltodextrin sample and (b and c) two glycans cleaved from pooled human plasma. The top spectra (blue) were analyzed using HILIC-MS and the bottom spectra (red) were analyzed with RP-MS. The difference in ammonium adduction is observed for several different types of glycans.

negatively impacts the profiling of *N*-linked glycans because the ammonium adduction spreads the signal of one glycan composition into multiple *m/z* channels. Additionally, **Figure 5.2a** and **Figure 5.2c** show that for certain types of glycans in HILIC, the $[M+nH^+]^{n+}$ peak is not detected in the mass spectrum, making detection and identification more difficult.

The observations discussed above have led to several conclusions on the mechanism of *N*-linked glycan separation by HILIC and RP chromatography. **Figure 5.3** summarizes the observations made in the separation of *N*-linked glycans, both

native and derivatized, in HILIC (**Figures 5.3a** and **5.3b**) and RP chromatography (**Figures 5.3c** and **5.3d**). The mechanisms of both HILIC^{4, 21-22, 70-72} and RP chromatography^{41, 73} are frequently debated, and often, the compromise is that the separation techniques both involve a combination of partitioning and adsorption depending on the molecular properties of the analytes. These properties permit the native glycans to interact significantly with the HILIC stationary phase and allow them to be retained on the HILIC column (**Figure 5.3a**). However when derivatized, the glycan molecules become more hydrophobic, and the hydrophobic tag causes the glycan to partition more into the organic mobile phase, which decreases the

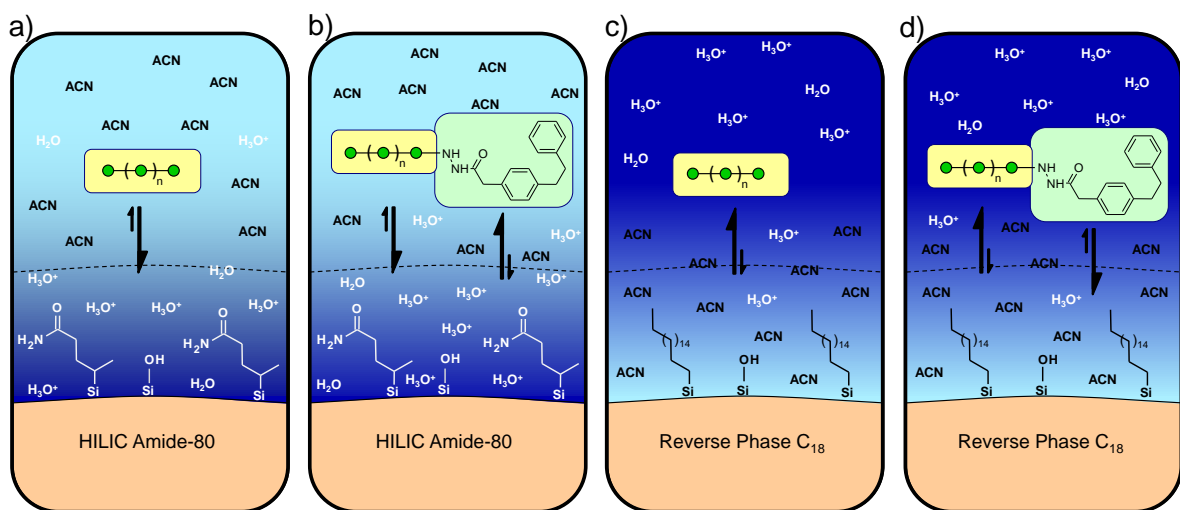


Figure 5.3 – The observed retention behavior of native and derivatized *N*-linked glycans in HILIC and RP chromatography. The magnitude of the arrows indicates the observed relative amount of interaction of the glycan with the stationary phase. The *N*-linked glycan shown is a general hexose structure to demonstrate the collective behavior of the maltodextrin glycans.

retention time (as seen in **Figure 5.1b**). In the case of RP chromatography, the native glycan interacts very little with the hydrophobic C₁₈ stationary phase (**Figure 5.3c**), but when derivatized (**Figure 5.3d**), the glycan molecule becomes hydrophobic enough to interact with the C₁₈ stationary phase, and the derivatized glycans are retained and separated (as seen in **Figure 5.1d**).

The magnitude of the arrows in **Figure 5.3** are used to portray the likelihood of the analyte interaction with the stationary phase and mobile phase and is dependent on the physical properties of the molecule. Molecules that are hydrophobic will tend to interact more with the C₁₈ stationary phase, whereas hydrophilic molecules will interact more with the mobile phase. A molecule that has both hydrophobic and hydrophilic character (such as the derivatized glycans) will have competing interaction between the mobile phase and stationary phase. **Figure 5.3c** implies that there is little to no interaction between the native glycans and the RP stationary phase because no retention is observed. However, because separation of derivatized *N*-linked glycans is observed on a RP column, the glycans must have some interaction with the stationary phase in order to have different retention times. If the glycan molecules are assumed to have no interaction with the stationary phase, then all possible retention would be due to the hydrophobic tag interaction, and since all the glycans are derivatized with the identical tag, one would assume that there would be no separation of the glycans. Since this was not observed, the partitioning of derivatized glycans was estimated by calculating the ratio of the hydrophobic surface area (NPSA) and the hydrophilic surface area (MW)

(equation development in supplemental **Equation C.1**). A plot of both retention time and $\frac{NPSA}{MW}$ vs. the number of hexose monosaccharide units is shown in **Figure 5.4**.

It is seen that the estimated hydrophobicity:hydrophilicity ratio predicts a similar trend as experimentally observed for the retention of derivatized glycans. This supports a partitioning mechanism for derivatized glycans based on both the hydrophobic and hydrophilic character of the molecule. However, eventually (based on the extrapolation of **Figure 5.4**), the glycans will be so large, adding an additional

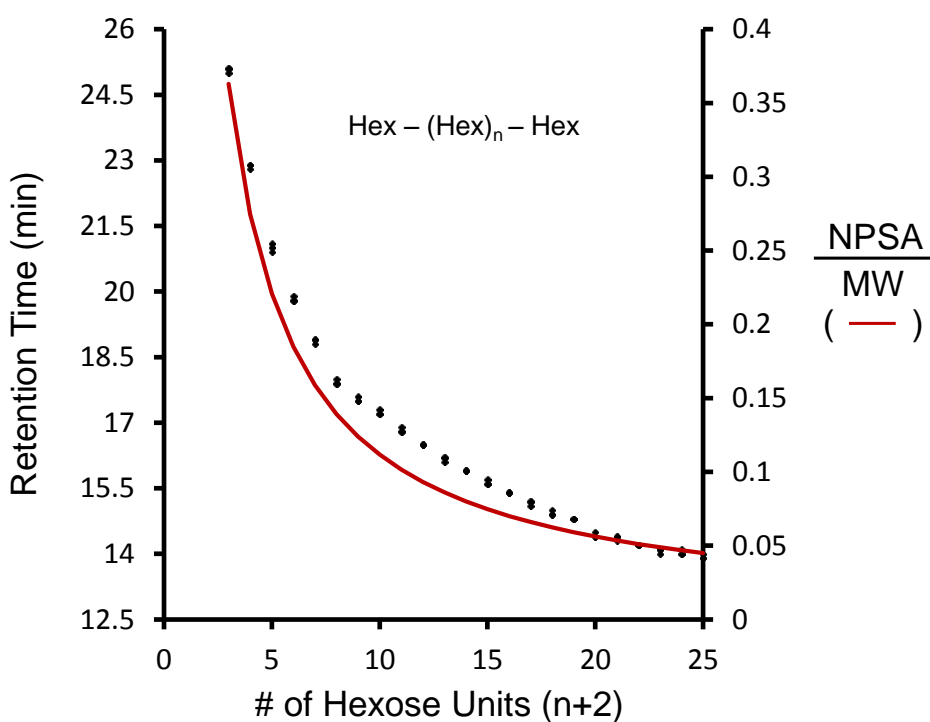


Figure 5.4 – The retention times (left y-axis) of the maltodextrin ladder with respect to the size of the maltooligosaccharide. The calculated partitioning trend of derivatized glycans is overlaid (right y-axis).

hexose monosaccharide (Hex_{n+1}) will not afford any chromatographic separation from the previous oligosaccharide (Hex_n). Thus, a limitation of the *N*-linked glycan RP separation will be at the most hydrophilic glycan molecules, where separation of the analytes will be limited, and competition in the electrospray droplet could occur. HILIC could be a possible alternative to RP for these large glycans; however, due to the competition in the ESI droplet with underivatized glycans (*vide supra*), HILIC does not perform better than RP for glycans derivatized by hydrazone formation.

In order to apply and study the advantages of RP separation over HILIC to complex mixtures, *N*-linked glycans cleaved from pooled human plasma were used to further compare the two chromatographic techniques. The maltodextrin oligosaccharide ladder is composed only of hexose monosaccharide residues; thus, it was necessary to test and compare more complex glycans (containing fucose and sialic acid residues) and glycan mixtures on the RP system. The base peak HILIC and RP chromatograms for derivatized *N*-linked glycans are shown in **Figure 5.5a** and **Figure 5.5b**, respectively (the native glycan chromatograms were not shown due to the results presented above – *vide supra*). These chromatograms are a complex mixture of glycans. However, **Figure 5.5a** shows that several glycans in HILIC are dominating the glycan retention window with large abundances and retention times on the order of minutes. This is not seen in the RP chromatogram, implying less spectral competition due to the most abundant analytes. In **Figure 5.5c**, it is seen that all glycans that were detected in HILIC (42 unique compositions) were also detected in RP. Moreover, 18 additional *N*-linked glycans were detected

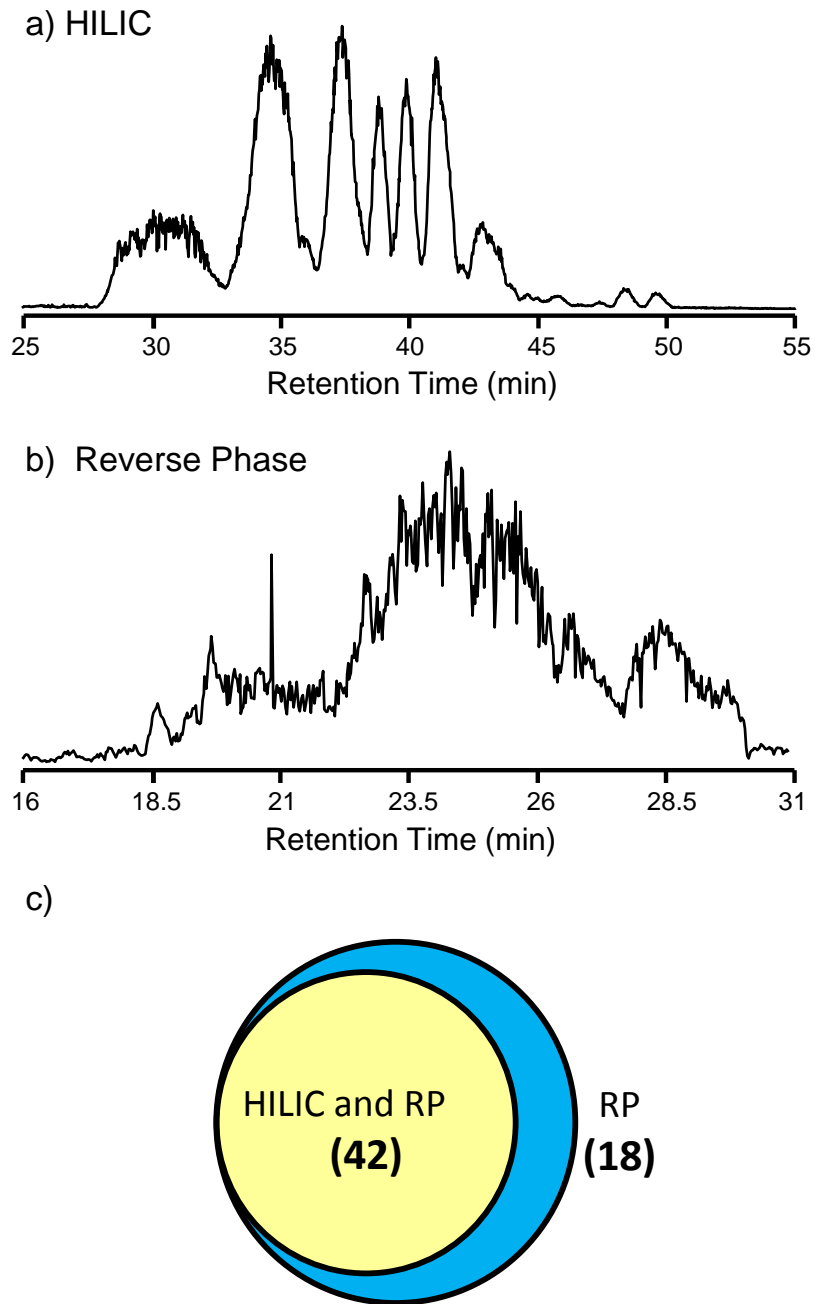


Figure 5.5 – The (a) HILIC and (b) RP chromatography base peak chromatograms for derivatized *N*-linked glycans. (c) Venn diagram of the total number of unique *N*-linked glycan compositions cleaved from pooled human plasma and analyzed by online HILIC- and RP-MS.

using RP separation rather than HILIC. The majority of these glycans were of the large, highly sialylated, complex glycan type that are typically low abundant and hydrophilic, two properties that make detection by ESI-MS difficult. By increasing the chromatographic resolution, reducing ammonium adduction, and reducing the competition in the ESI droplet, the effective detection limit of the instrument was decreased so that one is able to delve deeper into the *N*-glycome of human plasma. In a few cases (mostly sialylated glycans), it was observed that the glycan compositional mass was detected at two distinct retention times. This could possibly be due to isomeric separation, which would allow for quantification of glycan isomers. However, this needs to be investigated more thoroughly in order to determine the cause and utility of this peak splitting.

Table C.3 in the supplemental material details the glycan compositions that were detected and their respective molecular weights that were detected using both HILIC and RP chromatographic techniques. It is seen that numerous large complex glycans are only detected with RP separation. The charge state has also been listed in **Table C.3** for each glycan, and it was observed that glycans separated and analyzed in the RP solvent system are detected in higher charge states. This could be due to the elution of the glycans in different organic:aqueous solvent ratios and the difference in acidic buffer (formic acid or ammonium acetate). In comparison to other studies, the 60 unique *N*-linked glycan compositions detected using this method is on par with current literature. Reinhold and coworkers were able to detect 53 unique compositions,⁷⁴ and this was increased to 106 by using plasma depletion

methods. Lebrilla and coworkers report up to 64 unique compositions,⁶⁸ and Ruhaak and coworkers report 47 unique compositions.⁷⁵ However, utilizing the hydrazide quantification strategy presented previously,²³ each sample consisted of a 1:1 combination of a light and heavy derivatized sample, and only the glycans that were detected with a light and heavy pair in the spectra were determined to be identified. Thus, each of the glycans that was detected is also capable of being relatively quantified using stable-isotope labeled derivatization.

5.4 Conclusions

RP separation of *N*-linked glycans, both simple and cleaved from pooled human plasma, was more efficient than HILIC with respect to both separation and detection by MS. The discussed benefits of separating *N*-linked glycans by RP chromatography are in addition to the practical advantages that will increase the efficiency of 'multi-omics' laboratories. The opportunity to use the same chromatographic instrumentation, solvents, columns, and set-up as are used with proteomic analyses is a practical advantage that cannot be understated. Since many mass spectrometry groups who study glycosylation often study proteomics as well, the use of RP (C₁₈) chromatography for both analyses nearly eliminates the time it takes to switch between techniques (which takes at least one day to fully switch out solvents and equilibrate the columns when transitioning to HILIC from RP chromatography and vice versa), greatly increasing the efficiency of instrument time.

Furthermore, the ability to use a derivatization strategy that adds only 4 hr to the glycan sample preparation time while being able to analyze the samples on a RP-MS platform allows researchers to apply this derivatization strategy to glycans from any protein sample. This compatibility with numerous research labs combined with the previously demonstrated advantages including relative glycan quantification²³ and increased ESI efficiency¹³ make this a versatile, high-throughput strategy for the enhanced profiling and quantification of *N*-linked glycans cleaved from proteins. Additionally, the ability to acquire data in nearly any laboratory studying proteomics or glycomics using the exact same LC-MS strategy will allow for more accurate comparisons across laboratories, reproducibility studies, and ultimately allow the field of glycomics to stride toward a more in-depth biological understanding of glycosylation including aberrant glycosylation in disease, cellular interactions, and biomarker discovery efforts.

5.5 References

- (1) Apweiler, R.; Hermjakob, H.; Sharon, N. On the frequency of protein glycosylation, as deduced from analysis of the SWISS-PROT database. *BBA-Gen. Subjects*, **1999**, *1473*, 4-8.
- (2) Begley, T. P., *Wiley Encyclopedia of Chemical Biology* **2009**, *2*, 785.
- (3) Varki, A.; Cummings, R. D.; Esko, J. D.; Freeze, H. H.; Stanley, P.; Bertozzi, C. R.; Hart, G. W.; Etzler, M. E., *Essentials of Glycobiology* **2009**.
- (4) Wuhrer, M.; Deelder, A. M.; Hokke, C. H. Protein glycosylation analysis by liquid chromatography-mass spectrometry. *J. Chromatogr. B: Anal. Technol. Biomed. Life Sci.*, **2005**, *825*, 124-133.
- (5) Ruhaak, L. R.; Zauner, G.; Huhn, C.; Bruggink, C.; Deelder, A. M.; Wuhrer, M. Glycan labeling strategies and their use in identification and quantification. *Anal. Bioanal. Chem.*, **2010**, *397*, 3457-3481.
- (6) Lamari, F. N.; Kuhn, R.; Karamanos, N. K. Derivatization of carbohydrates for chromatographic, electrophoretic and mass spectrometric structure analysis. *J. Chromatogr., B*, **2003**, *793*, 15-36.
- (7) Zaia, J. Mass Spectrometry and Glycomics. *OMICS*, **2010**, *14*, 401-418.
- (8) Dixon, R. B.; Bereman, M. S.; Petite, J. N.; Hawkrigde, A. M.; Muddiman, D. C. One-year plasma N-linked glycome intra-individual and inter-individual variability in the chicken model of spontaneous ovarian adenocarcinoma. *Int. J. Mass Spectrom.*, **2011**, *305*, 79-86.
- (9) Bereman, M. S.; Williams, T. I.; Muddiman, D. C. Development of a nanoLC LTQ Orbitrap Mass Spectrometric Method for Profiling Glycans Derived from Plasma from Healthy, Benign Tumor Control, and Epithelial Ovarian Cancer Patients. *Anal. Chem.*, **2009**, *81*, 1130-1136.
- (10) Bereman, M. S.; Young, D. D.; Deiters, A.; Muddiman, D. C. Development of a Robust and High Throughput Method for Profiling N-Linked Glycans Derived from Plasma Glycoproteins by NanoLC-FTICR Mass Spectrometry. *J. Proteome Res.*, **2009**, *8*, 3764-3770.
- (11) Wuhrer, M.; Koeleman, C. A. M.; Deelder, A. M.; Hokke, C. N. Normal-phase nanoscale liquid chromatography - Mass spectrometry of underivatized

- oligosaccharides at low-femtomole sensitivity. *Anal. Chem.*, **2004**, 76, 833-838.
- (12) Butler, M.;Quelhas, D.;Critchley, A. J.;Carchon, H.;Hebestreit, H. F.;Hibbert, R. G.;Vilarinho, L.;Teles, E.;Matthijs, G.;Schollen, E.;Argibay, P.;Harvey, D. J.;Dwek, R. A.;Jaeken, J.;Rudd, P. M. Detailed glycan analysis of serum glycoproteins of patients with congenital disorders of glycosylation indicates the specific defective glycan processing step and provides an insight into pathogenesis. *Glycobiology*, **2003**, 13, 601-622.
- (13) Walker, S. H.;Lilley, L. M.;Enamorado, M. F.;Comins, D. L.;Muddiman, D. C. Hydrophobic Derivatization of N-linked Glycans for Increased Ion Abundance in Electrospray Ionization Mass Spectrometry. *J Am. Soc. Mass Spectrom.*, **2011**, 22, 1309-17.
- (14) Walker, S. H.;Papas, B. N.;Comins, D. L.;Muddiman, D. C. Interplay of Permanent Charge and Hydrophobicity in the Electrospray Ionization of Glycans. *Anal. Chem.*, **2010**, 82, 6636-6642.
- (15) Bereman, M. S.;Comins, D. L.;Muddiman, D. C. Increasing the hydrophobicity and electrospray response of glycans through derivatization with novel cationic hydrazides. *Chem. Comm.*, **2010**, 46, 237-239.
- (16) Bowman, M. J.;Zaia, J. Comparative Glycomics Using a Tetraplex Stable-Isotope Coded Tag. *Anal. Chem.*, **2010**, 82, 3023-3031.
- (17) Xia, B. Y.;Feasley, C. L.;Sachdev, G. P.;Smith, D. F.;Cummings, R. D. Glycan reductive isotope labeling for quantitative glycomics. *Anal. Biochem.*, **2009**, 387, 162-170.
- (18) Snyder, L. R.;Kirkland, J. J.;Dolan, J. W., *Introduction to Modern Liquid Chromatography*, 3 ed.; Wiley: Hoboken, NJ, USA, 2009.
- (19) Kadar, E. P.;Wujcik, C. E. Remediation of undesirable secondary interactions encountered in hydrophilic interaction chromatography during development of a quantitative LC-MS/MS assay for a dipeptidyl peptidase IV (DPP-IV) inhibitor in monkey serum. *J. Chromatogr. B*, **2009**, 877, 471-476.
- (20) Thaysen-Andersen, M.;Engholm-Keller, K.;Roepstorff, P., in *Hydrophilic Interaction Liquid Chromatography (HILIC) and Advanced Applications*, ed. P. G. Wang, W. He. CRC Press: Boca Raton, FL, 2011, pp 551-575.^^

- (21) Ikegami, T.;Tomomatsu, K.;Takubo, H.;Horie, K.;Tanaka, N. Separation efficiencies in hydrophilic interaction chromatography. *J. Chromatogr. A*, **2008**, *1184*, 474-503.
- (22) Alpert, A. J. Hydrophilic-Interaction Chromatography for the Separation of Peptides, Nucleic-Acids and Other Polar Compounds. *J. Chromatogr.*, **1990**, *499*, 177-196.
- (23) Walker, S. H.;Budhathoki-Uprety, J.;Novak, B. M.;Muddiman, D. C. Stable-isotope labeled hydrophobic hydrazide reagents for the relative quantification of N-linked glycans by electrospray ionization mass spectrometry. *Anal. Chem.*, **2011**, *83*, 6738-45.
- (24) Andrews, G. L.;Shuford, C. M.;Burnett, J. C.;Hawkridge, A. M.;Muddiman, D. C. Coupling of a vented column with splitless nanoRPLC-ESI-MS for the improved separation and detection of brain natriuretic peptide-32 and its proteolytic peptides. *J. Chromatogr. B*, **2009**, *877*, 948-954.
- (25) Lattova, E.;Perreault, H. Labelling saccharides with phenylhydrazine for electrospray and matrix-assisted laser desorption-ionization mass spectrometry. *J. Chromatogr. B*, **2003**, *793*, 167-179.
- (26) Lattova, E.;Perreault, H. Profiling of N-linked oligosaccharides using phenylhydrazine derivatization and mass spectrometry. *J. Chromatogr. A*, **2003**, *1016*, 71-87.
- (27) Saba, J. A.;Shen, X. D.;Jamieson, J. C.;Perreault, H. Investigation of different combinations of derivatization, separation methods and electrospray ionization mass spectrometry for standard oligosaccharides and glycans from ovalbumin. *J. Mass Spectrom.*, **2001**, *36*, 563-574.
- (28) Anumula, K. R. Advances in fluorescence derivatization methods for high-performance liquid chromatographic analysis of glycoprotein carbohydrates. *Anal. Biochem.*, **2006**, *350*, 1-23.
- (29) Anumula, K. R. High-sensitivity and high-resolution methods for glycoprotein analysis. *Anal. Biochem.*, **2000**, *283*, 17-26.
- (30) Chen, X. Y.;Flynn, G. C. Analysis of N-glycans from recombinant immunoglobulin G by on-line reversed-phase high-performance liquid chromatography/mass spectrometry. *Anal. Biochem.*, **2007**, *370*, 147-161.

- (31) Nielsen, T. C.;Rozek, T.;Hopwood, J. J.;Fuller, M. Determination of urinary oligosaccharides by high-performance liquid chromatography/electrospray ionization-tandem mass spectrometry: Application to Hunter syndrome. *Anal. Biochem.*, **2010**, *402*, 113-120.
- (32) Mopper, K.;Johnson, L. Reversed-Phase Liquid-Chromatographic Analysis of Dns-Sugars - Optimization of Derivatization and Chromatographic Procedures and Applications to Natural Samples. *J. Chromatogr.*, **1983**, *256*, 27-38.
- (33) Prater, B. D.;Connelly, H. M.;Qin, Q.;Cockrill, S. L. High-throughput immunoglobulin G N-glycan characterization using rapid resolution reverse-phase chromatography tandem mass spectrometry. *Anal. Biochem.*, **2009**, *385*, 69-79.
- (34) Wing, D. R.;Garner, B.;Hunnam, V.;Reinkensmeier, G.;Andersson, U.;Harvey, D. J.;Dwek, R. A.;Platt, F. M.;Butters, T. D. High-performance liquid chromatography analysis of ganglioside carbohydrates at the picomole level after ceramide glycanase digestion and fluorescent labeling with 2-aminobenzamide. *Anal. Biochem.*, **2001**, *298*, 207-217.
- (35) Rudd, P. M.;Colominas, C.;Royle, L.;Murphy, N.;Hart, E.;Merry, A. H.;Hebestreit, H. F.;Dwek, R. A. A high-performance liquid chromatography based strategy for rapid, sensitive sequencing of N-linked oligosaccharide modifications to proteins in sodium dodecyl sulphate polyacrylamide electrophoresis gel bands. *Proteomics*, **2001**, *1*, 285-294.
- (36) Kuraya, N.;Hase, S. Analysis of pyridylaminated O-linked sugar chains by two-dimensional sugar mapping. *Anal. Biochem.*, **1996**, *233*, 205-211.
- (37) Makino, Y.;Omichi, K.;Hase, S. Analysis of oligosaccharide structures from the reducing end terminal by combining partial acid hydrolysis and a two-dimensional sugar map. *Anal. Biochem.*, **1998**, *264*, 172-179.
- (38) Yoshino, K.;Takao, T.;Murata, H.;Shimonishi, Y. Use of the Derivatizing Agent 4-Aminobenzoic Acid 2-(Diethylamino)Ethyl Ester for High-Sensitivity Detection of Oligosaccharides by Electrospray-Ionization Mass-Spectrometry. *Anal. Chem.*, **1995**, *67*, 4028-4031.
- (39) Delaney, J.;Vouros, P. Liquid chromatography ion trap mass spectrometric analysis of oligosaccharides using permethylated derivatives. *Rapid Commun. Mass Spectrom.*, **2001**, *15*, 325-334.

- (40) Alley, W. R.;Madera, M.;Mechref, Y.;Novotny, M. V. Chip-based Reversed-phase Liquid Chromatography-Mass Spectrometry of Permethylated N-Linked Glycans: A Potential Methodology for Cancer-biomarker Discovery. *Anal. Chem.*, **2010**, *82*, 5095-5106.
- (41) Vailaya, A.;Horvath, C. Retention in reversed-phase chromatography: partition or adsorption? *J. Chromatogr. A*, **1998**, *829*, 1-27.
- (42) Tarentino, A. L.;Trimble, R. B.;Plummer, T. H. Enzymatic Approaches for Studying the Structure, Synthesis, and Processing of Glycoproteins. *Meth. Cell Biology*, **1989**, *32*, 111-139.
- (43) Poulter, L.;Burlingame, A. L. Desorption Mass-Spectrometry of Oligosaccharides Coupled with Hydrophobic Chromophores. *Methods Enzymol.*, **1990**, *193*, 661-688.
- (44) Bowman, M. J.;Zaia, J. Tags for the stable isotopic labeling of carbohydrates and quantitative analysis by mass spectrometry. *Anal. Chem.*, **2007**, *79*, 5777-5784.
- (45) Harvey, D. J. Electrospray mass spectrometry and fragmentation of N-linked carbohydrates derivatized at the reducing terminus. *J. Am. Soc. Mass Spectrom.*, **2000**, *11*, 900-915.
- (46) Hase, S.;Ikenaka, T.;Matsushima, Y. A Highly Sensitive Method for Analyses of Sugar Moieties of Glycoproteins by Fluorescence Labeling. *J. Biochem.*, **1981**, *90*, 407-414.
- (47) Suzuki, S.;Kakehi, K.;Honda, S. Comparison of the sensitivities of various derivatives of oligosaccharides in LC/MS with fast atom bombardment and electrospray ionization interfaces. *Anal. Chem.*, **1996**, *68*, 2073-2083.
- (48) Honda, S.;Akao, E.;Suzuki, S.;Okuda, M.;Kakehi, K.;Nakamura, J. High-Performance Liquid-Chromatography of Reducing Carbohydrates as Strongly Ultraviolet-Absorbing and Electrochemically Sensitive 1-Phenyl-3-Methyl-5-Pyrazolone Derivatives. *Anal. Biochem.*, **1989**, *180*, 351-357.
- (49) Avigad, G. Dansyl Hydrazine as a Fluorimetric Reagent for Thin-Layer Chromatographic Analysis of Reducing Sugars. *J. Chromatogr.*, **1977**, *139*, 343-347.
- (50) Naven, T. J. P.;Harvey, D. J. Cationic derivatization of oligosaccharides with Girard's T reagent for improved performance in matrix-assisted laser

- desorption/ionization and electrospray mass spectrometry. *Rapid Commun. Mass Spectrom.*, **1996**, *10*, 829-834.
- (51) Johnson, D. W. A modified Girard derivatizing reagent for universal profiling and trace analysis of aldehydes and ketones by electrospray ionization tandem mass spectrometry. *Rapid Commun. Mass Spectrom.*, **2007**, *21*, 2926-2932.
- (52) Shinohara, Y.;Sota, H.;Kim, F.;Shimizu, M.;Gotoh, M.;Tosu, M.;Hasegawa, Y. Use of a Biosensor Based on Surface-Plasmon Resonance and Biotinyl Glycans for Analysis of Sugar Binding Specificities of Lectins. *J. Biochem.*, **1995**, *117*, 1076-1082.
- (53) Karamanos, N. K.;Tsegenidis, T.;Antonopoulos, C. A. Analysis of Neutral Sugars as Dinitrophenyl-Hydrazones by High-Performance Liquid-Chromatography. *J. Chromatogr.*, **1987**, *405*, 221-228.
- (54) Miksik, I.;Gabriel, J.;Deyl, Z. Microemulsion electrokinetic chromatography of diphenylhydrazones of dicarbonyl sugars. *J. Chromatogr. A*, **1997**, *772*, 297-303.
- (55) Lattova, E.;Perreault, H. Method for investigation of oligosaccharides using phenylhydrazine derivatization. *Methods Mol. Biol.*, **2009**, *534*, 65-77.
- (56) Hull, S. R.;Turco, S. J. Separation of Dansyl Hydrazine-Derivatized Oligosaccharides by Liquid-Chromatography. *Anal. Biochem.*, **1985**, *146*, 143-149.
- (57) Gil, G. C.;Kim, Y. G.;Kim, B. G. A relative and absolute quantification of neutral N-linked oligosaccharides using modification with carboxymethyl trimethylammonium hydrazide and matrix-assisted laser desorption/ionization time-of-flight mass spectrometry. *Anal. Biochem.*, **2008**, *379*, 45-59.
- (58) Domon, B.;Costello, C. E. A Systematic Nomenclature for Carbohydrate Fragmentations in Fab-Ms Ms Spectra of Glycoconjugates. *Glycoconjugate J.*, **1988**, *5*, 397-409.
- (59) Zhao, C.;Xie, B.;Chan, S. Y.;Costello, C. E.;O'Connor, P. B. Collisionally activated dissociation and electron capture dissociation provide complementary structural information for branched permethylated oligosaccharides. *J. Am. Soc. Mass Spectrom.*, **2008**, *19*, 138-150.

- (60) Reinhold, V. N.;Reinhold, B. B.;Costello, C. E. Carbohydrate Molecular-Weight Profiling, Sequence, Linkage, and Branching Data - Es-MS and CID. *Anal. Chem.*, **1995**, *67*, 1772-1784.
- (61) Orlando, R. Quantitative Glycomics. *Methods Mol. Biol.*, **2010**, *600*, 31-49.
- (62) Orlando, R.;Lim, J. M.;Atwood, J. A.;Angel, P. M.;Fang, M.;Aoki, K.;Alvarez-Manilla, G.;Moremen, K. W.;York, W. S.;Tiemeyer, M.;Pierce, M.;Dalton, S.;Wells, L. IDAWG: Metabolic Incorporation of Stable Isotope Labels for Quantitative Glycomics of Cultured Cells. *J. Proteome Res.*, **2009**, 3816-3823.
- (63) Atwood, J. A.;Cheng, L.;Alvarez-Manilla, G.;Warren, N. L.;York, W. S.;Orlando, R. Quantitation by isobaric labeling: Applications to glycomics. *J. Proteome Res.*, **2008**, 367-374.
- (64) Alvarez-Manilla, G.;Warren, N. L.;Abney, T.;Atwood, J.;Azadi, P.;York, W. S.;Pierce, M.;Orlando, R. Tools for glycomics: relative quantitation of glycans by isotopic permethylation using (CH₃)₂C-13. *Glycobiology*, **2007**, 677-687.
- (65) Kang, P.;Mechref, Y.;Kyselova, Z.;Goetz, J. A.;Novotny, M. V. Comparative glycomic mapping through quantitative permethylation and stable-isotope labeling. *Anal. Chem.*, **2007**, 6064-6073.
- (66) Pabst, M.;Kolarich, D.;Poltl, G.;Dalik, T.;Lubec, G.;Hofinger, A.;Altmann, F. Comparison of fluorescent labels for oligosaccharides and introduction of a new postlabeling purification method. *Anal. Biochem.*, **2009**, *384*, 263-273.
- (67) Arnold, J. N.;Saldova, R.;Galligan, M. C.;Murphy, T. B.;Mimura-Kimura, Y.;Telford, J. E.;Godwin, A. K.;Rudd, P. M. Novel Glycan Biomarkers for the Detection of Lung Cancer. *J. Proteome Res.*, **2011**, *10*, 1755-1764.
- (68) Kronewitter, S. R.;de Leoz, M. L. A.;Peacock, K. S.;McBride, K. R.;An, H. J.;Miyamoto, S.;Leiserowitz, G. S.;Lebrilla, C. B. Human Serum Processing and Analysis Methods for Rapid and Reproducible N-Glycan Mass Profiling. *J. Proteome Res.*, **2010**, *9*, 4952-4959.
- (69) Takegawa, Y.;Deguchi, K.;Ito, H.;Keira, T.;Nakagawa, H.;Nishimura, S. Simple separation of isomeric sialylated N-glycopeptides by a zwitterionic type of hydrophilic interaction chromatography. *J. Sep. Sci.*, **2006**, *29*, 2533-40.

- (70) Nguyen, H. P.;Schug, K. A. The advantages of ESI-MS detection in conjunction with HILIC mode separations: Fundamentals and applications. *J. Sep. Sci.*, **2008**, *31*, 1465-1480.
- (71) Wuhrer, M.;de Boer, A. R.;Deelder, A. M. Structural Glycomics Using Hydrophilic Interaction Chromatography (Hilic) with Mass Spectrometry. *Mass Spectrom. Rev.*, **2009**, *28*, 192-206.
- (72) Hemstrom, P.;Irgum, K. Hydrophilic interaction chromatography. *J. Sep. Sci.*, **2006**, *29*, 1784-1821.
- (73) Rafferty, J. L.;Zhang, L.;Siepmann, J. I.;Schure, M. R. Retention mechanism in reversed-phase liquid chromatography: A molecular perspective. *Anal. Chem.*, **2007**, *79*, 6551-6558.
- (74) Stumpo, K. A.;Reinhold, V. N. The N-Glycome of Human Plasma. *J. Proteome Res.*, **2010**, *9*, 4823-4830.
- (75) Ruhaak, L. R.;Huhn, C.;Waterreus, W. J.;de Boer, A. R.;Neususs, C.;Hokke, C. H.;Deelder, A. M.;Wuhrer, M. Hydrophilic interaction chromatography-based high-throughput sample preparation method for N-glycan analysis from total human plasma glycoproteins. *Anal. Chem.*, **2008**, *80*, 6119-6126.

CHAPTER 6

The Use of a Xylosylated Plant Glycoprotein as an Internal Standard Accounting for *N*-linked Glycan Cleavage and Sample Preparation Variability

The following work was reprinted from the recently accepted manuscript: Walker, S. H.; Taylor, A. D.; Muddiman, D. C. *Rapid Communications in Mass Spectrometry* **2013**, *Accepted*: March 26, 2013. Copyright 2012 John Wiley & Sons.

5.1 Introduction

The roles of glycosylation in biological systems are becoming increasingly evident,¹⁻³ and numerous strategies have recently been developed using mass spectrometry to relatively quantify the amount of glycans in different samples.⁴⁻¹³ In this type of experiment, two (or more) samples are differentially labeled, processed in parallel, and mixed prior to analysis. The relative amounts of each glycan in the two samples can then be quantified in one liquid chromatography mass spectrometry (LC-MS) analysis. The disadvantage to these types of techniques is the variability introduced into the quantification by processing the samples in parallel. The analysis of *N*-linked glycans from a complex biological sample, such as human plasma, involves numerous sample preparation steps that each introduces variability into quantitative analysis. Though efforts are taken to keep conditions constant between samples, slight variances in the digestion efficiency, derivatization efficiency, and solid phase extraction (SPE) recovery can skew the relative amounts of glycans detected. Previous studies have utilized free sugars (simple, branched, and/or complex) to normalize or correct for sample preparation variability.^{4, 14-19}

However, these spiked-in sugars are unable to account for the *N*-linked glycan cleavage variability between samples.

The total variability (σ^2_{Total}) of these measurements is comprised of both analytical ($\sigma^2_{\text{Analytical}}$) and biological ($\sigma^2_{\text{Biological}}$) variability (**Equation 6.1**).

$$\sigma^2_{\text{Total}} = \sigma^2_{\text{Biological}} + \sigma^2_{\text{Analytical}} \quad (6.1)$$

Because the main objective is to measure biological change, it is necessary to minimize and account for the analytical variability such that true and significant biological change can be detected. However, when numerous samples must be processed in parallel, the samples are often grouped into ‘batches’. This allows experiments containing hundreds of samples to be divided into smaller groups in order to facilitate sample preparation. However, ‘batch’ processing has a cost due to all samples not being processed in parallel, and there are two main issues with multiple ‘batch’ processing in the same biological data set: 1) samples are often processed slightly different between samples and (to a larger degree) batches (*e.g.*, cleavage temperature and time can be variable), and 2) often the same lot of enzyme is not able to be used for all batches introducing activity variability. These issues pose inherent problems when trying to compare glycan abundances across not only samples but also across entire batches of data. Thus, an internal standard that is capable of monitoring and correcting for sample preparation variability

(including *N*-linked glycan cleavage variability) becomes a necessity in large-scale biological studies of glycosylation.

It is shown in **Equation 6.2** that many steps in the sample preparation and/or the human error contribute to the total variability of the measurement.

$$\sigma^2_{\text{Total}} = \left[\sigma^2_{\text{Solid Phase Extraction}} + \sigma^2_{\text{Derivatization}} + \sigma^2_{\text{Individual}} + \sigma^2_{\text{Technical}} \right] + \sigma^2_{\text{Incubation Temperature/Time}} + \sigma^2_{\text{Enzyme Activity}} + \sigma^2_{\text{Enzyme Matrix}} + \sigma^2_{\text{Biological}} \quad (6.2)$$

The dashed box and the solid box represent the variability that can be accounted for by spiking in a free oligosaccharide and a glycoprotein standard, respectively, at the onset of sample preparation. Thus, if there is significant variability in the enzymatic cleavage efficiency, the currently used free oligosaccharide internal standard would not be able to correct for this, a problem that will have an effect on the relative quantification of batch processed samples. It is necessary to monitor this cleavage variability when analyzing numerous biological samples because often the biological matrix of each sample is different and undefined. The matrix could have protease inhibitors or other physical properties that affect the enzymatic release of *N*-linked glycans. Additionally, when processing large numbers of samples, lot to lot variation, enzyme activity over time, and incubation conditions can all vary. This variability can significantly contribute to quantification results and must be controlled for in order to elucidate real and significant biological change.

A glycoprotein containing *N*-linked glycans would be an ideal candidate for having the potential to account for all aspects of sample preparation variability,

including variation in the cleavage efficiency between samples. However, the glycoprotein must have several favorable properties to be able to be used as an internal standard including commercial availability, cost effectiveness, the ability for the glycans to be cleaved by PNGase F, and most importantly, the glycoprotein must contain *N*-linked glycans that are not already found in the biological system being studied. Horseradish peroxidase (HRP) is a plant glycoprotein that is frequently used as a colorimetric indicator for antigen-antibody analyses. Previous studies have reported that HRP contains *N*-linked glycans with a xylosylated and often α 1,3-fucosylated core.²⁰⁻²³ This makes it a good candidate for a glycoprotein internal standard due to the inability of most mammals to produce xylosylated glycans.

Herein, we report on the utility of spiking in HRP at the onset of sample preparation. This allows one to monitor the PNGase F cleavage efficiency across samples, whereas maltoheptaose, a simple sugar internal standard, cannot. This leads to skewed quantification results when there is variability introduced in the cleavage reaction due to differences in enzymatic activity, sample matrix, or degradation. A time course digestion experiment of 6 identical pooled human plasma aliquots is used to simulate variability in digestion efficiency across samples. It is shown that comparing the ratios of the two internal standards do not produce the same correction factor when there is a discrepancy in the efficiency of the cleavage reaction (*i.e.* at short incubation times). Thus, HRP is a successful internal standard for monitoring and controlling for not only the variation in the parallel sample preparation but also any variability in the enzymatic cleavage process.

6.2 Experimental

6.2.1 Methods

N-linked glycans cleaved from 50 μ L aliquots of pooled human plasma (Sigma Aldrich, St. Louis, MO) were used to simulate variability in cleavage efficiency by allowing different samples to be incubated for various times ranging from 0 to 24 hr. *N*-linked glycans were cleaved with PNGase F (New England Biolabs, Ipswich, MA), an ethanol protein precipitation was performed, and the *N*-linked glycans were separated from the plasma matrix and remaining proteins as previously reported.²⁴ Both maltoheptaose (1 μ g) and HRP (200 μ g) were purchased from Sigma Aldrich (St. Louis, MO) and spiked into the plasma aliquots at the onset of sample preparation. Upon completion of the solid phase extraction of the *N*-linked glycans, derivatization was performed in parallel as previously reported.^{4, 24-26} Samples were derivatized with either the 'light' (natural) or 'heavy' (stable-isotope labeled) P2GPN hydrazide reagent.^{4, 25}

6.2.2 nano-Flow Reversed Phase Chromatography Coupled Online to Q Exactive MS

The derivatized glycan samples were reconstituted in 200 μ L of a 5% ACN solution. The sample was vortexed for 1 min and centrifuged for 5 min at 14,000 rpm. The supernatant was extracted and samples were mixed together in equal volumes for relative quantification per the experimental design (*vide infra*). An EASY-nLC II autosampler and liquid chromatography (LC) system (Thermo Fisher

Scientific, San Jose, CA) was used to load 10 μ L of the sample at 650 nL/min onto a cHiPLC column system (Eksigent, Dublin, CA) set up in the vented column configuration.²⁷ Immediately after loading, the sample was washed with an additional 2 μ L of mobile phase A. A ChromXP C18-CL 75 μ m x 15 cm analytical column (Eksigent, Dublin, CA) was used for both the trap and the analytical column, allowing for an effective column length of 30 cm. The EASY-nLC II was used to perform gradient elution, where mobile phase A consisted of a 2% acetonitrile (ACN) and 0.2% formic acid solution, and mobile phase B consisted of a 98% ACN and 0.2% formic acid solution. Glycans were separated at a constant flow of 300 nL/min. The initial solvent condition was 2% mobile phase B and held for 1 min. The mobile phase B composition was then increased to 22% over 1 min and further increased to 35% over 35 min. The column was washed with 90% mobile phase B and then re-equilibrated in the initial conditions for 15 min. The LC eluent was detected online by a QExactive mass spectrometer equipped with a nanospray source (Thermo Fisher Scientific, San Jose, CA). Electrospray ionization was achieved by applying 2.25 kV at the union adjoining the emitter tip and the outlet capillary of the LC. The capillary was heated to 225 °C, and the instrument was calibrated per the manufacturer specifications. Data dependent acquisition was performed, such that up to 5 MS/MS spectra were taken per precursor scan, where the most abundant ions were chosen for fragmentation. After a precursor ion has been chosen for fragmentation, it is put on an exclude list for 25 s. The precursor ions were detected in the orbitrap mass analyzer at 70,000 resolving power at $m/z = 200$ with a 1×10^6

automatic gain control (AGC) and a maximum injection time of 250 ms. The ions chosen for fragmentation were subjected to higher energy collision dissociation (HCD) at a normalized collision energy (NCE) of 20. The product-ion spectra were collected in the orbitrap as well and detected at 17,500 resolving power at $m/z = 200$, with a 2×10^4 AGC and a maximum injection time of 120 ms. The unique glycan compositions were identified manually using accurate mass and analyzed using Xcalibur software (v.2.2).

6.3 Results and Discussion

Two 200 μg samples of HRP were prepared, derivatized with the natural and SIL hydrazide tags, combined in equal volumes, and analyzed as a control using the same glycan extraction procedure as that in plasma to determine the complexity HRP would add when spiked into a plasma sample. Only two *N*-linked glycans were detected in the spectra, $\text{Hex}_3\text{HexNAc}_2\text{Xyl}_1$ and $\text{Hex}_3\text{HexNAc}_2\text{Fuc}_1\text{Xyl}_1$, and both of these glycans contain xylose (as reported in the literature)²⁰⁻²³, which is not found in human biosynthetic pathways. However, the $\text{Hex}_3\text{HexNAc}_2\text{Fuc}_1\text{Xyl}_1$ has a low signal to noise ratio, which could introduce technical variation; thus, the more abundant $\text{Hex}_3\text{HexNAc}_2\text{Xyl}_1$ (**Figure 6.1b**) will be referred to as the “HRP” internal standard and used to determine the effectiveness of accounting for the total sample preparation variability using a xylosylated *N*-linked glycoprotein. **Figure 6.1a** shows a generic plant protein with xylosylated *N*-linked glycan cores. The lack of xylose found in mammalian biosynthetic pathways allows plant *N*-linked glycans to be

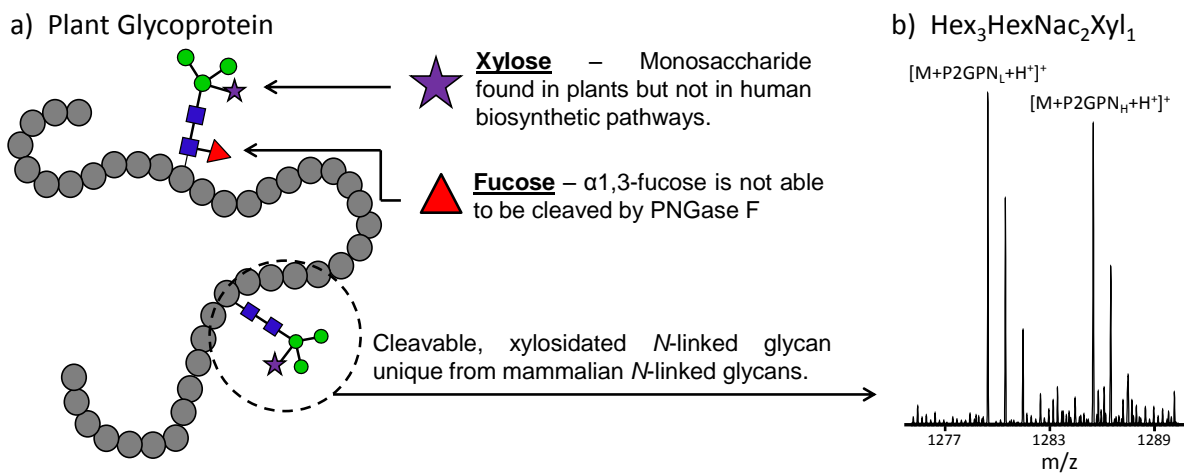


Figure 6.1 – a) Generic plant glycoprotein showing core α 1,3-fucose and core xylose containing glycans; b) HRP internal standard, $\text{Hex}_3\text{HexNac}_2\text{Xyl}_1$, detected after treating the two control samples with PNGase F, differential derivatization, and combining the samples in equal volumes.

unique from the *N*-linked glycans of interest. An additional property of many plant glycoproteins is the presence of α 1-3 fucosylated core, and glycans containing this motif are not able to be cleaved by PNGase F. This is also the reason only two *N*-linked glycans were detected from HRP. These attributes, along with the commercial availability, make HRP a great candidate for a glycoprotein internal standard.

A time course glycan deglycosylation experiment was used to simulate different enzymatic cleavage efficiencies in aliquots of the same pooled human plasma sample. Six pooled human plasma samples were denatured and subjected to PNGase F digestion. One sample was removed at each of the following time

points: 0, 4, 8, and 12 hr. Two samples were incubated for a full 24 hr (24a and 24b). When removed from the incubator, each sample was immediately quenched with ethanol and placed in the -80°C freezer. After the final 24 hr samples were removed from the incubator, all samples were allowed to incubate at -80°C for 1 additional hr, centrifuged, and dried. All aliquots were processed identically aside from the amount of time they were incubated for deglycosylation and the amount of time spent in the -80°C ethanol incubation. Each sample will be referred to by the PNGase F deglycosylation incubation time for the sample. The 0, 8, and 24a samples were derivatized with the 'light' P2GPN reagent, and the 4, 12, and 24b samples were derivatized with the 'heavy' P2GPN reagent. This allowed for comparisons between each adjacent (in time) sample and a comparison between each sample and one of the 24 hr time points.

Figure 6.2a shows the utility of using a glycoprotein as an internal standard by plotting the HRP glycan (corrected by the maltoheptaose internal standard) at different PNGase F incubation times. It is shown at the early time points that the maltoheptaose is incapable of taking into account poor efficiency in the PNGase F cleavage reaction. This is experimental evidence that the free oligosaccharide can only account for the variability in the dashed box in **Equation 6.2**. However, because the PNGase reaction efficiency can be monitored over time using the HRP glycan, all of the variability in the solid box in **Equation 6.2** can be accounted for, making the HRP glycoprotein a more effective internal standard.

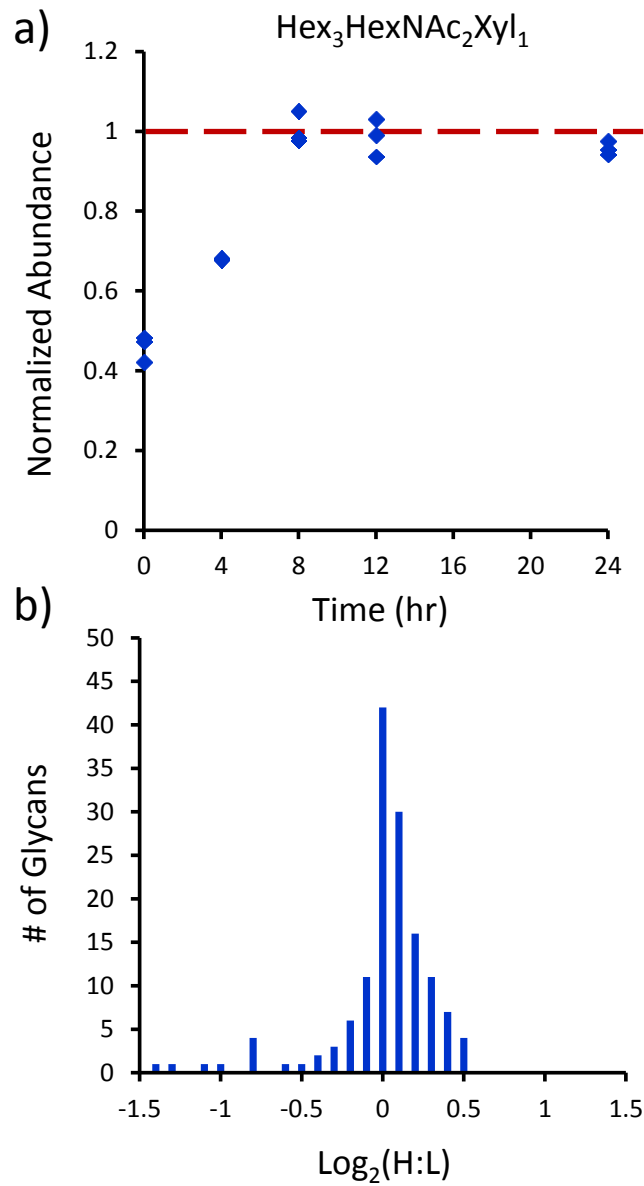


Figure 6.2 – a) The HRP glycan relative abundances, corrected by maltoheptaose and normalized to the 24-hr time point, at each of the 5 PNGase F incubation times. The abundances are normalized to the 24-hr time point, where 100% cleavage efficiency is assumed. **b)** Histogram plotting the $\text{log}_2(\text{Heavy:Light})$ for the 24a-24b sample and corrected by HRP.

Though it is shown that the HRP is effective in accounting for enzymatic cleavage variability, in order for it to be a productive internal standard, it must also account for the additional sample preparation variability shown in **Equation 6.2**. Thus, the two aliquots of plasma that were incubated for 24 hours were used to determine the effectiveness of the HRP glycan as an internal standard for correcting for σ^2_{Total} in glycan relative quantification experiments. The 24a-24b comparison sample is assumed to have no biological variability ($\sigma^2_{\text{Biological}} = 0$). Thus, any systematic variability in the measurement should be able to be corrected using an internal standard. **Figure 6.2b** shows the relative quantification histogram of the 50 most abundant *N*-linked glycans in the 24a-24b comparison corrected by HRP. The mean \pm 95% confidence interval for the heavy:light glycan ratio is 1.001 ± 0.037 , which statistically encompasses the expected 1:1 ratio. Histograms for other time points have not been shown due to the large variation in the cleavage efficiencies of different glycans at short digestion times. Neither internal standard is capable of reducing the *random* variability due to the variable cleavage rates of each glycan composition. This is why glycan cleavage is performed for >18 hr. Additionally, matrix effects on the cleavage efficiency would be systematic to all glycans, thus correctable using HRP.

Figure 6.2b also shows the analytical variability of this relative quantification strategy of *N*-linked glycans in a complex biological mixture. Because two aliquots of the same plasma sample were used for the 24a-24b time points, zero biological variability can be assumed. Thus, it is shown by the distribution in **Figure 6.2b** that

a ratio with more than $\pm 40\%$ deviation from unity can be deemed as a biologically significant change. By introducing HRP as an internal standard, the systematic variability of analytical sample preparation can be minimized, and if there are negligible differences in the cleavage reaction efficiency, HRP as an internal standard performs as well as spiking in a standard oligosaccharide. However, in situations where there is significant variation in the cleavage efficiency, the HRP internal standard out-performs the free oligosaccharide (**Figure 6.2a**) and is more suited to correct for analytical systematic variation than a free oligosaccharide. Importantly, for a large number of samples that are carried out in batches, the approach described herein is critical to make quantitative comparisons.

6.4 Conclusions

The use of a glycoprotein as an internal standard has the potential to correct for both the cleavage and sample preparation variability between two samples, and HRP has been shown to be an effective glycoprotein for this task. HRP will be used in future studies as the primary internal standard for correcting sample preparation and PNGase F cleavage efficiency for *N*-linked glycan large scale relative quantification studies. Additionally, maltoheptaose will also be used as a secondary internal standard. This will allow one to measure the systematic variability due to parallel sample preparation alone (maltoheptaose ratio), and by comparing the HRP light and heavy abundances to those of the maltoheptaose, the variability solely due to the enzymatic cleavage reaction can be determined. By monitoring this, we can

systematically account for any enzyme lot to lot variability, variation in the enzyme activity over time, variation in incubation conditions between batches, and the variability of each undefined biological matrix (e.g. plasma) which can inhibit glycan cleavage. Though it is often assumed that the glycan cleavage efficiency between samples has little variation due to the long incubation times, it would be analytically improper to not incorporate a suitable control for this assumption when studying biological change over a large number of samples. Thus, HRP provides a widely available, cost-effective tool that is easily incorporated into a majority of *N*-linked glycan relative quantification workflows.

6.5 References

- (1) Apweiler, R.; Hermjakob, H.; Sharon, N. On the frequency of protein glycosylation, as deduced from analysis of the SWISS-PROT database. *BBA-Gen. Subjects*, **1999**, *1473*, 4-8.
- (2) Begley, T. P., *Wiley Encyclopedia of Chemical Biology* **2009**, *2*, 785.
- (3) Varki, A.; Cummings, R. D.; Esko, J. D.; Freeze, H. H.; Stanley, P.; Bertozzi, C. R.; Hart, G. W.; Etzler, M. E., *Essentials of Glycobiology* **2009**.
- (4) Walker, S. H.; Budhathoki-Uprety, J.; Novak, B. M.; Muddiman, D. C. Stable-isotope labeled hydrophobic hydrazide reagents for the relative quantification of N-linked glycans by electrospray ionization mass spectrometry. *Anal. Chem.*, **2011**, *83*, 6738-45.
- (5) Alvarez-Manilla, G.; Warren, N. L.; Abney, T.; Atwood, J.; Azadi, P.; York, W. S.; Pierce, M.; Orlando, R. Tools for glycomics: relative quantitation of glycans by isotopic permethylation using (CH₃)-C-13. *Glycobiology*, **2007**, 677-687.
- (6) Atwood, J. A.; Cheng, L.; Alvarez-Manilla, G.; Warren, N. L.; York, W. S.; Orlando, R. Quantitation by isobaric labeling: Applications to glycomics. *J. Proteome Res.*, **2008**, 367-374.
- (7) Kang, P.; Mechref, Y.; Kyselova, Z.; Goetz, J. A.; Novotny, M. V. Comparative glycomic mapping through quantitative permethylation and stable-isotope labeling. *Anal. Chem.*, **2007**, 6064-6073.
- (8) Bowman, M. J.; Zaia, J. Comparative Glycomics Using a Tetraplex Stable-Isotope Coded Tag. *Anal. Chem.*, **2010**, *82*, 3023-3031.
- (9) Bowman, M. J.; Zaia, J. Tags for the stable isotopic labeling of carbohydrates and quantitative analysis by mass spectrometry. *Anal. Chem.*, **2007**, *79*, 5777-5784.
- (10) Xia, B. Y.; Feasley, C. L.; Sachdev, G. P.; Smith, D. F.; Cummings, R. D. Glycan reductive isotope labeling for quantitative glycomics. *Anal. Biochem.*, **2009**, *387*, 162-170.
- (11) Orlando, R.; Lim, J. M.; Atwood, J. A.; Angel, P. M.; Fang, M.; Aoki, K.; Alvarez-Manilla, G.; Moremen, K. W.; York, W. S.; Tiemeyer, M.; Pierce, M.; Dalton, S.; Wells, L. IDAWG: Metabolic Incorporation of Stable Isotope Labels for

- Quantitative Glycomics of Cultured Cells. *J. Proteome Res.*, **2009**, 3816-3823.
- (12) Hahne, H.;Neubert, P.;Kuhn, K.;Etienne, C.;Bomgarden, R.;Rogers, J. C.;Kuster, B. Carbonyl-Reactive Tandem Mass Tags for the Proteome-Wide Quantification of N-Linked Glycans. *Anal. Chem.*, **2012**, *84*, 3716-3724.
- (13) Zhang, P.;Zhang, Y.;Xue, X. D.;Wang, C. J.;Wang, Z. F.;Huang, L. J. Relative quantitation of glycans using stable isotopic labels 1-(d0/d5) phenyl-3-methyl-5-pyrazolone by mass spectrometry. *Anal. Biochem.*, **2011**, *418*, 1-9.
- (14) Dixon, R. B.;Bereman, M. S.;Petitte, J. N.;Hawkrigde, A. M.;Muddiman, D. C. One-year plasma N-linked glycome intra-individual and inter-individual variability in the chicken model of spontaneous ovarian adenocarcinoma. *Int. J. Mass Spectrom.*, **2011**, *305*, 79-86.
- (15) Bereman, M. S.;Muddiman, D. C. The effects of abundant plasma protein depletion on global glycan profiling using NanoLC FT-ICR mass spectrometry. *Anal. Bioanal. Chem.*, **2010**, *396*, 1473-1479.
- (16) Bereman, M. S.;Young, D. D.;Deiters, A.;Muddiman, D. C. Development of a Robust and High Throughput Method for Profiling N-Linked Glycans Derived from Plasma Glycoproteins by NanoLC-FTICR Mass Spectrometry. *J. Proteome Res.*, **2009**, *8*, 3764-3770.
- (17) de Leoz, M. L. A.;Young, L. J. T.;An, H. J.;Kronewitter, S. R.;Kim, J. H.;Miyamoto, S.;Borowsky, A. D.;Chew, H. K.;Lebrilla, C. B. High-Mannose Glycans are Elevated during Breast Cancer Progression. *Mol. Cell Proteomics*, **2011**, *10*, 1-9.
- (18) Snovida, S. I.;Perreault, H. A 2,5-dihydroxybenzoic acid/N,N-dimethylaniline matrix for the analysis of oligosaccharides by matrix-assisted laser desorption/ionization mass spectrometry. *Rapid Commun. Mass Spectrom.*, **2007**, *21*, 3711-3715.
- (19) Kaneshiro, K.;Watanabe, M.;Terasawa, K.;Uchimura, H.;Fukuyama, Y.;Iwamoto, S.;Sato, T. A.;Shimizu, K.;Tsujiimoto, G.;Tanaka, K. Rapid Quantitative Profiling of N-Glycan by the Glycan-Labeling Method Using 3-Aminoquinoline/alpha-Cyano-4-hydroxycinnamic Acid. *Anal. Chem.*, **2012**, *84*, 7146-7151.
- (20) Kamerling, J. P. Xylose-Containing Carbohydrate Chains Derived from N-Glycoproteins. *Pure & Appl. Chem.*, **1991**, *63*, 465-472.

- (21) Wuhrer, M.;Hokke, C. H.;Deelder, A. M. Glycopeptide analysis by matrix-assisted laser desorption/ionization tandem time-of-flight mass spectrometry reveals novel features of horseradish peroxidase glycosylation. *Rapid Commun. Mass Spectrom.*, **2004**, *18*, 1741-1748.
- (22) Lee, B. S.;Krisnanchettiar, S.;Lateef, S. S.;Lateef, N. S.;Gupta, S. Oligosaccharide analyses of glycopeptides of horseradish peroxidase by thermal-assisted partial acid hydrolysis and mass spectrometry. *Carbohydrate Res.*, **2005**, *340*, 1859-1865.
- (23) Matsuo, K. Small-scale, high-throughput method for plant N-glycan preparation for matrix-assisted laser desorption/ionization time-of-flight mass spectrometry analysis. *Anal. Biochem.*, **2011**, *413*, 200-202.
- (24) Walker, S. H.;Carlisle, B. C.;Muddiman, D. C. Systematic Comparison of Reverse Phase and Hydrophilic Interaction Liquid Chromatography Platforms for the Analysis of N-Linked Glycans. *Anal. Chem.*, **2012**, *84*, 8198-8206.
- (25) Walker, S. H.;Lilley, L. M.;Enamorado, M. F.;Comins, D. L.;Muddiman, D. C. Hydrophobic Derivatization of N-linked Glycans for Increased Ion Abundance in Electrospray Ionization Mass Spectrometry. *J Am. Soc. Mass Spectrom.*, **2011**, *22*, 1309-17.
- (26) Walker, S. H.;Papas, B. N.;Comins, D. L.;Muddiman, D. C. Interplay of Permanent Charge and Hydrophobicity in the Electrospray Ionization of Glycans. *Anal. Chem.*, **2010**, *82*, 6636-6642.
- (27) Andrews, G. L.;Shuford, C. M.;Burnett, J. C.;Hawkridge, A. M.;Muddiman, D. C. Coupling of a vented column with splitless nanoRPLC-ESI-MS for the improved separation and detection of brain natriuretic peptide-32 and its proteolytic peptides. *J. Chromatogr. B*, **2009**, *877*, 948-954.

CHAPTER 7

Individuality Normalization when Labeling with Isotopic Glycan Hydrazide Tags (INLIGHT): A Novel Glycan Relative Quantification Strategy

The following work was reprinted from the recently submitted manuscript: Walker, S. H.; Taylor, A. D.; Muddiman, D. C. *Journal of the American Society for Mass Spectrometry*. Submitted: April 5, 2013.

7.1 Introduction

The ubiquity of glycosylation in biological systems is evident in that the majority of translated gene products are glycosylated,¹⁻² and glycosylation is involved in cellular recognition, cell-cell interactions, cell division and adhesion, protein folding and stability, and protein function.³ Due to the importance of glycosylation in biological systems, it is necessary to develop high-throughput strategies to profile and quantify glycans in a high-throughput and reproducible manner. This applies to not only sample preparation and the analysis platform (often liquid chromatography coupled online to mass spectrometry (LC-MS)), but also to the bioinformatic processing strategy. Recently, numerous strategies have been described in the literature for the relative quantification of *N*-linked glycans using LC-MS-based stable-isotope labeled derivatization strategies.⁴⁻¹¹ However, because these strategies have only recently been developed and there are limited bioinformatic platforms for the analysis of LC-MS glycomics data, few glycomics experiments can be repeated, compared, or even reproducibly analyzed across laboratories.

Stable-isotope labeled (SIL) derivatization strategies involve differentially labeling two glycan samples *via* either a 'light' or 'heavy' reagent. This allows the two samples to be mixed together, analyzed in the same LC-MS run, and separated by mass. The relative ion abundances of a specific 'light' and 'heavy' glycan pair can then be measured, and the relative amounts of the glycan in each sample can be quantified. In these types of studies, there are numerous decisions that must be made on how to reproducibly measure the relative amounts of the light- and heavy-labeled glycans. These decisions include whether to quantify based on ion abundance ratios or extracted ion chromatogram (EIC) peak area ratios, whether to use the monoisotopic peak or the entire isotopic distribution for quantification, how to control for differential isotopic shift and/or isotopic overlap, and how to normalize for any systematic variability introduced due to the parallel sample preparation and systematic biological variability. Thus, a strategy must be developed in order to process SIL relative quantification LC-MS data in a reproducible manner.

Stable-isotope labeling for the relative quantification of glycans has been described for metabolic SIL⁴ and several different types of SIL glycan derivatization strategies including permethylation,^{5, 7, 11} reductive amination,^{6, 10} PMP derivatization,⁸ and hydrazone formation.⁹ Each of these strategies is unique such that one must process the data slightly differently. For example, the isotopic permethylation strategies and IDAWG will have a different m/z shift for each glycan depending on the size, branching, and constituent monosaccharides present. In contrast, techniques such as reductive amination, PMP derivatization, and

hydrazone formation introduce a fixed number of stable-isotopes resulting in a fixed m/z shift. The stable-isotope label also must be noted. Because ^{13}C and ^{15}N are not chromatographically resolved from ^{12}C and ^{14}N , respectively, it is practical to use LC-MS and quantify by EIC peak area. However, SIL techniques which incorporate deuterium should use caution when paired with LC-MS due to the possibility of chromatographic separation,¹²⁻¹⁴ which can lead to skewed quantification based on different mobile phase composition and different electrospray ionization efficiency. Thus, these studies will be the most effective using direct infusion ESI or MALDI and quantifying based on ion abundance.

Because the purpose of developing glycan relative quantification strategies is most often to measure differences in the glycan profiles of biological systems, it is necessary to minimize the random analytical variability and account/correct for any systematic analytical and biological variability such that the biological change of interest can be elucidated. The most effective strategy for minimizing sample preparation variability in glycan SIL relative quantification studies are those that involve metabolic labeling (e.g. IDAWG) due to the mixing of the two samples at the onset of sample preparation. However, the majority of glycan relative quantification studies are not capable of being performed in cell culture. Thus, many of the glycan SIL strategies involve parallel sample preparation in which variability is introduced at each step and must be controlled and corrected for in order to avoid detecting differences in relative abundance due to sample preparation variability. This can be accomplished by incorporating internal standards at the onset of sample preparation

and has been demonstrated in previous glycan literature.^{9, 15-20} The most common internal standards used in glycan relative quantification experiments include free sugars (such as maltoheptaose). While these internal standards are capable of correcting for sample preparation variability in the purification of *N*-linked glycans, derivatization efficiency, and other technical variability, studies which require the release of *N*-linked glycans from proteins often continue to use free glycans as internal standards. However, variability can be introduced when using enzymatic cleavage (PNGases) due to lot-to-lot variability, loss of enzyme activity over time, and when using an enzyme in an undefined biological matrix that could contain endogenous species which may inhibit the enzyme. Thus, a recent report has demonstrated the use of a plant glycoprotein (horseradish peroxidase) as an internal standard that can be used to account for all sample preparation systematic variability, including enzymatic release efficiency, when processing samples in parallel.¹⁹

Though using a single internal standard has been shown to be effective for samples with similar biological matrices (aliquots of pooled human plasma),¹⁹ often very little is known about the specific matrix of each sample. For example, when comparing a biological specimen from two individuals, the total protein concentration may be different, the total glycosylation may be different, and/or inhibitors to PNGase F may be present. Thus, each of these situations complicates relative quantification, and a single internal standard will not be able to account for these situations. Additionally, a single glycan internal standard may act significantly

different than other types of glycans (e.g. high mannose, complex, hybrid, fucosylated, acidic), creating a biased correction based on the chosen internal standard. Attempts can be made to normalize to the total protein concentration; however, this is not always proportional to the total glycosylation between different biological samples and biological states.

When measuring changes in a biological system (e.g. onset of disease) every effort must be made to define the inter-individuality (*i.e.* the variability of biological constituents in a population²¹⁻²²) of a specific biological sample set. Though these changes are often random between samples and can only be defined but not minimized, the previously mentioned systematic variations in individuality between samples must be accounted for in order to elucidate biological change. Because these situations cannot be accounted for using a spiked-in internal standard, other methods must be developed such that both analytical and biological systematic variability can be accounted for. Strategies for normalization in proteomic label free relative quantification experiments have been reported.²³⁻²⁸ These studies discuss how to elucidate biological change while accounting for variations in the sample preparation. Three proteomic normalization strategies can be applied to glycans: 1) normalization to selected proteins (analogous to spiking in a glycan internal standard – *vide supra*),²⁸ and 2) normalization based on total spectral counts (TSpC).^{23-24, 28-29} These two normalization strategies have been recently compared²⁸ and show that TSpC normalization performs more effectively than the normalization to selected proteins. This gives insight into possible glycan normalization methods and leads

one to believe that normalization to the total glycosylation of each sample may be a more effective strategy than using an individual spiked-in internal standard.

Herein, the INLIGHT method for generating and analyzing glycan SIL relative quantification data is described in detail, where *N*-linked glycans are derivatized with fixed mass shift SIL reagents⁹ via hydrazone formation³⁰⁻³¹ and analyzed by reversed phase liquid chromatography (RPLC) coupled to a Q Exactive mass spectrometer. The reagents used for derivatization have been previously reported,⁹ and offer significant advantages (increased ionization efficiency,³⁰⁻³¹ near stoichiometric derivatization,³⁰⁻³¹ analysis by RPLC,³² no post-derivatization clean up step, and <4 hr derivatization time) in addition to the ability to perform relative quantification in LC-MS. The INLIGHT strategy for relative quantification involves generating an extracted ion chromatogram for each light- and heavy-derivatized glycan based on the monoisotopic peak at a MMA of ± 5 ppm, correcting for the isotopic overlap of large molecular weight (MW) glycans, correcting for systematic analytical and biological variability, and determining the relative amounts of *N*-linked glycans in each sample. A method for isotopic overlap correction of glycan SIL relative quantification data is presented, and a post-acquisition data normalization strategy is described that is capable of accounting for both analytical and biological systematic variability. The INLIGHT strategy is demonstrated to be effective for the relative quantification of glycans using both a standard glycan ladder and pooled human plasma while minimizing the systematic variability in the measurement. The success of the INLIGHT strategy is ultimately demonstrated by the detection of

significant change in *N*-linked glycan abundances when a glycoprotein is spiked into pooled human plasma.

7.2 Experimental

7.2.1 Materials

Maltodextrin was purchased from V-Laboratories, Inc. (Covington, LA), and horseradish peroxidase, pooled human plasma, and other consumable chemicals were purchased from Sigma Aldrich (St. Louis, MO). Peptide: *N*-glycosidase F (PNGase F) was purchased from New England BioLabs (Ipswich, Ma). HPLC grade solvents were purchased from Burdick & Jackson (Muskegon, MI). The hydrazide reagent, 4-phenethylbenzohydrazide, was synthesized previously in both the natural and stable-isotope labeled form in the Department of Chemistry at North Carolina State University.⁹

7.2.2 *N*-linked Glycan Derivatization Procedure

Maltodextrin and *N*-linked glycans cleaved from pooled human plasma were derivatized with either the light or heavy 4-phenethylbenzohydrazide (P2GPN) using the method previously described.³¹ Briefly, a 1 mg/mL solution of each reagent was made immediately prior to reaction in 25:75 acetic acid:methanol (v/v). To the dried glycan sample, 200 μ L of the reagent solution was added. The sample was vortexed, centrifuged, and incubated at 56°C for 3 hr. The samples were dried *in vacuo* at 55°C, and the lyophilized powder was stored until analysis at -20°C.

7.2.3 Maltodextrin Sample Preparation

The maltodextrin sample has been prepared such that each vial contains a 50 μg aliquot of dried glycan powder. The samples were either derivatized with the light or heavy P2GPN reagent, according to the procedure detailed above. Before analysis, the samples were reconstituted in 200 μL of the initial LC conditions. The samples were then vortexed, centrifuged, and the supernatant was extracted and analyzed.

7.2.4 N-linked Glycan Extraction from Pooled Plasma

N-linked glycans were cleaved from pooled human plasma aliquots following methods detailed previously.^{20, 32} Briefly, at the onset of sample preparation 200 μg of a plant glycoprotein internal standard, horseradish peroxidase (HRP), was added. PNGaseF was used to liberate the *N*-linked glycans from 50 μL aliquots of pooled human plasma, the reaction was incubated for 18 hr, and an ethanol precipitation step was performed immediately after glycan cleavage to remove a majority of the plasma proteins. The remaining glycans were further purified using solid phase extraction (SPE). Following SPE, the samples were dried and stored at -20°C until analysis. The samples were either derivatized with the light or heavy P2GPN reagent, according to the procedure detailed above. Before analysis, the samples were reconstituted in 200 μL of the initial LC conditions. The samples were then vortexed, centrifuged, and the supernatant was extracted and analyzed.

7.2.5 *cHiPLC nano-Flow Reverse Phase Chromatography*

The derivatized glycan samples were analyzed using reverse phase liquid chromatography. Ten microliters of the glycan samples were injected onto the column using an EASY-nLC II autosampler and liquid chromatography (LC) system (Thermo Fisher Scientific, San Jose, CA) in mobile phase A at 650 nL/min. The sample was then washed with an additional 2 μ L of mobile phase A. Mobile phase A and B consist of 98/2/0.2% and 2/98/0.2% water/acetonitrile/formic acid, respectively. The separation of derivatized *N*-linked glycans was performed on a cHiPLC system (Eksigent, Dublin, CA) in the vented column configuration,³³ using a ChromXP C18-CL 75 μ m \times 15 cm analytical column for both the trap and analytical column. This dual-analytical column setup allowed for a total column length of 30 cm, and glycans were separated at a flow rate of 300 nL/min. The initial conditions of 2% mobile phase B were held for 1 min, and then, mobile phase B was ramped to 22% over 1 minute. The mobile phase B composition was further ramped to 35% over 35 min, and the column was washed at 95% mobile phase B and re-equilibrated for 15 min at the initial solvent conditions.

7.2.6 *Q Exactive Mass Spectrometry*

The RP chromatography system is coupled online to a Q Exactive mass spectrometer equipped with a nanospray source (Thermo Fisher Scientific, San Jose, CA).³⁴ Glycans were ionized by applying 2.25 kV to the union between the outlet of the LC system and the emitter tip. The MS inlet capillary was heated to

225°C. Glycans were detected using data dependent acquisition, where up to 5 precursor ions per full scan were chosen for MS/MS fragmentation. The 5 precursor ions were chosen based on ion abundance, and once an ion is chosen, it is put on an exclusion list for 25 s so that other precursors may be fragmented in the next cycle. In the full scan, precursor ions are detected in the Orbitrap at a resolving power of 70,000 (FWHM) at $m/z = 200$. The automatic gain control (AGC) was set to 1×10^6 ions, and the maximum injection time was set to 250 ms. Upon selection for fragmentation, the precursor ions are isolated and fragmented in the higher energy collision dissociation (HCD) cell at a normalized collision energy (NCE) of 20. In the product ion scan, ions are detected in the Orbitrap at a resolving power (FWHM) of 17,500 at $m/z = 200$. The AGC was set to 2×10^4 ions, and the maximum injection time was set to 120 ms. The instrument was calibrated just before the data set per the manufacturer's specifications. Unique glycan compositions were manually identified *via* accurate mass (± 5 ppm) and analyzed using the manufacturer's software (Xcalibur v.2.2). The *N*-linked glycan database, detailed integration, and processing strategy are all included in the supplementary material (**Appendix D**).

7.3 Results and Discussion

In this study, two samples, a hexose sugar ladder and pooled human plasma, were used to develop and demonstrate the effectiveness of the INLIGHT relative quantification strategy. Maltodextrin, a linear glucose polymer, was used as a

standard for developing a reproducible strategy for the analysis of SIL glycan relative quantification data. Using maltodextrin as a standard affords several advantages including minimized sample preparation variability in comparison to a biological sample, a large molecular weight range (~150-10,000 Da), and a wide abundance range (>5 orders of magnitude). This allows one to determine the effectiveness of the glycan quantification strategy and processing method at a wide variety of glycan sizes and abundances, mimicking a biological sample, while minimizing the variability.

The native and SIL P2GPN reagents (described previously⁹) were used in this experiment to derivatize glycans and have a nominal mass difference of 6 Da. At low molecular weights (~1000 Da), a 6 Da shift in the SIL tag mass is sufficient to fully separate the isotopic distributions (**Figure 7.1a**). However, as the molecular weight of the glycans becomes larger, the isotopic distributions begin to overlap (**Figure 7.1b-d**). This poses a problem because the current method for analyzing SIL relative quantification data is by generating extracted ion chromatograms of both the light and heavy monoisotopic peaks and creating a peak area ratio. Because the monoisotopic peaks (A peak) are used to extract the chromatograms for quantification, any overlapping isotopic distribution from the light-labeled sample will contribute to the area of the heavy-labeled sample. In order to account for this isotopic overlap of large molecular weight glycans, the isotopic distribution was modeled for each maltodextrin analyte detected. Using the theoretical isotopic distribution, the ratio of the $A+6_{\text{Light}}$ peak to the A_{Light} peak can be determined for

each molecular weight. This ratio can then be used to determine the amount of area contributed by $A+6_{Light}$ peak and subtracted from the $\Sigma[M+nH^+]^{n+}_{Heavy}$ area. Thus the corrected heavy peak area ($\Sigma[M+nH^+]^{n+}_{Heavy_Corrected}$) can be calculated using **Equation 7.1**, and the H:L ratio can be calculated using **Equation 7.2**.

$$\Sigma[M + nH^+]^{n+}_{Heavy_Corrected} = \Sigma[M + nH^+]^{n+}_{Heavy} - \left[\left(\frac{A+6_{Light}}{A_{Light}}\right)^{n+}\right] \times \Sigma[M + nH^+]^{n+}_{Light}$$

(Equation 7.1)

$$Relative\ Glycan\ Abundance\ Ratio = H:L = \frac{\Sigma[M+nH^+]^{n+}_{Heavy_Corrected}}{\Sigma[M+nH^+]^{n+}_{Light}}$$

(Equation 7.2)

In order to demonstrate contribution of the isotopic overlap to the relative quantification data and the effectiveness of correcting the data using **Equations 7.1** and **7.2**, two aliquots of maltodextrin were differentially labeled (one with the light and one with the heavy reagent), the two samples were mixed in a 1:1 ratio, and analyzed. It is shown in **Figure 7.2a** that the expected 1:1 glycan ratios are not correctly measured in the raw data. Additionally, **Figures 7.2b** and **7.2c** show that the ratios of these data are skewed by a combination of both the increasing molecular weight and the decreasing ion abundance in the spectra. Upon closer observation, it is clear that at low glycan ion abundances, the incorrect measured ratio is due to the glycan concentrations in the sample approaching the detection limits of the instrument. Here, one peak of the ion pair is at or just above the

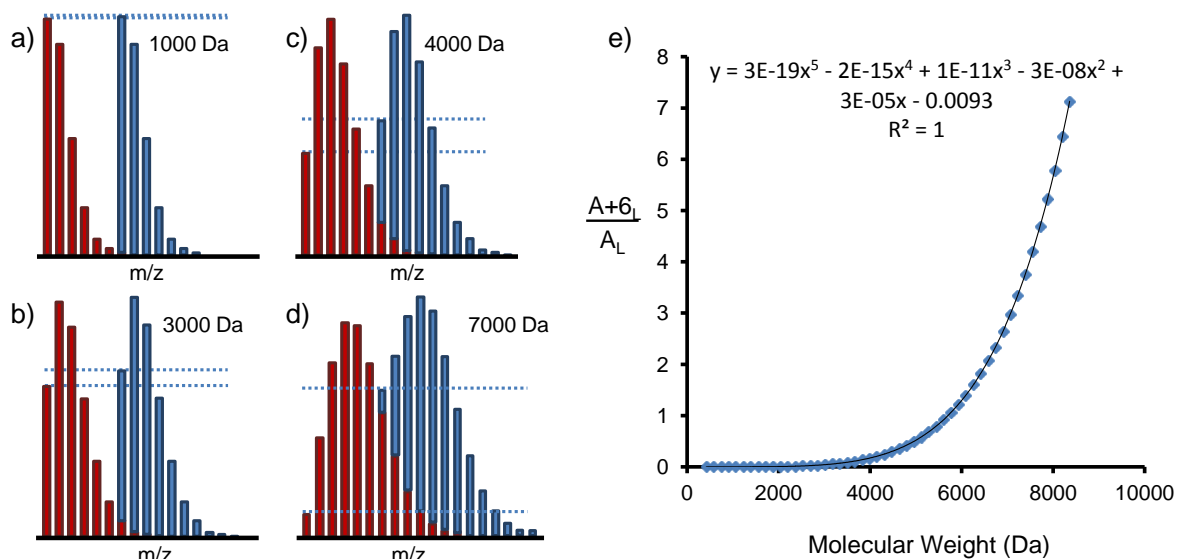


Figure 7.1 – a-d) Theoretical isotopic distributions for light and heavy glycan pairs in a 1:1 ratio at 1000, 3000, 4000, and 7000 Da, respectively. The dotted lines represent the abundance of the light and heavy $[M+nH^{+}]^{n+}$ peaks and show the discrepancy in quantification if isotopic distribution overlap is not taken into account. **e)** A plot of the theoretical $A+6_L$ to A_L ratio vs. the molecular weight of the maltodextrin ladder.

detection limit, causing the detected glycan ratios to be non-representative of the data. These glycans are shaded in the blue box in both **Figures 7.2b** and **7.2c**. Thus, based on this observation and the specification of our instrument, the data will be truncated below a normalized abundance value of 1×10^{-4} .

After the normalized abundance cutoff was applied, the data were further corrected using **Equations 7.1** and **7.2**. By correcting for the isotopic overlap of the glycans, the molecular weight dependence of the ratio is eliminated (**Figure 7.2e**). Although it is shown that the isotopic overlap can be corrected for, the glycans are

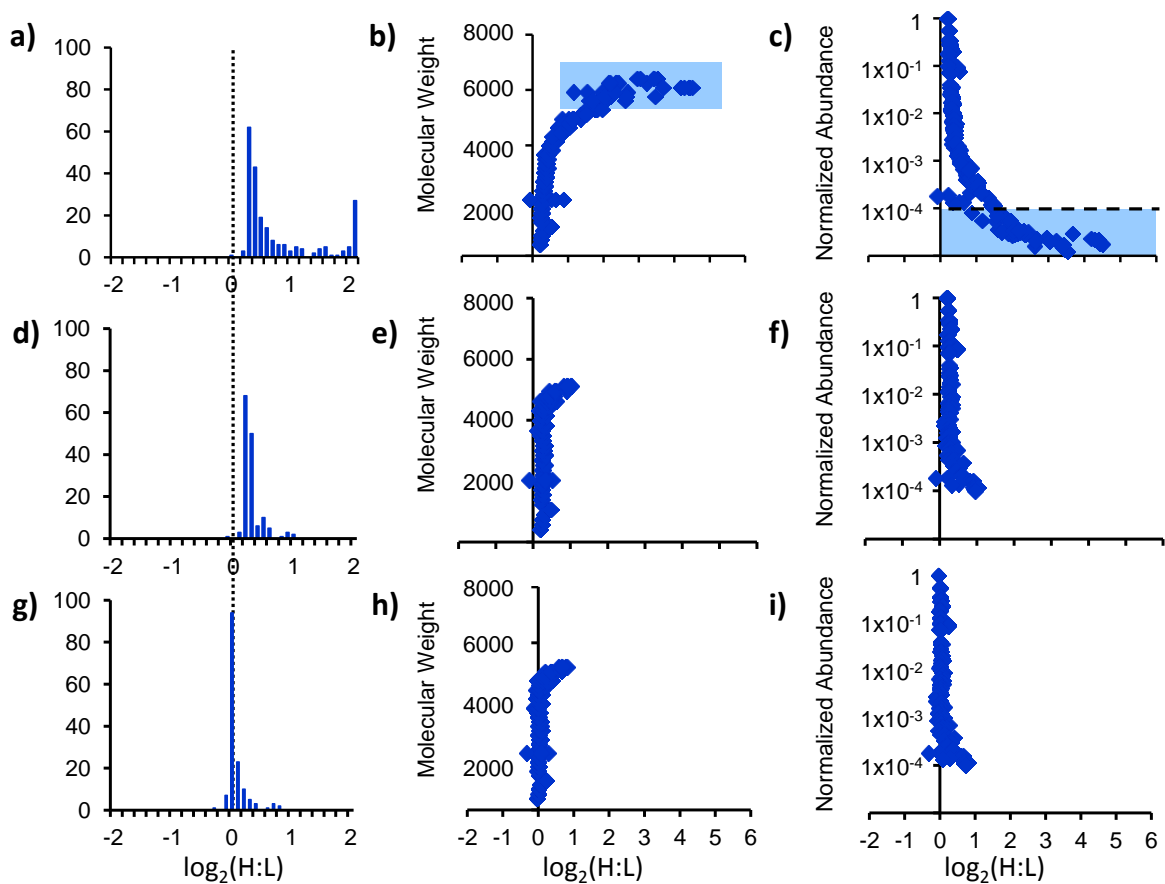


Figure 7.2 – Maltodextrin 1:1 (H:L) mixture. **a-c)** Raw data; **d-f)** abundance truncated and isotopic overlap corrected data; **g-i)** abundance truncated, isotopic overlap, and TGNF corrected data. For each of these situations, the histogram, molecular weight, and normalized abundance have been plotted.

still not detected with the ideal 1:1 ratio in **Figure 7.2d-f**. Thus, this data set was used to demonstrate the effectiveness of a Total Glycan Normalization Factor (TGNF) for the correction of systematic variability in the sample and sample preparation (**Figures 7.2g-i**). This TGNF is analogous to TSpC normalization^{23-24, 28} in label free proteomic methods and is described by **Equation 7.3**. This method

sums both the heavy glycan areas and light glycan areas and takes the ratio in order to calculate TGNF (larger value always on top). This factor is then multiplied by each of the glycan areas in the sample with the smaller of the two sums in order to normalize the two data sets. **Equation 7.3** sums the 30 most abundant glycan areas for each sample. All glycans are not used due to the mentioned adverse effects of low abundant glycans (*vide supra*).

$$TGNF = \frac{\sum_{i=1}^{30} GlycanArea_{Heavy}}{\sum_{i=1}^{30} GlycanArea_{Light}} \quad \text{(Equation 7.3)}$$

It is shown in **Figures 7.2g-i** that the TGNF (in combination with the molecular weight correction and abundance truncation) is capable of correcting for nearly all of the systematic variation of the sample preparation and analysis method. This allows for accurate relative quantification for 4 orders of magnitude when using the INLIGHT strategy, and after filtering out the low-abundance data (< the normalized value of 1×10^{-4}), the mean \pm 95% confidence interval for the TGNF and molecular weight corrected H:L ratio is calculated to be 1.06 ± 0.02 . In contrast, the mean \pm 95% confidence interval for the raw data (**Figures 7.2a-c**) after truncating using the abundance cutoff is calculated to be 1.37 ± 0.04 . Additionally, a two-tailed f-test for different variances was performed, and it was shown that the variance of the corrected data was significantly less than the variance of the raw data. This is

attributed to the molecular weight correction, and the reduction in variability will allow for lower cutoffs when determining significant biological change.

An additional data set was prepared such that the light- and heavy-labeled maltodextrin samples were mixed in the following ratios to generate a total of 7 samples: 5:1, 2:1, 1.5:1, 1:1, 1:1.5, 1:2, and 1:5. **Figure 7.3** plots the TGNF and molecular weight corrected experimental H:L ratio vs. the calculated H:L ratio for 3 representative glycans of different molecular weights: Hex₄, Hex₁₄, and Hex₂₄. The data are plotted in triplicate for each of the three glycans, and a weighted least squares regression was calculated. The slope \pm 95% confidence interval of the regression in **Figure 7.3** was found to be 1.01 ± 0.03 , and the intercept \pm 95% confidence interval was found to be 0.004 ± 0.06 . These data show that the INLIGHT strategy is capable of statistically measuring the ideal slope of unity and ideal intercept of 0, and the linear range of quantification spans a 5-fold change in glycan abundance in both directions.

The maltodextrin ladder has been used as an effective model for *N*-linked glycans in mammalian biological systems, and it has been shown that the INLIGHT strategy is capable of quantifying glycans in a sample with ~50 oligosaccharides. However, this model glycan ladder required minimal sample preparation, thus allowing for minimal sample preparation variability. The following studies were performed in aliquots of pooled human plasma in order to determine the effectiveness of the INLIGHT strategy in samples requiring significantly more complex sample preparation strategies. Thus, variability (both systematic and

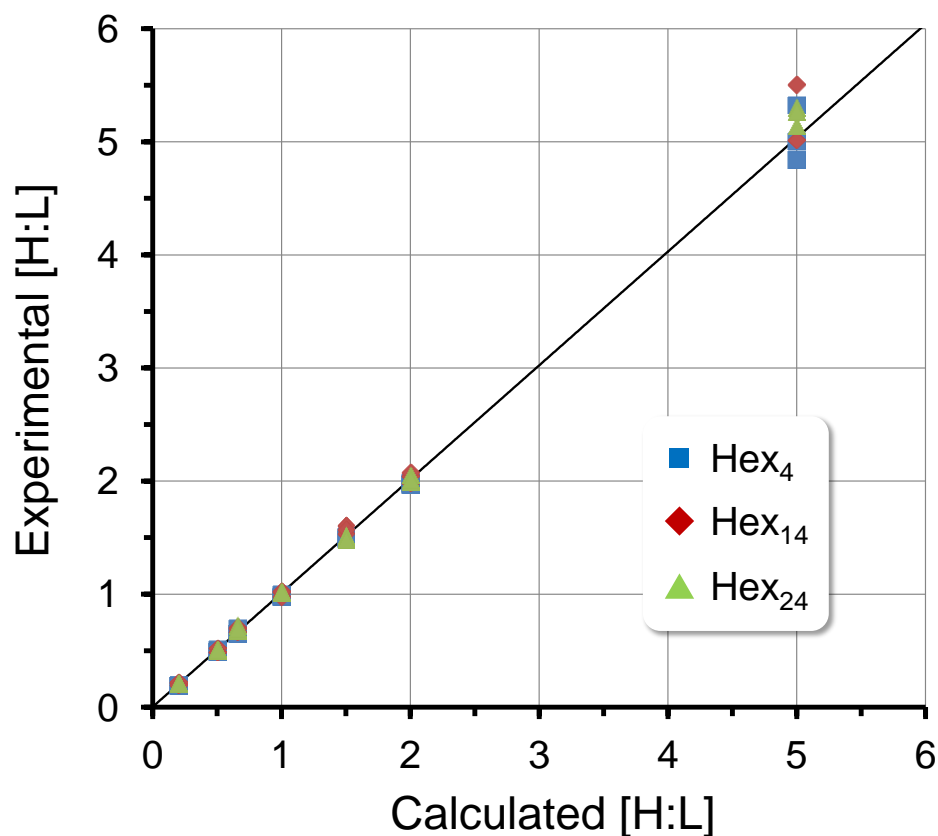


Figure 7.3 – A plot of the experimental vs. the calculated H:L ratio for the 5:1, 2:1, 1.5:1, 1:1, 1:1.5, 1:2, and 1:5 maltodextrin mixtures. The data have been plotted for 3 glycans, each in triplicate, of substantially different molecular weights (902.35, 2522.88, and 4143.41 Da). A weighted linear least squares regression is plotted for the data.

random) is incorporated at each step of the sample preparation (e.g., glycan cleavage, solid phase extraction, derivatization) due to the samples being quantified having to be processed in parallel. Pooled plasma aliquots were prepared according to **Figure 7.4**, where the internal standard glycoprotein (HRP) was added to each of the 10 aliquots, and 100 μg of α_1 -acid glycoprotein (AGP) were spiked into two

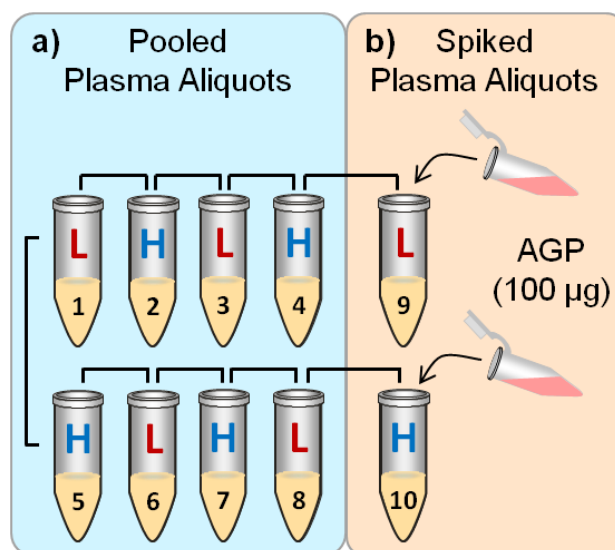


Figure 7.4 – The experimental design for demonstrating the effectiveness of the INLIGHT strategy in pooled plasma. Black brackets denote samples that were mixed together, and samples labeled with a red ‘L’ and blue ‘H’ are derivatized with the light and heavy P2GPN reagents, respectively. Samples in **(a)** were used to determine the variability of the internal standard and TGNF correction. The spiked plasma aliquots **(b)** were used to demonstrate the measurement of changing glycan abundances using the INLIGHT strategy.

aliquots to determine the effectiveness of using INLIGHT to relatively quantify *N*-linked glycans in complex biological matrices (*vide infra*).

The 8 pooled plasma samples that did not contain spiked AGP were derivatized and compared according to **Figure 7.4a** in order to measure and compare the variability of using the previously reported HRP internal standard correction vs. using the TGNF post-acquisition correction. **Figure 7.5** shows histograms of the $\log_2(\text{H:L})$ for these 7 samples in triplicate for the internal standard (**7.5a**) and TGNF (**7.5b**) corrected samples. It is shown that in these samples where

the biological variability is assumed to be zero (*i.e.*, pooled plasma), that both the internal standard and the TGNF methods are capable of measuring the expected 1:1 ratio with distributions centered around zero. However, qualitatively the distribution for the TGNF method is narrower than the internal standard corrected distribution, and there are ~33% more glycans in the TGNF corrected center-most bin (0 ± 0.05). Thus, an f-test was performed, and it was shown that the TGNF method allows for significantly less variance after correction than when using the internal standard correction.

The 2 spiked AGP plasma samples (one light and one heavy) were compared to a corresponding light or heavy sample of the normal pooled plasma samples analyzed in the previous experiment. These comparisons were made in order to test whether or not the INLIGHT strategy is capable of detecting change in arguably the most complex of biological samples and matrices, plasma. Because a glycoprotein was spiked in and not a standard free glycan, there is no way to know the added glycan concentration or what the expected change should be. However, it has been shown in the literature that AGP is significantly glycosylated with bi- tri- and tetra-antennary complex-type *N*-linked glycans containing *N*-acetylneuraminic acid.³⁵⁻³⁶ Thus, it would be expected that one would observe significantly different glycan abundances for large, acidic glycans, whereas neutral glycans would not be determined statistically different.

The glycan abundance ratios measured in the analyses comparing the AGP-spiked and normal pooled plasma samples are compared to the measured glycan

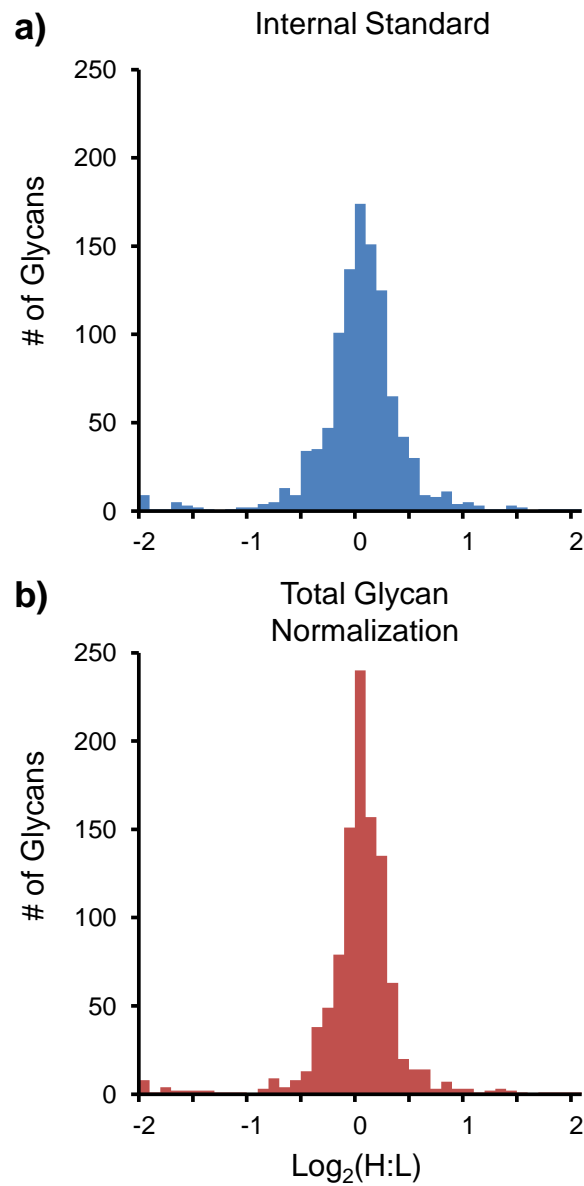


Figure 7.5 – Histograms of the **a)** internal standard (HRP) and **b)** TGNF corrected neat pooled plasma 1:1 N-linked glycan samples. An f-test confirms that there is less variation in the data corrected using the TGNF strategy.

ratios from the seven normal plasma comparisons in the previous experiment. **Table 7.1** shows example glycan abundance ratios from the comparison of the AGP-spiked and normal plasma samples. The *N*-linked glycans shown in the top of **Table 7.1** are examples of 4 multi-antennary glycans containing acidic monosaccharide moieties, and it is observed that when the AGP-spiked glycan ratios are compared to the normal pooled plasma glycan ratios, the $\log_2(\text{H:L})$ ratios significantly deviate from zero (\pm depending on whether the AGP-spiked sample was labeled light or heavy). In contrast, examples of neutral glycan abundance ratios from the same samples are shown on the bottom half of **Table 7.1**, and no significant difference is detected. All the glycan ratios in **Table 7.1** were compared to the glycan ratios of the 7 normal pooled plasma samples comparisons (in triplicate), and using a t-test, only the glycans with acidic monosaccharide residues were found to have significantly different abundance ratios. Furthermore, the light-labeled AGP-spiked sample ratios are detected as statistically significant negative values, whereas the heavy-labeled AGP-spiked samples ratios are measured as statistically significant positive values. This demonstrates the lack of labeling bias and further gives confidence to the fact that the molecular weight correction sufficiently minimizes the effects due to isotopic overlap. These *N*-linked glycans in which change is significantly detected are large molecular weight glycans (~3000-4000 Da), and if the change detected was due to the isotopic overlap, then the ratios would be the same for both samples instead of change in opposite directions, as seen in **Table 7.1**. Additionally, it must be noted that the amount of change detected in the AGP-spiked samples is less than a 2-fold

change, which is often used as a cutoff in determining biological significance. Furthermore, as little as a 20% change in the glycan abundance ($H_6N_5F_1A_2$ glycan) was determined to be significantly different. This is a testament to the precision and utility of the INLIGHT strategy for the relative quantification of *N*-linked glycans in complex biological samples.

Table 7.1 – Abundance ratios for example glycans in both AGP-spiked plasma samples.

	$H_6N_5F_1A_2$		$H_7N_6A_3$		$H_7N_6F_1A_3$		$H_8N_7A_3$		Up-Regulated Heavy Sample
	$\log_2(H:L)$	$ t /t_{Table}$	$\log_2(H:L)$	$ t /t_{Table}$	$\log_2(H:L)$	$ t /t_{Table}$	$\log_2(H:L)$	$ t /t_{Table}$	
α_1 -Spiked Light	-0.23	2.5	-0.64	9.0	-0.57	12	-0.63	3.7	
α_1 -Spiked Heavy	0.30	2.5	0.79	1.4	0.71	1.03	0.87	1.7	
	H_3N_5		H_7N_2		H_5N_4		$H_5N_5F_1$		Up-Regulated Light Sample
	$\log_2(H:L)$	$ t /t_{Table}$	$\log_2(H:L)$	$ t /t_{Table}$	$\log_2(H:L)$	$ t /t_{Table}$	$\log_2(H:L)$	$ t /t_{Table}$	
α_1 -Spiked Light	-0.05	0.04	-0.26	0.82	-0.09	0.39	-0.02	0.03	
α_1 -Spiked Heavy	0.06	0.93	0.02	0.10	0.04	0.16	0.07	0.36	

H – Hexose; N – *N*-acetylhexosamine; F – Fucose; A – *N*-acetylneuraminic acid.

7.4 Conclusions

The strategy presented herein, Individuality Normalization when Labeling with Isotopic Glycan Hydrazide Tags (INLIGHT), demonstrates the effective quantification of *N*-linked glycans both in simple and in complex biological samples. This method has been developed such that the SIL derivatization can be coupled to nearly any *N*-linked glycan (or any oligosaccharide with a free aldehyde at the reducing terminus)

sample preparation strategy with minimal time and monetary cost (<4hr of additional sample preparation time). Because of the possible benefits to many glycomics experiments, a detailed strategy for the relative quantification of INLIGHT has been presented.

In order to measure significant biological change, up-front sample preparation strategies and back-end data analyses must be optimized in order to minimize systematic variability introduced into the measurement. These efforts have been described for the INLIGHT strategy, where variation due to isotopic overlap has been corrected. Additionally, the ability to more effectively correct for systematic analytical and biological variability using a post-acquisition normalization strategy rather than a single internal standard is presented for the first time in a glycan sample. This attention to minimizing the variability and the inherent advantages of INLIGHT make this an attractive and easily implemented strategy for those interested in measuring biological changes in glycosylation.

7.5 References

- (1) Apweiler, R.; Hermjakob, H.; Sharon, N. On the frequency of protein glycosylation, as deduced from analysis of the SWISS-PROT database. *BBA-Gen. Subjects*, **1999**, *1473*, 4-8.
- (2) Begley, T. P., *Wiley Encyclopedia of Chemical Biology* **2009**, *2*, 785.
- (3) Varki, A.; Cummings, R. D.; Esko, J. D.; Freeze, H. H.; Stanley, P.; Bertozzi, C. R.; Hart, G. W.; Etzler, M. E., *Essentials of Glycobiology* **2009**.
- (4) Orlando, R.; Lim, J. M.; Atwood, J. A.; Angel, P. M.; Fang, M.; Aoki, K.; Alvarez-Manilla, G.; Moremen, K. W.; York, W. S.; Tiemeyer, M.; Pierce, M.; Dalton, S.; Wells, L. IDAWG: Metabolic Incorporation of Stable Isotope Labels for Quantitative Glycomics of Cultured Cells. *J. Proteome Res.*, **2009**, *8*, 3816-3823.
- (5) Atwood, J. A.; Cheng, L.; Alvarez-Manilla, G.; Warren, N. L.; York, W. S.; Orlando, R. Quantitation by isobaric labeling: Applications to glycomics. *J. Proteome Res.*, **2008**, *7*, 367-374.
- (6) Xia, B. Y.; Feasley, C. L.; Sachdev, G. P.; Smith, D. F.; Cummings, R. D. Glycan reductive isotope labeling for quantitative glycomics. *Anal. Biochem.*, **2009**, *387*, 162-170.
- (7) Kang, P.; Mechref, Y.; Kyselova, Z.; Goetz, J. A.; Novotny, M. V. Comparative glycomic mapping through quantitative permethylation and stable-isotope labeling. *Anal. Chem.*, **2007**, *79*, 6064-6073.
- (8) Zhang, P.; Zhang, Y.; Xue, X. D.; Wang, C. J.; Wang, Z. F.; Huang, L. J. Relative quantitation of glycans using stable isotopic labels 1-(d₀/d₅) phenyl-3-methyl-5-pyrazolone by mass spectrometry. *Anal. Biochem.*, **2011**, *418*, 1-9.
- (9) Walker, S. H.; Budhathoki-Uprety, J.; Novak, B. M.; Muddiman, D. C. Stable-isotope labeled hydrophobic hydrazide reagents for the relative quantification of N-linked glycans by electrospray ionization mass spectrometry. *Anal. Chem.*, **2011**, *83*, 6738-45.
- (10) Bowman, M. J.; Zaia, J. Comparative Glycomics Using a Tetraplex Stable-Isotope Coded Tag. *Anal. Chem.*, **2010**, *82*, 3023-3031.

- (11) Alvarez-Manilla, G.;Warren, N. L.;Abney, T.;Atwood, J.;Azadi, P.;York, W. S.;Pierce, M.;Orlando, R. Tools for glycomics: relative quantitation of glycans by isotopic permethylation using (CH₃)₂C=O-C-13. *Glycobiology*, **2007**, 677-687.
- (12) Filer, C. N. Isotopic fractionation of organic compounds in chromatography. *J. Labelled Compd. Radiopharm.*, **1999**, 169-197.
- (13) Filer, C. N.;Fazio, R.;Ahern, D. G. (+/-)-[methyl-H-3 and methyl-H-2]mianserin - participants in a dramatic instance of HPLC isotopic fractionation. *J. Org. Chem.*, **1981**, 3344-3346.
- (14) Gygi, S. P.;Rist, B.;Gerber, S. A.;Turecek, F.;Gelb, M. H.;Aebersold, R. Quantitative analysis of complex protein mixtures using isotope-coded affinity tags. *Nat. Biotechnol.*, **1999**, 994-999.
- (15) Dixon, R. B.;Bereman, M. S.;Petitte, J. N.;Hawkrige, A. M.;Muddiman, D. C. One-year plasma N-linked glycome intra-individual and inter-individual variability in the chicken model of spontaneous ovarian adenocarcinoma. *Int. J. Mass Spectrom.*, **2011**, 305, 79-86.
- (16) de Leoz, M. L. A.;Young, L. J. T.;An, H. J.;Kronewitter, S. R.;Kim, J. H.;Miyamoto, S.;Borowsky, A. D.;Chew, H. K.;Lebrilla, C. B. High-Mannose Glycans are Elevated during Breast Cancer Progression. *Mol. Cell Proteomics*, **2011**, 10, 1-9.
- (17) Snovida, S. I.;Perreault, H. A 2,5-dihydroxybenzoic acid/N,N-dimethylaniline matrix for the analysis of oligosaccharides by matrix-assisted laser desorption/ionization mass spectrometry. *Rapid Commun. Mass Spectrom.*, **2007**, 21, 3711-3715.
- (18) Kaneshiro, K.;Watanabe, M.;Terasawa, K.;Uchimura, H.;Fukuyama, Y.;Iwamoto, S.;Sato, T. A.;Shimizu, K.;Tsujiimoto, G.;Tanaka, K. Rapid Quantitative Profiling of N-Glycan by the Glycan-Labeling Method Using 3-Aminoquinoline/alpha-Cyano-4-hydroxycinnamic Acid. *Anal. Chem.*, **2012**, 84, 7146-7151.
- (19) Walker, S. H.;Taylor, A. D.;Muddiman, D. C. The Use of a Xylosylated Plant Glycoprotein as an Internal Standard Accounting for N-linked glycan Cleavage and Sample Preparation Variability. *Rapid Commun. Mass Spectrom.*, **2013**, In Press.
- (20) Bereman, M. S.;Young, D. D.;Deiters, A.;Muddiman, D. C. Development of a Robust and High Throughput Method for Profiling N-Linked Glycans Derived

- from Plasma Glycoproteins by NanoLC-FTICR Mass Spectrometry. *J. Proteome Res.*, **2009**, *8*, 3764-3770.
- (21) Harris, E. K. Effects of Intraindividual and Interindividual Variation on Appropriate Use of Normal Ranges. *Clin. Chem.*, **1974**, *20*, 1535-1542.
- (22) Hawkridge, A. M.;Muddiman, D. C. Mass Spectrometry-Based Biomarker Discovery: Toward a Global Proteome Index of Individuality. *Annual Review of Analytical Chemistry*, **2009**, 265-277.
- (23) Carvalho, P. C.;Fischer, J. S.;Chen, E. I.;Yates, J. R.;Barbosa, V. C. PatternLab for proteomics: a tool for differential shotgun proteomics. *BMC Bioinformatics*, **2008**, *9*.
- (24) Dong, M. Q.;Venable, J. D.;Au, N.;Xu, T.;Park, S. K.;Cociorva, D.;Johnson, J. R.;Dillin, A.;Yates, J. R. Quantitative mass spectrometry identifies insulin signaling targets in *C-elegans*. *Science*, **2007**, *317*, 660-663.
- (25) Zybailov, B.;Mosley, A. L.;Sardiu, M. E.;Coleman, M. K.;Florens, L.;Washburn, M. P. Statistical analysis of membrane proteome expression changes in *Saccharomyces cerevisiae*. *J. Proteome Res.*, **2006**, *5*, 2339-2347.
- (26) Florens, L.;Carozza, M. J.;Swanson, S. K.;Fournier, M.;Coleman, M. K.;Workman, J. L.;Washburn, M. P. Analyzing chromatin remodeling complexes using shotgun proteomics and normalized spectral abundance factors. *Methods*, **2006**, *40*, 303-311.
- (27) Sardiu, M. E.;Cai, Y.;Jin, J. J.;Swanson, S. K.;Conaway, R. C.;Conaway, J. W.;Florens, L.;Washburn, M. P. Probabilistic assembly of human protein interaction networks from label-free quantitative proteomics. *Proc. Natl. Acad. Sci. U.S.A.*, **2008**, *105*, 1454-1459.
- (28) Gokce, E.;Shuford, C. M.;Franck, W. L.;Dean, R. A.;Muddiman, D. C. Evaluation of Normalization Methods on GeLC-MS/MS Label-Free Spectral Counting Data to Correct for Variation during Proteomic Workflows. *J. Am. Soc. Mass Spectrom.*, **2011**, *22*, 2199-2208.
- (29) Collier, T. S.;Randall, S. M.;Sarkar, P.;Rao, B. M.;Dean, R. A.;Muddiman, D. C. Comparison of stable-isotope labeling with amino acids in cell culture and spectral counting for relative quantification of protein expression. *Rapid Commun. Mass Spectrom.*, **2011**, *25*, 2524-2532.

- (30) Walker, S. H.;Papas, B. N.;Comins, D. L.;Muddiman, D. C. Interplay of Permanent Charge and Hydrophobicity in the Electrospray Ionization of Glycans. *Anal. Chem.*, **2010**, *82*, 6636-6642.
- (31) Walker, S. H.;Lilley, L. M.;Enamorado, M. F.;Comins, D. L.;Muddiman, D. C. Hydrophobic Derivatization of N-linked Glycans for Increased Ion Abundance in Electrospray Ionization Mass Spectrometry. *J Am. Soc. Mass Spectrom.*, **2011**, *22*, 1309-17.
- (32) Walker, S. H.;Carlisle, B. C.;Muddiman, D. C. Systematic Comparison of Reverse Phase and Hydrophilic Interaction Liquid Chromatography Platforms for the Analysis of N-Linked Glycans. *Anal. Chem.*, **2012**, *84*, 8198-8206.
- (33) Andrews, G. L.;Shuford, C. M.;Burnett, J. C.;Hawkridge, A. M.;Muddiman, D. C. Coupling of a vented column with splitless nanoRPLC-ESI-MS for the improved separation and detection of brain natriuretic peptide-32 and its proteolytic peptides. *J. Chromatogr. B*, **2009**, *877*, 948-954.
- (34) Michalski, A.;Damoc, E.;Hauschild, J. P.;Lange, O.;Wiegghaus, A.;Makarov, A.;Nagaraj, N.;Cox, J.;Mann, M.;Horning, S. Mass Spectrometry-based Proteomics Using Q Exactive, a High-performance Benchtop Quadrupole Orbitrap Mass Spectrometer. *Mol. Cell. Proteomics*, **2011**, *10*.
- (35) Imre, T.;Schlosser, G.;Pocsfalvi, G.;Siciliano, R.;Molnar-Szollosi, E.;Kremmer, T.;Malorni, A.;Vekey, K. Glycosylation site analysis of human alpha-1-acid glycoprotein (AGP) by capillary liquid chromatography-electrospray mass spectrometry. *J. Mass Spectrom.*, **2005**, *40*, 1472-1483.
- (36) Fournier, T.;Medjoubi-N, N.;Porquet, D. Alpha-1-acid glycoprotein. *Biochim. Biophys. Acta - Protein Struct. Mol. Enzymol.*, **2000**, *1482*, 157-171.

APPENDICES

APPENDIX A

Supplemental Information to CHAPTER 3:

Hydrophobic Derivatization of *N*-linked Glycans for Increased Ion Abundance in Electrospray Ionization Mass Spectrometry

A.1 Non-Polar Surface Area Calculations

The NPSA were calculated according to **Figure A.1**. Standard molecular radii and bond lengths were used in order to estimate the surface area of each molecule in the reagent and the overlapping surface area. Only carbon and hydrogen molecules were considered to be hydrophobic, and when a carbon atom is

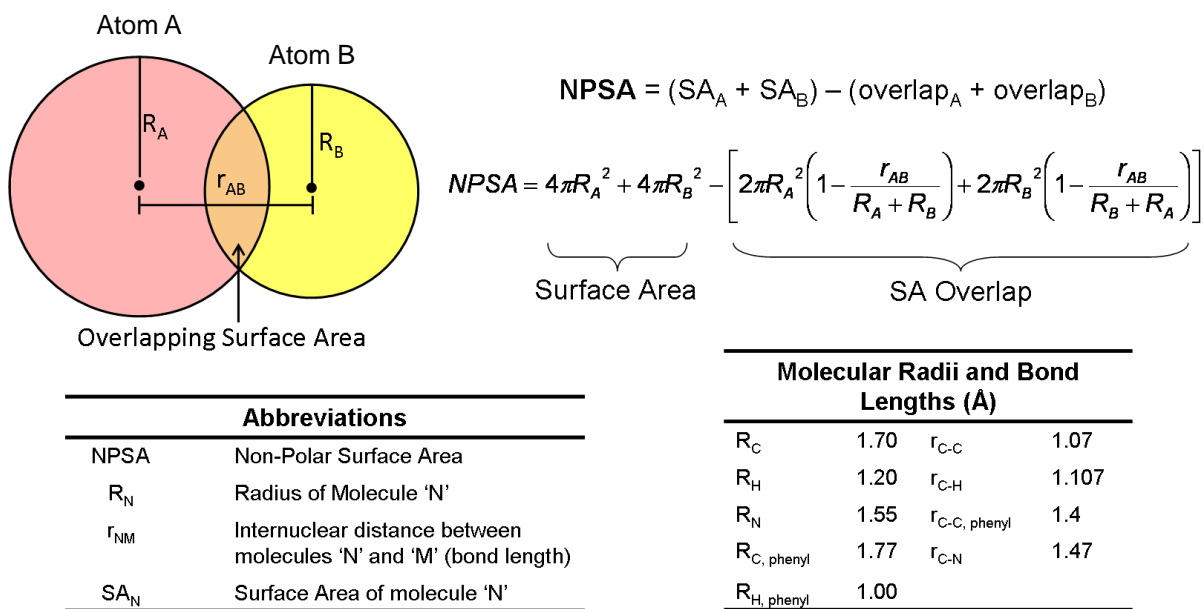


Figure A.1 – The formula, abbreviations, and molecular radii and bond lengths for the NPSA calculations of the hydrophobic hydrazide reagents.

bound to nitrogen, the overlapping surface area of the carbon/nitrogen is subtracted out as well. Additionally, a carbonyl carbon is not considered hydrophobic, so the surface area of a ketone is not factored into the NPSA. The polar surface area is not taken into account in the reagents because they are made of only non-polar functions, aside from the reactive site. This assumption reduces the complexity of the calculation and provides a simple calculation for the estimation of the hydrophobicity of the reagents.

A.2 Derivatization Reaction

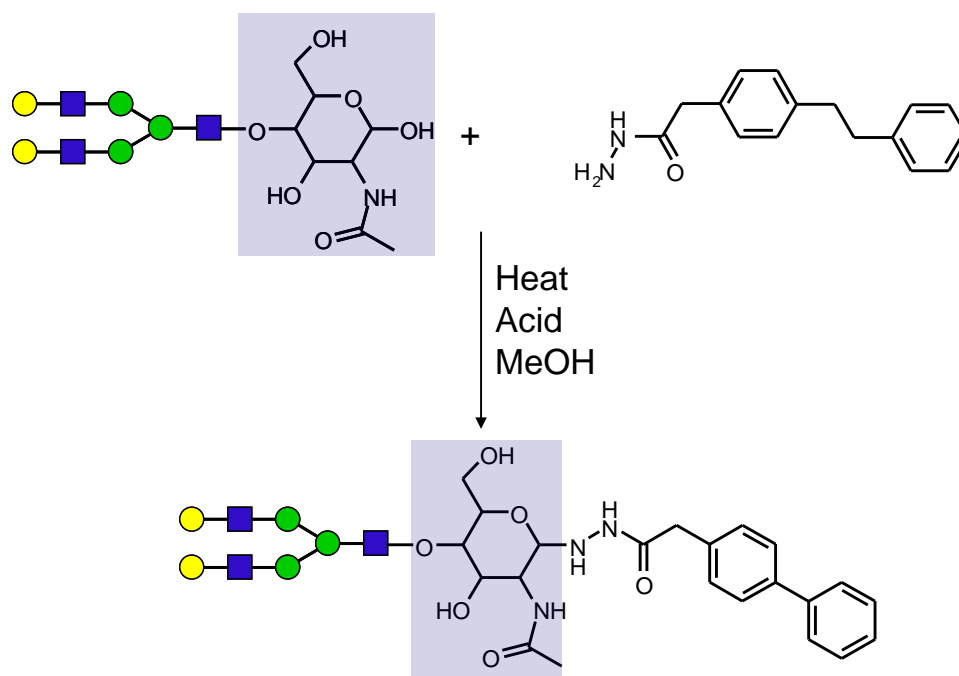
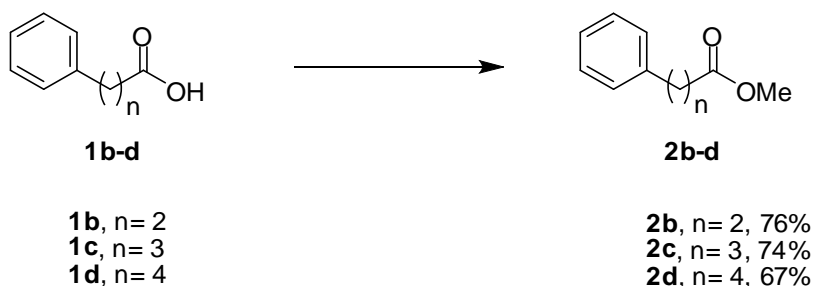


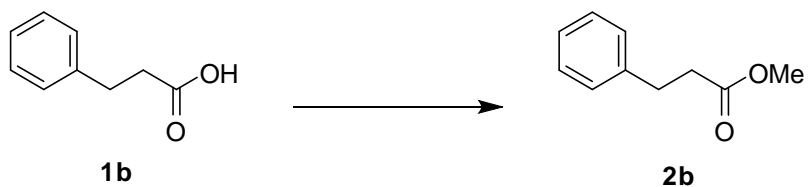
Figure A.2 – The hydrazone formation derivatization reaction. Portions shaded in light blue are the terminal GlcNAc (reducing terminus) chemical structure undergoing reaction.

A.3 Reagent Synthesis

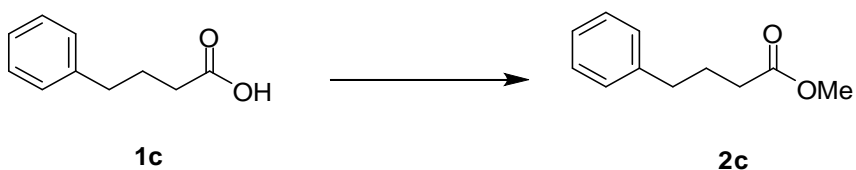
Many of the reagents and intermediates synthesized have been described previously in the literature and are referenced. These compounds, which have not been detailed in the literature, we have collected extensive characterization data, such as ^1H NMR, ^{13}C NMR, IR, and mass spectrometry.



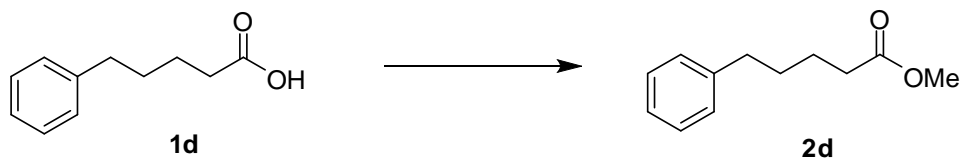
The corresponding carboxylic acid (**1b-d**) (5.0 g), was dissolved in a solution of concentrated hydrochloric acid (0.5 mL) in methanol (50 mL). The mixture was stirred for 20 h at rt. After 20 h at rt the mixture was extracted with ethyl ether (2x25 mL), washed with saturated aqueous NaHCO_3 (2x25 mL) and water (2x25 mL). The combined organic layers were dried over magnesium sulfate, filtered through a celite pad and the solvents removed *in vacuo*. Purification by distillation afforded the corresponding ester (**2b-d**).



Methyl 3-phenylpropanoate (2b).¹ $^1\text{H NMR}$ (400 MHz, CDCl_3) δ 7.16-7.32 (m, 5H), 3.66 (s, 3H), 2.95 (t, $J = 7.8$ Hz, 2H), 2.63 (t, $J = 7.8$ Hz, 2H); $^{13}\text{C NMR}$ (100 MHz, CDCl_3) δ 31.1, 35.9, 51.8, 126.4, 128.4, 128.7, 140.7, 173.5. **CAS:** 103-25-3



Methyl 4-phenylbutanoate (2c).² $^1\text{H NMR}$ (400 MHz, CDCl_3) δ 7.16-7.30 (m, 5H), 3.65 (s, 3H), 2.64 (t, $J = 8.0$ Hz, 2H), 2.32 (t, $J = 8.0$ Hz, 2H), 1.95 (m, 2H); $^{13}\text{C NMR}$ (100 MHz, CDCl_3) δ 26.6, 33.5, 35.2, 51.6, 126.1, 128.5, 128.6, 141.5, 174.0. **CAS:** 2046-17-5

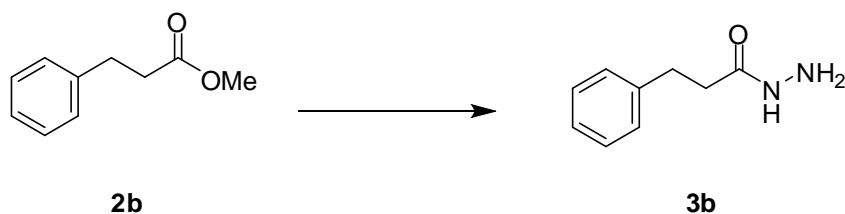


Methyl 5-phenylpentanoate (2d).³ $^1\text{H NMR}$ (400 MHz, CDCl_3) δ 7.14-7.30 (m, 5H), 3.65 (s, 3H), 2.62 (t, $J = 6.4$ Hz, 2H), 2.16 (t, $J = 6.4$ Hz, 2H), 1.65 (m, 4H); $^{13}\text{C NMR}$ (100 MHz, CDCl_3) δ 24.7, 31.1, 34.1, 35.7, 125.9, 128.4, 128.5, 142.3, 174.2. **CAS:** 20620-59-1



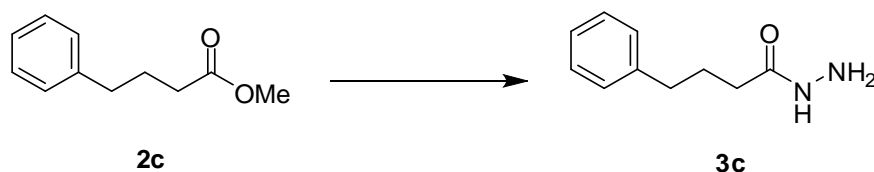
2-Phenylacetohydrazide (3a).⁴

Methyl 2-phenylacetate (**2d**) (1.0 mL, 6.66 mmol, 1.0 equiv) was dissolved in absolute ethanol (10 mL). The solution was cooled down to 0 °C and treated dropwise with hydrazine monohydrate (1.6 mL, 33.3 mmol, 5.0 equiv). The mixture was heated to reflux while stirring. After 20 h the mixture was allowed to cool down to rt and the solvent was removed *in vacuo* and the solid residue was recrystallized from isopropanol to yield 646 mg (65 %) of **3a** as white needle-like crystals. M.p. 118-118.2°C; ¹H NMR (400 MHz, CDCl₃) δ 7.22-7.38 (m, 5H), 6.75 (s, 1H), 3.83 (s, 2H), 3.56 (s, 2H); ¹³C NMR (100 MHz, CDCl₃) δ 42.1, 127.7, 129.2, 129.6, 134.1, 171.8. **CAS:** 937-39-3



3-Phenylpropanehydrazide (**3b**).⁵

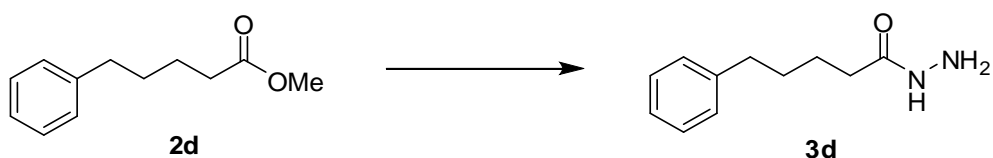
Methyl 3-phenylpropanoate (**2b**) (1.0 mL, 6.09 mmol, 1.0 equiv) was dissolved in absolute ethanol (10 mL). The solution was cooled down to 0 °C and treated dropwise with hydrazine monohydrate (1.5 mL, 30.5 mmol, 5.0 equiv). The mixture was heated to reflux while stirring. After 20 h the mixture was allowed to cool down to rt and the solvent was removed *in vacuo* and the solid residue was recrystallized from isopropanol to yield 589 mg (59 %) of **3b** as white needle-like crystals. M.p. 101.0-101.9 °C; ¹H NMR (400 MHz, CDCl₃) δ 7.14-7.34 (m, 5H), 6.75 (s, 1H), 3.85 (s, 2H), 2.97 (t, *J* = 7.2 Hz, 2H), 2.45 (t, *J* = 7.2 Hz, 2H); ¹³C NMR (100 MHz, CDCl₃) δ 31.6, 36.5, 126.6, 128.5, 128.8, 140.7, 173.1. **CAS:** 3538-68-9



4-Phenylbutanohydrazide (**3c**).⁵

Methyl 4-phenylbutanoate (**2c**) (1.0 mL, 5.6 mmol, 1.0 equiv) was dissolved in absolute ethanol (10 mL). The solution was cooled down to 0 °C and treated

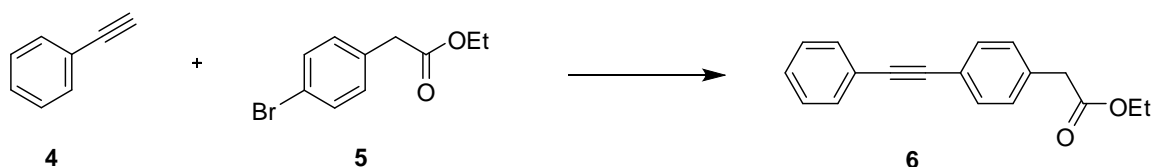
dropwise with hydrazine monohydrate (1.4 mL, 28.0 mmol, 5.0 equiv). The mixture was heated to reflux while stirring. After 20 h the mixture was allowed to cool down to rt and the solvent was removed *in vacuo* and the solid residue was recrystallized from isopropanol to yield 369 mg (37 %) of **3c** as white needle-like crystals. M.p. 80.0-80.5 °C; ¹H NMR (400 MHz, CDCl₃) δ 7.14-7.32 (m, 5H), 6.66 (s, 1H), 3.87 (s, 2H), 2.65 (t, *J* = 7.6 Hz, 2H), 2.15 (t, *J* = 7.6 Hz, 2H), 1.99 (m, 2H); ¹³C NMR (100 MHz, CDCl₃) δ 26.9, 33.8, 35.3, 126.3, 128.6, 128.7, 141.39. **CAS:** 39181-61-8



5-Phenylpentanehydrazide (**3d**).⁶

Methyl 5-phenylpentanoate (**2d**) (1.0 mL, 5.20 mmol, 1.0 equiv) was dissolved in absolute ethanol (10 mL). The solution was cooled down to 0 °C and treated dropwise with hydrazine monohydrate (9.8 mL, 203.0 mmol, 39.0 equiv). The mixture was heated to reflux while stirring. After 20 h was allowed to cool down to rt and the solvent was removed *in vacuo* and the solid residue was recrystallized from isopropanol to yield 387 mg (39 %) of **3d** as white needle-like crystals. M.p. 63.5-

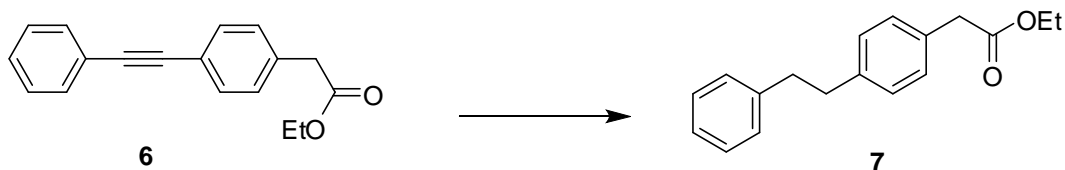
64.0 °C; ^1H NMR (400 MHz, CDCl_3) δ 7.12-7.32 (m, 5H), 6.72 (s, 1H), 3.88 (s, 2H), 2.63 (t, $J = 7.0$ Hz, 2H), 2.16 (t, $J = 7.0$ Hz, 2H), 1.65 (m, 4H); ^{13}C NMR (100 MHz, CDCl_3) δ 25.3, 31.2, 34.6, 35.8, 126.0, 128.5, 128.6, 142.2. **CAS:** 857482-61-2



Ethyl 2-(4-(phenylethynyl)phenyl)acetate (6).

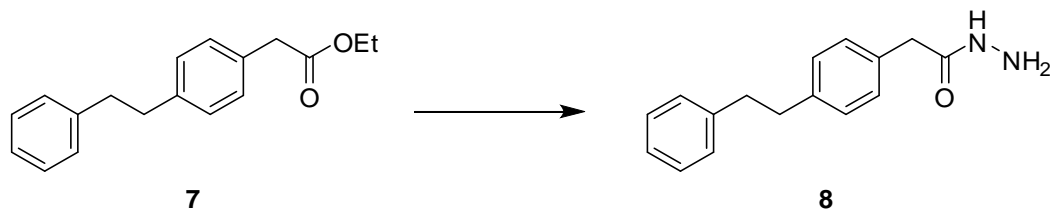
Ethyl 2-(4-bromophenyl)acetate (**5**) (360 μL , 2.06 mmol, 1.0 equiv) was added dropwise at rt to a mixture of bis(triphenylphosphine) palladium II chloride (5.8 mg, 0.0082 mmol, 0.004 equiv), copper (I) iodide (6.3 mg, 0.033 mmol, 0.016 equiv), and triphenylphosphine (6.5 mg, 0.025 mmol, 0.012 equiv) in freshly distilled triethylamine (4.0 mL) under a nitrogen atmosphere. The mixture was treated dropwise at rt with ethynyl benzene (**4**) (0.25 mL, 2.27 mmol, 1.1 equiv) and heated to 80 °C. After 24 h at 80 °C, the mixture was allowed to cool down to rt and then filtered through a pad of celite/silica gel 1:1. The solvent were removed *in vacuo*, the residue was dissolved in ethyl acetate (15 mL) and washed with brine (3x15 mL). The organic layer was concentrated under reduced pressure to afford the crude oil. Purification by Radial PLC (1% TEA/1% EtOAc/hexanes) afforded 433 mg (80 %) of

6 as a clear oil. ^1H NMR (400 MHz, CDCl_3) δ 7.24-7.62 (m, 9H), 4.16 (q, $J = 9.2$ Hz, 2H), 3.61 (s, 2H), 1.25 (t, $J = 9.2$ Hz, 3H); ^{13}C NMR (100 MHz, CDCl_3) δ 14.4, 41.5, 61.2, 89.3, 89.7, 122.2, 123.4, 128.4, 128.5, 129.5, 131.8, 131.9, 134.5, 171.4; IR (neat) 2981, 1733, 1512, 1252, 1155, 1030, 756, 690 cm^{-1} ; HRMS calcd for $\text{C}_{18}\text{H}_{16}\text{O}_2$ ($\text{M}+\text{H}$) $^+$ 265.1223, found 265.1219.



Ethyl 2-(4-phenethylphenyl)acetate (7).

Ethyl 2-(4-(phenylethynyl)phenyl)acetate (**6**) (433 mg, 1.64 mmol, 1.0 equiv) was dissolved in absolute ethanol (5.0 mL) and Pd/C 5% (43 mg, 10% w/w) was added. The mixture was stirred under a hydrogen atmosphere. After 20 h the mixture was filtered through a pad of celite, and the solvents were removed in vacuo. The residue was purified by Radial PLC (10% EtOAc/hexanes) to afford 237 mg (54%) of **7** as a clear oil. ^1H NMR (400 MHz, CDCl_3) δ 7.06-7.26 (m, 9H), 4.09 (q, $J = 7.2$ Hz, 2H), 3.52 (s, 2H), 2.85 (s, 4H), 1.19 (t, $J = 7.2$ Hz, 3H). **CAS:** 109135-23-1



4-phenethylbenzohydrazide (**8**).

Ethyl 4-phenethylbenzoate (**7**) (0.2465 g, 0.969 mmol, 1.0 equiv) was dissolved in absolute ethanol (4.0 mL). The solution was cooled down to 0 °C and treated dropwise with hydrazine monohydrate (0.23 mL, 4.85 mmol, 5 equiv). The mixture was heated to reflux while stirring. After 20 h in reflux the mixture was allowed to cool down to rt and the solvent was removed *in vacuo*. The solid residue was recrystallized from isopropanol, filtered and dried under vacuum for 20 h to yield 47.9 mg (21 %) of **8** as white round crystals. M.p. 158-160 °C; ¹H NMR (400 MHz, CDCl₃) δ 7.14-7.32 (m, 9H), 6.61 (s, 1H), 3.85 (s, 2H), 3.55 (s, 2H), 2.91 (s, 4H); ¹³C NMR (100 MHz, CDCl₃) δ 37.7, 38.0, 41.8, 126.2, 128.5, 128.6, 129.4, 129.6; IR (neat) 3648, 3029, 2983, 1733, 1510, 1265, 1157, 738 cm⁻¹; HRMS calcd for C₁₆H₁₉N₂O (M+H)⁺ 255.1492, found 255.1419.

A.4 References

- (1) Ramasamy, K.;Kalyanasundaram, S. K.;Shanmugam, P. Sodium Hydrogen Telluride - New Reagent for Hydrogenation of Carbon-Carbon Double-Bonds. *Synthesis*, **1978**, 545-547.
- (2) Ono, N.;Kamimura, A.;Miyake, H.;Hamamoto, I.;Kaji, A. New Synthetic Methods - Conjugate Addition of Alkyl-Groups to Electron Deficient Olefins with Nitroalkanes as Alkyl Anion Equivalents. *J. Organic Chem*, **1985**, *50*, 3692-3698.
- (3) Blomquist, A.;Stahl, R. E.;Smith, B. H.;Meinwald, Y. C. Many-Membered Carbon Rings .23. Restricted Rotation in a Simple Paracyclophane. *J. Org. Chem.*, **1961**, *26*, 1687-&.
- (4) Orrillo, A. G.;Escalante, A. M.;Furlan, R. L. E. Covalent double level dynamic combinatorial libraries: selectively addressable exchange processes. *Chem. Comm.*, **2008**, 5298-5300.
- (5) Demange, L.;Boeglin, D.;Moulin, A.;Mousseaux, D.;Ryan, J.;Berge, G.;Gagne, D.;Heitz, A.;Perrissoud, D.;Locatelli, V.;Torsello, A.;Galleyrand, J. C.;Fehrentz, J. A.;Martinez, J. Synthesis and pharmacological in vitro and in vivo evaluations of novel triazole derivatives as ligands of the ghrelin receptor. 1. *J. Med. Chem.*, **2007**, *50*, 1939-1957.
- (6) Kakimoto, S.;Sekidawa, I.;Yamamoto, K. Antitubercular compounds. VI. Antibacterial activity of acid hydrazides. *Yakugaku Zasshi*, **1955**, *75*, 353-4.
- (7) Williams, D. K.;Comins, D. L.;Whitten, J. L.;Muddiman, D. C. Evaluation of the ALiPHAT Method for PC-IDMS and Correlation of Limits-of-Detection with Nonpolar Surface Area. *J. Am. Soc. Mass. Spectrom.*, **2009**, *20*, 2006-2012.
- (8) Shuford, C. M.;Comins, D. L.;Whitten, J. L.;Burnett, J. C.;Muddiman, D. C. Improving limits of detection for B-type natriuretic peptide using PC-IDMS: An application of the ALiPHAT strategy. *Analyst*, **2010**, *135*, 36-41.
- (9) Bereman, M. S.;Comins, D. L.;Muddiman, D. C. Increasing the hydrophobicity and electrospray response of glycans through derivatization with novel cationic hydrazides. *Chem. Comm.*, **2010**, *46*, 237-239.
- (10) Walker, S. H.;Papas, B. N.;Comins, D. L.;Muddiman, D. C. Interplay of Permanent Charge and Hydrophobicity in the Electrospray Ionization of Glycans. *Anal. Chem.*, **2010**, *82*, 6636-6642.

- (11) Shuford, C. M.;Muddiman, D. C. Capitalizing on the hydrophobic bias of electrospray ionization through chemical modification in mass spectrometry-based proteomics. *Expert Rev. Proteomics*, **2011**, *8*, 317-323.

APPENDIX B

Supplemental Information to CHAPTER 4:

Stable-Isotope Labeled Hydrophobic Hydrazide Reagents for the Relative Quantification of *N*-linked Glycans by Electrospray Ionization Mass Spectrometry

B.1 *N*-linked Glycans Detected from Pooled Human Plasma

Table B.1 – Retention times for light and heavy glycan pairs in human plasma.

Glycan Composition	Retention Time Average (Light) (min)	Retention Time Average (Heavy) (min)	Average Retention Time Difference (s)
Hex ₅ HexNAc ₂	29.26	29.29	3.4
Hex ₃ HexNAc ₄	28.51	28.47	-1.4
Hex ₆ HexNAc ₂	32.48	32.48	-1.0
Hex ₃ HexNAc ₄ Fuc ₁	29.33	29.33	2.6
Hex ₃ HexNAc ₅	29.14	29.16	0.0
Hex ₇ HexNAc ₂	35.86	35.87	-1.8
Hex ₄ HexNAc ₄ Fuc ₁	32.37	32.37	0.0
Hex ₅ HexNAc ₄	34.59	34.53	0.0
Hex ₃ HexNAc ₅ Fuc ₁	30.38	30.36	2.0
Hex ₄ HexNAc ₃ NeuAc ₁ Fuc ₁	35.15	35.11	-1.0
Hex ₆ HexNAc ₂	38.23	38.19	1.0
Hex ₅ HexNAc ₃ NeuAc ₁	35.93	35.91	0.0
Hex ₅ HexNAc ₃ NeuAc ₁	35.93	35.91	2.8
Hex ₄ HexNAc ₅ Fuc ₁	32.96	32.93	0.8
Hex ₅ HexNAc ₅	34.87	34.86	-0.6
Hex ₉ HexNAc ₂	39.85	39.88	0.8
Hex ₅ HexNAc ₄ NeuAc ₁	37.25	37.25	0.0
Hex ₅ HexNAc ₄ NeuAc ₁ Fuc ₁	38.35	38.34	1.0
Hex ₄ HexNAc ₅ NeuAc ₁ Fuc ₁	36.56	36.54	3.0
Hex ₅ HexNAc ₅ NeuAc ₁	37.91	37.92	0.8
Hex ₅ HexNAc ₄ NeuAc ₂	39.41	39.41	2.0
Hex ₅ HexNAc ₅ NeuAc ₁ Fuc ₁	38.69	38.68	1.0
Hex ₆ HexNAc ₅ NeuAc ₁	40.23	40.26	0.8
Hex ₅ HexNAc ₄ NeuAc ₂ Fuc ₁	40.50	40.51	-0.8
Hex ₅ HexNAc ₅ NeuAc ₂ Fuc ₁	40.84	40.79	-1.6
Hex ₆ HexNAc ₅ NeuAc ₃	42.63	42.65	-1.4

The retention times for the ‘light’ and ‘heavy’ glycans detected in human plasma are presented in **Table B.1**. The data presented are average (n=3) retention times for technical replicates. The average retention time difference was calculated by first calculating the retention time difference for each of the replicates. Then, the retention time differences for each of the replicates were averaged. The glycan corrected and uncorrected abundance ratios are listed in **Table B.2**. The data were corrected by using the ratio of the spiked-in internal standard.

Table B.2 – Glycan relative abundance raw and corrected ratios

Glycan Composition	Uncorrected Ratio (H:L) Average (n = 3)	Corrected Ratio (H:L) Average (n=3)
Hex ₇ (Internal Standard)	1.30	1.00
Hex ₅ HexNAC ₂	1.38	1.05
Hex ₃ HexNAC ₄	1.29	0.98
Hex ₆ HexNAC ₂	1.48	1.13
Hex ₃ HexNAC ₄ Fuc ₁	1.31	1.00
Hex ₃ HexNAC ₅	1.27	0.98
Hex ₇ HexNAC ₂	1.39	1.05
Hex ₄ HexNAC ₄ Fuc ₁	1.40	1.08
Hex ₅ HexNAC ₄	1.33	1.03
Hex ₃ HexNAC ₅ Fuc ₁	1.31	1.01
Hex ₄ HexNAC ₃ NeuAc ₁ Fuc ₁	1.31	1.03
Hex ₈ HexNAC ₂	1.40	1.04
Hex ₅ HexNAC ₃ NeuAc ₁	1.40	1.08
Hex ₅ HexNAC ₃ NeuAc ₁	1.34	1.02
Hex ₄ HexNAC ₅ Fuc ₁	1.34	1.05
Hex ₅ HexNAC ₅	1.34	1.02
Hex ₉ HexNAC ₂	1.53	1.14
Hex ₅ HexNAC ₄ NeuAc ₁	1.52	1.13
Hex ₅ HexNAC ₄ NeuAc ₁ Fuc ₁	1.38	1.07
Hex ₄ HexNAC ₅ NeuAc ₁ Fuc ₁	1.41	1.12
Hex ₅ HexNAC ₅ NeuAc ₁	1.22	0.97
Hex ₅ HexNAC ₄ NeuAc ₂	1.33	1.06
Hex ₅ HexNAC ₅ NeuAc ₁ Fuc ₁	1.26	1.02
Hex ₆ HexNAC ₅ NeuAc ₁	1.33	1.03
Hex ₅ HexNAC ₄ NeuAc ₂ Fuc ₁	1.39	1.05
Hex ₅ HexNAC ₅ NeuAc ₂ Fuc ₁	1.55	1.10
Hex ₆ HexNAC ₅ NeuAc ₃	1.66	1.19

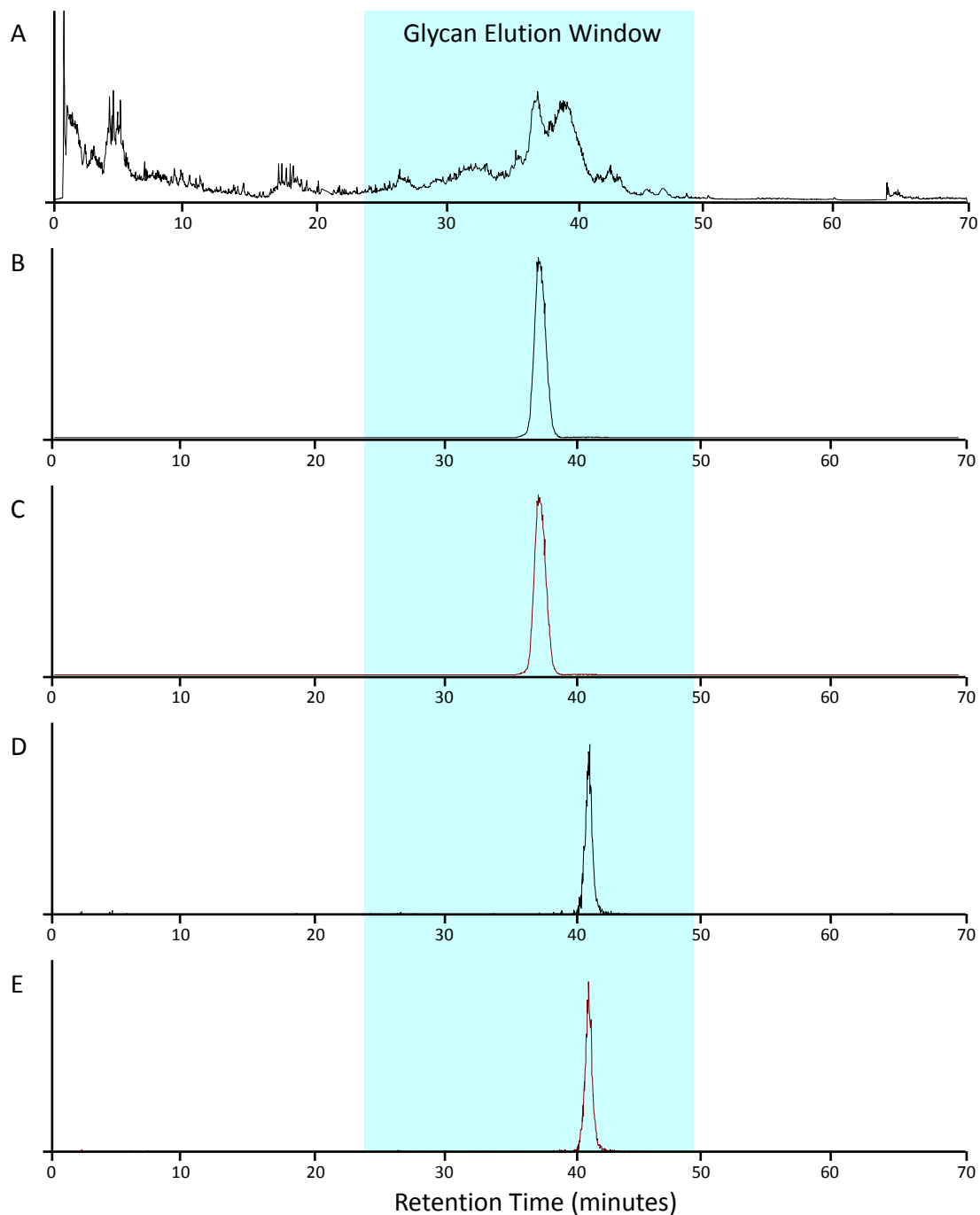
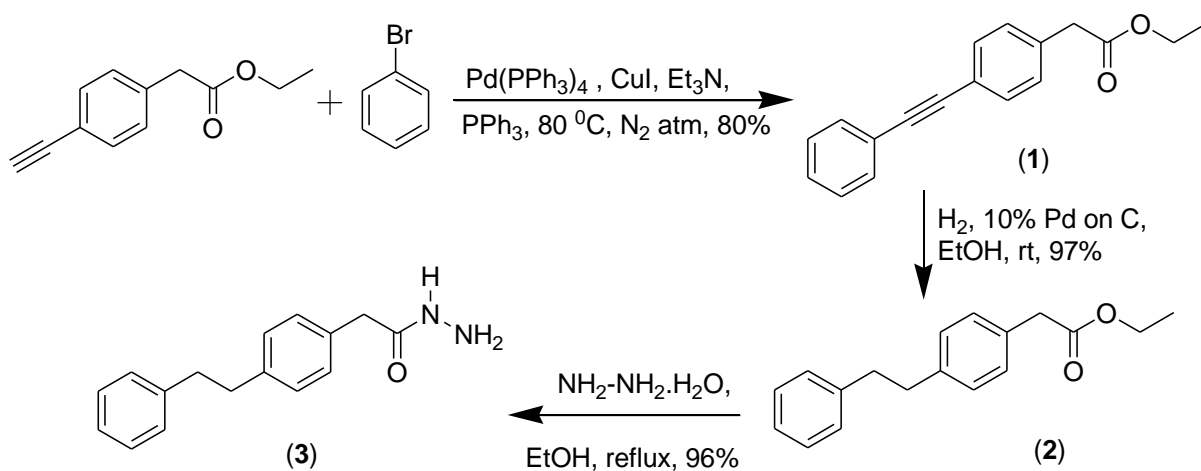


Figure B.1 – Total ion chromatogram for *N*-linked glycans cleaved from pooled human plasma in part A. Parts B and C are the ‘light’ and ‘heavy’ EIC’s of the Hex₅HexNAc₄NeuAc glycan, respectively. Parts D and E are the ‘light’ and ‘heavy’ EIC’s of the Hex₅HexNAc₅NeuAc₂Fuc glycan, respectively.

B.2 Reaction Schemes



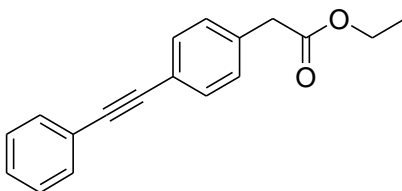
B.2.1 Experimental Section

General. The chemicals; bromobenzene, hydrazine monohydrate, tetrakis(triphenyl phosphine) palladium(0), triphenyl phosphine, copper(I)iodide, triethyl amine, palladium on charcoal were purchased from Sigma-Aldrich. Ethyl-4-ethynylphenylacetate was purchased from Spectra Group. Ltd. Inc. Isotopically labeled bromobenzene ($^{13}\text{C}_6$, 99%) was purchased from Cambridge Isotope Laboratories. Triethyl amine was dried with anhydrous sodium sulphate prior to use and all other chemicals were used as received. The Sonogashira coupling reaction was performed either inside a dry box filled with nitrogen gas or under nitrogen atmosphere. ^1H and ^{13}C NMR data were recorded on Mercury 300 or 400 MHz spectrometers (300 or 400 MHz for ^1H , 75 or 100 MHz for ^{13}C NMR) at room temperature. The chemical shift values were reported relative to TMS ($\delta = 0.00$ ppm) as an internal standard. IR spectra were obtained from JASCO FT/IR-410. Wave

numbers in cm^{-1} are reported for characteristic peaks. Mass spectra were obtained at the NCSU Department of Chemistry Mass Spectrometry Facility using electro spray ionization (ESI) on an Agilent Technologies 6210 LC-TOF mass spectrometer.

B.2.2 Synthesis of Unlabeled Compounds

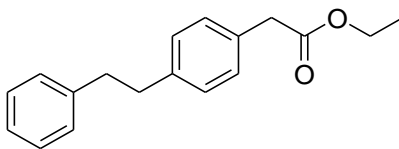
Synthesis of ethyl-2-(4-(2-phenylethynyl) phenyl) acetate, (1)



Bromobenzene (0.464g, 2.848 mmol) was added to ethyl-2-(4-ethynylphenyl)acetate (0.50g, 2.66mmol) taken in a clean and dry vial with a magnetic stir bar. $\text{Pd}(\text{PPh}_3)_4$ (0.150g, 0.129 mmol), PPh_3 (0.120g, 0.457 mmol) and triethyl amine (5.0mL) were added in sequence to the reaction mixture while stirring under nitrogen atmosphere. The reaction mixture was then heated in an oil bath at 80 °C for six hours. The completion of the reaction was determined from FTIR analysis of the reaction mixture by complete disappearance of the sharp absorption band at 3290 cm^{-1} of terminal alkyne C-H. The crude product was extracted from the heterogeneous mixture by hexane and further purified by column chromatography on silica gel using hexane: ethyl acetate mixture (9:1 v/v) to give **1** (0.580g, 80% yield) as clear oil. ^1H NMR (300 MHz, CDCl_3 , δ ppm) 7.53-7.18(m, 9H), 4.14(q, $J = 7.2$ Hz, 2H), 3.60(s, 2H), 1.24(t, $J = 7.2$ Hz, 3H); ^{13}C NMR (75 MHz, CDCl_3 , δ ppm) 171.8, 134.9, 132.3,

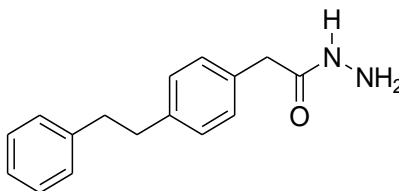
132.2, 129.9, 128.9, 128.8, 123.8, 122.6, 90.08, 89.7, 61.6, 41.9, and 14.8; IR (KBr film, cm^{-1}) 3062, 3033, 2981, 2931, 1735(carbonyl ester).

Synthesis of ethyl-2-(4-phenethylphenyl) acetate, (2)



To the stirring solution of (1), ethyl-2-(4-(2-phenylethynyl) phenyl) acetate, (0.56g, 2.072 mmol) in 5.0 mL absolute ethanol was added 10% Pd on charcoal (0.05g, ~9% w/w). The mixture was stirred under hydrogen atmosphere for four hours. The completion of the reaction was determined by TLC on silica gel plate using mixture of hexane and ethyl acetate (9:1 v/v). The mixture was filtered through a short column of silica gel. The solvent (ethanol) was removed by rotavap and the product was dried under reduced pressure to give **2** (0.551g, 97% yield) as a clear oil. ^1H NMR (300 MHz, CDCl_3 , δ ppm) 7.30-7.12 (m, 9H), 4.14(q, $J = 7.2$ Hz, 2H), 3.57(s, 2H), 2.89(s, 4H), 1.24(t, $J = 7.2$ Hz, 3H); ^{13}C NMR (75 MHz, CDCl_3 , δ ppm) 172.4, 142.3, 141.1, 132.2, 129.8, 129.2, 129.0, 128.9, 126.5, 61.4, 41.6, 38.4, 38.1, 14.8; IR (KBr film, cm^{-1}) 3085, 3058, 3025, 2981, 2931, 2857, 1735(carbonyl ester).

Synthesis of ethyl-2-(4-phenethylphenyl)acetohydrazide, (3)

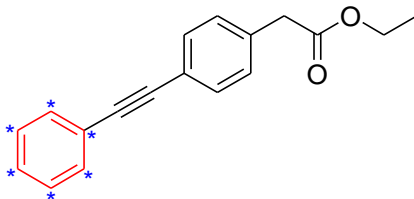


To the stirring solution of ethyl-2-(4-phenethylphenyl) acetate (**2**) (0.535g, 1.95 mmol) in 0.7mL absolute ethanol was added hydrazine hydrate (0.488g, 9.75 mmol) at room temperature under nitrogen atmosphere. The mixture was then refluxed for two hours. The completion of the reaction was determined by TLC on silica gel using mixture of hexane and ethyl acetate (9:1 v/v). Solvent was removed by rotavap and the product was purified by recrystallization from isopropanol. The white crystalline solid was dried under reduced pressure to give **3** (0.487g, 96% yield). ^1H NMR (400 MHz, DMSO- d_6 , δ ppm) 9.22(s, 1H), 7.29-7.12(m, 9H), 4.20 (s, 2H), 3.29 (s, 2H), 2.83 (s, 4H); ^{13}C NMR (100 MHz, DMSO- d_6 , δ ppm) 170.3, 142.2, 140.2, 134.3, 129.4, 129.0, 128.9, 128.8, 126.4, 40.7, 37.7, 37.3; IR (KBr film, cm^{-1}) 3351, 3208, 3080, 3050, 3023, 2981, 2969, 2933, 2911, 2850, 1648, 1619.

B.2.3 Synthesis and characterization of Stable Isotope Labeled (SIL) compounds

**The similar procedure as above was followed except that the SIL bromobenzene ($^{13}\text{C}_6$, 99%) was used as a starting material.

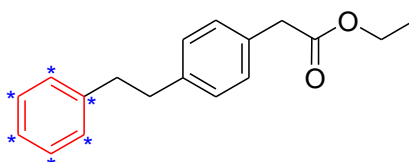
Characterization of **SIL (1); ethyl-2-(4-(2-phenylethynyl) phenyl) acetate**



^1H NMR (400MHz, CDCl_3 , δ ppm) 7.73-7.71(m, br, 1H), 7.53-7.48(m, overlap, 3H), 7.33-7.26 (m, overlap, 3H), 7.15-7.12(m, br, 2H), 4.15(q, $J = 7.2$ Hz, 2H), 3.62(s,

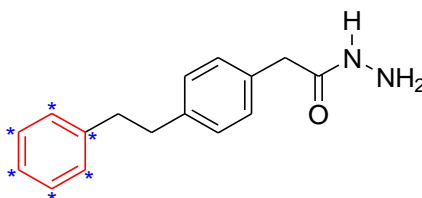
2H), 1.25(t, $J = 7.2$ Hz, 3H); ^{13}C NMR (100 MHz, CDCl_3 , δ ppm) 171.8, 134.9, 132.8-130.7(m overlap), 129.5-127.5(m, overlap), 124.0-122.7(m, overlap), 61.2, 41.5, and 14.4; IR (KBr film, cm^{-1}) 3052, 2981, 1733(carbonyl ester). HRMS: Calculated for $[\text{M}+\text{H}]$: 271.1424; found: 271.1425.

Characterization of **SIL(2); ethyl-2-(4-phenethylphenyl) acetate**



^1H NMR (400 MHz, CDCl_3 , δ ppm) 6.98-7.47 (m, 9H), 4.14 (q, $J = 7.2$ Hz, 2H), 3.58 (s, 2H), 2.90 (s, 4H), 1.25(t, $J = 7.2$ Hz, 3H); ^{13}C NMR (100 MHz, CDCl_3 , δ ppm) 171.8, 142.5-141.3(m, overlap), 132.2, 129.4, 129.3-128.3(m, overlap), 128.0-125.2(m, overlap), 61.0, 41.2, 38.0, 37.7, 14.4; IR (KBr film, cm^{-1}) 3046, 2981, 2929, 2857, 1735(carbonyl ester); HRMS: Calculated for $[\text{M}+\text{H}]$: 275.1737; found: 275.1740

Characterization of **SIL(3); ethyl-2-(4-phenethylphenyl)acetohydrazide**



^1H NMR (400 MHz, DMSO-d_6 , δ ppm) 9.18(s, 1H), 7.46-6.98 (m, 9H), 4.20 (s, 2H), 3.29 (s, 2H), 2.83 (s, 4H); ^{13}C NMR (100 MHz, DMSO-d_6 , δ ppm) 169.6, 142.3-140.5(m, overlap), 139.8, 133.6, 129.0-124.8(m, overlap), 37.2, 36.8, 36.6; IR (KBr

film, cm^{-1}) 3349, 3208, 3048, 3031, 2933, 2911, 2850, 1647, 1618.; HRMS:
Calculated for $[\text{M}+\text{H}]$: 261.1693; found: 261.1693.

APPENDIX C

Supplemental Information to CHAPTER 5:

Systematic Comparison of Reverse Phase and Hydrophilic Interaction Liquid Chromatography Platforms for the Analysis of *N*-linked Glycans

C.1 Supporting Data and Figures

Herein, the supplemental material presents further data to support the results and discussion of the manuscript. In **Figure C.1**, the EIC's for the same 3 glycans (Hex₅, Hex₉, and Hex₁₃) show extremely different retention widths in HILIC, with the largest being over 10 min. The RP EIC's all have retention widths less than 1 min. This is a significant advantage for RP chromatography when moving to more complex samples and analyzing samples with dynamic ranges that are several orders of magnitude, such as plasma.

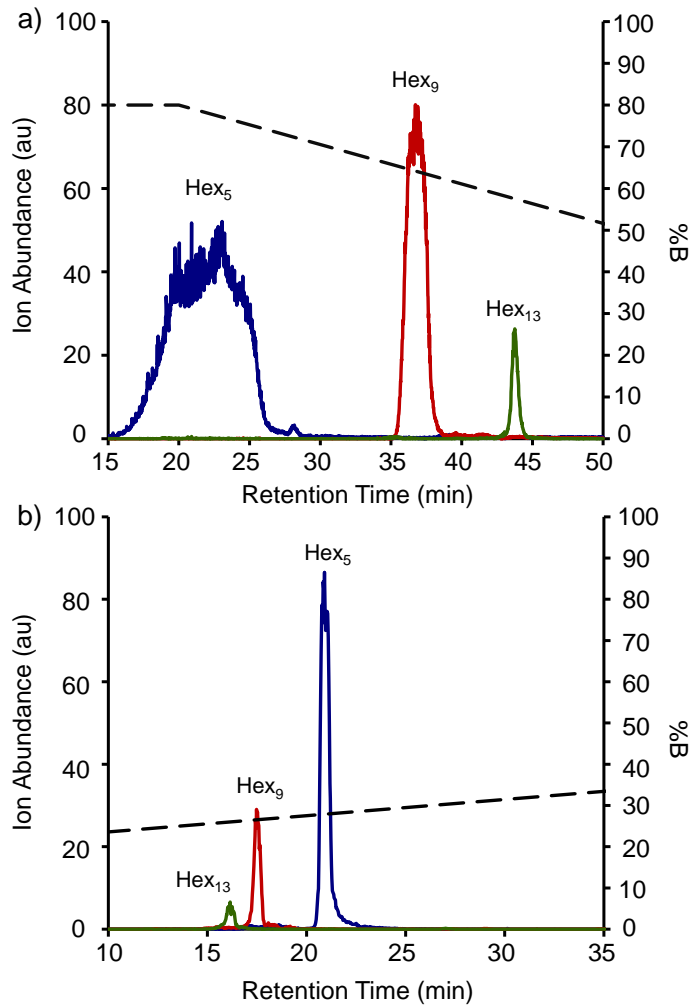


Figure C.1 – Extracted ion chromatograms for 3 example hexose glycan in HILIC (a) and RP chromatography (b).

Table C.1 – RP chromatography peak widths.

Carbohydrate	Peak Width (FWHM)
Hex ₃	1.1
Hex ₄	0.58
Hex ₅	0.5
Hex ₆	0.51
Hex ₇	0.45
Hex ₈	0.49
Hex ₉	0.56
Hex ₁₀	0.36
Hex ₁₁	0.38
Hex ₁₂	0.34
Hex ₁₃	0.43
Hex ₁₄	0.42
Hex ₁₅	0.39
Hex ₁₆	0.4
Hex ₁₇	0.42
Mean	0.488667
Standard Deviation	0.183259

Table C.3 – HILIC peak widths.

Carbohydrate	Peak Width (FWHM)
Hex ₃	1.7
Hex ₄	6.4
Hex ₅	10.37
Hex ₆	5.08
Hex ₇	2.53
Hex ₈	1.61
Hex ₉	1.05
Hex ₁₀	0.83
Hex ₁₁	0.65
Hex ₁₂	0.51
Hex ₁₃	0.82
Hex ₁₄	0.39
Hex ₁₅	0.58
Hex ₁₆	0.34
Hex ₁₇	0.6
Mean	2.230667
Standard Deviation	2.874254

In order to model the partitioning behavior of the derivatized glycans in **Figure 5.4**, the ratio of the hydrophobicity:hydrophilicity was theoretically calculated. Here, the hydrophobicity has been estimated by the nonpolar surface area⁷⁻¹¹ of the tag ($NPSA_{tag}$) and glycan ($NPSA_{glycan}$). However, due to the hydrophilicity of the glycans, the $NPSA_{glycan}$ is assumed to be negligible, leaving only the $NPSA_{tag}$. The hydrophilicity term was estimated by the molecular weight (MW) of the glycan.

$$\frac{Hydrophobicity}{Hydrophilicity} = \frac{NPSA_{tag} + NPSA_{glycan}}{MW} = \frac{NPSA_{Tag}}{MW} = \frac{NPSA}{MW} \quad \text{(Equation C.1)}$$

Table C.3 – List of the *N*-linked glycans cleaved and detected from pooled human plasma using HILIC and RP chromatography.

Glycan Composition	Molecular Weight	HILIC Charge State	RP Charge State	Glycan Composition	Molecular Weight	HILIC Charge State	RP Charge State
Hex ₅ HexNAC ₂	1236.11	1+, 2+	1+, 2+	Hex ₄ HexNAC ₅ Fuc ₁ NeuAc ₁	2120.94	2+	2+
Hex ₄ HexNAC ₃	1277.16	2+	2+	Hex ₅ HexNAC ₅ NeuAc ₁	2136.94	2+	2+, 3+
Hex ₃ HexNAC ₄	1318.21	1+, 2+	2+	Hex ₅ HexNAC ₄ NeuAc ₂	2225.00	2+	2+, 3+
Hex ₆ HexNAC ₂	1398.25	2+	2+	Hex ₅ HexNAC ₅ Fuc ₁ NeuAc ₁	2283.08	2+	2+, 3+
Hex ₅ HexNAC ₃	1439.30	2+	2+	Hex ₆ HexNAC ₅ NeuAc ₁	2299.08	2+	2+, 3+
Hex ₃ HexNAC ₄ Fuc ₁	1464.36	2+	2+	Hex ₅ HexNAC ₄ Fuc ₁ NeuAc ₂	2371.15	2+	2+, 3+
Hex ₄ HexNAC ₄	1480.36	2+	2+	Hex ₅ HexNAC ₅ NeuAc ₂	2428.20	2+	2+, 3+
Hex ₃ HexNAC ₅	1521.41	2+	2+	Hex ₆ HexNAC ₅ Fuc ₁ NeuAc ₁	2445.22	N/A	2+, 3+
Hex ₇ HexNAC ₂	1560.39	2+	2+	Hex ₅ HexNAC ₅ Fuc ₁ NeuAc ₂	2574.34	2+, 3+	2+, 3+
Hex ₄ HexNAC ₃ NeuAc ₁	1568.42	2+	2+	Hex ₆ HexNAC ₅ NeuAc ₂	2590.34	2+, 3+	2+, 3+
Hex ₆ HexNAC ₃	1601.44	2+	2+	Hex ₇ HexNAC ₆ NeuAc ₁	2664.42	N/A	2+, 3+
Hex ₄ HexNAC ₄ Fuc ₁	1626.50	2+	2+	Hex ₆ HexNAC ₅ Fuc ₁ NeuAc ₂	2736.48	2+, 3+	2+, 3+
Hex ₅ HexNAC ₄	1642.50	2+	2+	Hex ₇ HexNAC ₆ Fuc ₁ NeuAc ₁	2810.56	N/A	2+, 3+
Hex ₃ HexNAC ₅ Fuc ₁	1667.55	2+	2+	Hex ₆ HexNAC ₅ NeuAc ₃	2881.59	2+, 3+	2+, 3+
Hex ₄ HexNAC ₅	1683.55	2+	2+	Hex ₇ HexNAC ₆ NeuAc ₂	2955.67	3+	3+
Hex ₄ HexNAC ₃ Fuc ₁ NeuAc ₁	1714.56	2+	2+	Hex ₆ HexNAC ₅ Fuc ₁ NeuAc ₃	3027.73	2+, 3+	2+, 3+
Hex ₈ HexNAC ₂	1722.53	2+	2+	Hex ₇ HexNAC ₆ Fuc ₁ NeuAc ₂	3101.81	N/A	3+
Hex ₅ HexNAC ₃ NeuAc ₁	1730.56	2+	2+	Hex ₆ HexNAC ₅ Fuc ₂ NeuAc ₃	3173.87	N/A	3+
Hex ₄ HexNAC ₄ NeuAc ₁	1771.61	2+	2+	Hex ₇ HexNAC ₆ NeuAc ₃	3246.93	N/A	3+
Hex ₅ HexNAC ₄ Fuc ₁	1788.64	2+	2+, 3+	Hex ₆ HexNAC ₇ NeuAc ₂	3321.00	N/A	3+
Hex ₄ HexNAC ₅ Fuc ₁	1829.69	2+	2+, 3+	Hex ₇ HexNAC ₆ Fuc ₁ NeuAc ₃	3393.07	N/A	3+
Hex ₅ HexNAC ₅	1845.69	2+	2+	Hex ₆ HexNAC ₇ Fuc ₁ NeuAc ₂	3467.15	N/A	3+
Hex ₉ HexNAC ₂	1884.67	2+	2+	Hex ₇ HexNAC ₆ NeuAc ₄	3538.18	N/A	3+
Hex ₆ HexNAC ₃ NeuAc ₁	1892.70	2+	2+	Hex ₆ HexNAC ₇ NeuAc ₃	3612.26	N/A	3+
Hex ₄ HexNAC ₄ Fuc ₁ NeuAc ₁	1917.75	N/A	2+, 3+	Hex ₇ HexNAC ₆ Fuc ₁ NeuAc ₄	3684.32	N/A	3+
Hex ₅ HexNAC ₄ NeuAc ₁	1933.75	2+	2+, 3+	Hex ₆ HexNAC ₇ Fuc ₁ NeuAc ₃	3758.40	N/A	3+
Hex ₄ HexNAC ₅ NeuAc ₁	1974.80	2+	2+, 3+	Hex ₇ HexNAC ₆ Fuc ₂ NeuAc ₄	3830.46	N/A	3+
Hex ₅ HexNAC ₅ Fuc ₁	1991.83	2+	2+, 3+	Hex ₆ HexNAC ₇ NeuAc ₄	3903.51	N/A	3+
Hex ₁₀ HexNAC ₂	2045.81	2+	2+	Hex ₉ HexNAC ₈ NeuAc ₃	3977.59	N/A	3+
Hex ₅ HexNAC ₄ Fuc ₁ NeuAc ₁	2079.89	2+	2+, 3+	Hex ₆ HexNAC ₇ Fuc ₁ NeuAc ₄	4049.65	N/A	3+

Appendix D

Supplemental Information to Chapter 7

Individuality Normalization when Labeling with Isotopic Glycan Hydrazide Tags (INLIGHT): A Novel Glycan Relative Quantification Strategy

D.1 Glycan Database

Herein, the supplemental material presents further data to detail the processing method used to reproducibly apply the INLIGHT strategy to multiple samples. **Table 1** displays the *N*-linked glycan compositions (generated previously from pooled plasma samples) used in the Xcalibur processing method. Additionally, the *m/z* values for all charge states in both the light and heavy samples that have been detected are listed.

Table D.1 – Glycan database and previously detected charge states.

Glycan Composition	2+ charge state Nat	2+ charge state SIL	3+ Charge State Nat	3+ Charge state SIL
H ₅ N ₂	736.2898126	739.2998826	N/A	N/A
H ₄ N ₃	756.8028126	759.8128826	N/A	N/A
H ₃ N ₄	777.3163126	780.3263826	N/A	N/A
H ₆ N ₂	817.3163126	820.3263826	N/A	N/A
H ₅ N ₃	837.8293126	840.8393826	N/A	N/A
H ₃ N ₄ F ₁	850.3453126	853.3553826	N/A	N/A
H ₄ N ₄	858.3428126	861.3528826	N/A	N/A
H ₃ N ₅	878.8558126	881.8658826	N/A	N/A
H ₇ N ₂	898.3428126	901.3528826	N/A	N/A
H ₄ N ₃ A ₁	902.3508126	905.3608826	N/A	N/A
H ₆ N ₃	918.8558126	921.8658826	N/A	N/A
H ₄ N ₄ F ₁	931.3718126	934.3818826	N/A	N/A
H ₅ N ₄	939.3693126	942.3793826	N/A	N/A
H ₃ N ₅ F ₁	951.8848126	954.8948826	N/A	N/A
H ₄ N ₅	959.8823126	962.8923826	N/A	N/A
H ₄ N ₃ F ₁ A ₁	975.3798126	978.3898826	N/A	N/A
H ₈ N ₂	979.3688126	982.3788826	N/A	N/A
H ₅ N ₃ A ₁	983.3773126	986.3873826	N/A	N/A
H ₄ N ₄ A ₁	1003.890313	1006.900383	N/A	N/A
H ₅ N ₄ F ₁	1012.398313	1015.408383	N/A	N/A
H ₄ N ₅ F ₁	1032.911313	1035.921383	N/A	N/A
H ₅ N ₅	1040.908813	1043.918883	N/A	N/A
H ₉ N ₂	1060.395313	1063.405383	N/A	N/A
H ₆ N ₃ A ₁	1064.403813	1067.413883	N/A	N/A
H ₄ N ₄ F ₁ A ₁	1076.919313	1079.929383	718.2819672	720.2886672
H ₅ N ₄ A ₁	1084.916813	1087.926883	723.6136339	725.6203339
H ₅ N ₄ F ₂	1085.427313	1088.437383	N/A	N/A
H ₄ N ₅ A ₁	1105.430313	1108.440383	737.2893005	739.2960005
H ₅ N ₅ F ₁	1113.937813	1116.947883	742.9609672	744.9676672
H ₅ N ₄ F ₁ A ₁	1157.945813	1160.955883	772.2996339	774.3063339
H ₄ N ₅ F ₁ A ₁	1178.59313	1181.6032	785.9753005	787.9820005
H ₅ N ₅ A ₁	1186.456313	1189.466383	791.3066339	793.3133339
H ₁₀ N ₂	1141.416	1144.42607	N/A	N/A
H ₅ N ₄ A ₂	1230.464813	1233.474883	820.6456339	822.6523339
H ₅ N ₅ F ₁ A ₁	1259.485813	1262.495883	839.9929672	841.9996672
H ₆ N ₅ A ₁	1267.482813	1270.492883	845.3243005	847.3310005
H ₅ N ₄ F ₁ A ₂	1303.493313	1306.503383	869.3313005	871.3380005
H ₅ N ₅ A ₂	N/A	N/A	888.3386339	890.3453339

Table D.1 – continued

H ₆ N ₅ F ₁ A ₁	N/A	N/A	894.0103005	896.0170005
H ₅ N ₅ F ₁ A ₂	1405.033313	1408.043383	937.0246339	939.0313339
H ₆ N ₅ A ₂	1413.030813	1416.040883	942.3563005	944.3630005
H ₇ N ₆ A ₁	N/A	N/A	967.0353005	969.0420005
H ₆ N ₅ F ₁ A ₂	N/A	N/A	991.0423005	993.0490005
H ₇ N ₆ F ₁ A ₁	N/A	N/A	1015.721301	1017.728001
H ₆ N ₅ A ₃	1558.578313	1561.588383	1039.387967	1041.394667
H ₇ N ₆ A ₂	N/A	N/A	1064.066967	1066.073667
H ₆ N ₅ F ₁ A ₃	1631.607313	1634.617383	1088.073967	1090.080667
H ₇ N ₆ F ₁ A ₂	N/A	N/A	1112.752967	1114.759667
H ₆ N ₅ F ₂ A ₃	N/A	N/A	1136.759967	1138.766667
H ₇ N ₆ A ₃	N/A	N/A	1161.098634	1163.105334
H ₈ N ₇ A ₂	N/A	N/A	1185.777634	1187.784334
H ₇ N ₆ F ₁ A ₃	N/A	N/A	1209.784634	1211.791334
H ₈ N ₇ F ₁ A ₂	N/A	N/A	1234.463634	1236.470334
H ₇ N ₆ A ₄	N/A	N/A	1258.130634	1260.137334
H ₈ N ₇ A ₃	N/A	N/A	1282.809634	1284.816334
H ₇ N ₆ F ₁ A ₄	N/A	N/A	1306.816634	1308.823334
H ₈ N ₇ F ₁ A ₃	N/A	N/A	1331.495634	1333.502334
H ₇ N ₆ F ₂ A ₄	N/A	N/A	1355.502634	1357.509334
H ₈ N ₇ A ₄	N/A	N/A	1379.841301	1381.848001
H ₉ N ₈ A ₃	N/A	N/A	1404.520301	1406.527001
H ₈ N ₇ F ₁ A ₄	N/A	N/A	1428.527301	1430.534001
H ₈ N ₇ F ₂ A ₄	N/A	N/A	1477.213301	1479.220001
H ₉ N ₈ A ₄	N/A	N/A	1501.551967	1503.558667
H ₉ N ₈ F ₁ A ₄	N/A	N/A	1550.237967	1552.244667
H ₁₀ N ₉ F ₁ A ₃	N/A	N/A	1574.916967	1576.923667
H ₉ N ₈ A ₅	N/A	N/A	1598.583967	1600.590667
H ₁₀ N ₉ A ₄	N/A	N/A	1623.262967	1625.269667
H ₉ N ₈ F ₁ A ₅	N/A	N/A	1647.269967	1649.276667
H ₁₀ N ₉ F ₁ A ₄	N/A	N/A	1671.948967	1673.955667
H ₉ N ₈ F ₂ A ₅	N/A	N/A	1695.955967	1697.962667
H ₁₀ N ₉ A ₅	N/A	N/A	1720.294634	1722.301334

H – Hexose; N – *N*-acetylhexosamine; F – Fucose; A – *N*-acetylneuraminic acid.

D.2 Processing Method Details

This processing method was developed to make analyzing data for N-linked glycans more reproducible. This method uses Xcalibur software v.2.2 and MATLAB.

D.2.1 Before you begin

- 1) Generate a database or list of N-linked glycans with accurate calculated masses to 5 decimal places. If these glycans are derivatized, include this in the glycan mass. Calculate what the 2⁺ and 3⁺ *m/z* values will be.
- 2) If this is a stable-isotope relative quantification experiment, have both the *m/z* of the heavy-derivatized and light-derivatized glycan.

D.2.2 Getting Started

1. Open Xcalibur and click on Processing Setup (**Figure 1**)

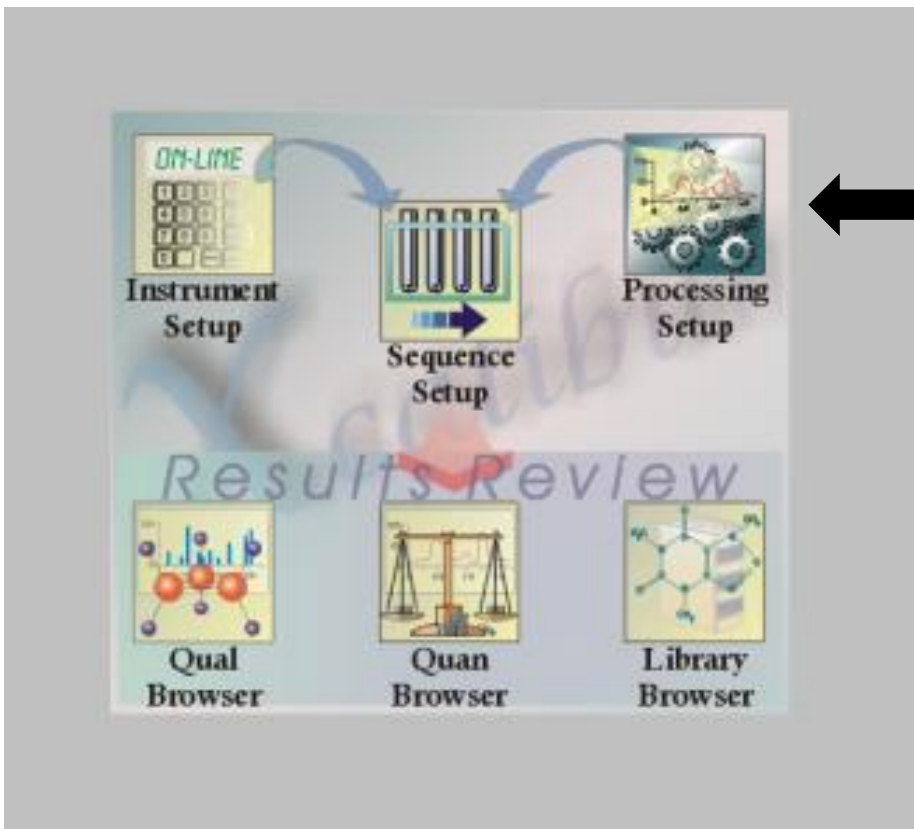


Figure D.1 – Xcalibur home page.

2. The following window will appear (Figure D.2).

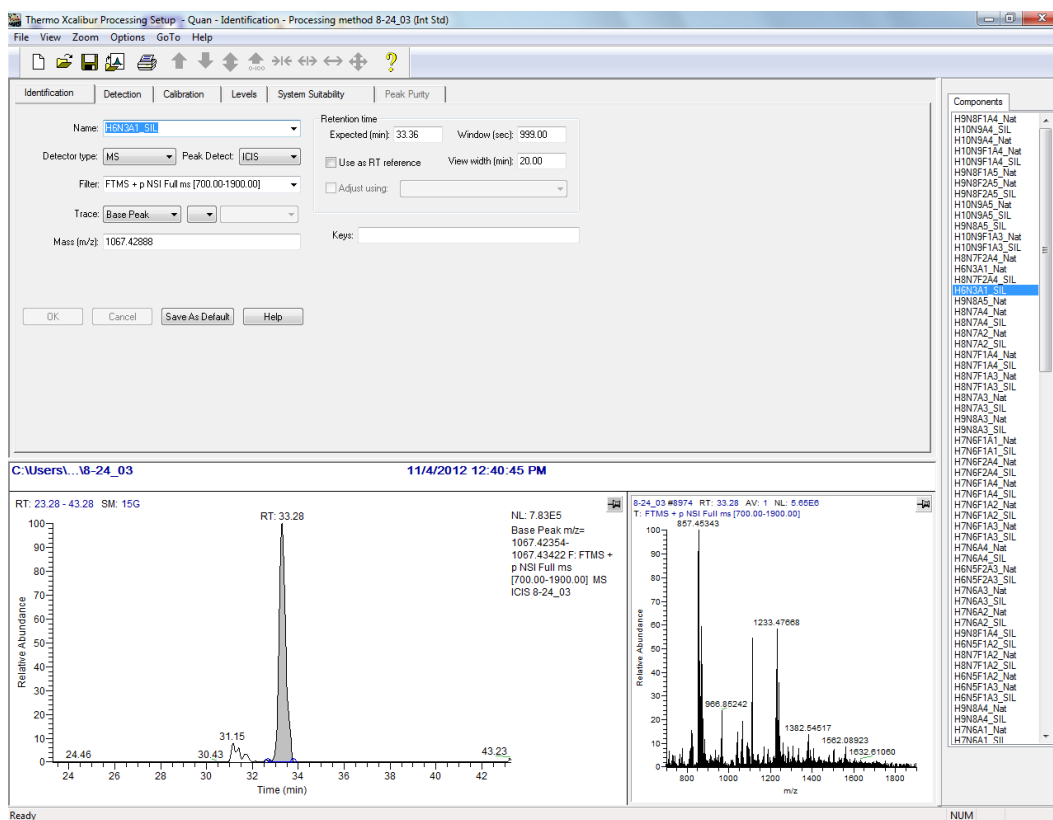


Figure D.2 – Processing method setup window.

3. Begin by adding glycans to the list on the right hand side by following the next steps.

A. Under 'Name' click on 'New' and type the name of your glycan. The following code was used:

- a. H = Hexose (Hex)
- b. N = N-acetylhexoseamine (HexNAc)
- c. F = Fucose (Fuc)
- d. A = N-acetylneuraminic acid (NeuAc)

B. The glycan tagged light should be named as follows:

Name_Nat

C. The glycan tagged heavy should be named as follows:

Name_SIL

D. For Example: H6N5_Nat and H6N5_SIL

4. Enter the following in the identification tab for each glycan:

Detector type = MS

Peak Detection = ICIS

Filter= FTMS + p NSI Full ms [700-1900] - (this must be identical to your scan header)

Trace = Base Peak

Mass (m/z) = respective mass for the glycan

Retention time:

Expected = where the peak is in the spectrum

Window = 999.00

View Width = 40.00

*If you need to check where the glycan elutes, you can do so in the spectrum to the right by pinning it and then scanning the data.

5. Detection:

Click on the detection tab at the top.

ICIS Peak Integration:

-Smoothing points = 15

-Baseline Window = 100

-Area noise factor = 5

-Peak noise factor = 10

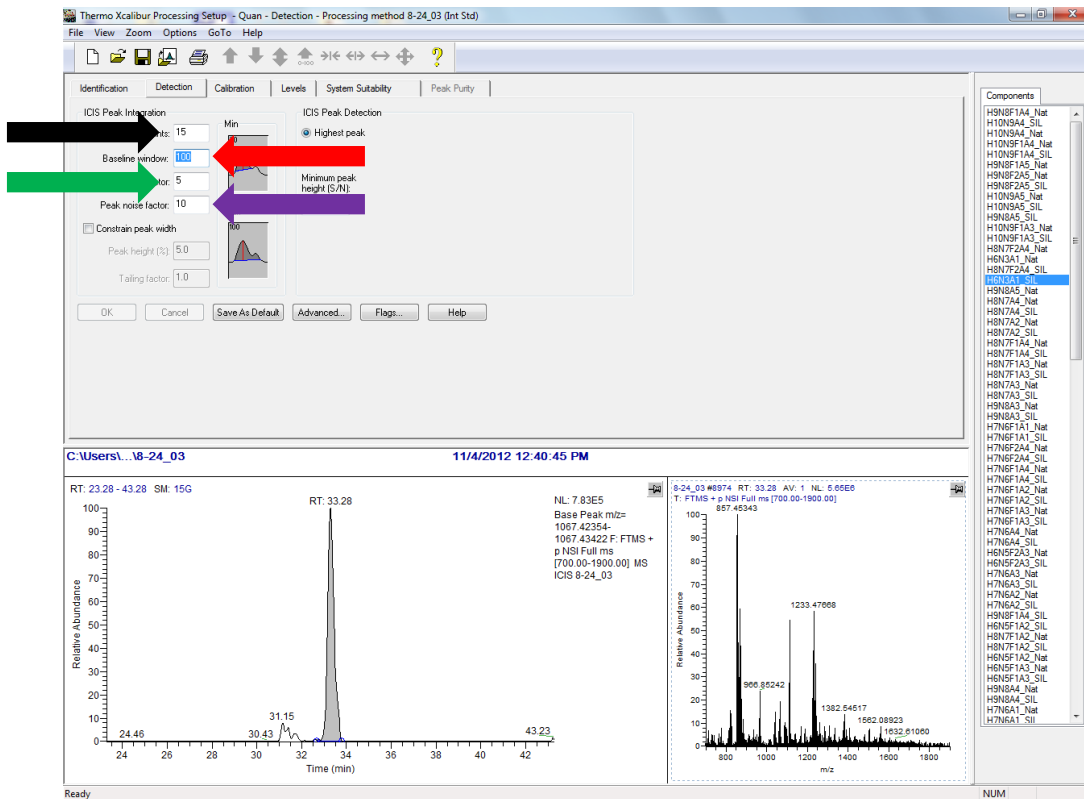


Figure D.3 – Detection tab and integration parameters.

6. Calibration:

-Click on the calibration tab next.

-For the Name_SIL glycans:

-ISTD (Internal Standard) should be checked

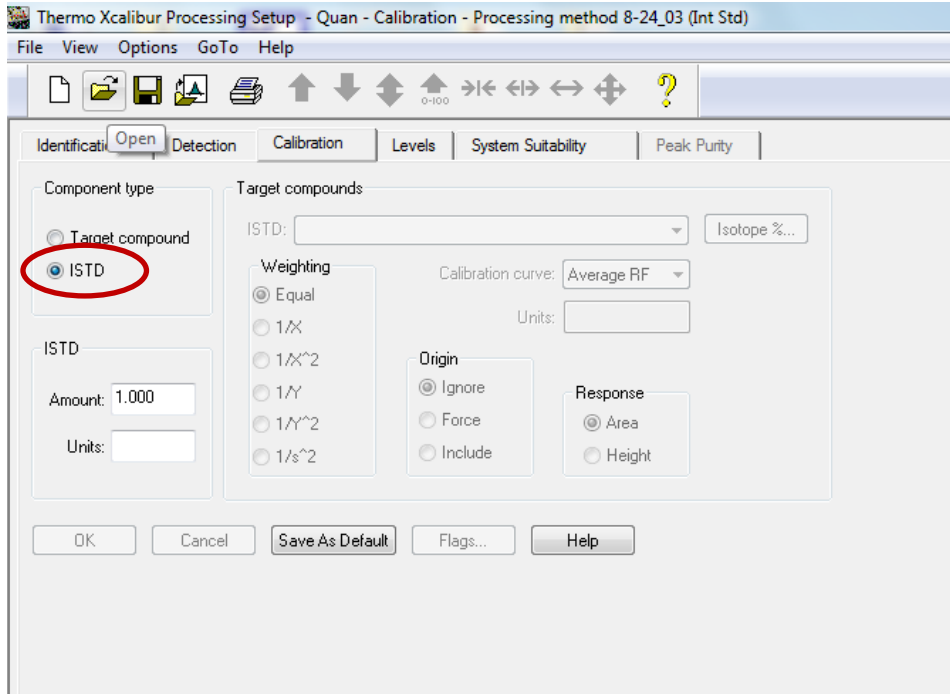


Figure D.4 – Calibration tab parameters.

-For the Name_Nat glycans:

-Target compound should be checked

-Under ISTD drop down box, select the matching Name_SIL glycan

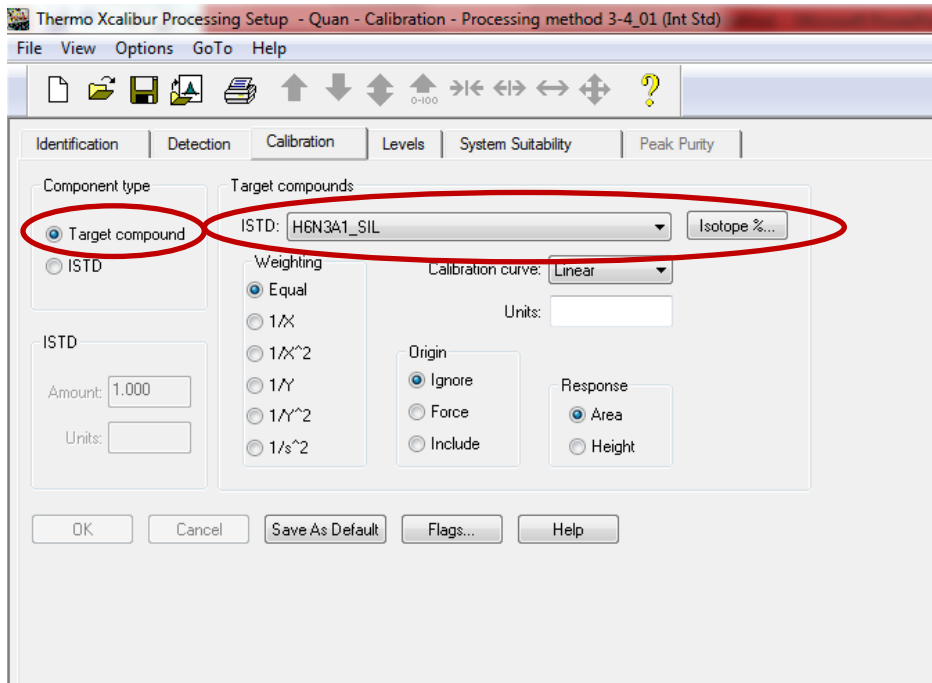


Figure D.5 – Calibration tab target compounds.

7. Levels:

-Click on the levels tab:

-Cal level 1 = 3

-Cal level 2 = 5

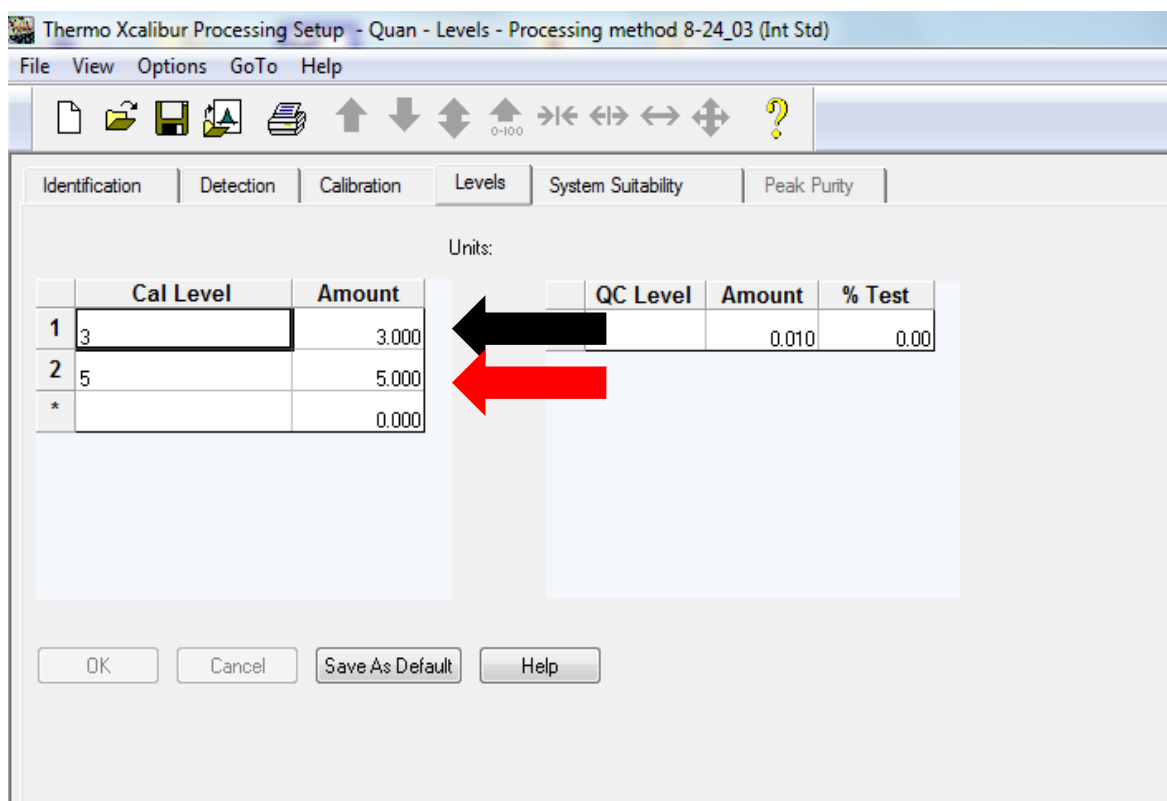


Figure D.6 – Levels tab parameters.

8. Save the processing method

-Because each processing method includes retention times for each glycan, it is advised to generate a processing method for each instrument method and LC gradient.

*A processing method must be saved for each raw file. For example if you ran in triplicate and your samples were named 1-2_01, 1-2_02 and 1-2_03, you would need to open each of these raw files in the processing method using 'File', 'Open Raw File', and then saving the processing method as something different for each

file. The following file name examples were used here: 'Processing method 1-2_01, Processing method 1-2_02, and Processing method 1-2_03'. This is important for the next step.

6.2.3 How to Process

A processing method has now been generated for each file that is to be processed.

1. Return to the Xcalibur roadmap and click on sequence setup.

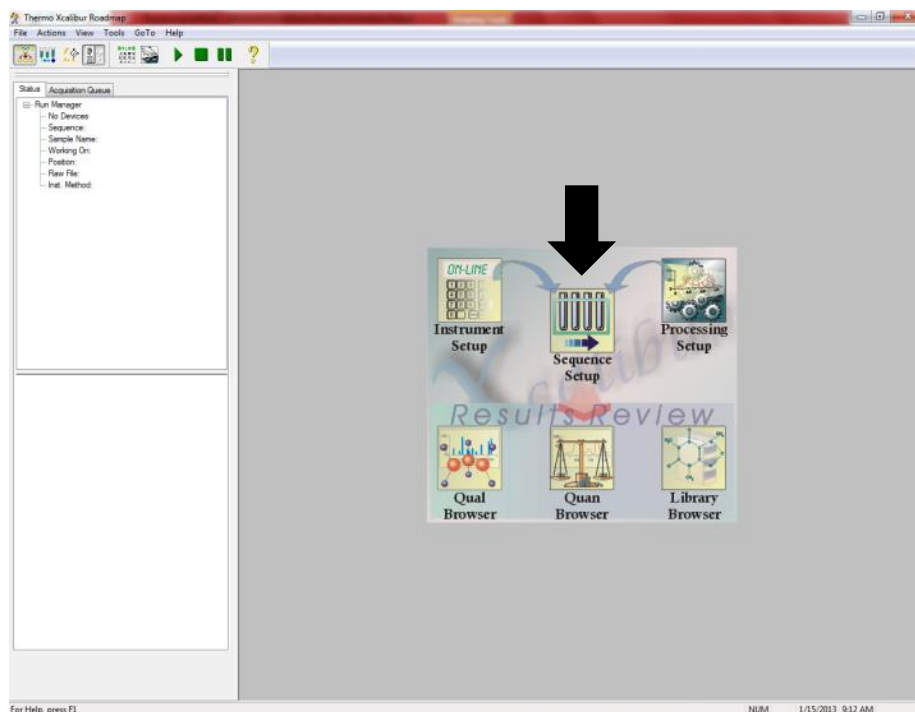


Figure D.7 – Xcalibur sequence and processing.

The following window will appear:

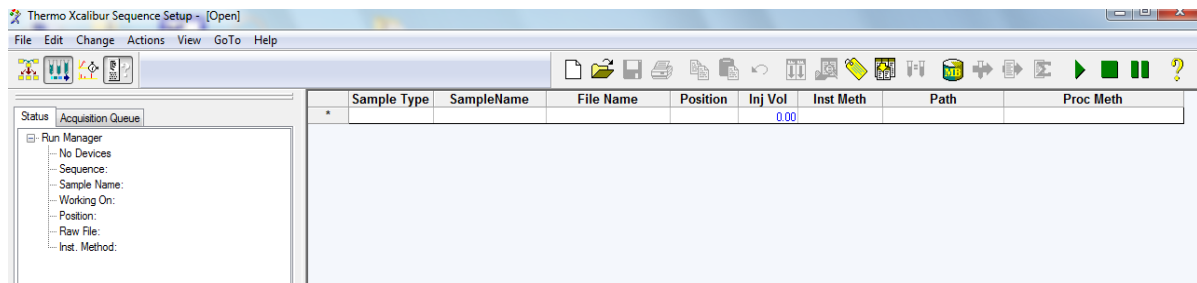


Figure D.8 – Xcalibur sequence setup.

2. Enter the following information:

-Sample Type = Unknown

-Sample Name = exact name of your file (i.e. 8-24_03)

-File Name = name of the file being processed (i.e. 8-24_03)

*The sample name and file name should match.

-Position = 1

-Inj. Volume = 10.00

-Instrument method = 'blank'

-Path = the location of the file (i.e C:/Users...etc)

-Processing Method = the exact name of the processing method you just created with the raw file (i.e. Processing method 8-24_03)

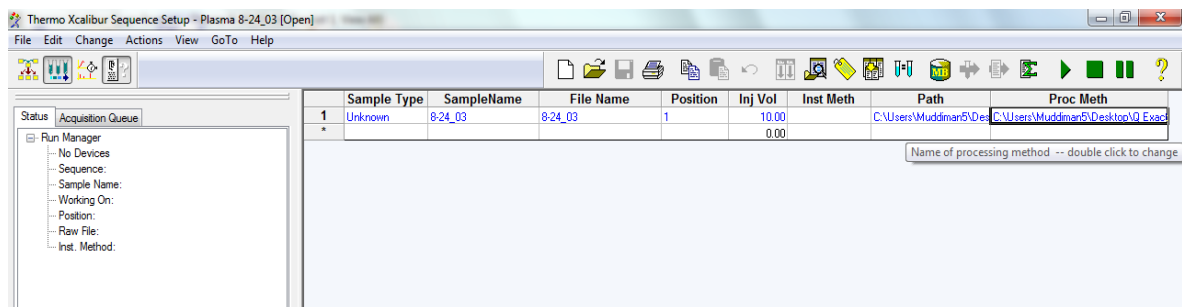


Figure D.9 – Xcalibur sequence example.

3. Once everything has been entered into the sequence, go to file and save as. Save as a file name directly related to the sample being processed. (e.g. Plasma 8-24_03)

-Click on 'actions' and select 'batch reprocess'

4. Return to the Xcalibur roadmap and select Quan Browser

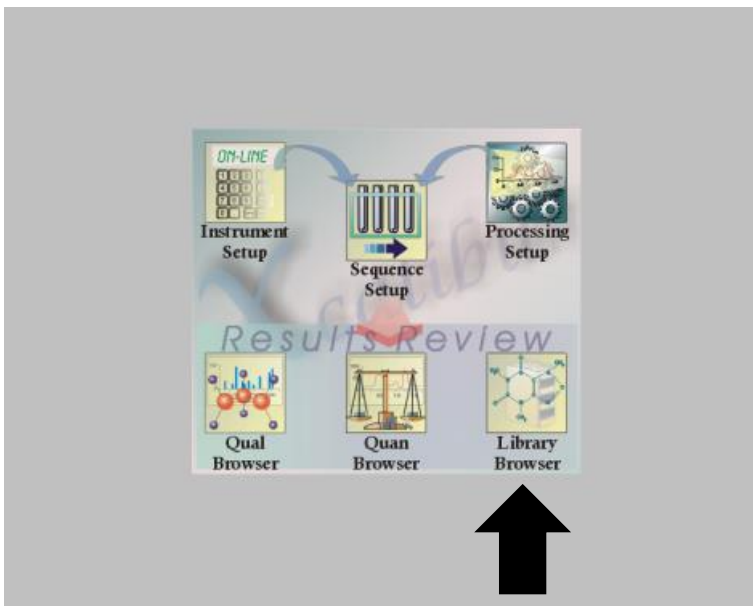


Figure D.10 – View processed data in Xcalibur Quan Browser.

-A box will open for you to select the file you just saved (i.e. Plasma 8-24_03)

-Click Open

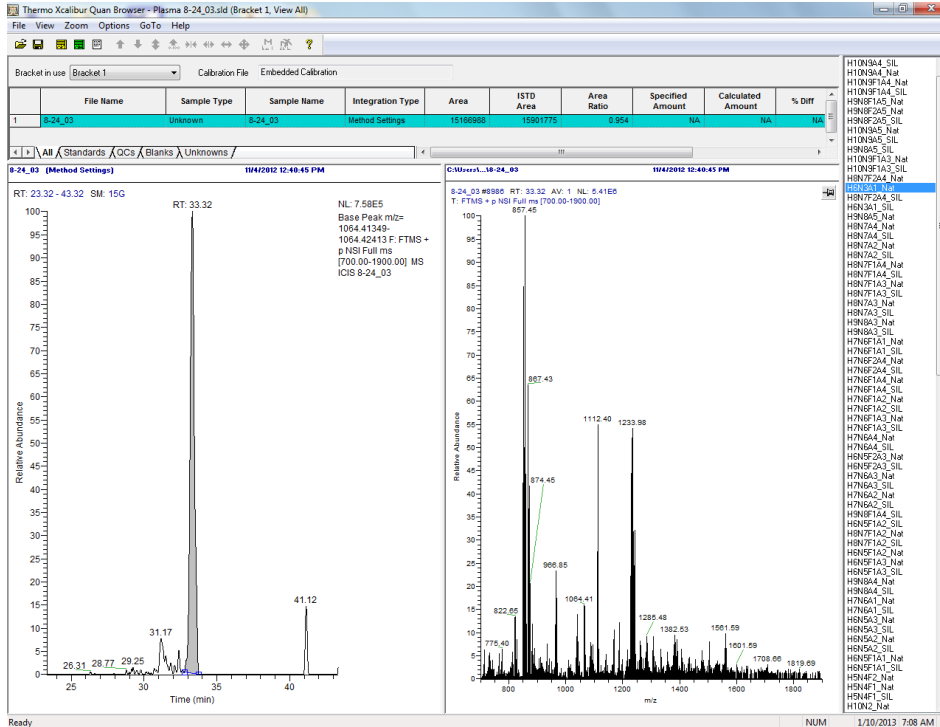


Figure D.11 – Area selection for each glycan extracted ion chromatogram.

-Use the boxes to capture the correct peak in the extracted ion chromatogram. Adjust accordingly for each of the glycans in the list to the right.

*If the peak is not perfect and you're not sure exactly which peak, or part of the peak includes your glycan, click on the green box in the toolbar to display your spectrum in the box to the right of your peak areas. You can then pin it and scroll to find the glycan. You can also select particular points within the peak on the left to determine if the glycan is present in that spot.

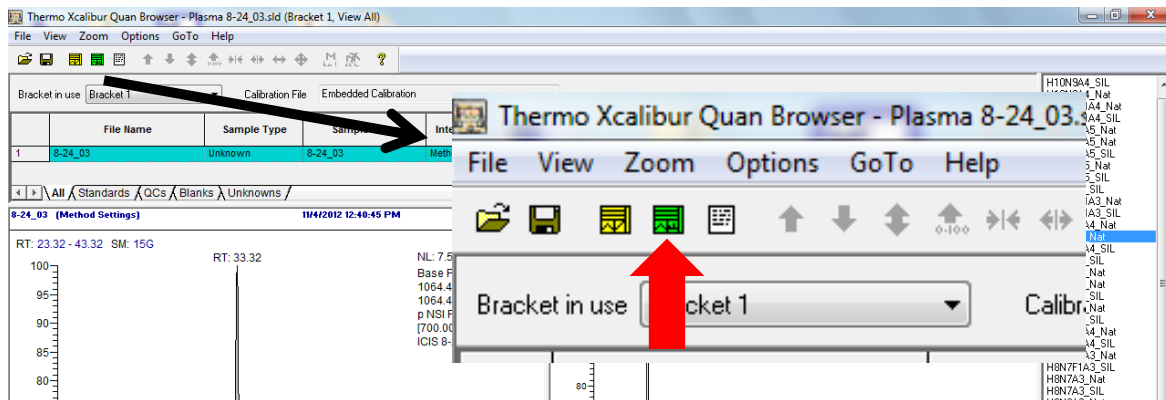


Figure D.12 – View spectra of the extracted ion chromatogram.

-Once you have finished, click file and save as. Save this file.

-Next click 'file' then 'export data to excel' then click 'export short excel report'

D.2.4 Extracting the Data to Excel

1. Open the MATLAB file called “processing method converter” *This is available by emailing the authors.*

-You must have a file such as Data List that contains all of the glycans so that peak areas can be extracted. It should look similar to the following:

	A	B	C	D	E	F	G	H	I	J	K	L	M	N	O	P	Q	R
1	Glycan Composition	Nat	SIL															
2	H5N2																	
3	H4N3																	
4	H3N4																	
5	H6N2																	
6	H5N3																	
7	H3N4F1																	
8	H4N4																	
9	H3N5																	
10	H7N2																	
11	H4N3A1																	
12	H6N3																	
13	H4N4F1																	
14	H5N4																	
15	H3N5F1																	
16	H4N5																	
17	H4N3F1A1																	
18	H8N2																	
19	H5N3A1																	
20	H4N4A1																	
21	H5N4F1																	
22	H4N5F1																	
23	H5N5																	
24	H9N2																	
25	H6N3A1																	
26	H4N4F1A1																	
27	H5N4A1																	
28	H5N4F2																	
29	H4N5A1																	
30	H5N5F1																	
31	H5N4F1A1																	
32	H4N5F1A1																	
33	H5N5A1																	
34	H10N2																	
35	H5N4A2																	
36	H5N5F1A1																	

Figure D.13 – Data list for MATLAB extraction program.

*The MATLAB program will automatically take all of the glycans labeled Name_Nat and place them in column B and all of the glycans labeled Name_SIL and place them in column C. It is very important that the glycans were named exactly in this way. The order of the list does not matter.

2. The processing method converter file **MUST** be in the folder where the short excel report is as well as the data list.

-Under **list_filename**: you should put the file name of the data list (i.e. data list 1.xlsx).

-Under **data_filename**: Plasma 8-24_03_Short.XLS (this is the filename you just created from the short report).

-Under **save_filename**: type what you would like the results file to be saved as (e.g. Plasma 8-24_03_results.xls).

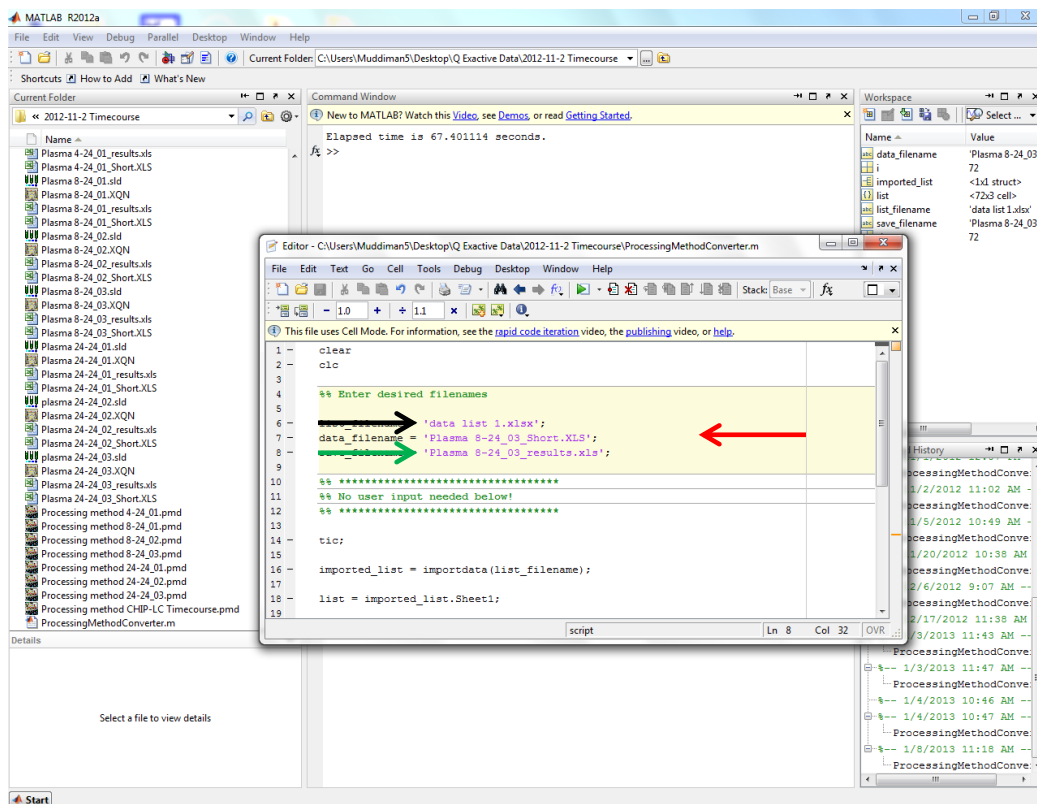


Figure D.14 - Input data into MATLAB.

-Press the **play button** at the top of the editor window.

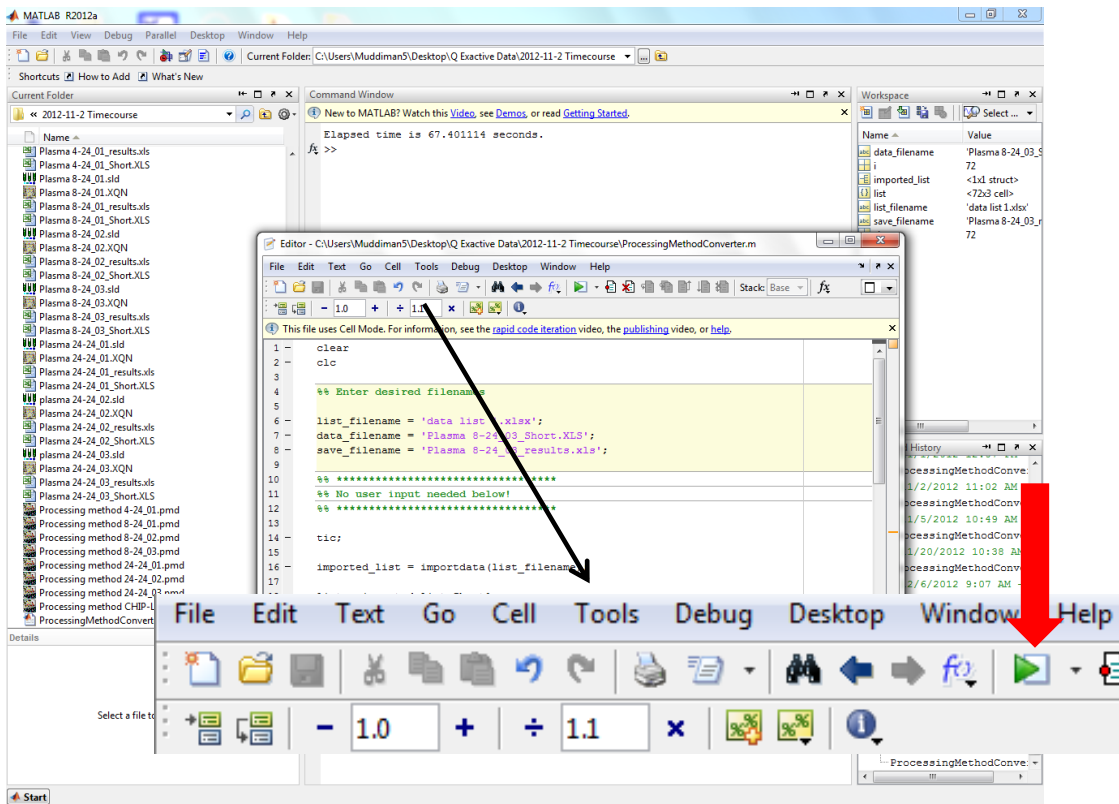


Figure D.15 – Execute MATLAB program for data extraction.

-Once the file has finished extracting the data an Elapsed time will appear in the main MATLAB window. You can then open your results file and manipulate the data as needed.

APPENDIX E

Glycan Sample Preparation Detailed Protocol

E.1 Reagents and Samples

N-linked Glycan Analysis from Plasma:

Batch Name:

Start Time/Date:

Reagents and Materials:

<u>Name</u>	<u>Manufacturer</u>	<u>P/N</u>	<u>L/N</u>
PNGase F (Glycerol Free)	New England Biolabs	P0705L	
Pooled Human Plasma	Sigma Aldrich		
Dithiothreitol	Sigma Aldrich		
Ammonium Bicarbonate	Sigma Aldrich		
Maltoheptaose	Sigma Aldrich		
Formic Acid	Sigma Aldrich		
Acetonitrile (HPLC)	Burdick & Johnson		
Water (HPLC)	Burdick & Johnson		
Methanol (HPLC)	Burdick & Johnson		
Acetic Acid			
Trifluoroacetic Acid	Sigma Aldrich		
Ethyl Alcohol			
Graphitized Carbon Cartridge	Alltech		
Horseshoe Peroxidase (HRP)	Sigma Aldrich		

Samples:

<i>Name</i>	<i>Description</i>
1)	
2)	
3)	
4)	
5)	
6)	
7)	
8)	
9)	
10)	
11)	
12)	

E.2 Sample PreparationPreparation of Plasma Samples and Addition of Internal Standard:

Start Time/Date:

Prepare 50- μ L aliquots of plasma.
Add 100 μ L of Horseradish Peroxidase (2 mg/mL)
Add 5 μ L of Maltoheptaose (0.2 mg/mL)

Denaturation and Digestion of Plasma:

Start Time/Date:

Turn on heat block to 95°C ~1 hr before beginning sample preparation.
Add 41 μ L of 100 mM Ammonium Bicarbonate
Pipette up and down, vortex, and centrifuge.

Denature: Add 2 μ L of 1M dithiothreitol (DTT) to each sample making the final concentration 10 mM DTT.

Incubate at 95°C for 15 s followed by immediate incubation at 25°C for 15 s.
Repeat previous step 3 additional times.

Vortex, centrifuge.

Digest: Add 2 µL (1000 Units – NEB; 15.3 mUnits – IUB) of NEB PNGase F to each sample.

Vortex, centrifuge.

Incubate samples for 18 hours at 37°C

Start Time/Date: _____

End Time/Date: _____

N-linked Glycan Extraction – Ethanol Precipitation and Solid Phase Extraction:

Start Time/Date:

Ethanol Precipitation: Remove samples from 37°C incubator and quench the reaction with 800 µL of chilled ethanol.

Vortex, centrifuge.

Incubate at -80°C for 1 hr.

Start Time/Date: _____

End Time/Date: _____

Centrifuge at 13200 rpm (check for 'rpm' on centrifuge) for 30 min.

Start Time/Date: _____

End Time/Date: _____

Pipette supernatant into fresh microcentrifuge tube.

Dry in SpeedVac at 45°C.

Start Time/Date: _____

End Time/Date: _____

Solid Phase Extraction: Prepare solvents for solid phase extraction (SPE) as follows.

Solvent #1 – Wash Solution: Water with 0.1% TFA.

Solvent #2 – Conditioning Solution: 80% ACN in Water with 0.05% TFA.

Solvent #3 – Elution Solution: 25% ACN in Water with 0.1% TFA.

Condition each of the solid phase extraction cartridges by adding two column volumes of Solvent #1, one column volume of Solvent #2, and two additional column volumes of Solvent #1.

During the conditioning of the columns, reconstitute the samples in 1 mL of Solvent #1.

Vortex, centrifuge

Load each of the samples into individual SPE cartridges by pouring into the top.

Wash each vial with 1 mL of Solvent #1, vortex, centrifuge, and pour into the same cartridge as the initial reconstitution.

Wash a second time with 800 mL of Solvent #1, vortex, centrifuge, and pipette into the same cartridge as the initial reconstitution.

Wash the cartridge and loaded sample with 40 mL of Solvent #1.

Let the final wash solution pass through until the bottom of the meniscus reaches the top of the white filter.

Elute the glycans with 1 mL of Solvent #3 and collect the 1 mL fraction in a microcentrifuge tube.

Repeat the previous step 3 additional times for a total of 4 fractions per sample.

Freeze the samples at -80°C.

Dry in SpeedVac at 45°C.

Start Time/Date: _____

End Time/Date: _____

Remove from SpeedVac and reconstitute fractions 1, 3, and 4 in 75 μ L DI water and add into the vial with fraction #2.

Freeze the samples at -80°C .

Dry in SpeedVac at 45°C

Start Time/Date: _____

End Time/Date: _____

Glycan Derivatization:

Start Time/Date:

Prepare the reaction buffer by making a 10 mL solution of 75:25 (v/v) methanol:acetic acid.

Make a 1 mg/mL solution of each the light and heavy tagging reagent in the reaction buffer.

(Make only enough tagging solution for the current number of experiments – make immediately prior to reaction)

Reconstitute the glycan samples separately in 200 μ L of either the light or heavy tagging reagent.

Pipette up and down, vortex, and centrifuge.

Incubate all samples in parallel at 56°C for 3 hr.

Start Time/Date: _____

End Time/Date: _____

Immediately dry in SpeedVac at 55°C .

Start Time/Date: _____

End Time/Date: _____

Store in -20°C freezer until ready for injection on LCMS.

LCMS Sample Preparation:

Start Time/Date:

Reconstitute the derivatized glycan samples in 200 μ L of 95:5 (v/v) water:ACN.

Pipette up and down several times, vortex for 30 s

Spin down in centrifuge at 14000 rpm for 5 minutes.

Remove supernatant.

If necessary, mix Light- and Heavy-derivatized samples together in a 1:1 (v/v) ratio.

APPENDIX F

Current Applications of the INLIGHT *N*-linked Glycan Relative Quantification Strategy

F.1 Current Applications and Collaborations

The INLIGHT relative quantification strategy has been designed such that it can be applied to nearly any *N*-linked glycan sample preparation methodology from any biological sample. The only requirements are that the glycans must be released from the proteins and contain a free aldehyde at the reducing terminus. These requirements are met nearly ubiquitously in the case of *N*-linked glycans due to common use of PNGase F, which provides released glycans in the exact form needed for hydrazone formation. Due to this, we have actively sought internal projects and external collaborations for the application of the INLIGHT strategy.

To date, the INLIGHT strategy has been successfully applied to several different samples within this group including human plasma (*vide infra*), chicken plasma, human embryonic stem cell lysates, and *Magnaporthe oryzae* fungus lysates. This broad range of biological samples demonstrates the utility of the INLIGHT strategy in different sample preparation strategies and biological systems. Externally, we have generated interest in this strategy by the presentation of data and discussions at various meetings including the American Society for Mass Spectrometry Conference, the Warren Workshop, Innovative Molecular Analysis Technologies principal investigators meeting, and United States Human Proteome

Organization Meeting. Through these discussions, collaborations have commenced with researchers at the Complex Carbohydrate Center at the University of Georgia, Pacific Northwest National Laboratory, Georgetown University, and GlaxoSmithKline. These collaborations will allow us to continually develop and improve the INLIGHT strategy to make it a more ubiquitous and applicable tool that can be widely used in the field of glycomics.

Finally, because these novel reagents used in the INLIGHT strategy have been synthesized here at North Carolina State University, the availability to others is a barrier to the widespread use of this strategy. Thus, we are currently in discussions with Thermo Scientific Pierce Protein Research (a division of Thermo Fisher Scientific) to evaluate our reagents with the possibility of developing the INLIGHT strategy for commercial availability. The ability to have these reagents manufactured and available to researchers throughout the world would allow for the INLIGHT strategy to reach its full potential, and it is envisioned that this strategy can become the mainstream process for the relative quantification of *N*-linked glycan profiles between two samples.

F.2 Application to Ovarian Cancer Biomarker Discovery Efforts

The first large-scale glycan relative quantification study using the INLIGHT strategy was the application to ovarian cancer biomarker discovery efforts. An ovarian cancer plasma repository has been collected in collaboration with the Mayo Clinic (Rochester, MN). The repository consists of 164 age-, menopausal-, and draw date-matched control and cancer plasma samples over all stages of ovarian cancer (**Figure F.1**). Because the repository contains single time point samples, it was necessary to collect matched control samples in an effort to minimize the biological variability due to age, menopause, and draw date. Additionally, the control samples were taken from women who presented ovarian cancer-like symptoms (e.g. benign tumor) but were not diagnosed with ovarian cancer. Thus, a biomarker that is

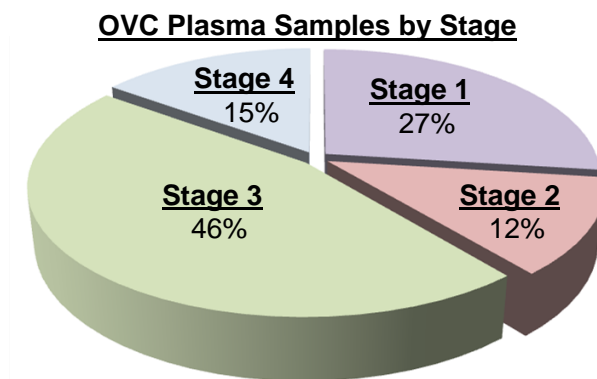


Figure F.1 – The percent of the total ovarian cancer plasma repository for each stage of cancer. It is seen that ~40% of the samples are from patients with early stage ovarian cancer.

capable of distinguishing between the control and cancer samples will likely be capable of screening for ovarian cancer vs. benign tumor without the necessity of a biopsy.

The *N*-linked glycan profiles were compared for each of the control-cancer matched pairs as detailed in **Figure F.2**. The sample pairs were divided into 7 batches for sample preparation and analysis. Each batch took one week to prepare, and the entire data set required continual MS analysis (24/7) of over 3 weeks. The data set is still being analyzed by the bioinformatic methods described in **Chapter 7**. Currently, ~25% of the data has been analyzed.

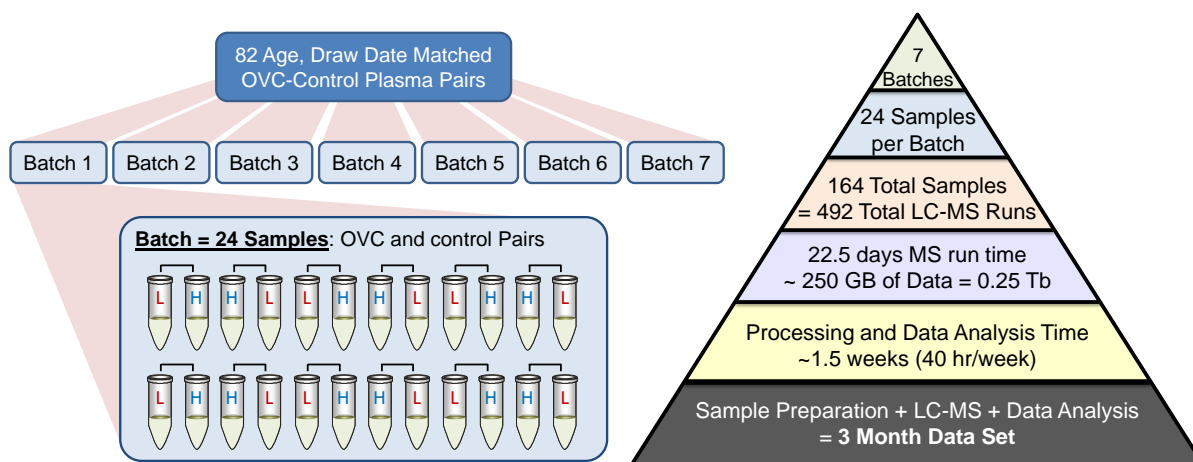


Figure F.2 – The sample preparation strategy for the entire cancer-control matched ovarian cancer plasma repository.

Two batches of the data have been processed, in which the relative quantification of each glycan for 24 sample pairs is presented as a heat map in **Figure F.3**. To further demonstrate the effectiveness of the INLIGHT strategy, **Figure F.3** presents a heat map for the glycan ratios in each sample corrected using the HRP internal standard (**Figure F.3a**) and normalizing based on TGNF (**Figure F.3b**). In **Figure F.3a**, it is seen that there is still systematic bias in certain samples. Certain columns (representing samples) are shown to be either all 'up' (red) or

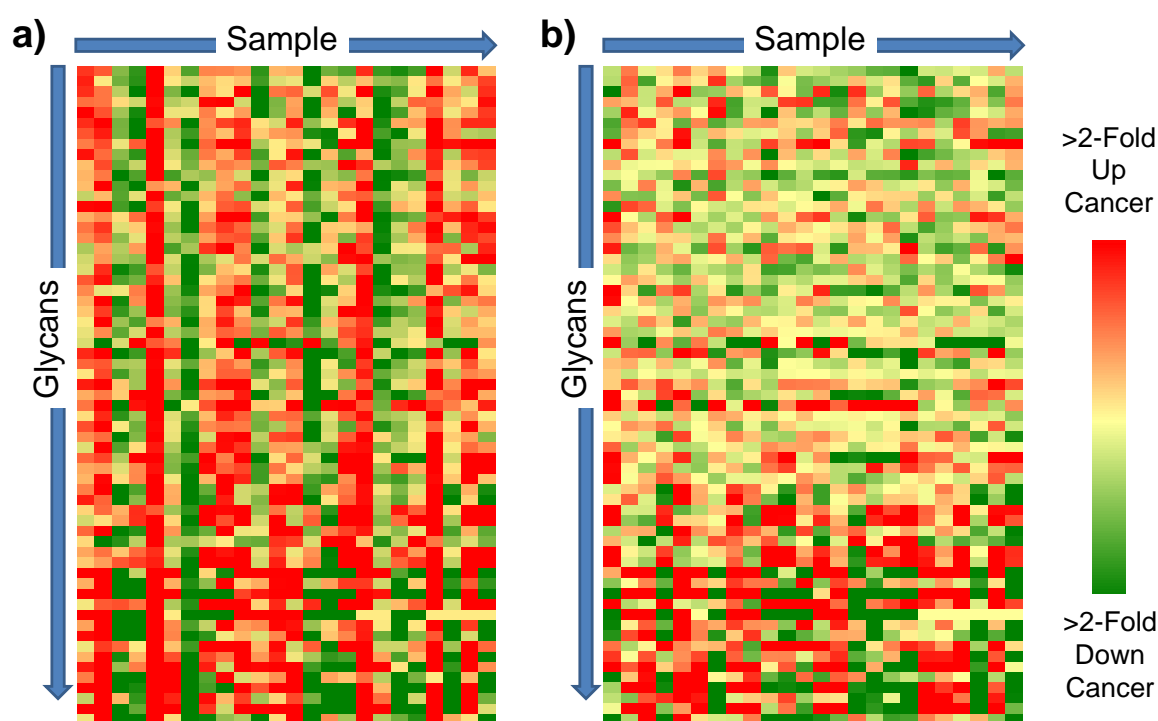


Figure F.3 – The individual glycan control:cancer ratios (depicted as a heat map) for each of the samples in the first two batches. Each glycan is listed along the vertical axis, and each sample is listed along the horizontal axis. **a)** HRP internal standard corrected data. **b)** TGNF normalized data.

‘down’ (green) regulated in cancer. However, this is unlikely due to ovarian cancer but the effects of different ‘glycan loading’ on proteins based on the individual. Thus, it can be seen in **Figure F.3b** that this systematic bias can be removed using the TGNF (*i.e.* no systematic red or green columns). Though this is very qualitative, histograms of the data are plotted in **Figure F.4**. Here, the analytical variability is plotted in **Figure F.4a** to demonstrate that the analytical variability is much less than the biological variability ($\sigma^2_{\text{Analytical}} \ll \sigma^2_{\text{Biological}}$), which allows for the detection of significant biological change. Additionally, it is seen that the HRP internal standard correction (**Figure F.4b**) contains more variation than when normalizing with TGNF.

Due to the more effective normalization strategy, the TGNF normalized heat map is presented in **Figure F.5a**, where the samples are grouped by stage, and the

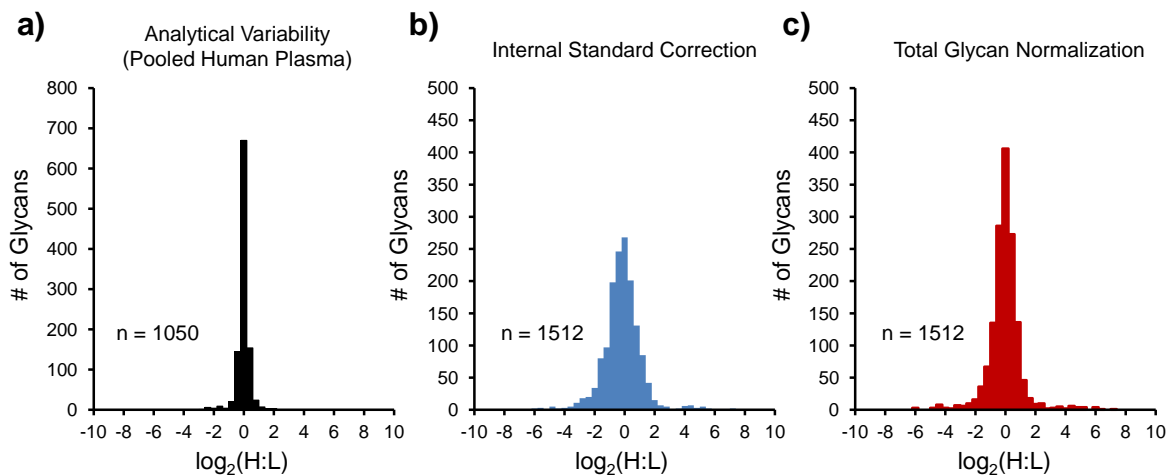


Figure F.4 – **a)** The analytical variability of the INLIGHT strategy as determined in **Chapter 7**. **b)** The histogram for the HRP internal standard corrected data. **c)** The histogram for the TGNF normalized data.

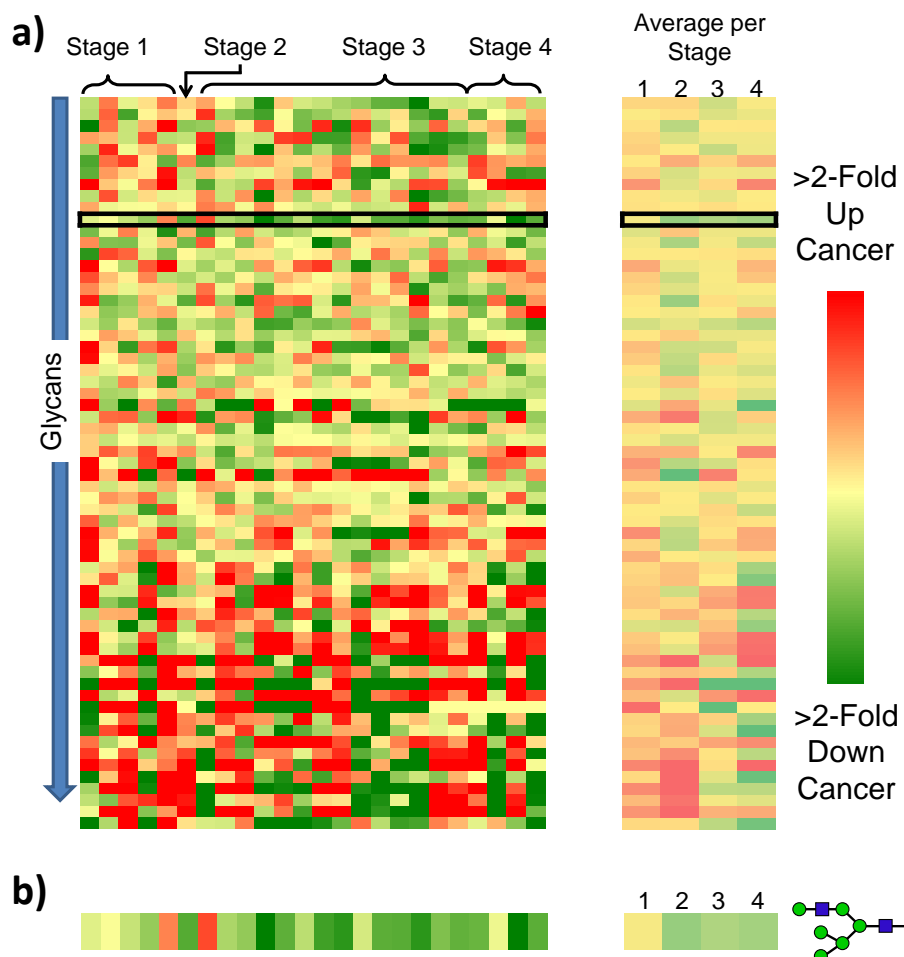


Figure F.5 – a) The TGNF normalized relative quantification data for each sample and the average glycan ratio (depicted as a heat map) in each stage. **b)** The glycan ratios for the Hex₆HexNAc₃ glycan over the first two batches.

average glycan ratios for each stage are shown. Using this data, one is able to begin to elucidate trends in certain glycans. For example, in **Figure F.5b**, it can be seen that the Hex₆HexNAc₃ glycan is down regulated in nearly every cancer sample that has been analyzed to date, and this data shows that on average, as ovarian

cancer progresses (in stage) this glycan becomes more down regulated. Though these are preliminary data, these examples demonstrate the effectiveness of the INLIGHT strategy toward large biological data sets. Thus, the entire data set will continue to be processed and analyzed in order to continue the search for glycan ovarian cancer biomarkers. Additionally, glycan relative quantification studies are underway utilizing the INLIGHT strategy and the chicken model of spontaneous ovarian cancer. This spontaneous model for ovarian cancer allows for longitudinal sampling of the onset of ovarian cancer, and because the variations in environment, age, feed, and strain are minimized, the biological variability is much less than single time point human data. Thus, these two large-scale glycan quantification studies will complement each other toward the discovery and development of glycan ovarian cancer biomarkers.